OECD/NEA
International Stripa Project
1980–1992

Overview Volume III

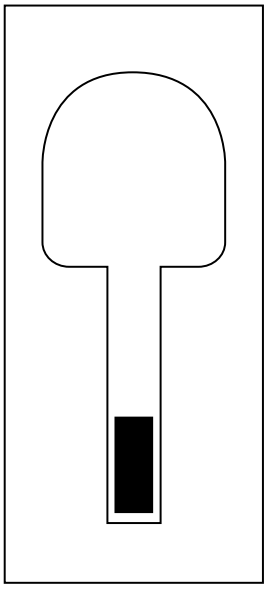

Engineered Barriers

Malcolm Gray

January 1993

OECD/NEA INTERNATIONAL STRIPA PROJECT

OVERVIEW VOLUME III

ENGINEERED BARRIERS

Malcolm N. Gray

January 1993

FOREWORD

This report results from a commission received in the Spring of 1991 from the Joint Technical Committee of the International Stripa Project. Interpreted and paraphrased, the description of work was deceptively simple - to produce a report that presented an overview of the studies into the engineered barriers which had been undertaken for the project. A focus on the work carried out between 1985 and 1991 for Phase 3 of the project was suggested.

At first, an attempt at an interpretive review of the studies was initiated. The personal goal of relating the findings of the project to the global purpose of total performance assessments of repository systems was set. An integration of results from all three phases of the project into a coherent whole was attempted. This objective proved to be unattainable. The regulatory environments in each of the member countries, the different repository designs being considered by the member organizations, the different levels of emphasis being placed in safety studies on the various components of disposal systems and an increasingly apparent disparity between the detailed objectives of the studies into the natural and engineered barriers demanded the less focused form that was finally adopted for the report. This form was derived from discussions between the five members of the reporting group (Drs. Fairhurst, Gera, Gnirk, Gray and Stillborg) and with members of each of the organizations that represented the seven nations that participated in Phase 3 of the Stripa Project.

Bounded by Chapter 1 (Introduction) and Chapter 6 (Conclusions), the four chapters that are the main body of the text discuss the research activities in the sequence in which they were carried out. Chapter 2 reviews the Buffer Mass Test that was undertaken for Phase 1 of the project, Chapter 3 reviews the Phase 2 Borehole, Shaft and Tunnel Plugging Tests, and Chapter 4 reviews the Phase 3 *In Situ* Grouting Experiments. Chapter 5 (Longevity of Sealants) is a remnant of the original concept for the report in that it deals with work carried out throughout the term of the project and is directly focused on issues that are specific to assessing the performance of sealing systems for repositories for heat-generating radioactive-wastes. In this context, because the review of the Buffer Mass Test given in Chapter 2 was written before the final structure of the document was fixed, this chapter contains more personal comment than Chapters 3, 4 and 5. The Chapters were written in the sequence 2, 3, 4, 5, 6, 1.

Although there was continuing personal involvement with the project from 1982, attempts were made to restrict the review to the contents of the Technical Reports that form the project record. Only where directly pertinent were findings from studies outside the Stripa Project used to clarify issues arising from the investigations. The Technical Reports on the Engineered Barriers investigations are informative, tantalizing and provocative. The completeness of the reports is attested by the fact that it was only necessary to meet with the principal investigators for one day to resolve misunderstandings arising from the review. Except where implied or explicitly stated, generally, the final text of this report is considered to represent the views of both the principal investigators and the author. Despite this, readers are encouraged to refer to the original documentation to gain a more complete understanding of the work for which this report provides a limited summary and singular view.

For Phases 1 and 2 of the project, Roland Pusch and Lennart Börgesson of Clay Technology AB (Sweden) were the Principal Investigators for the

Engineered Barriers investigations. Maria Onofrei (AECL Research, Canada), Daniel Meyer (IT Corporation, USA), William Coons (RE/SPEC Inc., USA) and Steven Alcorn (RE/SPEC Inc., USA) also acted as Principal Investigators for the Phase 3 investigations. With this small number of investigators it was probably less difficult to reconcile different views and interpretations of data obtained from the Engineered Barriers investigations than from those obtained from the studies into the Natural Barriers in which a larger number of investigators was engaged. From this perspective, the completeness, cohesiveness and objectivity of Volume II (Natural Barriers) of this report is admired.

The financial support and the encouragement received from the members of the Joint Technical Committee (JTC) of the OECD/NEA International Stripa Project are gratefully acknowledged. Specifically, the efforts of the JTC chairman, Mr. Per-Eric Ahlström, are recognized. Financial support was also provided by the CANDU Owners Group.

Special thanks are due to Drs. Steven Alcorn, Lennart Börgesson, William Coons, Maria Onofrei and Roland Pusch who were responsible for the work discussed in this document. Comments received from these individuals on early drafts of the document were comprehensive, constructive, valued and significantly enhanced the quality of the work. The comments and guidance received from the other members of the reporting group (Drs. Fairhurst, Gera, Gnirk and Stillborg) contributed significantly to the final product. In this regard, as peer reviewer to this volume, Dr. Ferruccio Gera's robust and patient comments and critique need special mention. Thanks are due to AECL Research, who released me from my normal duties to complete this document. In this respect, the outstanding support of the staff of the Fuel Waste Technology Branch and, specifically, the members of the Vault Sealing Section is recognized. The skills of those who turned scratchings into publishable figures added to the final quality of the document.

Malcolm N. Gray

Pinawa

1993, January

TABLE OF CONTENTS

SYNOPSIS

Underground laboratories are being used by the member countries of the OECD/NEA to obtain information to assist in the development of designs for repositories for heat-generating radioactive wastes. Work in the Stripa mine between 1980 and 1992 allowed for recognition of some of the conditions and difficulties that may be encountered in repositories in granite and for engineered solutions to be tailored and proffered. The studies were divided under the general headings of "natural" and "engineered" barriers investigations. From the overall objective of effective repository design the division is considered to be artificial and was required merely to provide effective management of the programmes.

The broad objective of the engineered barriers studies was to demonstrate and qualify the use of different materials and techniques for sealing water flow paths in the Stripa granite, the mine excavations and the excavation disturbed zones. The engineered barriers studies were carried out through the full period over which the agreements that formed the Stripa Project were in effect. The division of the programme into phases and the overlap in the timing of each of the three phases, Phase 1 (1980 to 1985), Phase 2 (1983 to 1988), and Phase 3 (1986 to 1992), allowed for developments achieved during the project and concerns arising from independent national programmes to be incorporated in the investigations. As may be anticipated from the application of the observational method that forms the basis for design of geotechnical structures, the programme evolved with the findings being made at Stripa and other underground laboratories.

During Phase 1, the engineered barriers investigations focussed on the heat affected zone of the repository. Specifically, the response of clay buffers and the interactions between waste containers, clay buffer materials and the rock were studied. The Phase 2 investigations examined the feasibility of sealing boreholes, shafts and tunnels with clay sealants. In Phase 3, studies of the ability to grout and seal fractured granite including the excavation disturbed zone were effected and specific studies into the longevity of cement- and clay-based sealing materials were undertaken. Major findings, observations and conclusions made through the progress of the work are summarized here.

PHASE 1 - THE BUFFER MASS TEST (BMT)

The Buffer Mass Test (BMT) was a half-scale mock-up of a waste deposition concept proposed by KBS of Sweden. Electrically powered heaters, simulating heat-generating waste containers, were embedded in highly compacted bentonite (HCB) clay buffer material and placed in six large diameter boreholes drilled in the floor of a room at the 340 m level of the Stripa mine. The room above two of the deposition holes was backfilled with bentonite-sand mixtures. The buffer, backfills and the rock were heated for periods of up to about four years and observations were made on the transient processes of heat and water transfer in the buffer and the ef-

fects of these processes on hydro-mechanical interactions between the rock and the buffer immediately following waste emplacement in a repository were studied. It was not possible, given the short duration of the test, to examine the radionuclide transport properties of the buffer, other than by implication.

The HCB used as the buffer was prefabricated by statically compacting the bentonite to a dry density of not less than 1.88 Mg/m^3. The sand-bentonite tunnel backfill materials were compacted *in situ* to minimum dry clay densities of approximately 0.43 Mg/m^3 (lower backfill) and 0.37 Mg/m^3 (upper backfill). At these densities the buffer probably has an osmotic efficiency approaching 100 per cent; the backfill materials probably have lesser efficiencies.

Calculations using numerical models based on Fourier's law for heat transfer in the backfill/buffer/rock system indicated that the test needed to be run for approximately 3 months to allow for observations on the validity of the model. Calculations for moisture transfer in the system, using numerical models based on isothermal moisture diffusivity equations, indicated a need for the experiment to be operated for a period of one or more years. Uncertainties were evident in the modelling exercises. These related principally to a lack of available data for the parameters employed in the field equations describing heat and moisture transfer. Experience indicated that it was likely that the uncertainties were more significant to the predictions of water transfer than to those for heat transfer.

During water uptake, the buffer and backfill materials were predicted to swell and develop swelling pressures acting against the other components of the test system. The buffer was expected to exert high ultimate pressures, 10 MPa or more, against the rock and the backfills. Pressures of hundreds of kPa were expected from the backfill materials. Deformations of decimetres at the buffer/ backfill boundary were predicted. Moreover, the swelling pressures could result in clay being extruded into open rock fractures that intersected the excavations in which the experiment was to be carried out.

The hydro-mechanical interactions, due to their largely unknown effects on the hydraulic boundary conditions acting at the buffer/backfill/rock interfaces, further decreased confidence in ability to predict numerically the heater/buffer/backfill/ rock performance and interactions. Observations to be made in the BMT were needed to qualify and refine conceptual models for performance and to provide an indication of the extent to which enhanced numerical prediction capabilities were required or, indeed, possible.

The work for the macropermeability experiment carried out under the Swedish-American Cooperative agreement, along with observations made in the large diameter holes (Φ = 760 mm) that were diamond drilled to a depth of 3 m for the BMT, provided information used to bound the initial hydraulic conditions around the BMT room. Excavating the room at right angles to the horizontal major principal stress resulted in an excavation disturbed zone with a radial hydraulic conductivity that was less than the value of 10^{-10} m/s estimated for the surrounding rock mass. Measurable water flows occurred principally in the fractures in the rock mass although there was evidence of flow in permeable "fracture free" rock. Only a small fraction of the observed fractures visibly carried water. A large number of the natural fractures were infilled with minerals or otherwise blocked to the transmission of water. The eastern wall and the back of the room appeared

likely to provide greater access of water to the backfills than the floor, the western wall and the end of the room. Natural water flows into the deposition boreholes varied between holes. Most of the water entered the open large diameter drill holes through discrete fractures which, reflecting excavation disturbance, were concentrated in the upper third of the holes and sub-parallel to the floor of the room. Three holes were classified as "wet"; the other three were classified as "dry".

A large number of instruments were installed in the buffer and backfills to monitor changes in temperature, total pressure, pore water pressure, moisture content and displacement during the progress of the tests. Commercially available instrumentation was used wherever possible: much of this instrumentation required modification and calibration for the harsh environmental conditions of temperature, pressure and water salinity expected in the test. Special moisture sensors were developed to monitor transients in the clay masses.

The heaters used in the six emplacement holes were specifically designed to facilitate single point measurements of moisture content in the HCB during careful decommissioning at the end of the test .

The response of the buffer and backfills to heating and to water supplied through the bounding rock mass depended on the original hydraulic boundary conditions, the test configuration and the interactions between the clays and the rock mass. The temperature distribution, final moisture content distributions and swelling pressures developed by the HCB buffer material were largely controlled by the rate at which water was supplied at the rock/buffer interface. The buffer in wet holes became saturated within the period of the test; the buffer in dry holes showed increasing water content from the heater to the buffer/rock interface with drying having occurred near the heater. Correspondingly, swelling pressures were higher in the wet holes than in the dry ones; temperatures were generally lower.

Under the force of the swelling pressure, HCB was extruded into fractures intersected the excavations . This prevented these fractures from acting as local water sources . Water uptake by the buffer took place through a thin layer of sealed rock which acted as a porous medium. The swelling pressures also ensured that the buffer mass, which originally contained construction joints, self sealed. In accordance with expectations, this self sealing was more pronounced in wet holes than in dry ones.

The results tended to confirm that an isothermal moisture transfer model could be applied to moisture transfer in the backfill materials. The model did not account for moisture transfer that occurred in the HCB buffer in which it was likely that an evaporation/condensation cycle was established down the temperature gradient developed in the unsaturated buffer. The temperature data, swelling pressure results, moisture redistribution data, results from tracer tests and retrospective analyses all support this hypothesis. This process is known to occur in loose clays and sands. Through the conduct of the BMT it is now known to be significant in dense bentonite materials under repository conditions and, depending on repository design, may need to be accommodated in models of near-field performance.

The heat conduction model used tended to overestimate the temperatures to be expected in saturated systems - the ultimate condition expected in a repository.

The mechanical performance of the backfill met all expectations by exhibiting more than adequate resistance to the uplift forces from the buffer. The magnitude of heave at the buffer/backfill interface was well predicted by a simple mathematical model. The effects of swelling pressures from the buffer on the rock mass were too low to be measured. However, the floor of the emplacement room exhibited heave, which was principally attributable to increases in the temperature of the rock and in accordance with understanding. The effects of this movement on water flow in the near-field rock mass could not be established.

Pore water pressures in the rock mass within one metre of the tunnel faces appear to have been controlled by an excavation disturbed zone (EDZ). Adding to the results from the SAC macropermeability experiment, the BMT results indicated that the hydraulic properties of the EDZ were anisotropic; hydraulic conductivity parallel with the tunnel axis appeared higher than radial hydraulic conductivity. The high axial conductivity fed groundwater to the top of the emplacement boreholes and to the bottom of the tunnel backfills. These data provided significant understanding of the near-field rock mass for the design of grouting experiments carried out during Phase 3 of the project.

PHASE 2 - BOREHOLE, SHAFT AND TUNNEL PLUGGING

Borehole plugging

Three borehole plugging/sealing tests were carried out. Each test was configured to allow for different aspects of borehole plugging with HCB to be investigated.

In all of the tests HCB was introduced into smooth walled, diamond drilled boreholes and observations made on the rate of water uptake and swelling of the HCB, the resistance of the maturing bentonite to piping under hydraulic gradients, and the mechanical resistance between bentonite plugs and the borehole wall. The differences between the three tests lay in the orientation of the boreholes - one horizontal borehole and two vertical boreholes were sealed - and in the type of plugs used - one vertical borehole was plugged using techniques which were virtually identical to those used in the horizontal borehole, the sealing system used for the second vertical borehole differed.

The sealing system in all cases consisted of hollow cylinders of HCB encased in an exoskeleton of perforated metal. The exoskeleton was needed to provide rigidity to the system as it was introduced into the borehole The perforations were required to allow water to access the HCB, causing the material to swell and seal unfilled sections of the boreholes. The axial central hole in the HCB allowed access for instrumentation leads and hydraulic tubing and will not be present in repository seals.

The horizontal borehole plugging test was carried out in a 96.6 m long, 56 mm diameter borehole that, in part, ran approximately parallel to the drift used for the BMT in Phase 1.

The vertical borehole plugging tests were carried out in two 14 m long, 76 mm diameter boreholes that were specially drilled for the purpose of the tests between two vertically separated, parallel tunnels near the BMT area.

The arrangement of the borehole plugging tests included mechanisms that allowed for the plugs to be subjected to high water pressure gradients so that the hydraulic properties of the sealed borehole could be examined. The resistance of the maturing bentonite to piping was specifically investigated. Moreover, total and pore water pressure sensors were included at strategic locations along the length of the plugs to assist with the interpretation of the flow measurements and to confirm aspects of bentonite behaviour and properties. After the *in situ* hydraulic testing of the borehole plugs had been completed the vertical borehole plugs were extruded and measurements were made to evaluate the water uptake and swelling behaviour of the HCB. At the end of the horizontal borehole plugging test a small volume of rock, through which the sealed borehole passed, was carefully excavated and the bentonite that it contained was examined.

The ease with which the borehole plugs were emplaced demonstrated the practicality of the design of the HCB sealing system for both horizontal and vertical borehole plugging operations.

Hydraulic testing of the horizontal plug as little as 14 days after plug installation proved that the bentonite plugs could sustain hydraulic gradients as high as approximately 450 without piping. A very effective seal at the HCB/rock interface was demonstrated by the pressure measurements taken in the vertical borehole plugging tests.

Examination of the recovered HCB plugs indicated that the clay was virtually fully water saturated and had expanded into the annular space between the plug and the borehole wall that was needed as a working clearance during plugging operations. This outer film of bentonite was less dense than the inner core indicating either incomplete consolidation of the bentonite or an ability for the bentonite to sustain significant stress gradients.

It can be concluded that bentonite plugs like the ones tested at Stripa will fail hydraulically by piping before they fail mechanically by extrusion. Within the pressure range in which they are effective they can be estimated to seal the borehole to an effective hydraulic conductivity in the range 10^{-12} m/s to 10^{-13} m/s.

Shaft and tunnel plugging

Shaft and tunnel plugging tests were carried out to determine the efficiency with which HCB could limit flow at the interfaces between bulkheads, backfills and excavated rock surfaces. The shaft plugging experiment was conducted near the vertical borehole plugging tests in a 14 m deep vertical, tapered shaft that had been excavated to a diameter of 1 m (top) and 1.3 m (bottom) between two vertically separated virtually horizontal tunnels. The tunnel plugging experiment was carried out in a specially excavated, 35 m long, dead-end tunnel. The tunnel was excavated by careful blasting to a cross-sectional area of about 11 m^2.

In both the shaft and tunnel plugging tests two bulkheads were constructed within the excavations to form a test cell. The inner surfaces of the bulkheads were lined with HCB and the enclosed volume was filled with sand.

The outer bulkheads, the inner, sand-filled part of the test cell and the rock acted as constraints to resist bentonite swelling. The inner sand-filled chambers were filled with water and pressurized and the resulting water flows through and around the HCB gaskets were measured.

Shaped HCB blocks with properties similar to the buffer material used in the BMT were used and tested. In the shaft plugging experiment HCB filled the entire cross-section of the excavation; in the tunnel plugging experiment the HCB was used to form a gasket (or "O" ring) on the perimeter of the inner surfaces of concrete bulkheads at the bulkhead/rock interface. The swelling and water pressures exerted on the bulkhead structures and at the HCB/rock and HCB/sand interfaces were measured along with the resulting deformations of the structures and the softer interfaces. Observations were made of the water uptake properties of the clays and, like the deformations, compared with pre-test predictions that were made using simple conceptual and numerical models of system performance based on developments made in Phase 1.

The clay plugs were readily emplaced. This demonstrated the practicality of the design of the plugging system. Moreover, the hydraulic testing showed that the HCB effectively stopped water flow through the shaft and tunnel excavations. The clays seals were less permeable than the surrounding Stripa granite through which, in both the shaft and tunnel plugging experiments, most of the water was lost from the test cells.

The Stripa rock was hydraulically variable on the scale of metres. The paths in the rock around the shaft plug through which water was lost were not defined. However, for the tunnel plugging test it was clear that a pegmatite zone and a series of discrete, steeply dipping, connected fractures in the floor of the tunnel allowed water to circumvent the plug.

Measured water content distributions in the HCB showed that at the end of the tests the inner cores of the HCB was not saturated. The measured water content distributions were compared with values calculated using a simple diffusivity model developed through the Phase 1 activities. The measured and calculated values were in reasonable agreement except for incomplete appreciation of the boundary conditions acting on the clay and, hence, erroneous assumptions used for the calculations. Thus, it appears possible to predict the water uptake properties of confined highly compacted bentonitic materials. In common with the results from the borehole plugging and the shaft plugging experiments, the variations in moisture content through the clay showed that the HCB was not homogenized over the period of the test. Differential stresses were sustained. An eventual equalization of the stresses within and densities of the clay in the very long term remains questionable.

Observations made during the disassembly of the test structures showed that the expanded bentonite conformed with the faces and edges of the inside of the bulkheads and the irregular rock surfaces. This evidence supported the conclusion that the swelling HCB can be used to effectively seal the interfaces between engineered barriers and the excavated rock surfaces. Observations of the limited penetration of the swelling HCB into fractures in the rock surface echoed findings of the BMT and the borehole sealing experiments, and further supported the suggestion that physical interactions between the rock and the clay controlled water ingress into the clay and effectively sealed the interface between the clay and the rock. Although the

clay had penetrated outwards from the seal into the fractures the outward movement was clearly limited in extent and there was no evidence of erosion of the clay under the high pressure gradients imposed on the groundwater. Moreover, it could be concluded that sand and clayey materials can be designed and used to confine HCB and preserve the long-term sealing functions of the clay.

PHASE 3 - GROUTS AND GROUTING

Materials

Scoping studies led to the selection of high-performance cement- and clay (bentonite)-based grouts for investigation in Phase 3. Laboratory studies of the rheological and hydraulic conductivity properties of these materials were undertaken to define the conditions under which they could be applied with maximum effect as grouts.

The results confirmed that decreasing the water content tends to increase strength (shearing resistance) and decrease the hydraulic conductivity of both material types. For these and other reasons it was anticipated that decreasing the water content would improve the long term performance of the materials. Methods allowing for the injection of the materials with low water content yet with sufficient fluidity to permit injection were developed.

Both the clay and cement grouts were determined to exhibit pseudo-plastic behaviour immediately after mixing with water. Moreover, the rheological behaviour could be modified by vibrating the freshly mixed materials. The effects of vibrations of different frequencies and amplitudes on the rheology of various grout mixtures were evaluated. It was generally concluded that applying vibrations to the grouts during injection would decrease the water content needed to provide adequate fluidity to the materials. Thus, a range of operating parameters was defined for the effective functioning of a grout injection pump that could apply vibrations as well as pressure to the grouts during injection.

It was shown that reductions in the water contents of both bentonite clay-based and cement-based grouts could be effected by the use of admixtures. For the clay grouts, NaCl added to the mixing water decreased the water content at which the materials were sufficiently liquid to be described as grouts. In addition to changing the rheological properties of freshly mixed grouts it was inferred from the results that the addition of salt to the grouts could improve the long-term strength and hydraulic properties of the materials.

The water content of cement grouts could be decreased by admixing superplasticizers. In addition, the inclusion of finely divided pozzolanic materials, in the form of silica fume, eliminated bleeding from the freshly mixed cement grouts, increased long-term strength, and decreased hydraulic conductivity.

Thus, clay grouts incorporating NaCl and cement grouts including superplasticizers were studied in the *in situ* experiments. Cement grouts with and without the pozzolan were tested in the Stripa mine.

Cement, pozzolanic and clay products exhibit inherent variability arising from natural source variability and changing production patterns. Ageing processes, post-production and prior to use, also influence the properties of cementitious materials. Effects of these factors on the particle size and rheological properties of freshly mixed grouts were determined. It can be deduced that practical grouting operations associated with repository sealing would be obliged to accommodate much of this variability and that experienced personnel will be required to effect control procedures and make field adjustments to mix composition. Ultimately, grout mixes will be selected through the application of understanding gained from observations made during the progress of the *in situ* grouting operations associated with repository sealing. In this latter context it is noted that the cement grouts used in the *in situ* experiments at the Stripa mine were selected on the basis of expected material variability and possible effects on the success of the grouting operations. The materials used were varied somewhat from the grouts preselected from the results of the laboratory studies. Modifications to the mix compositions were made as the *in situ* work progressed.

Grouting around deposition holes

The hydraulic conductivity of the rock in the floor of the BMT room around two BMT holes was measured before and after injection with clay-based grout and after the grouted rock had been heated to almost 100°C. The rock was grouted from the BMT holes using a large diameter packer and injection system that was specially developed for the purpose and linked to the dynamic injection device that had been developed and tested during preliminary activities.

The hydraulic conductivity of the rock was decreased by grouting. Heating caused the hydraulic conductivity of the grouted rock to increase. However the final values tended to be less than those of the ungrouted rock. The increase in hydraulic conductivity of the grouted rock caused by heating was associated with heave in the unrestrained floor of the test room. Grouting also caused the floor to heave. Thus, it was shown that the materials and techniques developed through the programme could be used successfully to decrease the hydraulic conductivity of discretely fractured rock with values before grouting as low as 10^{-8} m/s. It was shown that the Stripa granite with hydraulic conductivities in the range $10^{-10} < k < 10^{-8}$ could be grouted if the fractures were relatively free of natural infilling materials.

The upper 0.5 m to 1.0 m of floor of the BMT room was found to have been significantly disturbed by the excavation process and to have an hydraulic conductivity axially along the room that was as much as four orders of magnitude higher than the average value measured for the undisturbed rock. However, the values varied over three orders of magnitude on a scale of metres. This latter finding and the observed heave in the floor of the room, which was also locally variable at the same scale, led to the suggestion that, for the purposes of repository performance assessment, the only reasonable approach may be to attempt to predict the thermo-hydro-mechanical performance of ungrouted or grouted rock with less detail than the one achieved in this experiment.

Fracture zone grouting

The natural barrier investigations provided background information on the hydrogeological characteristics of the rock mass that was to be grouted and a concept for an experiment to determine the effectiveness with which high performance grouts could seal hydraulically active fracture zones in the rock mass was developed. Effectiveness was to be evaluated by measuring the extent to which grouting was able to decrease the rate of water flow into excavations.

The background information on the hydrogeological characteristics of the rock proved to be insufficient for the level of understanding of the rock required for the grouting experiment. Additional probes to locally characterize the rock indicated more complex hydrogeological characteristics than those originally envisaged and led to a revised concept of the hydrogeological conditions. The hydrogeological characterization activities associated with the experiment identified a subset of fracture features, providing local control (at the scale of tens of metres) on water flows. The subset had not been recognized by preceding, more globally orientated, natural barrier studies. Similar findings may be expected should grouting activities prove to be necessary to effect repository sealing. Such grouting activities will provide additional information on the detailed structural geology of the host rock and may be used to refine hydrogeological models used for site assessment.

Hydraulic testing of the rock locally around the test room provided estimates for the apparent hydraulic conductivities of the different structures through which the excavation had been made. With this information it was possible to construct a simple axisymmetric finite element model of the flow paths. Using known hydraulic pressures in the rock and making reasonable assumptions for the effects of grouting on the hydraulic conductivity of the rock, estimates were made for the effects of the grouting on the total flow into the room. The results showed that total inflows could be expected to be decreased by less than 10 %, which is less than the natural fluctuations measured before grouting. While some measure of this decrease may have been observed in the test results, alone, the measurements of total in-flow to the room were not sufficient to evaluate the effects of grouting. In light of the hydrogeological conditions that will exist in a sealed repository after the major disturbances to the groundwater flow caused by repository construction are removed, the rate at which water flows into a room may not be the appropriate criterion by which to evaluate the effectiveness of grouting.

The physical presence of grout in the fractures, the results of the tracer experiments and the rates of evaporation from the rock surfaces before and after grouting, the measured rates of inflow from holes drilled into the ungrouted and grouted hydraulically active volumes of rock, along with hydraulic testing of ungrouted and grouted rock, all indicated that the grouting activities changed the dominant water flow paths in the rock.

From these observations it could be concluded that, using the techniques and cement-based grouting materials developed and used through the programme, it would be possible to decrease the apparent hydraulic conductivity of fracture zones, such as that exemplified by the J zone in the Stripa rock mass, from $10^{-8} > k > 10^{-9}$ m/s to $5 \cdot 10^{-10} > k > 10^{-10}$ m/s. To achieve

this effect, borehole spacings would have to be closer than the ones used in the grouting experiment. Further improvements in grouting equipment, techniques and processes would add further confidence in an ability to achieve the result.

Grouting the excavation disturbed zone

In situ investigations were carried out in 3 500 m^3 of rock around the enclosed section of the tunnel used for the BMT. The hydraulic properties of the excavation disturbed zone (EDZ) around tunnels excavated in the Stripa granite and the ability to grout and decrease the hydraulic conductivity of the zone were investigated.

The EDZ was considered to consist of two parts: (i) a blast damaged zone (BDZ), which extended around the periphery of the room to a maximum depth of approximately 1 m from the surface of the excavation; and (ii) a stress disturbed zone, which theoretically extended to a depth of about 12 m into the rock and was investigated experimentally to a depth of 7 m. The hydraulic conductivity of the BDZ was measured locally , at the scale of metres, by water pressure injection tests. Attempts were made to measure the hydraulic conductivity of the stress disturbed zone over a distance of 13 metres with the longitudinal axis of the test tunnel. These measurements were supplemented by assessments of the hydraulic conductivity of the rock made through evaluations of the water inflows under the natural hydraulic gradients into openings in the rock. Hydraulic conductivity measurements were made before and after the BDZ was grouted using both static and dynamic injection techniques with Alofix cement-based grout. Practical difficulties, associated with sealing the surface of the test chamber, led to delays in the programme and cost concerns. Thus, a programme to test the effectiveness of grouting the stress disturbed zone was not completed.

Evaluation of the results from hydraulic tests required the development of conceptual models for the fracture features in and the hydraulic characteristics of the undisturbed and disturbed Stripa granite. These conceptual models were incorporated into available computer codes which were used to appraise the effects of excavation on the hydraulic properties of the granite. At the level of detail needed for the experiment, the conceptual models and computer codes, alone, were not sufficiently complete to describe the properties of the excavation disturbed rock mass and account for the test results. Combined with observations made in other parts of the Stripa mine throughout the SAC programme and Phases 1, 2 and 3 of the Stripa Project, the results of the modelling methods and the hydraulic testing led to the following conclusions with regard to the hydraulic properties of the rock around the BMT excavation. A blast damaged zone, which could be generally ascribed an hydraulic conductivity of approximately 10^{-8} m/s, existed in the rock within 1 m of the surface of the excavation. The hydraulic properties of the stress disturbed zone were generally anisotropic with axial and radial hydraulic conductivities of $5 \cdot 10^{-10}$ m/s and $5 \cdot 10^{-11}$ m/s, respectively. The undisturbed rock could be considered as isotropi with hydraulic conductivities in the range $3 \cdot 10^{-11}$ to $9 \cdot 10^{-11}$ m/s. The values given vary spatially within defined ranges.

With the techniques and grouting materials used for the experiment, despite clear evidence that grout had been injected into the EDZ, the hydraulic con-

ductivity of the zone was not measurably changed. Some possible explanations for this result include insufficiently close spacing of the holes through which the grout was injected and the effects of infilling materials in the natral fractures. Alternative grouting procedures may have given different results. The lack of opportunity to conduct a second grouting phase or to grout the stress disturbed zone left these issues unresolved.

LONGEVITY OF SEALANTS

The longevity of clay- and cement-based sealants was investigated by: investigation of natural analogues; laboratory studies of material properties; and, numerical modelling of thermodynamic processes.

For bentonite-based materials, attention focussed on developing detailed understanding of hydrothermal alteration of minerals; particularly, reactions causing transformation of smectite clays to hydrous clay-micas or causing silicification of the clay mass were studied. Both of these processes could decrease the swelling capacity of the bentonite and lead to loss in long-term function. For the cement-based sealants, mechanisms causing dissolution of cement in groundwater and, thereby, increasing the hydraulic conductivity of grouted rock were investigated: specifically, the leaching and hydraulic conductivity properties of the materials were studied. To allow for the development and application of numerical models of cement-grout longevity, a data base on the fundamental thermodynamic properties of cement grout phases was established and expanded. In addition to these basic studies, the mechanical stability of clay gels and unset cement pastes were investigated with respect to their ability to resist erosion. This information was needed to define the limiting groundwater flow conditions under which each of the materials could be applied.

The crystal structures of smectite minerals and hydrous clay-micas possess similar features. With particle sizes less than 2 mm, both mineral types consist of negatively charged lamellae of phyllosilicates comprised of covalently bonded silica and alumina layers. The lamellae in clay-mica are bonded by K^+. In smectites the lamellae are separate and discrete. Studies of the products of reaction between bentonite, finely ground silica, groundwater and rock over a wide range of temperatures and pressures showed that when K^+ is present in groundwater, the smectite in bentonite clay will convert to hydrous clay-mica. In contrast with HCB, for which the conversion reaction will take many tens of thousands of years, conversion in clay grouts will take a few thousand years or less. At temperatures above about 130°C, the conversion reaction will be accompanied by the precipitation of silica within the clay fabric. This latter process results in cementation and embrittlement of the grout. The effects of the conversion of smectite to hydrous clay-mica on the performance of a grouted rock mass were assessed by reviewing the structure of the grouts recovered from the *in situ* tests. It was estimated that after the smectite in the grouted rock mass has undergone complete conversion from smectite to hydrous clay-mica, the grouted rock could still possess an hydraulic conductivity that is significantly less than that of ungrouted rock. The conversion process was shown to be largely controlled by the coefficient for fickian diffusion of K^+ in the clay and the concentration of K^+ in the groundwater.

To evaluate the longevity of high-performance cement-based sealants, laboratory studies were coupled with geochemical modelling of the changes that may occur within the fabric of the material and a numerical assessment of the effects of these changes on performance. Initially, modelling studies were based on contemporary understanding of normal cements and concretes and were subsequently adjusted for laboratory findings on high-performance grouts.

The studies indicated that the grouts could endure between 100 000 and 1 000 000 years in a repository environment. These predictions did not account for unhydrated materials that were found in both ancient cements and modern high-performance materials. The long endurance was related to the low dynamic porosity of the high-performance materials.

The porosity-hydraulic conductivity relationship for conventional portland cements was found not to apply to high-performance materials, laboratory specimens of which were shown to be virtually impermeable at hydraulic gradients less than approximately 15 000. In this context, it is noted that the maximum hydraulic gradient in the Stripa facility was approximately 2 000; much lower gradients are expected in a sealed repository. Initially, based on conventional wisdom, it was assumed that cements would degrade by water percolating through the grouts; as the water passed through, the cement solids would dissolve and the consequent porosity increase would increase hydraulic conductivity. Given the very low hydraulic conductivity of the high-performance grouts, substantial flow through the body of the cement did not appear to be likely. While flow will occur around the grout, diffusion processes will operate within the grout to alter the mineralogical composition and chemistry of the grout. The slow diffusional processes virtually assure an approach to chemical equilibrium and it can be inferred, as shown in laboratory tests, that void spaces represented by micro-cracks or other microporosity will be filled by the precipitation of secondary reaction products. The chemical reaction of groundwater and cement yields secondary products which occupy more space than that occupied by the original solid cement phases.

The consequence of this new understanding is that during early repository evolution, cement grout performance will be dominated by surface-controlled mechanisms. Because these mechanisms are less efficient at mass removal than the assumed processes of percolation and dissolution, the reported estimated persistence times are considered to be a lower bound on the longevity of intact cement-based sealing materials. Several uncertainties rest with this judgment. Particularly, examination of the microstructure of grouts injected in the Stripa mine revealed an inhomogeneous structure that was not present in laboratory prepared and tested materials. The full implication of the Stripa findings need to be appraised after further *in situ* tests have established whether the results are specific to the Stripa site and to the injection technique applied in the Stripa field tests.

CONCLUSIONS

- The hydraulic conductivity of drill holes and excavated openings could be returned to values similar to those of intact granite by the judicious use of HCB.

- Models are now available to predict the response of HCB to changes in stress, thermal and hydraulic gradients. The models for water transfer are not rigorously precise. In contrast, thermal properties are reasonably well understood and heat fluxes through the material can be well described.
- The properties of advanced, high-performance bentonite- and cement-based materials pertinent to their successful injection as grouts in fractured rock have been well defined. Equipment and procedures for injection of the grouts have been developed and are available for use in repository design and construction. The limits of the application of the selected materials and methodologies were defined for the Stripa granite.
- Data at the level of detail derived for the application and qualification of general groundwater flow models such as those examined in the natural barrier studies of the Stripa Project are unlikely to provide sufficient information for grouting activities intended for repository sealing. As at Stripa, the information gained from the grouting activities at repository sites will likely lead to revisions in understanding of the rock mass.
- An excavation disturbed zone (EDZ) consisting of a blast disturbed zone enveloped by a stress disturbed zone existed in the rock surrounding tunnels in the Stripa granite. In the absence of alternative, preferably repository site specific information, the EDZ of the blast disturbed zone in granitic rocks similar to those at Stripa can be taken to have an hydraulic conductivity of about 10^{-9} to 10^{-8} m/s. At the locations in the Stripa mine studied by the engineered barriers research group, the stress disturbed zone appeared to be more conductive parallel to the axis of the excavations ($3 \cdot 10^{-10} \leq k \leq 9 \cdot 10^{-10}$ m/s) than normal to it ($7.5 \cdot 10^{-12} \leq k \leq 2.3 \cdot 10^{-11}$ m/s).
- Under the low hydraulic gradients expected in groundwater in a sealed repository site, chemical transformation of the minerals in clay- and cement-based sealants can be predicted, reasonably, to extend over tens of thousands to millions of years. The predicted period depends on the porosity of the as-placed materials and the ionic concentrations in the groundwater.
- The sealing properties of both clay- and cement-based sealants are most susceptible to change under high hydraulic gradients. Thus, both materials will be most vulnerable to adverse change during seal construction and the period over which the repository is open for the deposition of waste.
- The engineered barriers studies for the Stripa Project have increased confidence in the ability to engineer geological repositories for heat-generating radioactive wastes.
- Due to the perturbations caused by the presence of excavations it may never be possible to examine physically in underground laboratories, or from excavations at repository sites, the conditions under which radionuclides will migrate within either the engineered barriers or the host rocks that form the waste isolation system.

A number of unresolved items have been identified. These could be considered for resolution in future collaborative studies or national programmes of research and development related to repository design and construction.

1 INTRODUCTION

The International Atomic Energy Agency is clear in its view that consensus exists among member nations that heat-generating radioactive wastes can be safely isolated from man's environment in underground repositories located deeply in geological formations (IAEA, 1985; 1989; 1990). Alternative disposal concepts, such as sea bed disposal and less mature technologies such as transmutation and disposal in space, have steadily lost favour. The results of national and international programmes have built confidence in abilities to engineer the waste repositories in geological formations as different as clay beds, salt domes, welded tuff and basement rocks such as granite. To-date, the confidence has not been fully translated into working, acceptable repository designs.

To form the excavations for repositories, engineers will be faced by the many difficulties that are encountered in the modern day mining and civil engineering industries and for which there exist a variety of solutions. During site appraisal and selection, to minimize the possibility for radionuclide releases from the repository, regions of high groundwater flow rates will be identified and subsequently avoided. Thus, threats of excavations flooding and associated difficulties with ground stability should be negligible. Moreover, it can be expected that repositories will be built in thick, possibly massive geological structures. While underground work can never be regarded as trivial , it is reasonable to suppose that, with appropriate measures taken for workers safety, the creation of the repository openings in these massive formations will present less hazardous conditions than those encountered during the exploitation mining of thinner mineral seams. In these and other respects, the ground conditions to be encountered during repository construction can be expected to be less difficult and working conditions will be safer than those normally expected in contemporary mining and civil engineering practice.

To limit burdens on future generations and in view of the requirement to isolate heat generating radioactive wastes for many millennia, repositories are generally being designed as passive structures, which, once closed, will not require maintenance. The long design life of repositories will make them, once built, without precedent. In this regard much evidence is being collected to permit reasonable predictions of satisfactory repository performance which can be defined (OECD/NEA, 1988) as the lack of unacceptable radiological risks from possible releases of radionuclides from a repository. It is generally accepted that absolute safety, although possible, cannot be assured. Repository performance criteria limit the radiological risks to present and future generations of humans to very low levels that are comparable with relevant national and international safety requirements such as those recommended by the International Commission on Radiological Protection (ICRP, 1977, 1985, 1991). Ultimately all research and development associated with the geological disposal of heat-generating radioactive wastes and repository construction is focussed to provide evidence that reasonably assures that the safety criteria are met.

Figure 1-1 shows a general approach to repository design and how investigations in underground laboratories, such as those in the Stripa mine, contribute to the design process. For major geotechnical projects, once scheme designs have been effected, technical issues have been identified and social factors considered, access to the selected site can be made available, data on the

geotechnical conditions can be gained and detailed designs can be effected. Regulatory agencies in all of the member states of the NEA/OECD are yet to grant sufficient access for detailed investigations of possible repository sites, Underground laboratories are being used to obtain information to assist in design development. In this context, it is accepted that, as shown in Figure 1-1, the design of underground facilities and structures is an iterative process. Features and phenomena, that are revealed as excavations proceed and underground facilities are used, provide increasingly detailed information for inclusion in design. This iterative approach is so important to geotechnical works that it has been formalized by the term "the observational method" (Peck, 1969). The method recognizes the needs to identify the most likely geotechnical conditions that will be encountered at a site and to project possible extreme conditions. Engineering solutions for difficulties arising from both expected and extreme conditions need to be proferred prior to applying the design. Work in underground laboratories, such as the Stripa mine, allows for recognition of some of the conditions that may be encountered in repositories and for engineered solutions to be tailored. Geotechnical conditions encountered and engineering solutions offered at underground laboratories at different sites allow for the preliminary application of the observational method to repository design. In this regard, and in view of the high costs of *in situ* research and development work, the need for international collaboration is evident. Moreover, the final designs for repositories will need to be refined as conditions encountered at the sites selected in each country become increasingly clear.

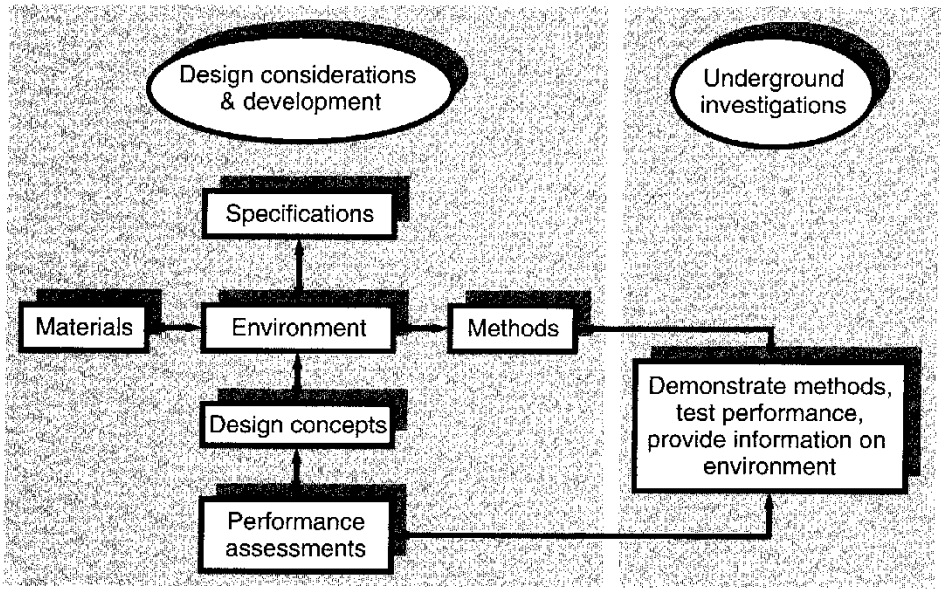

Figure 1-1 The role of underground investigations in repository design and performance assessment.

Studies into the natural barriers at a selected site, such as those carried out for the Stripa Project and described in Volume II of this report, are intended to provide much of the information on the geological environment needed for the preliminary design and assessment of the performance of a repository. Work in underground laboratories extends beyond this limited objective. For the Stripa Project, methods for investigating the rock mass were developed and

different approaches to the numerical modelling of hydrogeological conditions were appraised. Similarly, the research undertaken into the engineered barriers for the Stripa Project extended beyond *in situ* investigations. Laboratory- and theoretically-based investigations were needed to plan and interpret the results of the large scale *in situ* tests. Moreover, even though some *in situ* experiments lasted as long as five years, to project the performance of the engineered materials over millennia and, thereby, meet the needs of performance assessments, the development and application of methods for evaluating the longevity of selected sealing materials were undertaken.

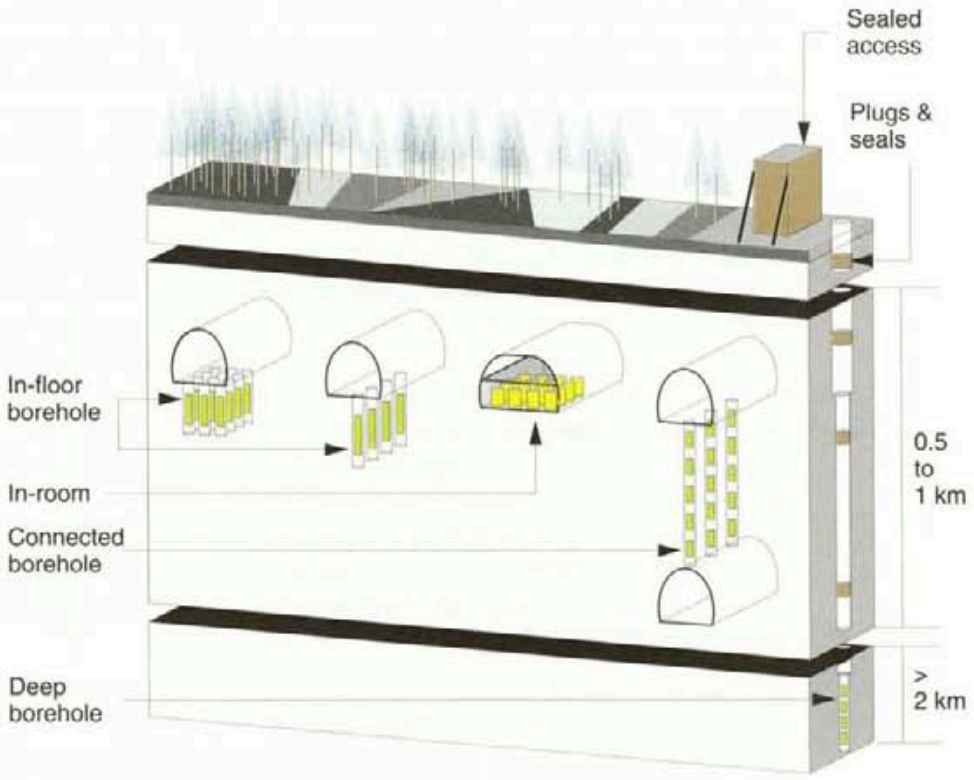

Figure 1-2 Waste container deposition options being considered for repositories in granite by member countries of the Stripa Project.

Countries that were members of the Stripa Project are evaluating concepts for repositories in a wide range of geological formations. In most cases, concepts are being developed for disposal of the waste beneath the water table. However, some studies include evaluation of unsaturated media above the water table. Furthermore, those countries for which granite rock formations are the prime prospect for a repository site are considering a variety of options for depositing the waste containers in the rock. Some of the possibilities are shown in Figure 1-2. Variations arise from differences in the physical and chemical characteristics of the waste form, different concepts for the structure of the waste containers, and, arising from these differences, various appreciations of the response of the rock to excavation and heating and the need to physically and chemically condition and buffer the environment in which the waste-containers will be entombed.

Each of the geological formations and the waste deposition methods present technical problems that are unique to the concept being considered. Inevitably these individual problems need to be resolved within the independent national programmes. However, there are common concerns which can form the foci for international cooperative studies. It was recognized before the Stripa Project (OECD/NEA, 1980) that all repository sites will be penetrated by investigation boreholes. Moreover, shafts, tunnels and adits will be excavated to provide access to the disposal levels. It is generally considered that structures will be required within these openings to control water flows and associated radionuclide movement in the repository. Suggested control strategies include the installation of lowly permeable plugs and seals in saturated rocks, and the construction of diversion dams and weirs in unsaturated media. Although not a significant concern to operational safety, the openings will be enveloped by a zone of rock that is disturbed by the excavation. Disturbances will arise from changes in the natural stress fields in the rock caused by the creation of the openings. Processes such as blasting used to create the openings may create another level of disturbance and change the properties of the rock near the openings. The possible effects of these excavation disturbances on water and, more importantly, radionuclide movement in the rock were seen to be suitable subjects for investigation in the Stripa mine. At the disposal levels the temperature will increase as the heat produced during the decay of radioactive elements in the waste dissipates through the rock. Temperature changes could result in hydro-mechanical effects that may alter the radionuclide transport properties of the rock. The countries that were members of the Stripa Project agreed, to more or less extent, that all of the above subjects were of interest and combined to support the studies. Aspects of each of the subjects were studied through the progress of the thirteen years long investigations. In addition to the resolution of specific technical issues and access to developing technologies, member countries were able to expose concepts being developed nationally to an international group of experts from whom they could receive the benefits of critical comment and peer review.

In common with many large civil engineering design and development projects, experts from a wide range of scientific and technical disciplines were drawn together to carry out the work within the framework of the Stripa Project. In view of the wide range of investigations the studies were broadly divided under the headings of studies into natural barriers and studies into engineered barriers. It is emphasised here that from the overall objective of effective repository design the division is considered to be artificial and was required merely to provide effective management of the programmes. In this context it is noted that as the studies progressed, investigators in each of the divisions found significant reasons to study the excavation disturbed zones.

The investigators involved with the studies into engineered barriers worked under the broad objective of demonstrating and qualifying the use of different materials and techniques for sealing water flow paths in the Stripa granite, the mine excavations and the excavation disturbed zones. The engineered barriers studies were carried out through the full period over which the agreements that formed the Stripa Project were in effect. The project was divided into the following three phases: Phase 1 (1980 to 1985), Phase 2 (1983 to 1988), and Phase 3 (1986 to 1992). The division of the programme into phases and the overlap in the timing of each of the phases allowed for developments achieved during the project and concerns arising from independent national programmes to be incorporated in the investigations. As may be anticipated from the appli-

cation of the observational method, the programme evolved with the findings being made at Stripa and other sites.

Table 1-1 Major issues examined by the engineeered barrier studies in each of the phases of the Stripa Project.

	Issues addressed			
Stripa phase	Engineering feasibility.	Laboratory studies of material properties and behaviour.	Numerical modelling of system performance.	*In situ* observations for design development.
Phase 1 (1980 to 1985)	• Deposition borehole drilling. • Waste and buffer placement. • Backfill placement.	• Buffer swelling. • Buffer hydraulic and thermal conductivity • Buffer and backfill longevity.	• Heat and water transfer in clay buffer and backfills. • Mechanical response of buffer and backfill.	• Buffer/backfill rock interactions. • Parameters to qualify performance models and knowledge of buffer & backfill behaviour.
Phase 2 (1983 to 1988)	• Remote sealing of investigation boreholes. • Construction of seals in tunnels and shafts.		• Water uptake by swelling clays in isothermal conditions. • Extrusion of swelling clays into fractures.	• Water uptake by clay seals. • Mechanical and hydraulic interactions between clay seals, rock and concrete plugs.
Phase 3 (1986 to 1992)	• Grouting fractured rock including fracture zones, discrete fractures and excavation disturbed rock.	• Rheological properties of clay and cement grouts. • Sealing properties of clay and cement grouts. • Longevity of clay and cement-based sealants.	• Porous media models of water flow in rock/seal systems. • Grout penetration in fractures. * Displacements in the rock mass caused by engineering activities. • Longevity of cement-based sealants.	• Limits of sealing achievable by grouting. • Morphology of injected grout materials. • Effects of heat on grouted rock.

During Phase 1, the engineered investigations focussed on the heat affected zone of the repository. Specifically, the response of clay buffers and the interactions between waste containers, clay buffer materials and the rock were studied. The Phase 2 investigations examined the feasibility of sealing boreholes, shaft and tunnels with clay sealants. In Phase 3, studies of the ability to grout and seal fractured granite including the excavation disturbed zone were effected and specific studies into the longevity of cement- and clay-based sealing materials were undertaken. Within this broad framework, a raff of detailed issues was considered. Significant progress was made in the major subjects and by the methods identified in Table 1-1. It can be seen from the table that the studies

focussed on both clay- and cement-based sealants and on the hydraulic properties of these engineered materials and the sealing structures which the materials were used to form. These limitations reflect the normal constraints applied to major projects. Clay- and cement-based materials were chosen for study through collective examination and harmonization of priorities within the member countries. The decision to study cement-based as well as clay-based materials during Phase 3 of the project and include investigations into the longevity of sealants shows a shift in the foci of the investigations between Phases 2 and 3. This provides an example of the evolving nature of the programme and is a reflection of the changing interests of the member countries.

This report presents an overview of the engineered barrier studies from1980 to 1992. The results of the technical programme are summarized and reviewed. Wherever considered relevant, results from the work undertaken during the Swedish-American-Cooperative activities, that preceded the OECD/NEA programme in the Stripa mine, and data from the natural barrier studies are referenced. The three phases of the Stripa Project are reviewed in sequence in Chapters 2, 3 and 4. In view of the importance of the subject, Chapter 5 is devoted to the studies into the longevity of clay- and cement-based sealants and seals.

2 PHASE 1 - 1980 TO 1985 BUFFER MASS TEST (BMT)

2.1 BACKGROUND AND SCOPE

Details of the Buffer Mass Test (BMT) are to be found in a series of internal reports of the Stripa Project. It is not the purpose here to re-present this information but to offer a critique of the experiment such that the significance of the work and its findings can be used in future developments for safety assessments related to long-lived radioactive waste disposal schemes. Brief descriptions of the perceived scope of the experiment and its objectives are presented prior to providing the analysis.

The BMT was a half-scale mock-up of a waste emplacement concept then proposed by KBS of Sweden and shown schematically in Figure 2-1. Interest in the test came from the participating international community for a number of technical and pragmatic reasons.

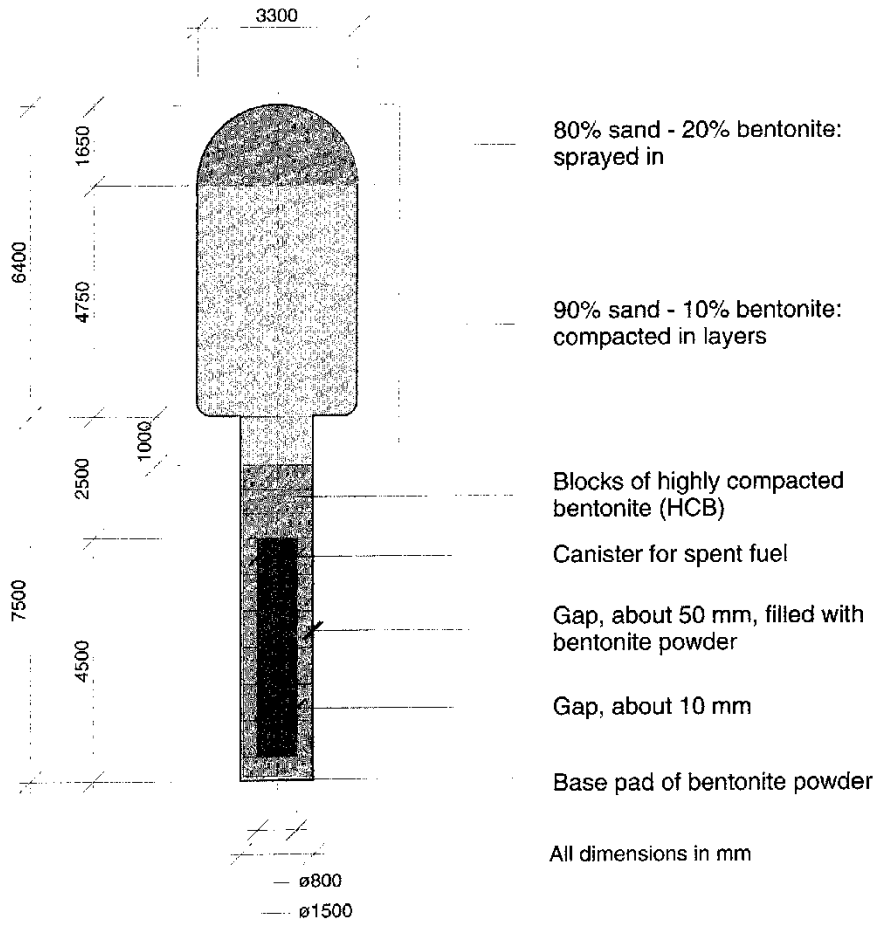

Figure 2-1 The KBS-3 fuel-waste disposal concept.

Technically, the "test" allowed for a demonstration of some of the methodologies available for the placement of waste containers in boreholes in the floors of emplacement rooms and the closure of the rooms. These methodologies included the following: the excavation of the large diameter boreholes needed for waste emplacement; the preparation of bentonite-based buffer materials and the encapsulation of the waste package; and the backfilling and sealing of rooms. The test was to be carried out in the "ventilation drift" developed and characterized by Lawrence Berkeley Laboratories, USA through previous Swedish-American cooperation at the 340 m level in the mine. The location and schematic layout of the test are shown in Figures 2-2 and 2-3.

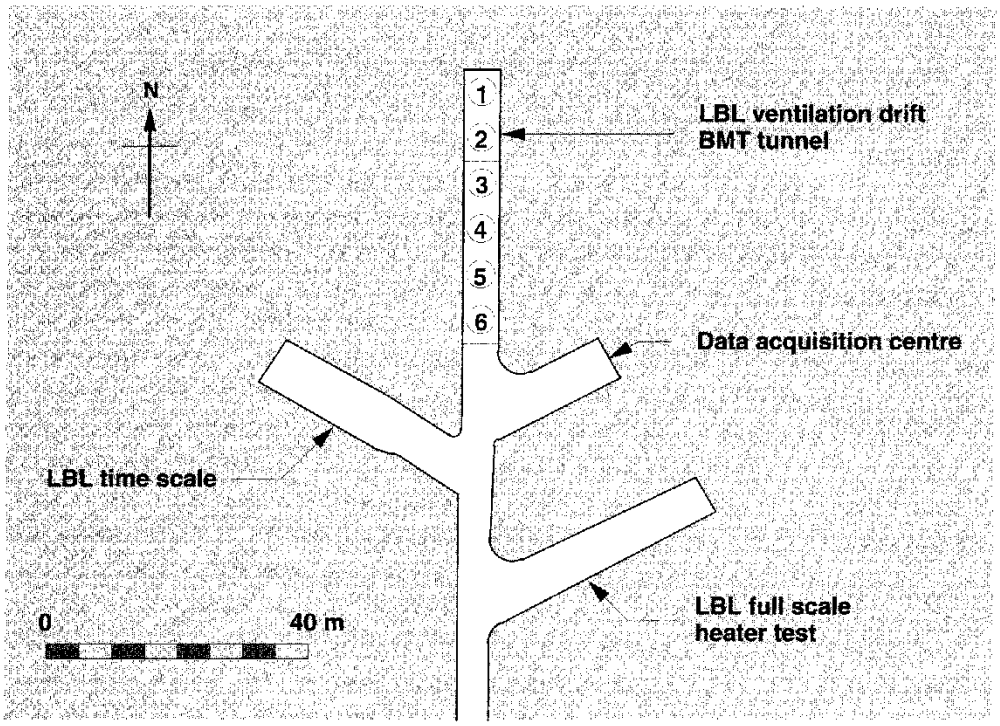

Figure 2-2 The location of the BMT at the 340 m level in the mine.

The BMT was to be the first ever *in situ* experiment in a granitic rock body through which a large volume of rock and repository sealing material were to be heated and the combined response of and interactions between the rock mass and sealants were to be observed. Spatial and temporal variations in temperature, water pressure, total pressure and water content in the sealing materials and at the seal-rock boundary were to be measured. Temperatures and water pressures in near-field rock mass were also to be monitored. These observations were to be compared with the predictions of the expected hygro-thermo-mechanical performance of the heater/seal/rock system. It was implicit at the outset that significant uncertainties existed in the performance models and it was expected that the observations would result in improved understanding of the system. This improved understanding would be translated into improved conceptual and numerical models of performance.

The KBS-3 concept for spent fuel disposal consists of a massive copper container for the used fuel enveloped by a highly compacted clay-based barrier material which separates the container from the host rock. Commonly referred to as buffer material, the clay barrier is intended to control and stop the groundwa-

ter flow in the vicinity of the container. Long after the repository is closed and finally sealed, when the integrity of the container is breached and radionuclides are released from the container, the buffer is intended to retard the rate of release to the rock. In the KBS concept highly compacted bentonite[1] clay (HCB) is proposed for use as buffer. Similar materials have been proposed as buffer materials in repository concepts being developed in co-operating countries (Pusch and Gray, 1989). The Buffer Mass Test (BMT), as its name suggests, was particularly focussed on enhancing knowledge of the engineering and performance characteristics of these buffer materials in a repository setting.

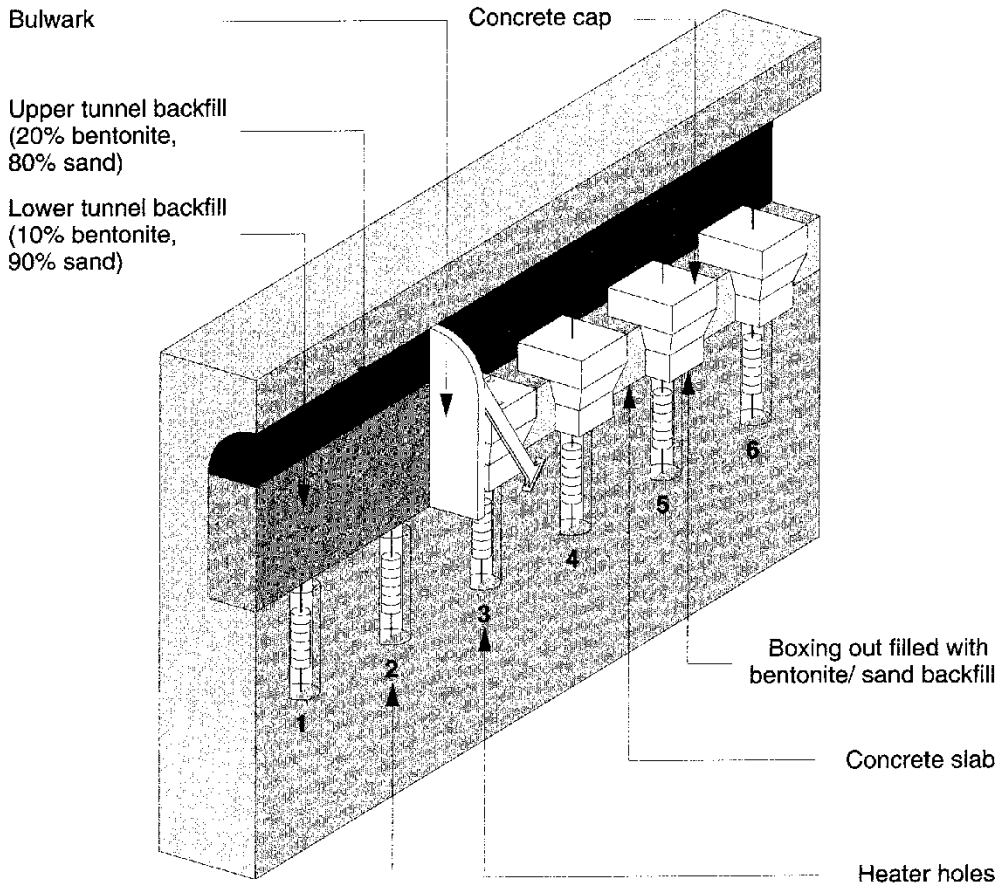

Figure 2-3 The general Buffer Mass Test arrangement.

Concurrent with the conduct of the BMT, NAGRA of Switzerland were developing the "in-room" waste emplacement concept shown in Figure 2-4 (NAGRA,1985). Here the buffer barrier (or overpack) envelopes a thick-walled ferrous waste-container to completely fill the excavated chamber. For the "borehole emplacement", KBS-3 concept, and similar concepts being considered in other participating countries, bentonite-based materials had been offered as suitable for filling and sealing the room above the sealed emplace-

1 Bentonite - a clay material comprising principally clay minerals belonging to the smectite group. These minerals are highly hydrophilic and will sorb water and, if unconfined, will swell (see Section 2.3.4).

ment boreholes. Engineering and performance issues related to such possible backfilling materials were to be investigated as part of the BMT.

2.2 PERFORMANCE ISSUES

The BMT was conducted to provide data that could lead to informed opinion on the practicality of use and expected performance of bentonite-based buffer and backfill materials. These engineered barriers are part of repository design concepts that accept the need to include natural and engineered components to assure the safety of a repository in granite. This need, which is internationally recognized (IAEA, 1985; 1989,1990), partly arises from uncertainties regarding the performance of each of the system components which are necessarily reflected in the results of total system performance analyses. Decreasing the uncertainty in performance of each of the barriers should lead to increased confidence in total system performance analyses.

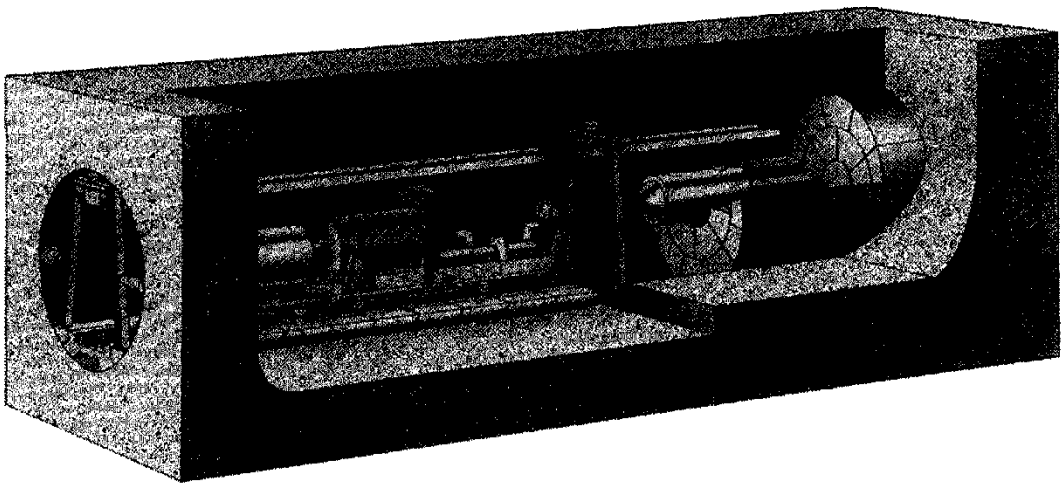

Figure 2-4 The "in-room" emplacement procedure proposed by NAGRA in Project Gewähr. The space between the container and the rock is filled with HCB.

For the KBS-3, and similar fuel-waste disposal concepts, buffer materials are quired to limit the rate of release of radionuclides into the natural barrier. The waste will be deposited deep in the rock mass. After closure the rock and the repository system will eventually become water saturated. For total system performance analyses it is generally assumed that radionuclides will be released through the mechanisms of waste dissolution and transport in the groundwater. The purpose of the buffer is to minimize the rate of water flow in the vicinity of the waste container and, thereby, minimize advective and convective radionuclide flux. Conventional wisdom (Mitchell, 1991) suggests that, for porous media with hydraulic conductivities lower than 10^{-9} m/s, advective (darcian) and convective fluxes of contaminants tend to become relatively insignificant compared to those arising from chemical (fickian) diffusion in the pore fluids. Consistent with the results of classical soil mechanics (Lambe and Whitman, 1969), Pusch (1980b) showed through laboratory tests that water saturated, highly compacted bentonite (HCB) could be expected to have an hydraulic conductivity of less than 10^{-11} m/s. This result, which subsequently has been con-

firmed by a number of workers (Cheung et al, 1987), tended to suggest that HCB would be a suitable buffer material. For an intact buffer barrier, fickian diffusion parameters are the prime input required for performance assessment models.

For the KBS-3 concept and all others that propose the use of HCB or similar buffer material, the compacted clay will be placed with a degree of saturation (S) of less than 100 per cent. Working clearances, construction joints and other discontinuities in the buffer could leave pathways for water flow in the vicinity of the container. Although laboratory tests and general experience with bentonite led to the opinion that, through water uptake, an HCB buffer could be expected to expand and seal the possible water pathways, observations on these phenomena were required at large scale. Furthermore, the extent to which, and the rate at which, this beneficial swelling process could be expected to proceed would depend on the availability of water at the buffer/rock boundary and the complicating effects of the heat flow from the container. The latter would tend to drive water away from the container. It remained to be demonstrated that cracks generated in the buffer due to drying shrinkage, if any, would be sealed by buffer swelling on wetting.

Available models that described the coupled hygro-thermo-mechanical processes in the buffer needed to be qualified through the improved understanding of buffer behaviour gained through observations of *in situ* performance. Realistic boundary conditions for input to these models were needed. The effective hydraulic boundary conditions were likely to depend on the structural geology of the site which would influence the hydraulic characteristics of the rock and the natural stress field in the rock mass. Furthermore, the geometry of the excavations and the excavation technology (drilling, blasting, boring) used to develop the cavities would influence both the stress field in the rock and the hydraulic characteristics of the rock in contact with the buffer. These characteristics could be expected to change due to contact with the buffer and due to temperature variations.

Redistribution of moisture within the buffer mass was known to change the thermal conductivity and specific heat capacity of the material (drier material has lower thermal conductivity and specific heat capacity than wetter material at the same dry density[2]). These factors would influence the temperature of the container and the temperature distribution in the buffer and rock mass. Temperatures and temperature distributions are required to be known with some confidence as corrosion mechanisms for container materials and performance parameters of the buffer, backfill and rock barriers were anticipated, from laboratory and desk studies, to depend functionally on temperature. With specific regard to bentonite buffer material, it was generally accepted that, to ensure a measure of predictable material performance, maximum temperatures (at the container/buffer interface) should be kept below approximately 95°C. This limit arose from an understanding of the fundamental thermodynamic properties of smectite (specifically montmorillonite[3]) clay - see Chapter 5 - and doubts on the

---

2 Dry density - the ratio of the mass of solids (dried at 105°C) to the total volume (solids + voids) of the system.

3 Montmorillonite - a clay mineral belonging to the smectite group (see Section 2.3.1).

predictability of material behaviour at temperatures above 100°C [4].

Many of the issues related to HCB buffer performance were also important when considering the room backfill. Specifically, the rate of water uptake and redistribution under changing temperatures and temperature gradients as well as varying boundary conditions were of concern. Understanding of the effects of these changes on the mechanical response of the backfill and the backfill/rock interactions was required.

One of the purposes of the backfill in the borehole emplacement concept used by KBS-3 is to restrain the buffer, as, unrestrained, the buffer would swell out of the borehole. Apart from the obvious consequence of undesirable container movement, this swelling would cause the porosity of the buffer to increase and adversely alter the mass transport characteristics of the material (radionuclide and water transport rate parameters would increase). It was necessary to show that a backfill placed with existing technology could effectively restrain this expansion.

2.3 MODELS AND CONSTRAINTS

The Oxford English Dictionary defines "model" as "a simplified description of a system to assist calculations and predictions". Complex conceptual models, based on a fundamental understanding of material characteristics and behaviour, provide the base for the construction of more simplified mathematical and numerical models. Predictions can be numerically based or extended from the conceptual models through logical sequencing. All three modelling approaches were used to predict system performance in the BMT. This section briefly describes the models used for these predictions. Where appropriate, attempt is made to describe alternative models that were available, define the constraints on the application of these models and provide pertinent results from the underlying research that led to the application of particular models.

2.3.1 Material characteristics

Bentonite, as proposed for use in sealing repositories for long-lived radioactive waste and specifically for the preparation of the HCB to be tested in the BMT, is a processed clay product. Processing includes the excavation and air drying of bentonite clay, further drying of these clays in kilns and subsequent grinding into powders and granulates. Used in civil engineering for purposes such as diaphragm wall construction, drilling muds and liners for waste containment structures, the material also finds many other uses, such as in foundry sands, animal foods, wine clarification and as a water sorbent. Some of these uses require chemical treament of the material prior to application or during production. For the purposes of nuclear waste disposal and the BMT, to simplify analyses and understanding, it was proposed to use a material that had not been

---

4 The use of bentonite was suggested from conventional geotechnical enginering practice. Understanding of material performance is well established for normal, ambient temperatures. Little knowledge is available for predicting performance at elevated temperatures.

chemically treated. A product called MX-80, manufactured by American Colloid Company, USA, was selected for use. Similar materials are produced by a number of manufacturers in North America and Europe. MX-80 was selected for use in the BMT in recognition of the significant materials characterization and development work that had been carried out under the auspices of KBS of Sweden prior to the initiation of the BMT.

As delivered, MX-80 is granular in character. Pusch et al (1982) report that when subjected to dry sieve analysis, the material is virtually completely retained on US sieve No. 80 (> 180 μm). Dispersed and subjected to wet sieve analysis (ASTM Test No. C117-80) over 85% of the material is clay sized (< 2 μm). Between 80 and 90 % of the clay fraction exhibits the characteristics of the clay mineral montmorillonite. The remaining fraction is dominated by quartz and feldspars.

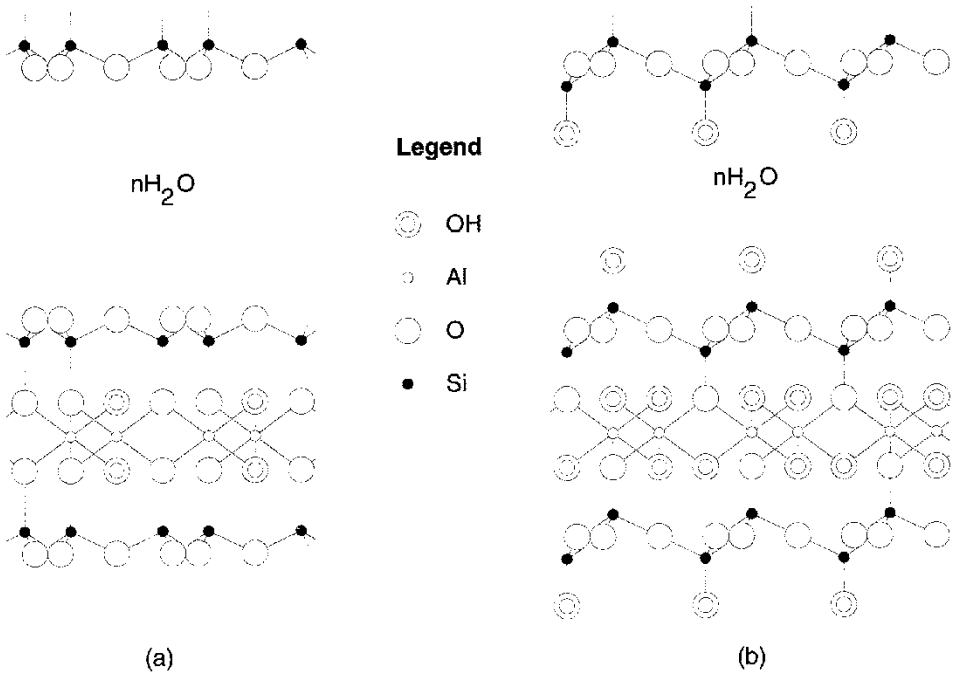

Figure 2-5 Crystal lattice models of montmorillonite: (a) the Endell/Hoffman/Wilm structure; and (b) the Edelman/Favejee structure.

Montmorillonite is one member of a class of clay minerals termed smectites. Clay minerals are a class of minerals characterized by a platey structure formed from sheets of silica and alumina. A generalized representation of the crystal structure of montmorillonite clay platelets is shown in Figure 2-5. With very small particle size, montmorillonite clays have very large specific surface areas (typically ~800 m^2/g). Combined with large negative charge deficiencies, caused by imperfections in the crystal lattices, the large specific surface area yields a high surface activity which accounts for many of the properties that render the material suitable for consideration as a buffer.

The electro-negative charge on the clay particles is offset by the attraction of positively charged exchangeable cations and the repulsion of anions. Na^+ is the predominant exchangeable cation on MX-80, which has a cation exchange capacity of approximately 80 meq/g. The material is colloidal in character and when dispersed in water will exchange the Na^+ for other cations in solution de-

pending on cation concentrations and their position in the lyotropic series. Thus, it is possible that the rate of migration of cationic radionuclide species through bentonite based sealing materials such as HCB could be retarded by sorption processes. Sufficiently dense, the clay may, through repulsive forces, exclude anionic radionuclide species and thereby severely limit their migration.

(a) (b)

Figure 2-6 (a) Isostatically compressed cylinders of HCB; (b) shaping HCB to suit the geometry of the experiment.

Water, being dipolar, is attracted to the clay mineral surfaces. Bentonite powders and granulates in normal use are exposed to the atmosphere, from which they sorb water. Pusch et al (1982) report that MX-80 used for the BMT had a hygroscopic water content [5] between 8 and 14 %. At an average hygroscopic water content of 11%, assuming a specific gravity for dry bentonite of 2.70 [6] (Pusch et al, 1982), the material can be theoretically compacted to a maximum dry density of 2.08 Mg/m^3. At this density, using the specific surface area of 800 m^2/g and a specific gravity of solids of 2.80 (see footnote 6) an average interparticle spacing of 6 Å can be calculated. In this context a monolayer of water can be attributed a thickness of 2.5 Å (Sposito, 1984). Depending on the predominant exchangeable cation, it is generally understood that montmorillonite will immobilize between 2 and 4 layers of water yielding dry densities of 1.68 and 0.56 Mg/m^3, respectively. HCB can be defined, theoretically, as bentonite in which no free water exists. A minimum buffer dry density of 1.88 Mg/m^3 was sought for the BMT [7] . This was achieved through cold "isostatic" compaction of air-dried bentonite powders which produced cylinders of HCB, 0.4 m in diameter and 2 m long. Blocks of predetermined

---

5 Water content (w) is the mass of water/mass of solids determined by drying the material at 105°C. Water content is normally expressed as a percentage.

6 Value typically measured for bentonite dried at 105°C. Calculated from the crystal structure the specific gravity of montmorillonite is approximately 2.80. The lower measured value is attributable to adsorbed water layers which are not removed by drying at 105°C.

7 Value calculated using specific gravity of solids = 2.8 and based on a saturated bulk density of 2.05. Bulk density is the total mass/unit volume and is the reporting measure used by Pusch et al.

shapes and sizes, configured to suit the geometry of the experiment, were sawn and shaped from the large cylinders. Some of the processes involved are shown in Figure 2-6.

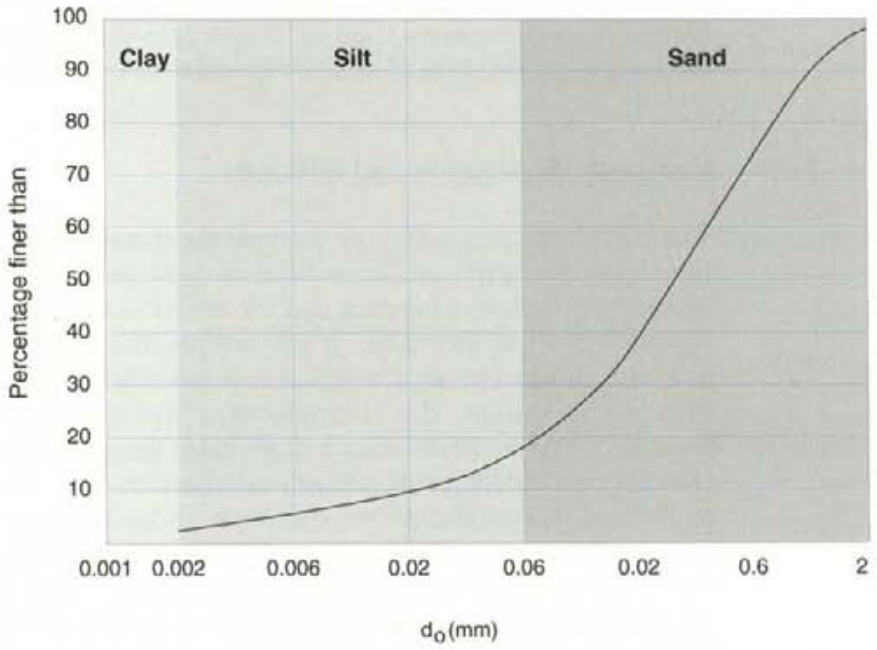

Figure 2-7 Particle size distribution of the sand-ballast material used in the backfills.

Consistent with the KBS-3 concept, which was developed through the progress of the BMT, compacted sand-bentonite mixtures were used to fill the portion of the boreholes unfilled by the heaters and HCB and to fill the room above heater holes 1 and 2 (see Figure 2-3). Two sand-bentonite mixtures were used. In both cases a sand ballast with the grain size distribution shown in Figure 2.7 was used. This material was mixed in 9:1 (sand:clay) dry mass proportions with MX-80 bentonite for the lower backfill and 4:1 dry mass proportions for the upper backfill. The lower backfill was placed in horizontal layers and compacted using a commercially available manually operated vibrating plate compactor[8]. Once headroom was reduced sufficiently to deny access to personnel and machinery (the top 2 m of the room) the upper material was placed using remote pneumatic stowing techniques. Laboratory compaction tests indicated that compacted dry densities as high as 1.92 and 1.82 Mg/m^3 may be achievable in the lower and upper backfill materials, respectively. These dry densities correspond to clay dry densities (ρ_c)[9] of 0.55 and 0.81 Mg/m^3, respectively. In practice in the BMT, mean dry densities of 1.75 and 1.19 Mg/m^3, corresponding to clay dry densities of 0.43 and 0.37 Mg/m^3, respectively, were obtained in the lower and upper backfill materials. These values are significant insofar as recent work (Cheung et al, 1987; Graham et al, 1989) suggests that clay dry density controls the mechanical and mass transport properties of compacted bentonite and bentonite-sand mixtures.

---

8 400 kg Dynapac LG 40.

9 In sand-clay mixtures clay dry density can be defined as the ratio of the dry mass of clay to the volume of clay plus voids. The sand fraction is ignored (Dixon et al, 1985). For the calculations here, the specific gravity of the sand was taken to be 2.65.

The clay dry density can be used as a design criterion for bentonite based seals. The backfill materials used in the BMT lie outside the range of density defining HCB ($\rho_c > 0.56$ to 1.68 Mg/m^3). Table 2-1 summarizes the density data along with the void ratios, porosities and degrees of saturation of the voids. These data indicate the range of conditions over which the properties of bentonite and bentonite-sand mixtures need to be understood and provide the initial parameters for input into performance models for the buffer and backfill sealants.

2.3.2 Radionuclide sorption and diffusion

The BMT was designed to investigate the transient processes of heat and water transfer in the buffer and the effects of these processes on hydro-mechanical interactions between the rock and the buffer in the early stages immediately following waste emplacement. It was not possible, given the short duration of the test, to examine factors that affect radionuclide transport in the near field, other than by implication. It is re-emphasized here that, from the perspective of total repository system performance modelling, the processes of radionuclide transport through buffer are of primary importance. The effects of the transient heat and moisture transport processes are only significant insofar as they affect the radionuclide transport properties of the near-field barrier materials and may effect delays to the onset of radionuclide release. Given their significance to radionuclide transport modelling the processes of sorption and diffusion in buffer and backfill materials are briefly discussed here.

Table 2-1 Density and porosity data for the buffer and backfills used in the BMT (immediately after placing).

Material	ρ_b *	Water * content (w)	ρ_d	ρ_c	Porosity (n)	Void ratio (e)	Degree of saturation (S)
	Mg/m^3	%	Mg/m^3	Mg/m^3	%		%
Buffer (HCB)	2.09 2.12	10 13	1.90 1.88	1.90 1.88	30 31	0.42 0.44	63 79
Lower backfill	1.92	10	1.75	0.43	35	0.54	50
Upper backfill	1.19	15.5	1.19	0.37	55	1.24	34

* Values provided by Pusch et al (1982) and Pusch et al(1985c). All other values were computed using specific gravities of 2.70 for bentonite and 2.65 for sand.

For the purposes of "post-closure" near-field performance assessment models it is generally assumed that the buffer/container system is fully water saturated - otherwise dissolution of the waste form cannot occur - and that the radionuclide transport properties of the buffer material can be represented by those measured in the laboratory. With the very low hydraulic conductivity of the buffer, radionuclide flux across the buffer barrier is assumed to occur

through chemical diffusion processes under a driving radionuclide concentration gradient: higher concentrations of radionuclides in the water in contact with the waste form drives the contaminants to the groundwater in the rock in contact with the outer buffer boundary or to the backfill. Hydraulic conditions in the rock and the backfill materials will determine the concentration of radionuclides in the water at the outer buffer boundary, which, in turn, will influence the radionuclide flux. In the absence of precise information, the worst case of "swept away" boundary conditions is often assumed in the rock mass providing an upper bound on radionuclide flux. Observations on a number of these assumptions can be made from the BMT. Specifically, the rock conditions around a borehole could be observed, an estimate of the time for saturation of the buffer could be made and the degree of homogeneity of the buffer after saturation, assuming this was achieved, could be appraised.

The chemical diffusion processes are described using Fick's first and second laws: these can be represented mathematically using Equations 2.1 and 2.2, respectively.

$$Q/A = J = - \frac{D_e}{f} \nabla c \qquad (2.1), \text{ and}$$

$$\frac{\partial c_p}{\partial t} = D_a \nabla^2 c_p \qquad (2.2),$$

where Q (M/T) is the rate of flow and J is the flux of the diffusing species, A (L^2) is the cross sectional area of the element through which flow occurs, t (T) is time, c (M/L^3) is the concentration of species , c_p (M/L^3) is the concentration of species in the pore fluid of the clay, ∇^2 (L^{-2}) is the spatial laplacian operator, f (dimensionless) is the formation factor, and D_e (L^2/T) and D_a (L^2/T) are the effective and apparent diffusion coefficients (diffusivities), respectively. The correct evaluation of f, D_a and D_e are essential to the succesful application of the theory and continue to be the subject of international research.

The formation factor, f, allows the diffusivity in pure water (D) to be related to the apparent diffusivity through Equation 2.3.

$$D_a = f D \qquad (2.3)$$

D_e and D_a can be related by the equation:

$$D_e = D_a n_e \qquad (2.4),$$

where n_e (dimensionless) is termed the effective porosity. For both loose and highly compacted bentonite, f and n_e can only be derived from laboratory diffusion experiments. Both require a knowledge of the fraction of the absolute porosity that is available for species to diffuse. The effective porosity, n_e, also includes an allowance for the sorption of species on the clay solid.

The electro-chemical and colloidal characteristics of smectite minerals are sufficient reason to suppose that the effective porosities for anionic species will tend to be less than those for cationic species. Increasingly available experimental evidence tends to confirm this suggestion. For example, Oscarson et al (1991) have shown that n_e for $^{129}I^-$ may be as little as 5% of n in compacted bentonite. In the absence of sufficient information for the total system perfor-

mance models, n is still being used to evaluate diffusive radionuclide flux (Brandberg and Skagius, 1991). This methodology is probably conservative for anionic radionuclide species, leading to an overevaluation of flux. The use of n will lead to less than realistic values for fluxes of cationic and other sorbing species.

For the diffusive flux calculations, the BMT provided direct evidence of the practically achievable densities of different bentonite-based sealants and allowed laboratory-based research to be realistically focussed.

2.3.3 Heat and water transfer

Mitchell (1976) and Yong and Warkentin (1975) describe the nested processes that cause direct and coupled heat, water, electrical and chemical transfer in porous media such as clays. Table 2-2 shows the inter-relationships between flux and gradient. Mitchell (1991) provides a detailed review of the current state of the art of application of these relationships in conventional geotechnical engineering practice. Aspects relevant to radioactive waste disposal, and to buffer and backfill materials and the BMT in particular, are briefly presented here.

It may be suggested from Table 2-2 that radionuclide flux through clays can occur not only through direct chemical diffusion in accordance with Fick's law but also be coupled with flows of heat, water and electrical energy. Generally, the total flux of a contaminant, J_C, is given by the sum of all fluxes from different forces as shown in Equation 2.5

$$J_C = L_{CC}\nabla(-C) + L_{CE}\nabla(-E) + L_{CH}\nabla(-H) + L_{CT}\nabla(-T) \qquad (2.5)$$

where L is the transfer coefficient under gradients of temperature (T), electrical potential (E), hydraulic head (H) and chemical concentration (C). The two subscripts on L denote first the flow type and second the driving gradient. The element $L_{CC}\nabla(-C)$ represents fickian diffusion.

Equations similar to 2.5 can be written for heat, water and electrical fluxes. For example, the equation for water flux would be:

$$J_W = L_{HH}\nabla(-H) + L_{HC}\nabla(-C) + L_{HE}\nabla(-E) + L_{HT}\nabla(-T) \qquad (2.6)$$

with the element $L_{HH}\nabla(-H)$ representing darcian flux.

From the perspective of total repository system performance modelling it is clear that the validity of the assumption that radionuclides are transferred through the water saturated buffer and backfill materials almost exclusively by fickian diffusion depends on all other terms in the flux equation tending towards zero. For this to be the case either the phenomenological coefficient or the gradient must tend to zero. Although buffer temperatures may be elevated, temperature gradients will be small at the time of radionuclide release: the Soret effect is ignored for this reason. Similarly, no significant electrical potential gradients can be reasonably envisaged in or around the repository. For water saturated clays, Shackelford (1988) has shown that streaming current effects - Table 2-2 - (advective transport) are virtually insignificant for materials with hydraulic conductivities less than 10^{-9} m/s. Moreover, hydraulic gradients of

less than 0.01 are likely in a sealed, fully saturated waste repository in granite (Chan, 1987).

Results reported by Pusch et al (1982) and, subsequently, by other workers (e.g. Cheung et al, 1987) show that the hydraulic conductivity, k (L_{HH}), of compacted bentonite decreases with increasing density (Fig 2.9). Saturated at ρ_d = 1.9 Mg/m^3, the density of emplacement of the HCB in the BMT, ρ_m = 2.20 Mg/m^3 (t/m^3), giving, from Figure 2.9, k < 10^{-13} m/s. At the emplaced densities of ρ_c = 0.43 and 0.37 Mg/m^3 , the upper and lower backfills used in the BMT had k values of between 10^{-9} m/s and 10^{-11} m/s. Hence, at the densities achieved in the buffer and backfill materials used in the BMT, fickian diffusion would be the overriding mechanism of radionuclide transport in water-saturated, bentonite-based near-field seals.

Table 2-2 Direct and coupled flows.

Flux, J	Gradient			
	Hydraulic head	Temperature	Electrical	Chemical concentration
Fluid	**Hydraulic conduction (DARCY's LAW)**	Thermo-osmosis	Electro-osmosis	Chemical osmosis
Heat	Isothermal heat transfer	**Thermal conduction (FOURIER's LAW)**	Peltier effect	Dufour effect
Current	Streaming current	Thermo-electricity: Seebeck effect	**Electric conduction (OHM's LAW)**	Diffusion & membrane potentials
Ion	Streaming current	Thermal diffusion: Soret effect	Electro-phoresis	**Diffusion (FICK's LAW)**

The BMT would principally investigate the processes of heat and moisture transfer in the HCB and backfill materials. In the notation adopted here, Equations 2.7 and 2.8, which ignore electrical and chemical gradients, would describe heat and water transfer:

$$J_W = L_{HH}\nabla(-H) + L_{HT}\nabla(-T) \qquad (2.7)$$

$$J_T = L_{TT}\nabla(-T) + L_{TH}\nabla(-H) \qquad (2.8).$$

For the present discussion the effects of the complicating coupling terms for flux from chemical concentration gradients, $L_{TC}\nabla(-C)$ and $L_{HC}\nabla(-C)$, are ignored. Their significance is discussed further in section 2.2.3.

Although still uncertain at low hydraulic gradients in compacted bentonite (Yong and Warkentin, 1975; Dixon et al, 1992), L_{HH}, the hydraulic conductivity is assumed to possess a singular value for water-saturated soils and in this case the HCB and backfill materials. It was shown by Gray (1969) for saturated clays that L_{HT} tends to zero and $L_{HT}\nabla(-T)$ can be ignored. Similarly, the isothermal heat transfer ($L_{TH}\nabla(-H)$) is insignificant in saturated clays and the heat transfer can be reasonably assumed to occur in ac-cordance with Fourier's law ($L_{TT}\nabla(-T)$ with L_{TT} being the thermal conductivity, more commonly defined by the symbol λ). In saturated clays λ can be reasonably ascribed a singular value that is readily measured in the laboratory. For the water-saturated materials used in the BMT, Börgesson (1982) suggests values for λ of 1.4 W/m.°K for bentonite, irrespective of ρ_d, and 2.4 W/m.°K for the sand-bentonite mixtures, irrespective of sand content. These values are consistent with those measured on alternative bentonites and bentonite-sand mixtures (Radhakrishna,1984; Radhakrishna et al, 1989) and can be used in the analyses of temperature fields in and around a long-lived radioactive waste repository in the long term after sealing and complete saturation.

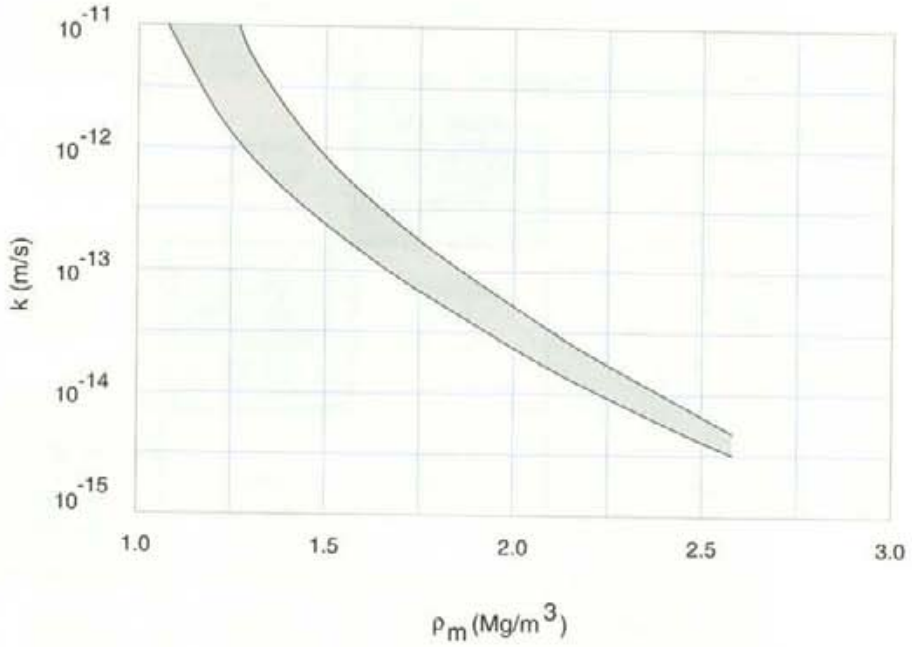

Figure 2-8 The influence of density [10] on the hydraulic conductivity of compacted MX -80 bentonite.

In unsaturated media, such as the HCB and the backfills used in the BMT, both heat and water are transferred by water in both liquid and vapour phases. Heat is also conducted through the solid phase of the material. In conventional geotechnical engineering practice the processes have been studied to provide insights on problems such as the effects of heat conduction on the stability of buried cables and other heat sources. The most commonly used solution, proposed by Philip and DeVries (1957), provides the general differential Equa-

10 ρ_m is the saturated bulk density of the material and is related to ρ_d by the expression $\rho_m = (1+w)\rho_d$. For saturated MX-80 bentonite $\rho_m = \rho_w$ ((1+w)/(0.37+w)), where ρ_w is the density of water.

tions 2.9 and 2.10, in which, through similarity with Equation 2.2 for fickian, chemical, diffusion, the transfer coefficients are termed "diffusivities":

$$\frac{\partial \Theta}{\partial t} = \nabla\bullet(D_{\Theta T}\nabla T) + \nabla\bullet(D_{\Theta\Theta}\nabla\Theta) + \frac{\partial K_\Theta}{\partial z} \qquad (2.9)$$

$$C\frac{\partial T}{\partial t} = \nabla\bullet(D_{TT}\nabla T) + \nabla\bullet(D_{T\Theta}\nabla\Theta) \qquad (2.10).$$

The terms t and T have their previously defined meanings, K_Θ is the unsaturated hydraulic conductivity, z is elevation from a datum and the term $\partial K_\Theta/\partial z$ describes the gravitational movement of water. Θ is the volumetric water content of the porous medium ($\Theta = n\bullet S$) and is used in place of hydraulic head, H, as the driving force on the supposition that in unsaturated media Θ is a more easily measured and understandable parameter than H. The material parameters K_Θ , $D_{\Theta\Theta}$, $D_{\Theta T}$, D_{TT} and $D_{T\Theta}$ all, to lesser or greater extents, functionally depend on Θ and T and are generally found to exhibit hysteresis.

The thermal moisture diffusivity, $D_{\Theta T}$, and the isothermal moisture diffusivity, $D_{\Theta\Theta}$, are each the sum of parts allowing for water transfer in the vapour and liquid phases. That is, $D_{\Theta\Theta} = (D_{\Theta vap\Theta} + D_{\Theta liq\Theta})$ and $D_{\Theta T}=(D_{\Theta vapT} + D_{\Theta liqT})$, where the subscripts liq and vap denote liquid and vapour, respectively. Thus, theoretically, the prediction of moisture movement under coupled heat and moisture gradients can be accomplished through knowledge of the individual vapour and liquid diffusivities or through use of lumped parameters.

General experience in the application of the Philip and DeVries equations has shown that, provided moisture content distribution is known and the thermal conductivity, λ, and the specific heat capacity, C, of the material(s) are known as a functions of Θ, then Equation 2.10, reduced to the form shown in 2.11, reasonably predicts temporal and spatial temperature distributions:

$$\frac{\partial T}{\partial t} = \nabla\bullet\left\{\frac{\lambda}{C}\nabla T\right\} \qquad (2.11).$$

The use of the equations - the theoretical model - is complicated by the fact that heat and moisture movement in clays is accompanied by volume changes and distortions associated with stress variations. These changes influence the porosity and pore size distribution of the clay. These complications have combined with others to limit the precision to which the model predicts performance. Mitchell (1991) notes that while both transient and steady state temperatures can be reasonably well predicted, an ability to accurately predict moisture movements and distributions (and, consequently, the effects of these changes on the mechanical properties of the materials) remains outside current capabilities.

Work is in progress (Thomas, 1992; Gens and Alonso, 1992) to further define the precision and bounds of application of the models. Some of these studies are particularly focussed on refining an ability to predict the performance of repositories proposed for construction in natural clay strata (such as the proposed repository at Mol in Belgium) or in unsaturated (vadose) zones in hard rocks (such as that being investigated at Yucca Mountain in the USA). The results of the BMT add insight into some of the processes likely to

be operating in repositories constructed in these 'non-granite' media by providing information on the hygro-thermal properties of dense porous media. However, the results of the BMT provide specific insights into the relative significance of thermo-osmosis, hydraulic conduction, vapour transfer, liquid transfer and the coupled effects of these process on heat flow related to the performance of HCB and backfill materials for repository concepts which include such seals in heat affected regions.

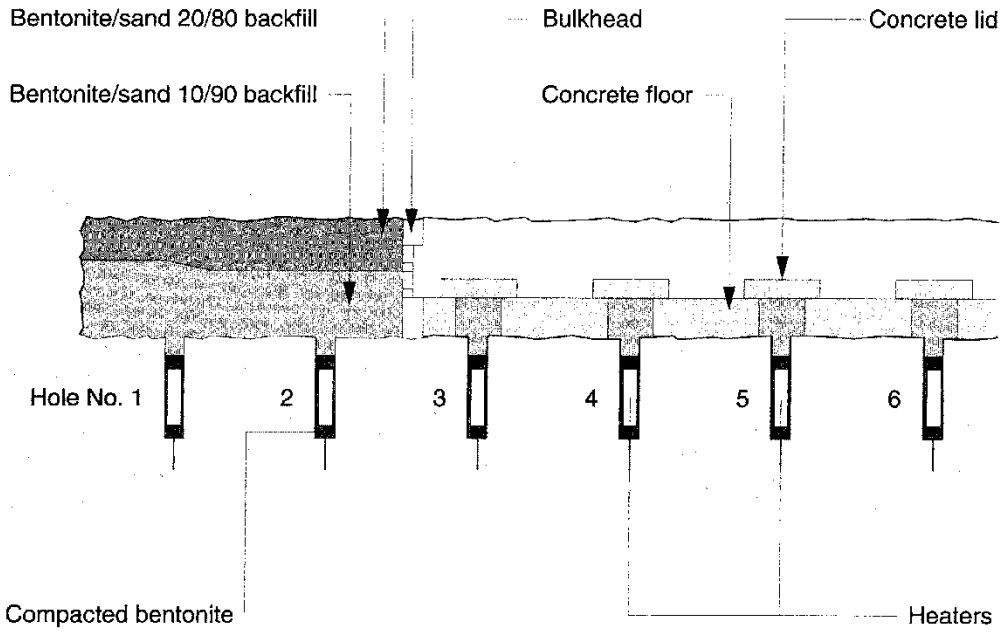

Figure 2-9 Longitudinal section of the BMT.

Predictions for moisture movement and temperature distribution in the BMT were largely conducted in accordance with the previously presented model but were limited by the information available on materials characteristics. The models were simplified to reflect these limitations.

Heat transfer and temperature distributions

For heat transfer, thermal finite-element codes, based on Equation 2.11, were applied (Börgesson, 1982). Since the performance of the buffer and backfill were of prime concern the meshes of elements were designed to provide information on the temperatures to be expected in these components of the test system. The meshes and boundary condititons were also adjusted to accomodate various configurations used in different sections of the test. Figure 2-9 presents a longitudinal section of the planned test. Different meshes were used for heater holes 1 and 2 than for holes 3 to 6 to accomodate the different thermal and boundary conditions. Moreover, during emplacement of the heater and HCB overpack a clearance (slot) of approximately 3 cm was required between the HCB and the borehole wall. This was left empty in holes 1, 2 and 5 and filled with bentonite powder in holes 3, 4 and 6. This feature was accomodated in the input parameters to the coded model.

Table 2-3 gives the parameters used for the analyses for which it was assumed for holes 1, 2 and 5 that the HCB, backfill and rock were completely water saturated. For holes 3, 4 and 6, the HCB and sand-bentonite backfill was assumed not to take up water. Constant heater power output rates of 600 W, 1200 W and 1800 W (values to be used in the test) were assumed in different computer runs. The principle of superposition was used to calculate the influence of heat transfer from neighbouring heater holes on the near field temperatures. It is clear from the table that some values were not measured but assumed based on background information. Moreover a comparison of the density values with those presented in Table 2-1 indicates significant overestimation of the densities of the backfill materials and, thereby, a probable error in the estimation of λ and C.

Table 2-3 Heat conduction parameters used in the finite element analyses for the BMT.

Element	λ (W/m.°K)	C (W.s/kg.°K)	Bulk density (Mg/m^3)
Heater	59	460	7.8
Bentonite:			
HCB-saturated	1.40	1600	2.10
HCB-as placed	1.00	1100	2.17
HCB-dry	0.39	800	1.90
Powder	0.30	1240	1.16
Bentonite-sand:			
Saturated	2.40	1400	2.20
As placed	1.50	1200	1.95
Dry	0.39	800	1.90
Sand:			
Saturated	2.10	1600	2.10
Dry	0.29	800	1.80
Rock-saturated	3.60	800	2.70
Concrete	1.80	920	2.30
Water	0.50	4200	1.00

Results of the form shown in Figure 2-10 were produced by the analyses. These gave an indication of the expected temperatures and rates of temperature change at different locations in the sealed volume of rock. Since one of the purposes of the test was to qualify predictive modelling capabilities for heat flow, the data were used to define appropriate locations for instrumentation and could be used as one of the guides needed to define a suitable duration for the BMT.

Moisture uptake and transfer

Numerical predictions for moisture uptake and redistribution in the buffer and backfill materials under the combined hydraulic and temperature gradients were restricted in the BMT by the lack of knowledge of the diffusion parameters in Equations 2.7 and 2.9. Moreover, the effects of hydro-mechanical interactions between the rock and the sealing materials were uncertain. These were likely to influence the hydraulic flux conditions at the buffer/backfill/rock boundaries. To begin to examine these phenomena, calculations of possible water transfer in the clay-based sealing materials were carried out using finite element codes based on the isothermal water transfer equation:

$$\frac{\partial w}{\partial t} = D \nabla^2 w \qquad (2.12),$$

where D is a lumped diffusivity coefficient for water transfer in the materials over a range of water contents, w, based on mass. The assumed values for D for different materials, taken from Börgesson (1985), are given in Table 2-4.

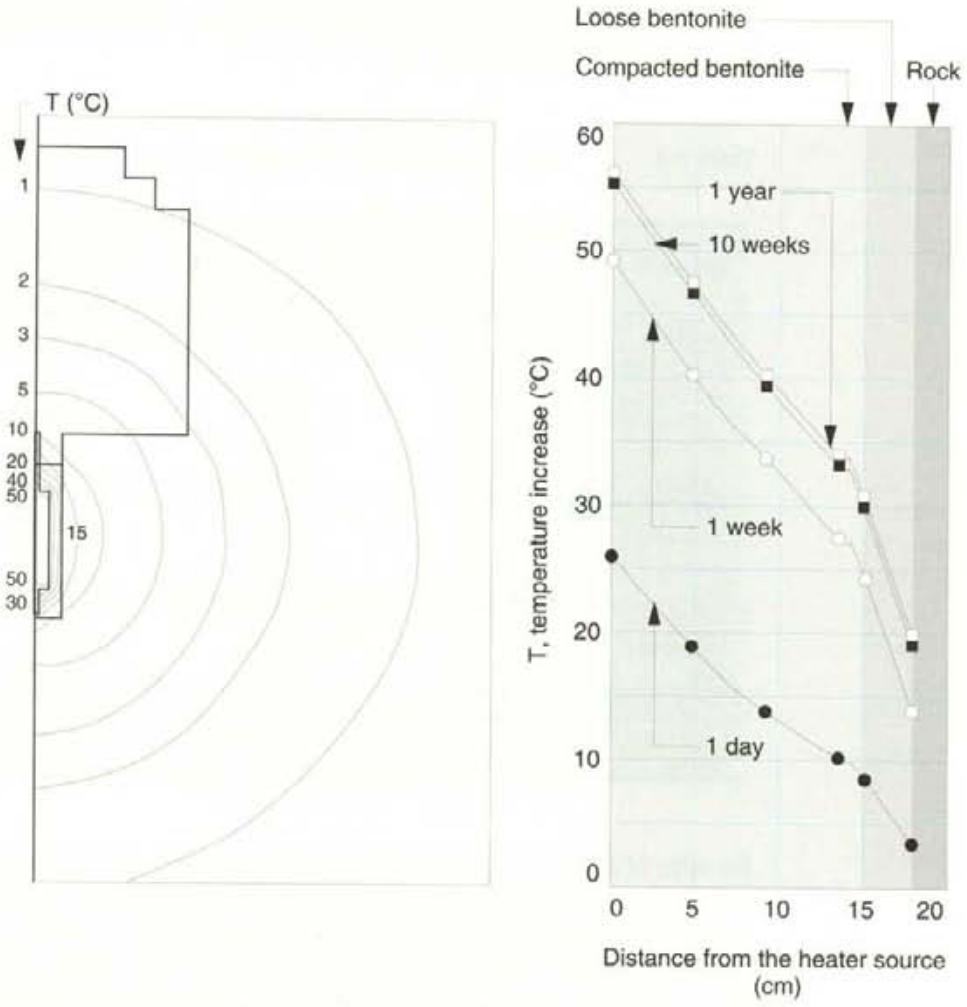

(a) Heater hole 2 (b) Heater hole 5

Figure 2-10 Typical output from heat transfer modelling for changes in (a) far field temperature distributions, and (b) temperatures to be expected in the HCB.

Different cases with boundary conditions ranging from unlimited water supply at the buffer/rock and backfill/rock boundaries to supply limited to a single water bearing fracture intersecting the emplacement borehole or the tunnel were computed. Typical results for these two extreme conditions in the HCB are given in Figure 2-11. Some typical results for the backfill are presented in Figure 2-12.

Table 2-4 Parameters used in the calculations of water transfer in the buffer and backfill materials.

Element	D** m^2/s	w_o * %	w_f* %
Buffer	4.10^{-10}	10	35
Backfill 80/20	1.10^{-8}	15	36
Backfill 90/10	1.10^{-8}	10	17
Contact zone	1.10^{-10}	15	36
Intact rock	1.10^{-50}	-	-

* w_o and w_f are the initial and final water contents of the material, respectively.

** D values are average values over a range of w and are based on laboratory measurements of water uptake in clay and clay-sand mixtures during confined swelling pressure tests (see section 2.3.4).

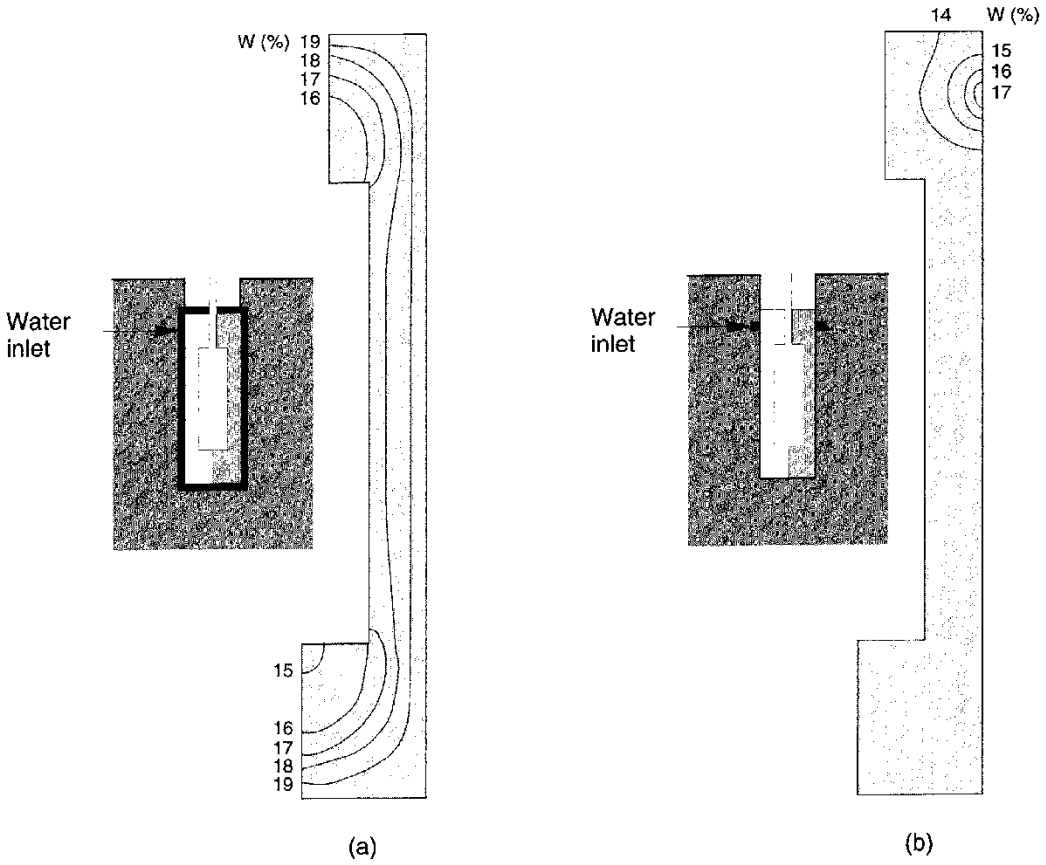

Figure 2-11 Predictions of water uptake in the buffer after 64 weeks for (a) unrestricted water supply, and (b) water supply restricted to one fracture at the outer buffer boundary.

The results indicated that, if water was freely available at the HCB/rock interface and isothermal moisture transfer was the dominant mechanism for moisture uptake and redistribution, the buffer would saturate in three to four years. A significantly longer period would be required for the backfill. Water inflow through discrete fractures in the rock would cause localised water uptake. Under these latter conditions complete saturation would take much longer to attain than if water was freely available at the buffer and backfill

surfaces. The predicted rates at which water would be taken up by the buffer and backfill with time are summarized in Figure 2-13. Based on the measured rates at which water flowed into the open individual boreholes drilled for the BMT and into the tunnel recorded during the ventilation experiment, carried out for the Swedish American Cooperative agreement, the data indicated that the buffer and backfills should retard flow into the excavated cavities.

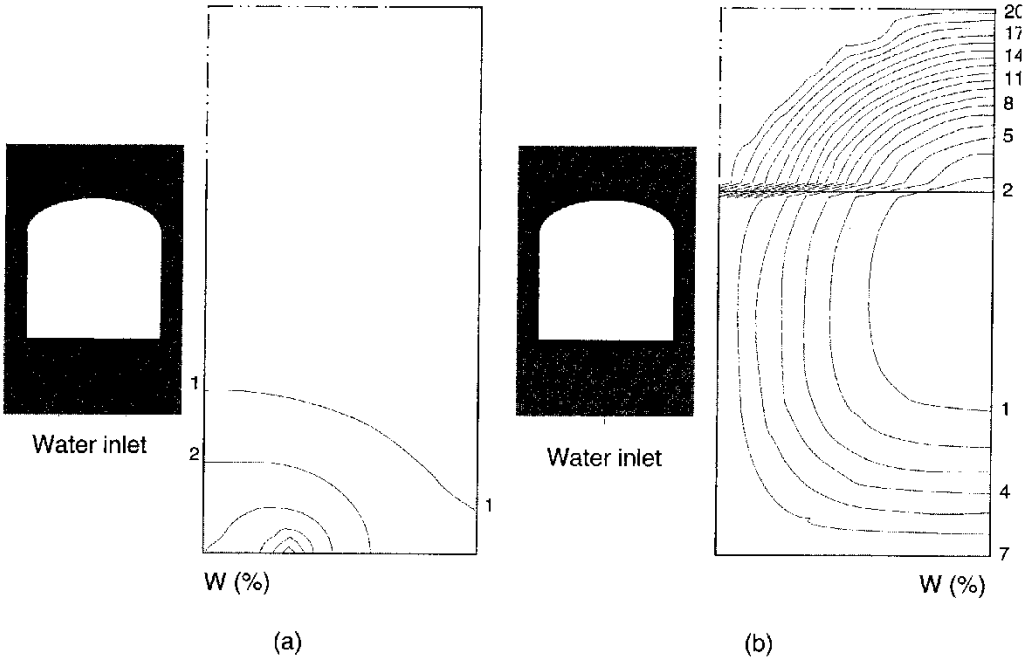

Figure 2-12 Predictions for water uptake in the tunnel backfills after (a) 3.4 years with limited water supply, and (b) 1 year with unlimited water supply at the backfill/rock boundary.

Moreover, the results suggested that the experiment needed to be run for one or more years to allow for reasonable comparisons between measured and predicted water uptakes. It is recognized that the predictions not only ignored the effects of thermally induced moisture transfer but also did not accommodate for the possible effects of hydraulic potential change at the buffer/backfill rock boundaries. Instrumentation in the experiment had to be configured to allow for these processes to be assessed. Due to the delaying effects of the bentonite on the in-flow to the cavities, it could be predicted that the hydraulic pressures should increase in the near field rock mass.

2.3.4 Swelling and swelling pressures

Unrestrained and in contact with free water, saturated compacted bentonite and bentonite-sand mixtures will sorb water and swell. In addition to their low hydraulic conductivity and diffusivity, this potential to swell makes compacted bentonite-based materials attractive for use as buffer and backfill materials. It was noted in section 2.2.2 that the swelling should result in the closure of joints and voids left in the seals during construction. One intent of the BMT was to investigate the effects of the swelling processes on repository system performance.

Mechanistic models for the swelling processes, related to osmotic potential differences between free water and pore water in the clay, are presented by Mitchell (1976), Yong and Warkentin (1975) and Pusch (1980a). The lower total potentials that exist in pore water, due to the colloidal character of the clay particles, induce water flow into the clay primarily through the process of chemical osmosis (see Table 2-2). Discussed in section 2.3.3, the water flow may or may not be accompanied by the advective movement of electrolytes from the free water source into the clay depending on the density of the clay. It has been shown (Bresler, 1973) that clays act as semi-permeable membranes with varying degrees of osmotic efficiency that depend on a number of factors which include density. At the densities used in the BMT, it can be suggested from Bresler that the buffer material has an osmotic efficiency that probably approaches 100 per cent. It is likely that the backfill materials have lesser efficiency.

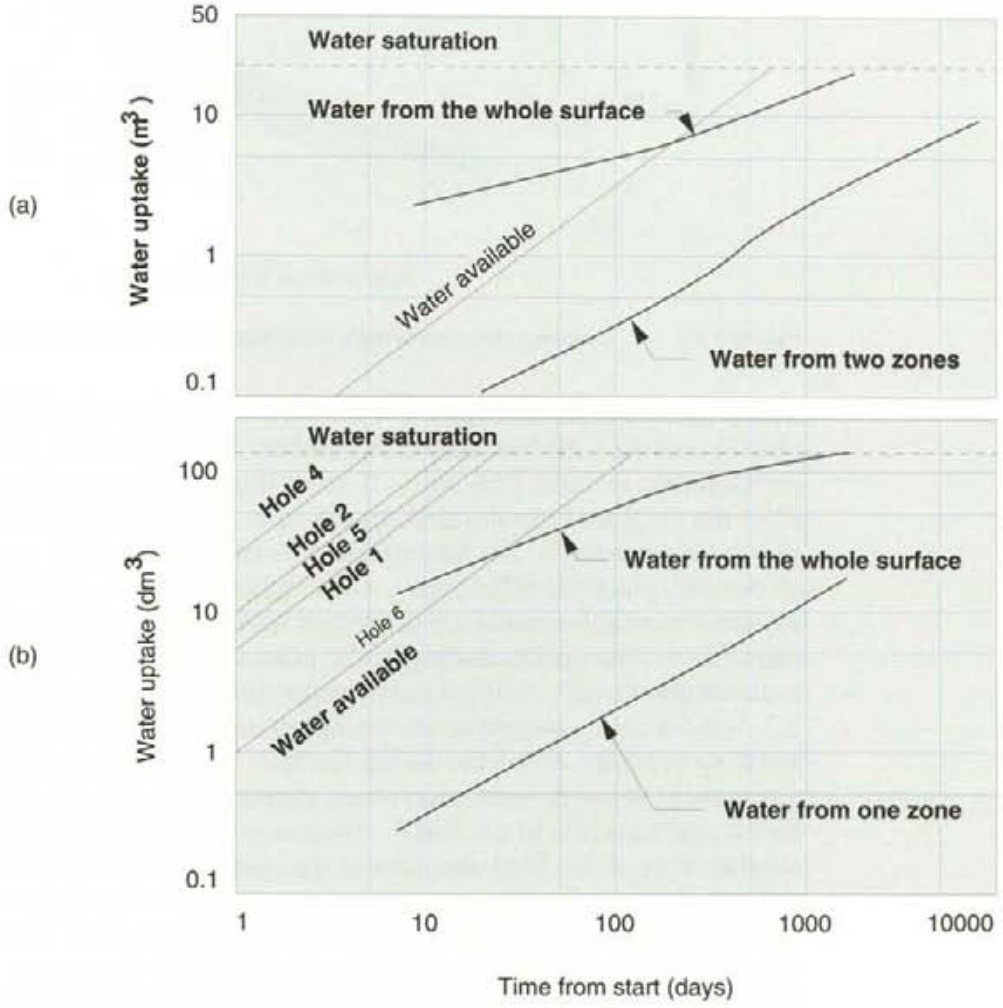

Figure 2-13 Predictions for the times for (a) the backfill, and (b) the buffer to attain various degrees of saturation.

Virtually totally confined, like the buffer and backfill materials in the BMT, water cannot physically flow from the rock to cause the saturated clays to swell. The total potentials in the soil water and the free water in the rock must equilibrate. This equilibration results in a pressure (the swelling pressure) being exerted by the buffer and the backfill on the confinement. These pressures

were measured by Pusch (1980a) for totally confined compacted MX-80 and shown, as expected, to depend on density. The range in possible values is shown as a function of density in Figure 2-14. Swelling pressure-density relationships for the sand-bentonite backfill materials were not available. Subsequent work (Gray et al; 1985, Graham et al, 1989) has shown that the swelling pressures are directly related to the clay dry density (see footnote 9).

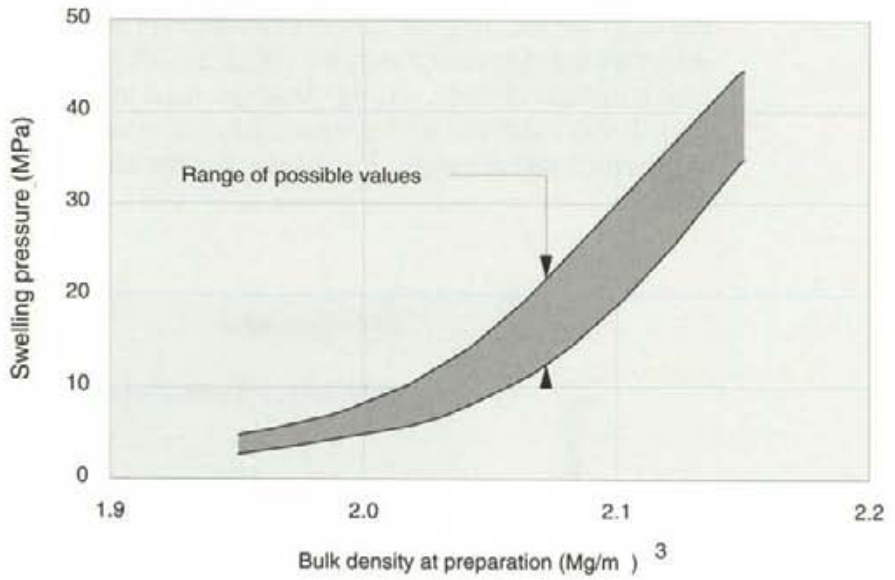

Figure 2-14 Swelling pressure/density relationships for HCB (after Pusch, 1980).

The pressures given in Figure 2-14 are the final pressures exerted by saturated clay in contact with free water. A number of processes are involved in the development of these pressures. Two of these are the wetting-up of the clay from the as-placed unsaturated condition to saturation and the equilibration of the water potentials. The first of these involves water flow via capillary as well as osmotic potential differences. Little information was available on the flow parameters which control the processes leading to saturation. Combined with the lack of clear understanding of the processes of water uptake and redistribution under coupled temperature and hydraulic gradients (see section 2.3.3) it was not appropriate to attempt to model numerically the change of swelling pressure with time during the test. Predictions were thus restricted to a statement of the possible maximum pressure that may be observed in the buffer and backfills in the BMT. These could be read off Figure 2-14, or similar chart, if the final densities of the materials were known. These were estimated from a knowledge of the initial density of the materials used and the volumes that they would be required to occupy once fully saturated and swollen. These volumes would not only depend on the empty space left during material emplacement but also on the mechanical interactions between the buffer, backfill and rock.

2.3.5 Mechanical interactions and processes

At a dry density of 1.88 Mg/m^3 (the emplaced density) the saturated HCB could be expected to exert an ultimate pressure of betweeen 10 and 20 MPa on the backfill and the rock. The backfill could be expected to exert swelling pressures only in the range of hundreds of kPa on the buffer and rock. The

differential between the pressures was expected to cause compression of the backfill by the buffer. Moreover, the swelling pressures would tend to extrude the buffer and backfill into any fissures in the rock mass that intersect the excavations. Arguably beneficial, insofar as the effective boundary of the buffer would be extended by the extrusion, extrusion and buffer/backfill interactions would both tend to reduce the density of the buffer and increase the radionuclide transfer coefficients. These processes also complicated modelling of the heat and mass transfer processes both in the test and in a repository setting by imposing dynamic conditions at the buffer/ backfill/rock interfaces. In addition, the pressures exerted on the rock by the clay materials also, possibily, could change the hydraulic conditions in the rock mass near the test. Available models were, and remain, insufficiently advanced or accessible to accurately describe these links between the hydraulic properties of the near-field rock mass and stress variation. Added to these difficulties, the heat pulse imposed on the system would tend to cause displacements of the interfaces and affect hydraulic performance. A complete numerical analysis of these processes would require a large quantity of information. This would include data on the thermal expansion properties of the materials, the temperature dependent compression and consolidation properties of the HCB and backfill (both in the saturated and unsaturated states), knowledge of the frictional factors that control slip at the interfaces and within the materials, and an understanding of the relevance of laboratory derived parameters to *in situ* performance. This knowledge was not available.

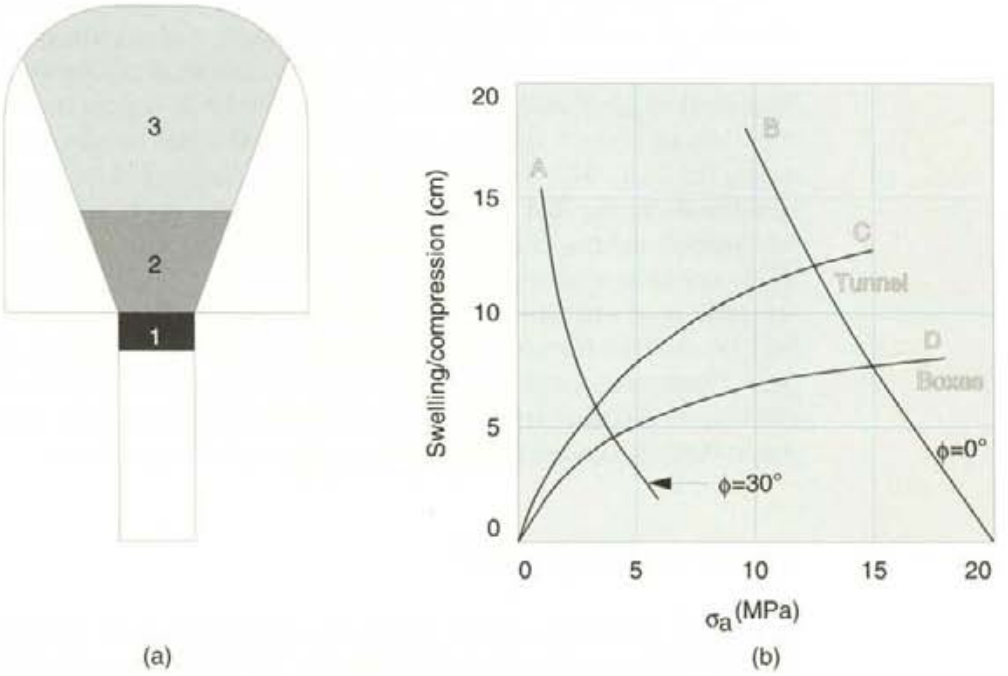

Figure 2-15 (a) Assumed distribution of load in the backfill to calculate (b) deformation at the buffer/backfill interface depending on buffer swelling pressure, test configuration and buffer/rock interface friction angle.

Observation in the BMT offered a means through which a conceptual model of the mechanical performance of the total buffer/backfill /rock system could be established. Some attempts at enumerating the interacting effects and

processes could be made. Limited laboratory and theoretical exercises were undertaken to allow for broad predictions of the effects of mechanical interactions. An analysis of the possible maximum deformation of the buffer/backfill interface and the measurement of the extrusion properties of HCB into artificial fissures under different conditions were effected.

Recognizing the uncertainties in the calculations and the deficiency of the laboratory derived data base on material properties, a relatively simple confined compression computation was made (Börgesson, 1982) to estimate the deformation of the buffer/backfill interface using the measured compression characteristics of the lower (9:1) saturated backfill material. Calculations were carried out to allow for the various buffer/backfill configurations to be used in the experiment and to accomodate a range of possible swelling pressures from the buffer and possible coefficients of friction between the buffer and the rock. In common with some methods for calculating deformations of foundations on clay soils, the pressures from the buffer were assumed to distribute in the backfill as shown in Figure 2-15(a). Predicted swelling of the buffer (compression of the backfill) is shown in Figure 2-15(b).

Laboratory tests (Pusch, 1983a) indicated that the empirical relationship shown in equation 2.13 reasonably represented the rate at which HCB would self-inject into planar, simulated fractures in rock:

$$x = Ad^2\log(t+1) \qquad (2.13),$$

where x is the distance moved by the clay front, d is the aperture, t is time of onset of flow under the developing swelling pressure and A is an empirically derived parameter depending on temperature, water salinity, clay type and fracture characteristics. The experiments consisted of confining HCB in stainless steel or granite chambers, allowing the HCB access to water through planar slots of known aperture and observing the rate of advance of a clay front along the slot. The veracity of this relationship could be examined for *in situ* conditions in the BMT and observations on the applicability of the equation to bentonite/sand backfill materials could be made. Deviations from the relationships could be expected due to the irregularity of natural fissures in rock and the effects of fracture infills on clay movement. In addition, the laboratory tests had shown that the advancing front of clay would have the consistency of a soft gel. There was some concern that this material would be eroded by the water flowing in the rock fractures. Observations on these phenomena could be made during a careful decommissioning of the experiment.

2.4 ROCK CONDITIONS

The BMT was to be carried out in the ventilation (later termed macropermeability) drift developed and used during the Swedish-American Cooperative (SAC) programme to evaluate the permeability and hydraulic conductivity characteristics of the Stripa granite (Gale et al, 1983). Work under the SAC agreement provided a wealth of information relevant to the conduct of the BMT. The pertinent de-tails are reviewed by Pusch and Nilsson (1983) and Pusch et al (1985b). For ease of reference these details are summarized in this section along with new information gained during the developments preceding the installation of the BMT. It is noteworthy that the BMT/macropermeability test room was used for experiments in Phase 3 of the Stripa Project.

The information provided in this section is relevant to both the BMT and the Phase 3 experiments.

The BMT room was excavated using careful drill-and-blast techniques (Andersson and Halén, 1978) into the medium grained, massive grey/reddish granite at the Stripa site. The blast rounds were designed, as far as then practicable, to limit disturbance of the rock. The rock, which was virtually water saturated, had a temperature of 12.5 to 13.0 °C a short distance from the face of the excavations, where air temperature was maintained at 15 °C. The stresses in the rock immediately adjacent to the BMT room had not been measured but were presumed from measurement in the locale (Pusch et al, 1985b) to be related to a general stress field with $\sigma_1 \sim 20$ MPa acting horizontally and at right angles to the axis of the room, $\sigma_2 \sim 10$ MPa acting horizontally and parallel with the room axis and $\sigma_3 \sim 4$ MPa acting vertically.

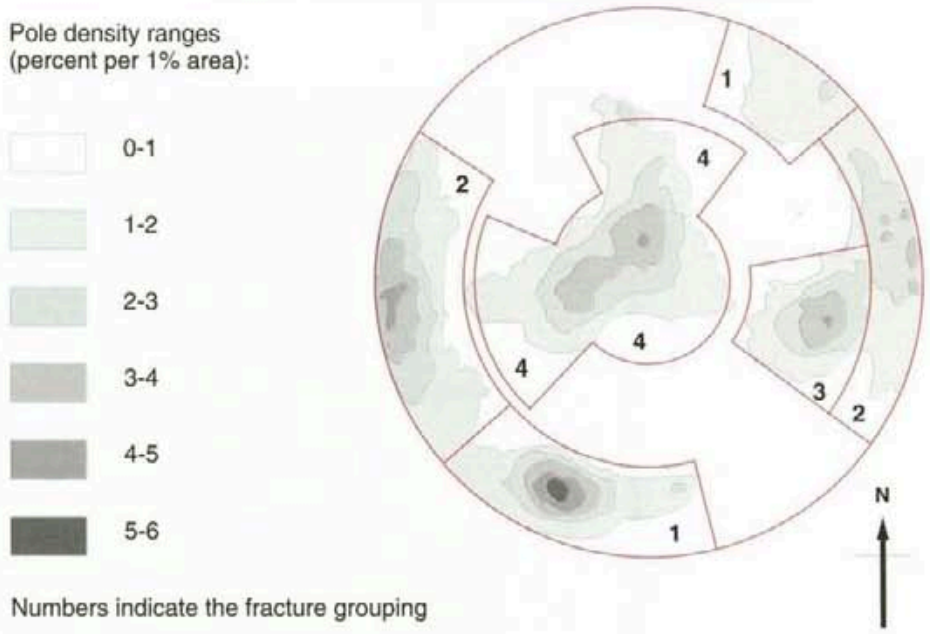

Figure 2-16 Lower hemisphere plot of poles to planes of fractures in the rock mass near the BMT drift (after Gale et al, 1983).

At the time of initiation of the BMT the results of the Phase 3 investigations that led to a more complete understanding of the effects of the presence of the mine on the regional hydrology were not available. Mapping of the faces of the excavation combined with the careful analysis of fractures that intercepted boreholes, emanating radially and longitudinally from the test room, had provided the polar plot shown in Figure 2-16 as partial explanation of the hydrological characteristics of the rock mass. The radial and longitudinal boreholes had also been instrumented for the measurement and monitoring of hydraulic head in the rock around the room. This instrumentation was to be maintained and monitored during the conduct of the BMT. The heads measured in the radial holes during the SAC macropermeability experiment are shown in Figure 2-17.

It was shown in section 2.3.3 that the rate of water uptake by the buffer and the backfill may be influenced by the nature and distribution of water bearing frac-

tures intercepting the BMT room and boreholes. For a number of reasons, including mineralogical infilling and small hydraulic aperture, not all the fractures mapped in Figure 2-16 were water bearing. A subjective attempt was made to identify the water bearing fractures and the permeable rock that allowed flow into the BMT room in the region which was to be backfilled above heater holes 1 and 2 (see Figure 2-9). The assessment was effected by drying the room and observing the re-wetting of the surfaces of the excavation. Maps of the water bearing fractures and moistening rock zones were produced. These showed that water did not flow evenly into the open room. The end of the tunnel was the driest. Inflow was apparently highest along the eastern wall with flow occuring through fractures and zones of permeable rock. Water bearing fractures largely controlled water inflow through the western wall and the back of the room. There is no recorded attempt to relate these observations to local variations in the geomorphology. The flow rate into the 12 m long section of the room was estimated from the macropermeability experiment to be approximately 25 ml/min (Pusch et al, 1985c).

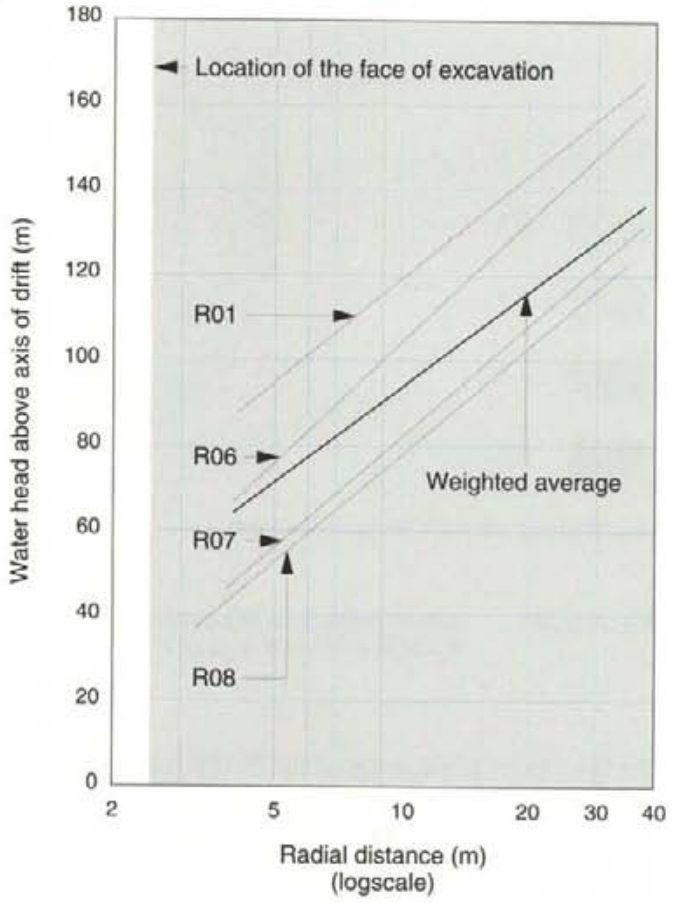

Figure 2-17 Hydraulic heads measured with radial distance from the axis of the BMT room before the initiation of the test (after Wilson et al, 1981).

The head data shown in Figure 2-17 and the known inflow rates to the room were used by Gale et al (1983) as input to a porous medium model for the rock to estimate the average hydraulic conductivity of the monitored rock mass. A value for k of 10^{-10} m/s was determined. Specific note was made of the fact that the head data shown in Figure 2-17, if projected to the wall of the room, indicate a higher head than the actual value. This indicates a skin - or excava-

tion disturbed zone - with a lower radial conductivity than the rock mass. This zone was one of the focii for the engineered barrier studies for Phase 3 of the Stripa Project and accounted for some of the difficulties encountered in the interpretation of data collected during the hydrogeological investigations throughout the entire Stripa Project.

Some of the characteristics of the excavation disturbed zone were identified during the excavation and mapping of the large diameter (Φ = 760 mm) 3 m deep boreholes that were diamond-drilled into the floor of the experiment room to accommodate the buffer and heater systems.

Figure 2-18 presents a fracture map of the wall of borehole No.1. The thicker lines denote distinct water bearing fractures. The fracture maps for the boreholes typically show that the water bearing fractures were concentrated in the upper third of the boreholes and were sub-parallel with the floor of the room. Natural fractures, containing infills of calcite, chlorite, epidote or pegmatite, had been opened possibly by stress redistribution. Near the floor of the room new fractures, with no infilling materials, were identified as the progeny of room excavation.

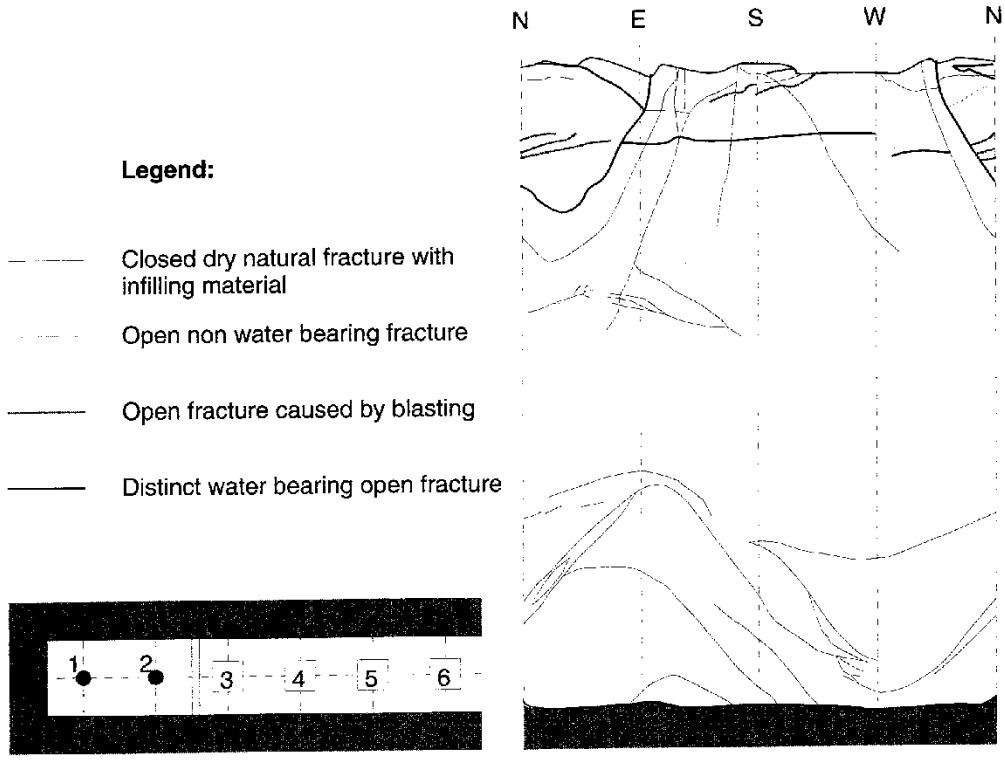

Figure 2-18 Mapping of major fractures intersecting emplacement borehole No.1 of the BMT.

The natural inflows of water into the upper, middle and bottom sections of each of the six emplacement boreholes were measured using a moveable collecting system. The results are shown in Table 2-5 along with the inflows measured in pilot holes (Φ = 56 mm) drilled to centre the large diameter holes.

Table 2-5 Average inflow rates measured in the pilot holes and the BMT emplacement boreholes.

Hole No.	Water inflow l/d: Upper half	Lower half less bottom 20cm	Bottom 20cm	Total inflow	Total into pilot holes
1	3.7	1.1	0.7	5.5	6.2
2	8.0	1.2	1.6	10.8	5.6
3	nm	nm	nm	nm	3.0
4	2.7	3.2		5.9	0.2
5				6.7	1.9
6			0.2	1.0	0.2

nm = measurements not made.

Disturbance in the hydrologic regime during the measurement of flows into the 760 mm diameter holes, caused by construction activities, rendered the in-flow data for these holes uncertain. The principal effect was to cause unaccountable fluctuating flows in the excavation disturbed zones. The data from the pilot holes were taken to reflect the background hydrologic conditions (Pusch et al, 1985c). These data show that emplacement holes 1 and 2 were significantly "wetter" than the others. It was noted in section 2.3.3 that after the emplacement of the heater/buffer systems, powdered bentonite was poured in the annular gap between the buffer and the rock in holes 3, 4 and 6. The gap was left open in holes 1, 2 and 5.

2.5 INSTRUMENTATION

Instruments were installed in the buffer and backfills to monitor changes in temperature, total pressure, pore water pressure, moisture content and displacement during the progress of the tests. Measurements of water pressure and temperature were made in the near-field rock mass. The interfaces between the buffer and the rock, the buffer and the backfill, and the backfill and the bulkhead - separating the backfill from the open section of the test room (see Figure 2-9) - were instrumented for total pressure. It was noted in section 2.4 that inflow into emplacement hole No. 5 was the highest for the four capped boreholes (Nos. 3 to 6). Thus, hole No. 5 was selected for extra instrumentation. This was intended to measure the swelling forces from buffer and backfills acting on the cap of the hole and to measure the rock displacements arising from the combined effects of temperature changes and the swelling forces. Details of all the instrumentation, the monitoring and recording systems, and the identification codes used for each of the instruments are provided by Pusch et al (1985b). Table 2-6 presents a summary of the instrumentation used. Insofar as they limit data interpretation or influenced the conduct of the experiment, some specific aspects of the instrumentation require mention here.

Details of the operating principles of commonly used geotechnical instruments and a discourse on the "state of the art" of instrumentation are provided by Dunnicliff (1988). Specific note is made here of the nature of errors that can occur in measurement with attention to the level of certainty in the data from the BMT instrumentation. Types of error, causes and remedies are given in

Table 2-6 Instrumentation used in the BMT.

Measurement	Location	Instrument	Supplier	Range	Accuracy*	Number used	Comments
Temperature	Buffer/ backfill/ rock	Type T thermo-couple	Pentronic, Sweden	0 to 90 °C & 100 to 160 °C	+/- 0.5 °C	1242	
Total pressure	Buffer/rock interface Backfill/bulkhead interface Inside buffer/backfill masses	Constant volume, fluid filled pressure cells	Gloetzl Baumesstechnik, Germany	0 to 4 MPa & 0 to 16 MPa	+/- 4% range +/- 4% range	128	The same instrument was used for both ranges. Recording device offers stated accuracy. Values are affected by temperature and require interpretation.
Water pressure	Near field rock mass	Hydraulic piezometers, constant volume piezometers, and manometers	Constant volume piezometers: Gloetzl Baumesstechnik, Germany	0 to 3 MPa	+/- 10 kPa for u>100 kPa	28	Values are affected by temperature and require interpretation. High air entry ceramic employed.
	Backfill	Hydraulic piezometers and constant volume piezometers	Hydraulic piezometers: Bengt-Arne Torstensson AB, Sweden	0 to 3 MPa	+/- 1 kPa	25	High air entry ceramic. Remote sensing improves precision.

Table 2-6 Instrumentation used in the BMT (Cont'd).

Measurement	Location	Instrument	Supplier	Range	Accuracy*	Number used	Comments
Water content	Buffer Backfill	Electrical capacitance gauges	University of Luleå, Sweden			560	Regarded as imprecise device. Records passage of wetting or drying front.
Deformation	Buffer/backfill interface	Copper coins			+/- 3 mm	240	Precise survey allows for stated accuracy. End values only.
	Near field rock mass	Sliding micrometer	Solexperts Ltd., CH		+/- 10 mm	4	Hole 5 only instrumented.
Force	Restraining bolts on cell caps	Electrical resistance load cells	Geo-Beräkningar AB, Sweden	0 to 1 MN	+/- 2 % range	12	Hole 5 only instrumented.

* Accuracy stated by Pusch et al (1985b) based on assessments of the compound performance of the instruments and the data aquisition systems.

Table 2-7 Types, causes and remedies for measurement errors*.

Type of error	Causes of error	Remedies for error
Gross	Inexperience Misreading Misrecording Computational error	Training Care Duplicate recording Cross checking
Systematic	Improper calibration Loss of calibration Hysteresis Nonlinearality	Proper calibration Recalibration Use of standards Consistent procedures
Conformance	Inappropriate installation details Instrument design limitations	Proper instrument installation Improve instrument design
Environmental	Weather Temperature Vibration Corrosion	Apply temperature corrections Use appropriate materials
Observational	Variation between observers	Training Automatic data aquisition
Sampling	Variability in the measured parameter	Install sufficient number of instruments
Random	Noise Friction Environmental effects	Statistical analysis Noise elimination Multiple readings
Murphy's law	If something can go wrong, it will	None

* From Dunnicliff (1988) p.77.

Table 2-7. Systematic error, conformance error, environmental error and random error are the focii of this discussion.

All of the instruments used, except the water content gauges, were commercially available instruments used in conventional geotechnical engineering monitoring systems.

To minimize systematic error, temperature sensors were specially calibrated and linked to a data acquisition system with an electronic ice point reference. Knowledge of temperatures within the accuracy shown in Table 2-6 allowed for appropriate temperature corrections to be made to other instruments. A large number of thermocouples were used to allow for accurate recording of the spatial and temporal temperature distributions. This also reduced sampling error for the temperature distributions.

Calibration curves for the total pressure sensors and the fluid pressure gauges and transducers were supplied by the manufacturers and traceable to relevant national standards in the country of origin. Readings from the Gloetzl total pressure and water pressure sensors were corrected for temperature in accordance with the manufacturer's recommendation by a factor of 0.02 MPa/°C. Some uncertainty rests in this number. The recorded values required judgement and experience with the instruments. The hydraulic piezometers were read remotely: thus, readings were not influenced by temperature. It was not possible to recalibrate many of the instruments during the progress or after completion of the test.

Figure 2-19 shows the locations of total pressure sensors in the vicinity of emplacement boreholes Nos. 1 and 2. Uncertainties exist in the interpretation of the results from the cells due to possible lack of conformance of the gauges and due to the method of operation. With regard to the latter, each of the cells was pressurized over a period of between 1 and 10 minutes to return the device to zero volume strain (Pusch et al, 1985b). For saturated clays this corresponds to undrained loading and will cause an error in measurement of the swelling pressure (the effective stress). This error is expected to have been present in all gauges in varying magnitude depending on several factors including the degree of saturation of the clays and the value of the swelling pressure. The stiffnesses of the gauges differ from those on the buffer and the backfill. This causes conformance errors as shown by Selig (1964). The gauges were probably stiffer than the soil masses in which they were embedded which gives rise to an overestimation of the actual stresses in the clays. For these reasons, it is considered that the measurements may not lie in the accuracy range given in Table 2-6. The fluid pressure calibrations provided by the manufacturer may not truly reflect the actual pressures experienced by the cells. The results from the interfaces are likely to be more accurate than those from the embedded cells.

Compressed bentonite pellets are often used to seal boreholes above piezometer tips. It is known (Government of Hong Kong, 1979) that the osmotic potential differences between the bentonite and the groundwater can give rise to undermeasurement of hydraulic potential in saturated media. The readings from the piezometers in the near field rock mass may have been subjected to such distortions from the suctions generated by the buffer and backfill materials. Due to cavitation effects, readings from the sealed diaphragm cells were not relied on at water pressures less than 100 kPa. The double tube, rechargeable hydraulic piezometers fitted with high air entry ceramic tips could be relied on to read pressures down to -80 kPa (i.e. 80 kPa

below atmospheric pressure). These latter instruments were read using a single, quick-connect water pressure transducer. It is not clear that elastic phenomena in the instrumentation and tubing did not cause measurement distortions. For these reasons, the accuracies of the measurements are likely to be less than those shown in Table 2-6.

The equipment was required to be serviceable for a number of years. This criterion, combined with high temperatures and possibly corrosive conditions, called for substantial protection of the instrumentation and the leads to the data acquisition system and operating devices. The selected protection measures described by Pusch et al (1985b) proved to be very successful: the greater proportion of all instrument types remained serviceable throughout the period of the test. This also testifies to an appropriate choice of instruments. Difficulties in interpretation of results noted above were accepted for the benefits of robustness and reliability.

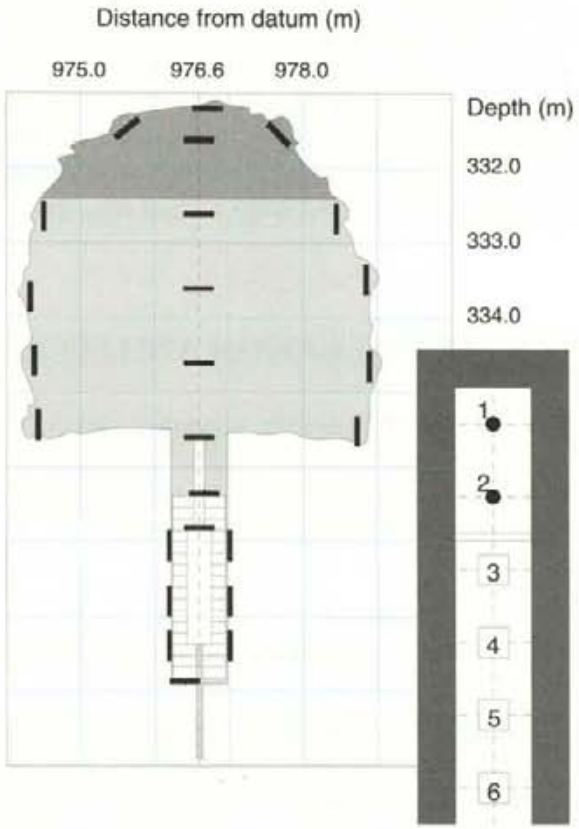

Figure 2-19 Location of total pressure sensors in and above heater holes 1 and 2 (From Pusch et al, 1985b).

Commercially available soil-moisture sensors are designed for use in agronomy and are used in loose porous media. There was no known moisture sensor with the robustness and reliability required for the BMT available for use in dense clays. A special miniature sensor to measure the capacitance of the clays (a parameter that varies with moisture content) was developed in an attempt to meet the requirements of the BMT. The accuracy of these devices varied with moisture content and other factors (measurements in the sand-bentonite backfill were considered to be less accurate than those in the HCB) and the recorded values were taken only as an indication of wetting or drying of the clays in which the instruments were embedded (Pusch et al,

1985b). The clays were destructively sampled during the decommissioning of the experiment. Moisture contents of the sampled materials were determined by oven drying at 105 °C.

To facilitate decommissioning, a special segmental heater, representing the waste package, was designed for the tests. The wedged outer aluminium construction allowed for rapid disassembly during excavation and thereby minimized the time to sample the buffer. Due to the requirements for manual operations, it was not possible to sample the buffer at high temperatures. Some redistribution of moisture content must have occurred in the buffer and backfills prior to sampling.

In common with other instrumentation, the heaters had to be robust and reliable over a test period extending into several years. Unlike other instrumentation, which was applied with redundancy, malfunctioning heaters could result in abandonment of the test. Thus, significant effort was expended in the design, construction and reliability testing of the heaters. Details of this work are provided by Pusch et al (1985b). The heater cores were designed to be run at constant power up to 3 kW. Each core was supplied with three heating elements with each being capable of supplying the necessary power to an accuracy of approximately +/- 1.5 % of output. In testimony to the care with which this work was effected, apart from the failure of one heater element, all six heaters and their controls behaved according to expectations for the four year period over which they were operated.

2.6 TEST INSTALLATION AND SEQUENCING

For ease of reference the schematic layout of the BMT shown in Figure 2-3 is re-presented in Figure 2-20. Table 2-8 shows the periods over which the heaters were operated and the power supplied. The following brief explanations pertain to the history of the test.

Table 2-8 Significant event dates for BMT activities.

Location	Heater power W	Turn-on date	Turn-off date	Comments
Hole No.1 (wet)	600 1800 1400	5 Oct 81 20 Mar 84 10 Apr 84	20 Mar 84 10 Apr 84 1 Feb 85	
Hole No.2 (wet)	600	7 Oct 81	14 Nov 84	
Hole No.3 (dry)	600 1200 1800	20 Jan 82 13 Jun 83 17 Jan 84	12 Apr 83 17 Jan 84 21 May 84	Heater/buffer system withdrawn and replaced before high power test.
Hole No.4 (dry)	600	20 Jan 82	1 Dec 83	
Hole No.5 (wet)	600	24 Mar 82	7 Jun 84	
Hole No.6 (dry)	600	24 Mar 82	6 Apr 84	
Tunnel backfill: completed excavated		 Dec 81 Nov 84	 Jan 85	Outer half of backfill over hole No.2 excavated by Nov 84. Complete excavation by Jan 85.

All the preliminary engineering activities including the drilling of the boreholes, the prefabrication of the steel bulkhead, the casting of the concrete slabs and caps, the installation of the data acquisition and heater control systems, and the acquisition and demonstration of materials preparation and placement systems had been successfully completed by the end of summer of 1981. These activities allowed for a demonstration of some of the activities needed for the construction of a repository. Perhaps the most significant of these was the successful blind diamond coring of the large diameter emplacement boreholes.

The heaters were to be emplaced and turned on sequentially from 1 to 6, initially at a power of 600 W. This allowed for early start-up of the test and limited the time over which the buffer and backfill would draw water from the rock without an applied temperature gradient. In this context, heat was applied to hole Nos. 1 and 2 two months prior to the completion of the backfill and the installation of the bulkhead.

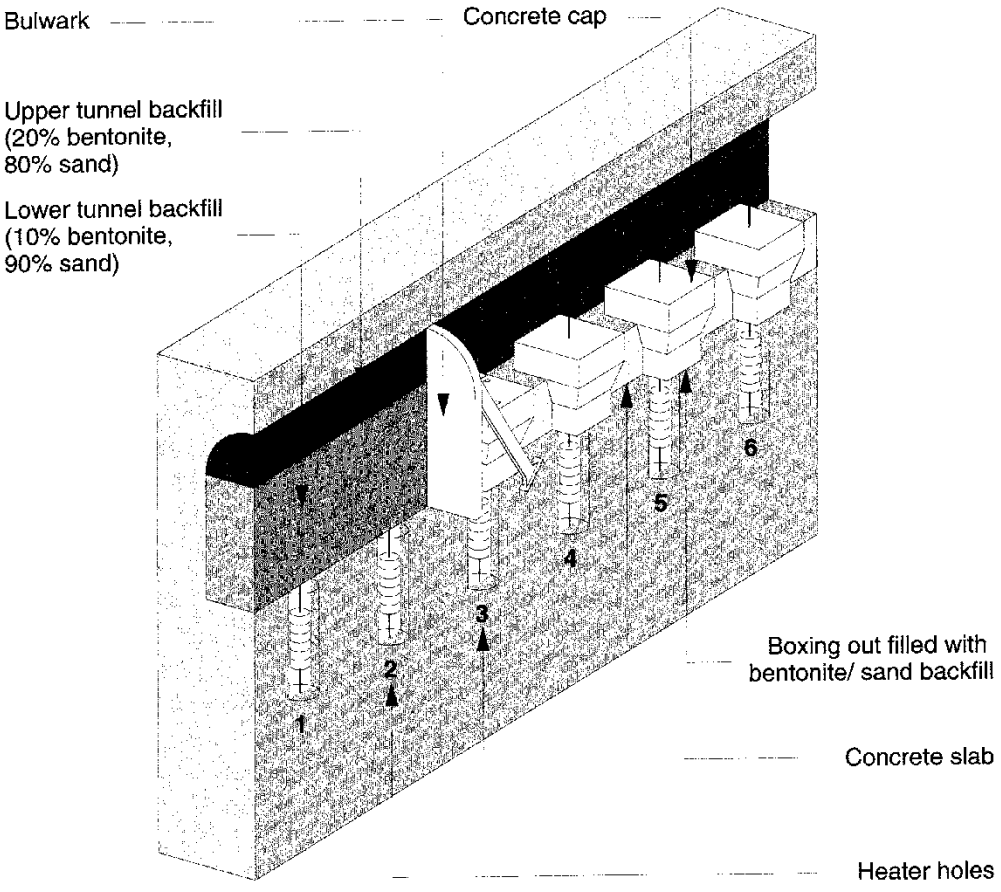

Figure 2-20 A perspective of the BMT room arrangement.

Powered at 600 W, the heaters were expected not to increase temperatures above approximately 90°C. To examine the effects of higher temperatures, one dry hole (No.3) and one wet hole (No.1) were chosen in which to in-

crease power to 1400 or 1800 W. This was effected after the experiment had been operating for more than 12 months and some quasi-equilibrium had been established. Prior to the increase in power in hole No.3, the system was excavated and replaced. This provided preliminary insights into the buffer response and also allowed for a different method of buffer and heater placement to be demonstrated. In the initial installation the buffer/heater system had been placed as a complete package. During the second installation in hole No.3 the buffer was placed as an annular brickwork and the heater was lowered into the resulting cylindrical cavity. The short term high power test in hole No.3, which acted as a precursor for the longer test in hole No.1, allowed for an interim review of predictive models and formed the basis for decisions regarding the conditions for the high power test in hole No.1.

2.7 RESULTS

2.7.1 Heat and Water Transfer

The results presented by Pusch et al (1985a) show that water uptake and temperature changes in the HCB were affected by the original boundary conditions and the test configuration. In holes Nos. 1, 2 and 5, which had been classified as "wet" holes before the installation of the heater/buffer systems, and in which no powdered clay had been placed in the annular gap between the buffer and the rock, towards the end of the test measured temperatures tended to be lower than the predicted values (see Table 2-9).

The opposite was true for "dry" holes 3, 4 and 6. The data in Table 2-9 for holes Nos. 5 and 6 are typical of data acquired for "wet" and "dry" holes, respectively. Throughout the test period measured temperatures were higher than predicted for the dry holes. In wet holes measured temperatures were initially higher than predicted ones: the difference between measured and predicted values decreased with time.

The differences in the temperature patterns are explained by the moisture redistributions in and water uptake by the HCB during the progress of the tests. On excavation, it was found that the HCB in wet holes 2 and 5 was virtually completely water saturated. In wet hole No.1, in which high power tests had been carried out, the degree of saturation (S) remained above 90 per cent. In contrast, S varied across the section of the dry holes, largely as shown in Figure 2-21 for hole No.3. The gradients in temperature across the buffer correspond to a decrease in the thermal conductivity with increasing S. The results confirm that the predictive methodology applied did not accommodate all the physical processes present in the buffer under combined hydraulic and temperature gradients (see section 2.3.3). A recent analysis (Ohnishi, 1988) has confirmed the observation (Pusch et al, 1985a) that heat and moisture transfer in the water vapour phase were the major causes of deviations from the predicted performance of the HCB. Ohnishi (1988) concludes that the effects were more significant to moisture transfer and mechanical effects than to heat transfer and temperature distributions.

Table 2-9 Measured and predicted values of temperature at the mid-section of the heater under power outputs of 600 W at various times after the initiation of the BMT.

Hole No.	Heater power W	Lapsed time	Temperature at heater * °C	Temperature at rock/buffer* °C
1 (wet)	600	2.4 years	65/68	35/36
2 (wet)	600	3.1 years	60/75	38/42
3 (dry)	600	1.0 years	79/71	33/35
4 (dry)	600	0.9 years	81/71	33/34
5 (wet)	600	1 week	70/56	30/27
		10 weeks	70/62	32/32
		1 year	66/64	33/34
		2.2 years	63/64	34/34
6 (dry)	600	1 week	78/62	30/27
		10 weeks	83/69	34/32
		1 year	84/70	35/34
		2.1 years	81/71	35/35

* First value is measured / second value is predicted.

A retrospective analysis of the temperature fields observed in the wet hole (see Table 2-9 for hole No.5) indicates that the moisture redistribution observed in the dry holes initially occurred in the wet ones (i.e. moisture was driven away from the heater towards the rock under the temperature gradient). This was followed by a general resaturation of the buffer resulting from water influx from the rock. In both the wet and the dry holes, it appears that the local effects of water availability that were predicted using isothermal moisture transfer equations (see Figure 2-11) were largely masked by the effects of thermo-osmosis and vapour transport. The dominating influence of thermo-osmosis and vapour transport in dry holes became fully evident during the first excavation of hole No. 3. A modified heat conductivity model was used to estimate the temperatures expected during the high power test. This "series" model included buffer elements with different thermal conductivities. The thermal conductivity (λ) of saturated HCB was assigned a value of 2.0 W/m°K as opposed to the value of 1.4 W/m°K used in preliminary analyses (see Table 2-3). It appears that the use of laboratory derived values of λ led to an underestimate of field performance and that this difference may have accounted for the separation between measured and predicted final temperatures in the wet holes. Figure 2-22 shows for the new model that the numerical results fitted well with the measured values. The appreciation of the moisture distribution in the buffer provided by the BMT allowed for this numerical solution. The solution cannot be applied readily to conditions other than those encountered at Stripa in the BMT.

Water uptake by the room backfills was not complicated by high temperatures and temperature gradients. Testing during the excavation of the backfills was interpreted (Pusch et al, 1985a) as showing that the bottom 3 m of the lower 10/90 bentonite/sand backfill was virtually water saturated - isolated pockets of compressed gases (air) were enveloped in a saturated mass. The periphery of the backfill next to the walls and back of the room were also saturated to thicknesses ranging from 0.5 m in the 20/80 bentonite/sand upper backfill to 2 to 3 m next to the walls. The saturation profile through a cross-section of the backfill above hole No.1 is shown in Figure 2.23 along with the water pressure in the near-field rock above holes 1 and 2. The total water taken up by the backfill exceeded by a factor of approximately two the

quantity determined from the inflow measurements into the open excavations.

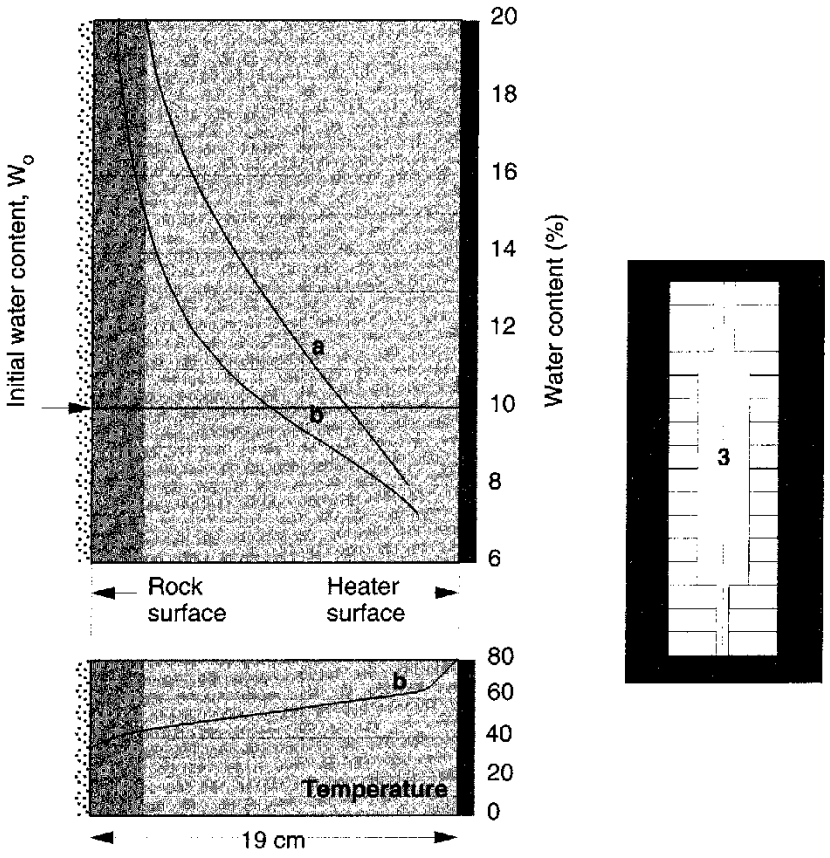

Figure 2-21 Water content and temperature distributions at cross-sections (a) and (b) at the end of the 600 W test in hole No.3 (from Pusch et al,1985a). W_o is the original water content.

The water uptake results in the backfills were reasonably consistent with the results of calculations based on isothermal moisture transfer shown in Figure 2-13(b) for water inflow from the whole tunnel surface. The discrete water bearing fractures intersecting the room did not appear to cause significant local variations in saturation conditions. This was accounted for by the mechanical interactions between the backfill and the rock (see section 2.7.3 and Pusch et al, 1985a). The recorded water pressures in the near-field rock mass were considered to be less than those that could be anticipated from the SAC macropermeability test results and consistent with an hydraulic gradient downwards from the end of the room towards the confining bulkhead. The low measured pressures were attributed to the following two possible causes: the high suction (low potential) in the bentonite-based backfill - this is similar to the effect of bentonite pellets on piezometers noted in section 2.5; and, the connectivity of the excavation disturbed zone (EDZ); this was particularly pronounced in the floor of the room where water flowed along the EDZ longitudinally towards the open parts of the excavation. In the latter context, the rates of inflow into boreholes No.3 when the hole was open were observed to be less after the excavation of the backfills than prior to it. These observations provided the basis for initial analyses on the properties of the

EDZ which were studied extensively during Phase 3 of the Stripa Project. The pronounced anisotropy in the hydraulic properties of the EDZ was found to be significant to both the engineered and natural barrier investigations.

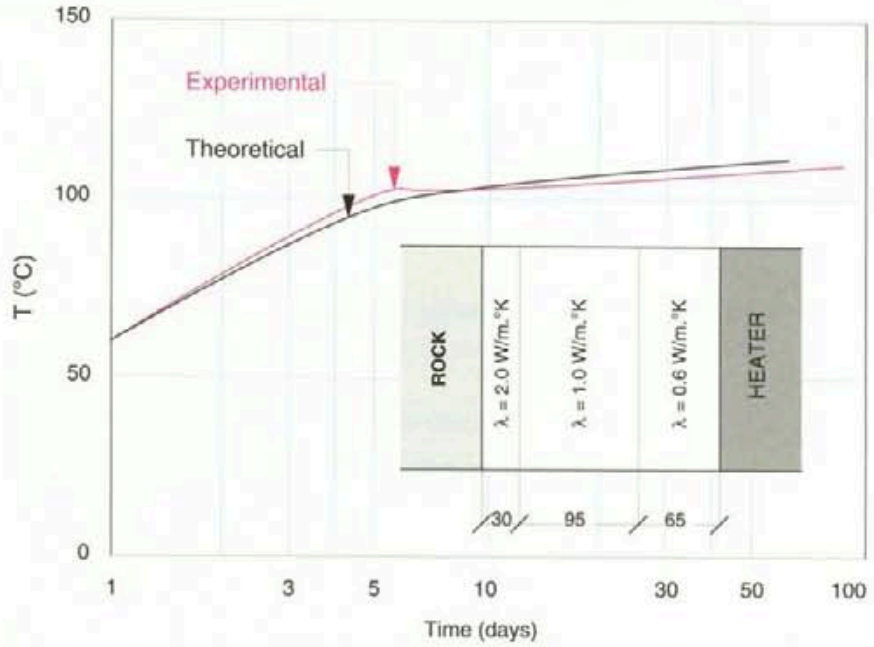

Figure 2-22 A comparison between measured temperatures in the high power (1200 W) test in hole No.3 with values predicted using a revised conductivity model.

2.7.2 Swelling and swelling pressures

The changes in moisture content in the HCB were associated with variations in total pressure in the buffer mass and at the buffer/rock and buffer/backfill interfaces. These were measured in each of the holes by ten Gloetzl cells located as shown in Figure 2-24. The values measured with time by each of the cells in hole No.1 over the full duration of the test are also shown in the figure. Table 2-10 presents the maximum value recorded on each of the cells in all the holes. The values in the table are interpreted to the nearest 100 kPa from the data provided by Pusch et al (1985a). In almost all cases the tabulated values are the final ones measured: swelling pressure tended to increase continuously with time over the period of the test as shown for hole No.1 in Figure 2-24.

The data show that higher swelling pressures were recorded from the wet holes. The maximum values recorded in hole No.2, exceeding 10 MPa, compare well with the values predicted from the laboratory measurements. In the wet holes, the cells used to measure vertical pressure (Nos. 1 to 4) tended to indicate lower pressures than those used to measure lateral pressure (Nos. 5 to 10), with cells 1 and 2 tending to indicate higher pressures than cells 3 and 4. A number of explanations are possible for these differences. These include the following: differential wetting of the HCB arising from temperature gradients - results from the 1400 W test in hole No.1 (Figures 2.65 to 2.67 in Pusch et al, 1985a) tend to indicate drier material nearer the heater; a higher degree of saturation in the HCB at the bottom of the holes -

the pilot holes extended beneath the emplacement holes and were known in some cases, e.g. hole No.5, to provide access to a source of flowing groundwater, and gravitational potentials may have caused water to flow downwards in the annular space at the periphery of the wet holes; and, as described in section 2.3.5, movement at the buffer/backfill interface under the applied swelling pressure. The latter mechanism is emphasized by Pusch et al (1985a).

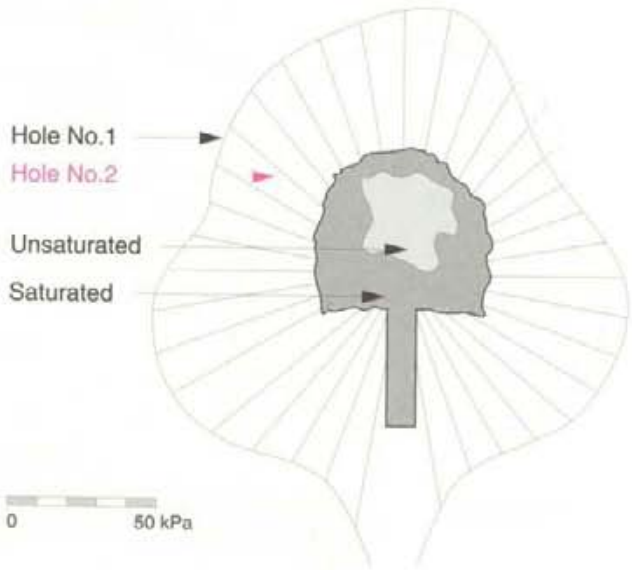

Figure 2-23 Moisture content distribution in the backfill in the cross-section above hole No.1, and water pressures at the backfill/rock interface in the cross-ections above holes Nos. 1 and 2 at the end of the test.

The horizontal pressures acting on the walls of the wet boreholes were remarkably even. Within each of the holes, given consideration of the accuracy of the instruments, the maximum values indicated by cells 5 to 10 were virtually indistinguishable. This conforms with the water uptake and redistribution data presented previously and may be taken to indicate that inflows from discrete fractures intersecting the boreholes were secondary to the overall influx and the effects of thermo-osmosis and the transport of water in the vapour phase.

The slow moistening of the buffer in the dry holes accounts for the lower pressures measured at these sites. Low pressures were measured even at the HCB/rock interface, where the buffer was saturated. No measurements are available to confirm that the rock in contact with the buffer remained saturated nor is it clear that the HCB swelled sufficiently to completely fill the borehole and thus allow for the transmission of stress. Both of these factors could account for the low measured pressures.

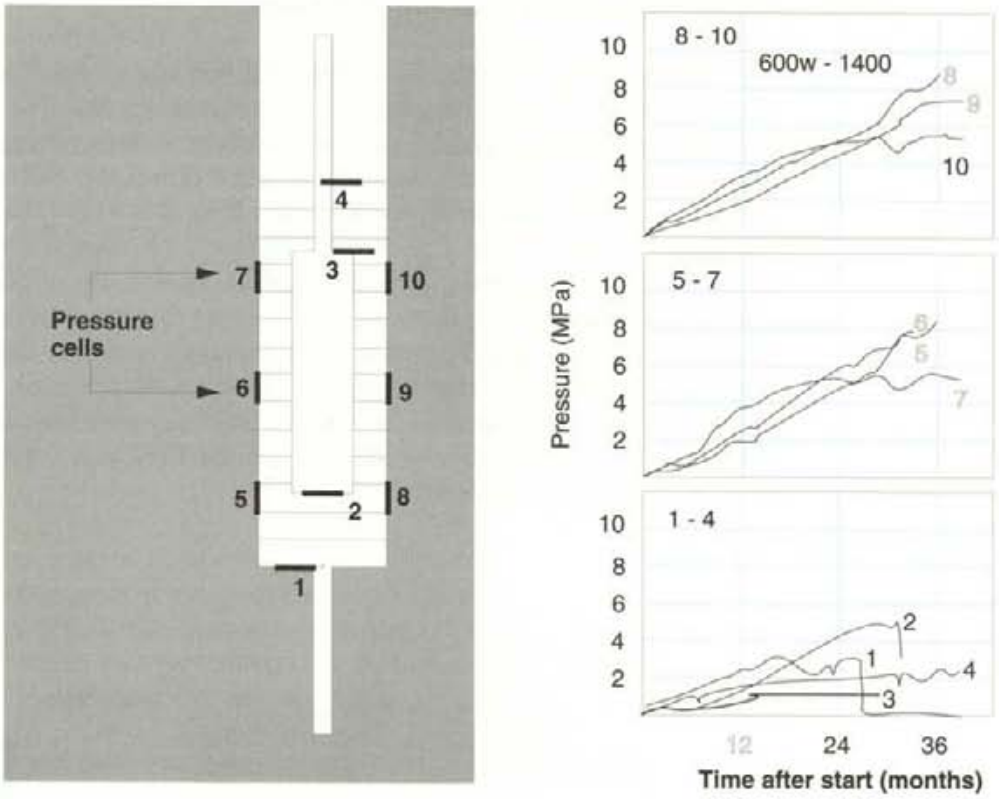

Figure 2-24 Location of Gloetzl total pressure sensors in the borehole with recordings made for hole No. 1.

Table 2-10 Maximum pressures recorded from the Gloetzl total pressure sensors during the 600 W test.

Hole No.	Maximum recorded pressure (MPa)									
	Pressure sensor location No.									
	1	2	3	4	5	6	7	8	9	10
1 (wet)	3.0	5.0	1.0	2.0	5.0	6.8	5.3	6.0	5.2	5.2
2 (wet)	4.0	6.8	1.0	2.1	10.4	*7.8	*5.2	10.8	10.2	*5.0
3 (dry)	1.8	0.4	0.5	1.2	0.4	0.4	0.8	0.4	0.1	0.8
4 (dry)	1.0	0.4	0.4	0.8	0.6	0.1	0.2	0.3	0.1	0.1
5 (wet)	*5.0	4.0	0.6	1.8	5.0	4.6	3.9	3.5	3.5	3.5
6 (dry)	0.6	0.5	0.2	0.8	0.5	0.3	0.8	0.5	0.3	0.8

* Instrument failed prior to test completion.

2.7.3 Mechanical interactions and processes

The measured heave of the buffer/backfill boundary varied between 40 and 70 mm with the maximum value being measured in hole No.1 (a wet hole with the longest test duration) and the minimum value being measured in hole No.4 (a dry hole with the minimum test duration). Although the values tend to be higher than predicted for holes Nos. 3 to 6 and lower than predicted for holes Nos. 1 and 2 (see Figure 2-15) they are of the same order of magnitude as the predictions and tend to confirm the applicability of the simple deformation model used. It is evident that, as predicted, the backfill above holes Nos. 1 and 2 acted as an adequate restraint to the buffer material. In the wet holes 2 and 5 the heave was concave (Pusch et al, 1985a) with greater upward movement at the rock/buffer boundary than along the axis of the hole. The higher rate of water flow in the EDZ was considered to account for this phenomenon.

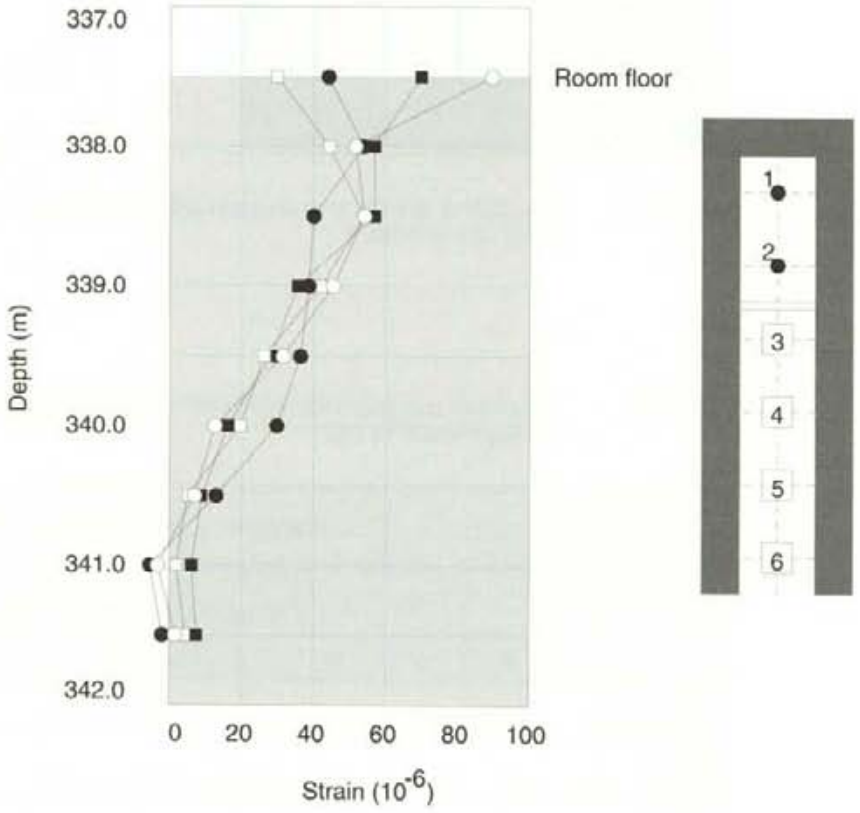

Figure 2-25 Vertical strain in the rock around hole No.5.

The vertical strains recorded in the near-field rock mass around hole No.5 are shown in Figure 2-25. The data points are mean values derived from four reading cycles during the progress of the experiment. This plot is possible as the readings did not vary significantly within the accuracy of the instrument once the initial heave caused by the thermal perturbation of the rock mass had occurred. The results are remarkably consistent for all four of the instrument holes which were drilled across two diameters set at right angles on a circle

1 m in diameter centred on the vertical axis of the emplacement hole. Effects arising from a fracture with a dip of approximately 60 degrees and intersected by instrument holes Nos. 1 and 3 cannot be discerned from the data. Predictions of the extent of heave of the rock were not available nor, indeed, possible other than by broad evaluation. The effects of the heave on the water carrying characteristics of the fractures could not be established during the BMT. However, the thermally induced heave was also observed during the engineered barrier studies for Phase 3 of the project in which it was shown to have significant influence on the function of some engineered barrier materials.

The fractures intersecting the excavations were examined after the buffer and backfills had been removed. There was clear evidence of the penetration of the bentonite and bentonite/sand mixtures into the intersecting fractures (see Figure 2-26). It was not possible to measure the depth of penetration or the density of the bentonite in the slots. However, the observation partly reaffirmed the observations made from the laboratory slot tests described in section 2.3.5. There was no visible evidence of erosion of the bentonite.

Figure 2-26 Penetration of swelling bentonite into fractures in the rock.

It was concluded (Pusch et al, 1985a) that the self injection of the bentonite into the fractures was a control on the rate of water uptake by the clay sealants from the rock. Insofar as the injected bentonite has hydraulic conductivities less than or equal to the intact rock mass and penetrated fissures as fine as 0.1 mm, the injection process developed a thin skin of self-sealed, porous medium around the HCB through which water had to pass to reach the clay mass. This phenomenon combined with the effects of the temperature gradients was used to account for the evenness of water uptake by both the HCB and the backfills.

2.7.4 Additional tests and observations

The installation in hole No.5 included filters at the rock/buffer and heater/buffer interfaces. The filters were originally included to provide for the possibility of carrying out chemical diffusion tests in the buffer. Due to the complexities encountered in the interpretation of moisture transfer phenomena, the filters were used to carry out tracer tests intended to clarify relevant physical processes acting in the buffer mass. Methylene blue was

released from the filters at the buffer/rock interface to trace water flow. Hydrogen sulphide (H_2S) was released at the buffer/heater interface to trace vapour transport. The H_2S was expected to react with the small quantities of iron in the HCB and thereby discolour (blacken) the buffer. The methylene blue maintains its colour in the bentonite. The areal extent of staining of the buffer caused by the H_2S/Fe reaction and the methylene blue could be identified during excavation of the borehole and used to define the limits of acting processes. The tracers were released without elevated pressures shortly before the test in hole No.5 was terminated.

Observations made during the excavation revealed that the methylene blue was confined to very short distances from the points of injection. In contrast, the H_2S had migrated distances of up to 30 mm from the source at the base of the heater and up to 60 mm from the source at the top of the heater. The discolouration caused by the FeS was localized. The lack of movement of the methylene blue reflects the very low diffusion coefficient of large organic molecules in compacted bentonite and is consistent with a high degree of saturation and maturity[11] of the HCB. The zones of blackened bentonite may be considered to reflect an unsaturated vadose halo around the heater in which moisture and heat are transferred in an evaporation/condensation cycle. The moisture contents measured in the HCB were considered to be too high to support this suggestion (Pusch et al, 1985a). In this context it is pertinent that the tracers were injected while the heaters were operating and the moisture content determinations were made on cooled material. Insufficient data are available to precisely define the processes.

It had been speculated that the cyclic movement of water under the evaporation/condensation cycle could give rise to the transfer of salts in the buffer which may be deleterious to repository performance by creating corrosive conditions near the waste-container. Measurements of soluble salt concentrations in buffer materials recovered from the hole No. 5 showed no evidence to support the suggestion. However, it is noted that hole No.5 was wet and the period over which the cyclic processes operated was limited in duration.

The HCB was applied as blocks. Thus, as placed, the buffer masses contained known discrete vertical and horizontal discontinuities. During excavation of the wet holes it was observed that these possible flow paths had virtually disappeared. The buffer mass had swelled to become a self-sealed continuous "welded" body. In the dry holes the discontinuities could still be discerned during excavation and had been supplemented near the heaters by radial cracks caused by drying shrinkage. These cracks may have provided rapid pathways for vapour transport. Examinations of the microstructure of the clays sampled from the test holes (Pusch, 1985) showed no significant changes in the crystal structure of the clays. There was no reason to suppose that the construction joints or the shrinkage cracks in the dry holes would not be sealed by swelling of the HCB once sufficient water was present. This is discussed further in Chapter 5 of this review.

---

11 The fabric of bentonite is dynamic and changes as it wets. A mature bentonite is one in which the original tactoids formed in nature and during manufacture are expanded to their limit through inter-particle separation forces.

3 PHASE 2 - 1983 TO 1988 BOREHOLE, SHAFT AND TUNNEL SEALING TESTS

3.1 BACKGROUND AND SCOPE

Siting a repository for long-lived, heat-generating radioactive waste will require thorough investigation of the rock mass. Despite the significant advances made in geophysical investigation methods, through the international Stripa investigations and other programmes, it remains clear that the site investigations will include the penetration of the rock mass by investigation boreholes. These may be used for geological characterization exercises and for hydrogeological or geophysical studies related to total system performance assessment. Most preliminary designs for repositories in saturated granite masses are based on the assumption that investigation boreholes, like the shafts and tunnels used to develop and access the disposal levels of a repository, if left unfilled during repository closure, may act as preferential pathways for radionuclide migration and release. Phase 2 of the Stripa Project focussed on methodologies for sealing these possible pathways in mined repositories.

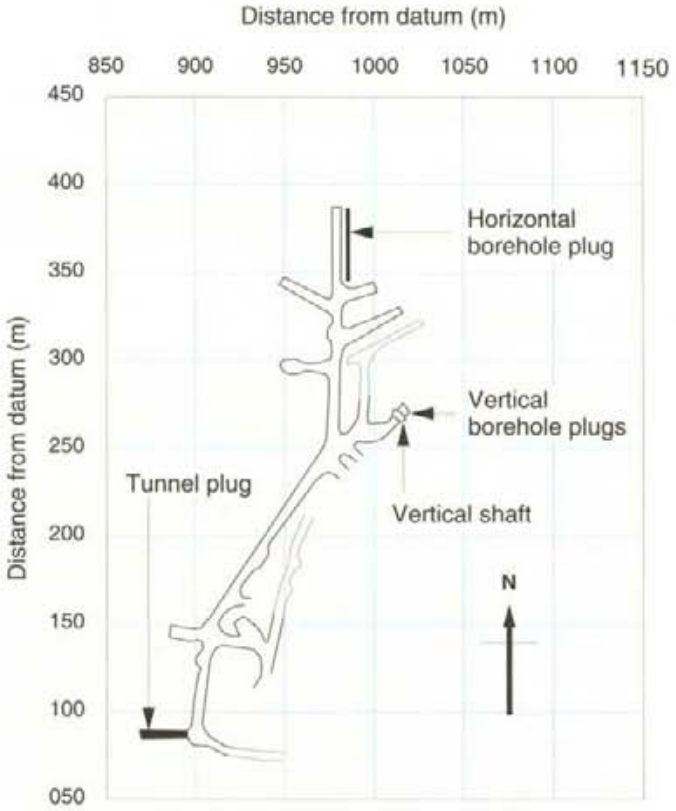

Figure 3-1 The locations of the borehole, shaft and tunnel seal tests.

Building on the experience gathered in Phase 1 and following the general approach being developed for repository sealing by SKBF of Sweden, the studies focussed on investigating the suitability of highly compacted bentonite (HCB) for sealing boreholes, shafts and tunnels.

The tests were carried out in the rock mass at the 340 m level of the mine near the BMT drift at the locations shown in Figure 3-1. For all three tests the objectives were as follows:

- demonstrate the ability to effectively emplace clay seals;
- observe the maturation of HCB with water uptake and compare the results with water uptake models developed during the conduct of the BMT;
- make observations on the effectiveness of the seal at the rock/clay interface.

Subsidiary to the third objective, observations were to be made on the ability of the HCB to penetrate and seal fractures in the rock intersected by the openings. Moreover, the effects of erosion on the effectiveness of the clay seals and the influence of clay swelling on the hydrology of the adjacent rock mass were to be examined.

Unlike the BMT, no heat was to be applied to the borehole, shaft and tunnel seals. For disposal concepts such as that presented by SKBF (KBS-3, 1988) borehole, shaft and tunnel seals will be placed some distance away from the waste packages. Although in some cases the seals may exist at elevated temperatures, temperature gradients will be small and are not expected to have a significant influence on the performance of the clay.

3.2 BOREHOLE SEALING TESTS

Complete details of these tests are provided by Pusch et al (1987a). Major points salient to this review of the work are presented in this section.

3.2.1 Test configurations

Three borehole plugging/sealing tests were carried out. Each test was configured to allow for different aspects of borehole plugging with HCB to be investigated.

In all of the tests HCB was introduced into smooth walled, diamond drilled boreholes and observations made on the rate of maturation (water uptake and swelling) of the HCB, the resistance of the maturing bentonite to piping under hydraulic gradients (with particular interest in the development of oedema within the bentonite body) and, the mechanical characteristics of the bond between matured bentonite plugs and the borehole wall. The differences between the three tests lay either in the orientation of the borehole - one horizontal borehole and two vertical ones were sealed - and in the type of plug used - one vertical borehole was plugged using techniques which were virtually identical to those used in the horizontal borehole, the sealing system used for the second vertical borehole differed.

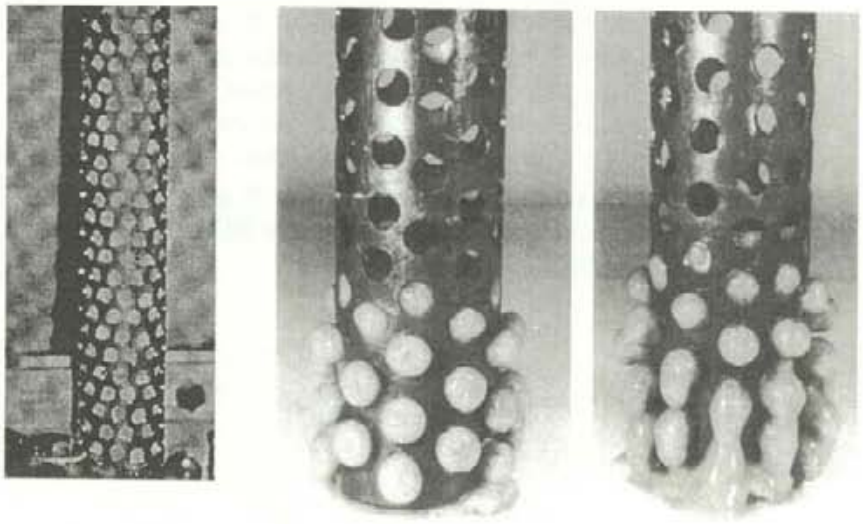

Figure 3-2 (a) HCB contained within a perforated copper sleeve, and the effects of immersing the sealing system in water for (b) 8 hours and (c) 24 hours showing the extrusion of the bentonite through the perforations.

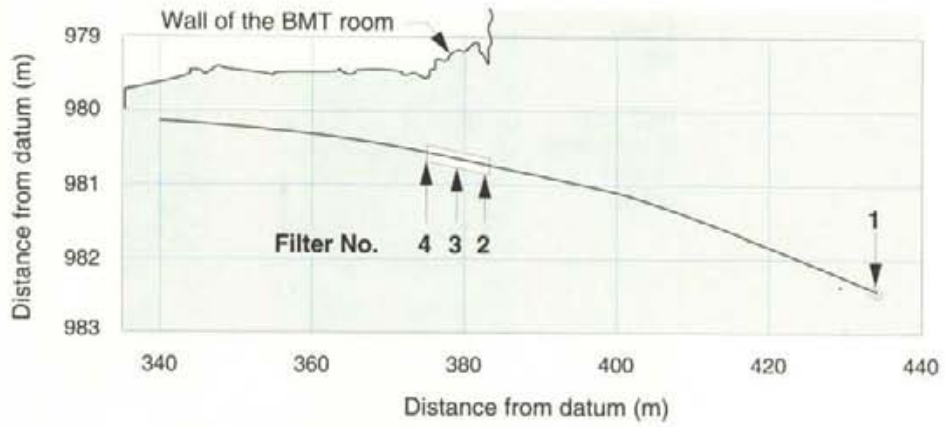

Figure 3-3 Location and layout of the horizontal borehole plugging test in DbH2.

The sealing system in all cases consisted of hollow cylinders of HCB encased in an exoskeleton of perforated copper or steel. The system used for the horizontal borehole test is shown in Figure 3-2(a). The exoskeleton was needed to provide rigidity to the system as it was introduced into the borehole and, thereby, assure the physical integrity and quality of the sealing system. The perforations were required to allow water to access the HCB, causing the material to swell and seal unfilled sections of the boreholes. This process is seen in Figure 3-2 (b & c). For the vertical borehole plugging tests, the perforation/solid ratio in the tubing was varied between the two tests. In one test (coded Ib), as previously noted, the perforation/solid ratio was identical to that of the sealing system used in the horizontal plug. In the other vertical test (coded Ic), a steel wire mesh was used to hold the HCB. With a significantly higher perforation/solid ratio the wire-mesh system might be expected to mature more quickly than the system confined in the copper tubing. However, the benefits of an increased rate of maturation had to be measured against practical difficulties in placing the more flexible, wire mesh plug.

The central axial hole in the hollow HCB cylinders allowed for copper tube connections to be run along the centre and length of the sealing system. These connectors added rigidity to the system and doubled as conduits for the wiring and hydraulic tubing needed to connect instruments to monitoring equipment and to feed water to different elements of the test arrangements. Thus, to prevent axial water flow along the length of the plug, the HCB was not only required to seal against the borehole wall but also against the inner copper connecting tube.

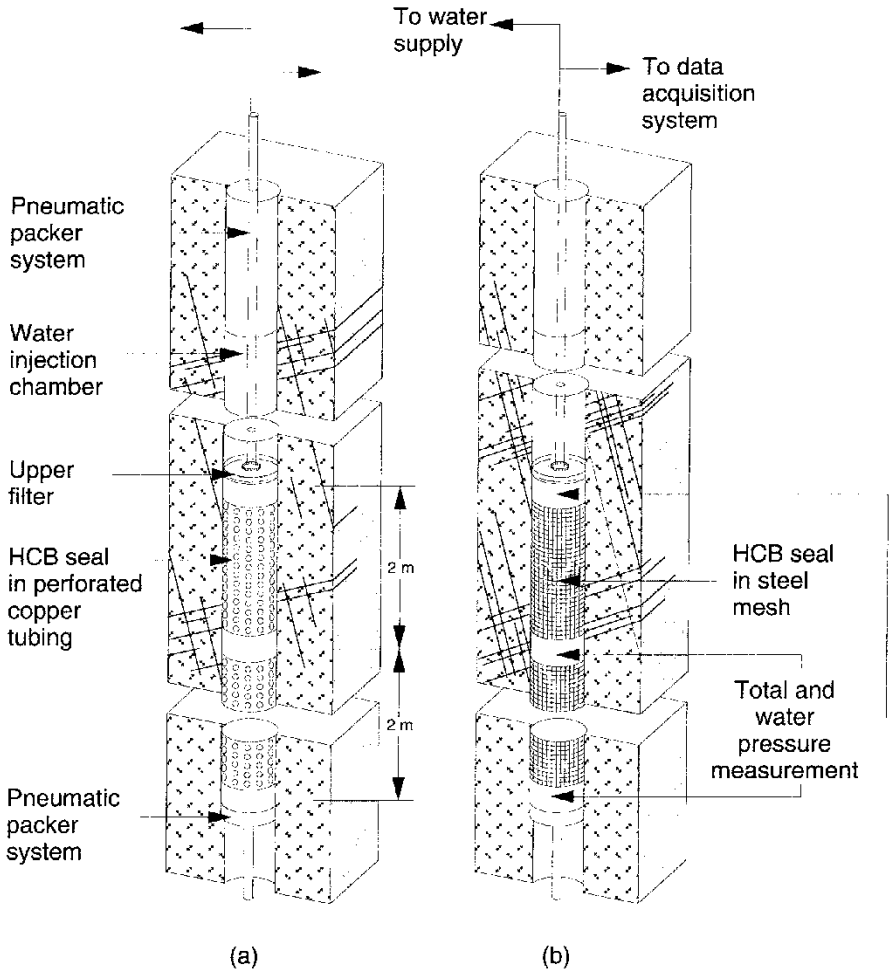

Figure 3-4 Layout of the vertical borehole sealing tests.

The horizontal borehole plugging test was carried out in the 96.6 m long, 56 mm diameter borehole DbH2 that was drilled as part of the SAC macropermeability experiment. Shown in Figures 3-1 and 3-3, the hole in part runs approximately parallel to and continues 50 m beyond the end of the BMT drift. In the region of the BMT drift the hole generally lies 1 to 1.5 m from the drift wall (that is within a zone of rock expected to have been disturbed by the excavations). At this location, hydrogeological conditions in the rock mass were not clear and the rates at which the HCB would take up water from the rock were uncertain. Analyses of the core from the drillhole and the information available from the macropermeability test and BMT results discussed in Chapter 2 indicated that the hydraulic conductivity of the rock could be assigned values in the range 10^{-12} to 10^{-10} m/s. Once sealed, pressures in the

vicinity of the borehole were anticipated to rise to values in the range 100 to 300 kPa (see Figure 2-18). Four filters, shown as 1 to 4 in Figure 3-3, were installed within the bentonite plug. These filters allowed for water to be injected into the plug at the preselected locations and the changes in water pressures at these locations to be monitored with time and test conditions. Filters 2 to 4 were located conveniently for excavation after the completion of the test. This allowed for visual examination of the physical condition of the matured bentonite. The inner 87 m of the borehole was to be plugged using an HCB system with an external diameter of 54 mm (giving an annular clearance from the borehole wall of approximately 1mm). The remaining outer 9.6 m of the borehole was to be filled with a cement grout which, when hardened, was to act as a virtually rigid restraint to the swelling HCB.

Table 3-1 Initial and expected final conditions of the HCB used in the borehole sealing experiments.

	As fabricated (S<100%)				After maturation (S=100%)		
Borehole	ρ_b Mg/m^3	w %	ρ_c Mg/m^3	S* %	ρ_b Mg/m^3	w %	ρ_c Mg/m^3
DbH2 horizontal	2.11	11	1.90	71	1.90	32	1.44
Vertical (lb)	2.10	10	1.91	66	1.82	40	1.30

* S based on a specific gravity of 2.70 for MX-80 bentonite.

The vertical borehole plugging tests were carried out in two 14 m long, 76 mm diameter boreholes that were specially drilled between two vertically separated, parallel tunnels at the location shown in Figure 3-1. The layout of the two tests is shown in Figure 3-4. The copper casings had a diameter of 68.6 mm leaving an annular clearance between the sealing system and the borehole wall of 3.8mm. Each of the bentonite plugs was equipped with specially designed combined pore-water pressure and total pressure sensors at locations 1 to 6 shown in Figure 3-4. The design and function of these devices is discussed in connection with the test results in section 3.2.3. These devices were intended to provide information on the rate of maturation of the bentonite as the material drew water from the rock. Later in the tests, the instrumentation was intended to provide information on the piping resistance of the bentonite as water pressures were increased in the water-filled spaces between the HCB sealing systems and the inflatable rubber packers that were used to close the upper sections of the boreholes. Despite their close proximity to each other, the hydrogeological conditions differed between the test boreholes. Water pressure injection tests using 1.2 m packed-off sections of the boreholes showed that the boreholes intersected two major, inclined, hydraulically conductive fracture sets separated by a vertical distance of approximately 1.5 to 3 m. The lower fracture set was approximately 2 m thick and more conductive than the upper set. The 4 m long HCB sealing systems were aligned to

straddle the lower fracture sets. The injection chamber was configured to be intersected by the upper fracture set. This configuration was chosen in order to enhance the rate of maturation of the HCB by the higher natural water inflows from the fracture sets and to increase the groundwater pressures in the vicintiy of the boreholes. In this latter respect, no data were available of the hydraulic pressures and flow conditions in the rock mass intersected by the boreholes. It was presumed that the pressures had been relieved by the previous excavations in the vicinity of the test area. In light of the results from the BMT room this assumption cannot be entirely confirmed.

The same bentonite, MX-80, as that used in the BMT was used to fabricate the borehole plugs. The densities and water contents of the materials at fabrication of the seals incorporating the perforated copper tubing are shown in Table 3-1. Calculated values of density and water content after complete maturation and homogenisation of the clay are also given. These latter values are based on data provided by Pusch et al (1987a) and allow for the solid volumes occupied by the copper tubing and connectors. The initial densities of the clays used in the wire-mesh sealing system were within the range shown in the table. Final dry densities of the homogenised , matured HCB could be expected to be lower and final water contents could be expected to be higher in the borehole sealed with the wire-mesh system. Average hydraulic conductivities and swelling pressures for the matured bentonites can be taken from Figures 2-9 and 2-15 to be approximately 10^{-13} m/s and 1.5 MPa, respectively.

3.2.2 Schedule, installation and sequencing

Significant event dates for the conduct of the borehole sealing experiments are given in Table 3-2. The testing programme overlapped the programme for the Buffer Mass Test (see Table 2-8). This affected the completion of the excavations associated with the horizontal plug test which were delayed until August 1986. At this time all of the Phase 1 *in situ* activities associated with the BMT had been completed.

Table 3-2 Significant event dates for the borehole sealing tests.

Borehole	Seal installation date	Natural maturation period	Hydraulic testing period	Excavation or extrusion
DbH2 horizontal	1983, June 7	14 days	1983, June 15 to July 6	1986, February
Vertical Ib	1983, August	3 days	August 1983 to Dec. 1984	1985, July
Vertical Ic	1983, August	3 days	August 1983 to Dec. 1984	1985, July

The horizontal plug was installed into the naturally draining DbH2 borehole (the borehole was slightly inclined to permit drainage). A 10 kN capacity hydraulic jack was sufficient to install the 87 m long instrumented plug in a pe-

riod of less than 2.5 h. The installation process was complicated by the instrumentation cabling and hydraulic tubing. It was estimated that without these complications the plug could have been installed in less than an hour. The ease with which the installation was effected demonstrated the practicality of the design of the bentonite plugging system. Within two days after installation, the hydraulic tubing connected to filters 1 to 4 were flooded with naturally flowing groundwater . The tubing and sealing system was locked off and the consequent increase in groundwater pressures at the filter locations was monitored. Within 15 days the water pressure in filter No.1 located at the distant, inner end of the plug had risen to 1200 kPa. Approximately 50 m away filters 2, 3 and 4 were registering pressures of 0, 0 and 400 kPa, respectively, corresponding to a maximum hydraulic gradient of 16 between filters 4 and 3. With these conditions stabilized a series of rapid pressure tests were carried out in filters 2, 3 and 4. In general the pressures in one filter were increased in steps and the pressure or water flow response in the other filters recorded. Subsequent to these tests, the hydraulic tubing was locked-off and water pressures in the filters were monitored continuously until final excavation of the rock and plug section containing filters 2,3 and 4.

The vertical borehole plugs were installed into holes Ib and Ic which had been packed off at the bottom with rubber packers and allowed to fill with groundwater. While special care and attention was needed for the installation of the wire-mesh plug in hole Ic, the perforated-copper-tube sealing system used in hole Ib was readily emplaced. Pusch et al (1987a) made specific note of the practical difficulties that could be expected in placing the wire-mesh plug in an upwardly inclined borehole and indicated that such operations would be particularly difficult in a plugging system that did not contain the central copper tube core. With the plugs installed the upper rubber packers were inflated to create and bring into service the upper water injection chambers. In general the pressures in the chambers were increased progressively and the flows required to maintain the chamber pressure were monitored along with the total and water pressures recorded by the gauges installed in the sealing systems. At the end of the hydraulic pressure testing, and with some attempts being made to ensure similar degrees of maturity in the bentonite throughout the length of the plug, the rubber packers were removed and the mechanical forces required to extrude upwardly the bentonite plugs from the boreholes were measured. After extrusion the plugs were examined and then sectioned. The water contents of the sections were determined to provide an indication of the physical condition of the matured bentonite along the length of the plugs. Moreover, measurements of water contents and other observations were made to determine any differences between the physical condition of the bentonite that remained within the copper tubing and the bentonite that had been extruded into the annular space between the tubing and the borehole wall.

3.2.3 Results and discussion

While keeping the other filters water saturated but drained, water pressure was increased alternatively in filters 2,3 and 4 in the horizontal borehole plugging test and the pressure at which a break in the bentonite seal occurred was recorded. Failure of the seal was identified by either a sudden increase in the flow into the injection point or an increase in pressure or flow at other locations in the plugged borehole. Table 3-3 shows the pressures and approximate hydraulic gradients at which the plug failed.

Table 3-3 Results of injection tests from the horizontal borehole plugging experiment.

Injection filter No.	Failure condition*	Observations
2 (Test 1)	1.4 (56)	Sudden inflow into the filter.
2 (Test 2)	2.0 (80)	Pressure increase in filter No. 3.
3	4.5 (40)	Slight flow into the filter occurred at 1 MPa. At 4.5 MPa leakage through the cement plug occurred.
4 (Test 1)	2.0 (80)	No failures observed.
4 (Test 2)	5.0 (200)	Inflow into filter No. 4. Flow from filter No. 3.

* First value gives water pressure in MPa, value in brackets is the minimum hydraulic gradient.

The results show that the segment of the borehole plug between filters 3 and 4 provided a greater resistance to flow than that between 2 and 3. This was considered to reflect the natural flows into the open borehole which, as evidenced by the build-up of natural water pressure in this filter, were greatest close to filter number 4. It was concluded that insufficient time had elapsed between installation and hydraulic testing to allow for full water uptake by and expansion of the HCB in the segment between filters 2 and 3. With this suggestion, the gradients sustained by the plug segment between filters 3 and 4 can be taken as minimum values sustainable by a fully matured bentonite borehole plug.

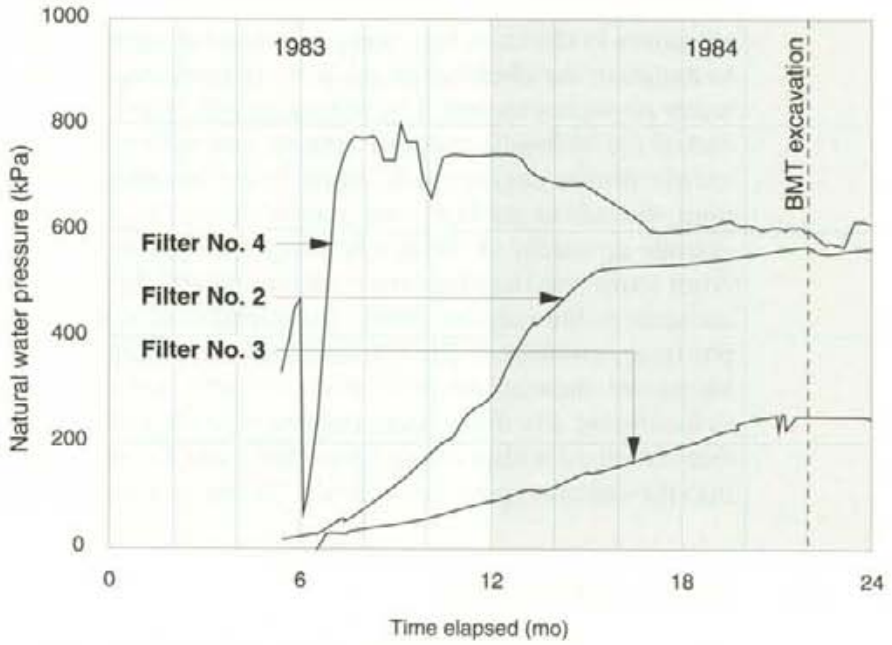

Figure 3-5 Rise in natural water pressure with time in filters 2,3 and 4 in the horizontal borehole plug.

During the pressurization of filter 3 flow occurred in the inner copper instrumentation tubing. Thus, the results from this test cannot be used in the interpretation of plug performance.

After the hydraulic testing, the natural water pressure rise in the filters was monitored for almost two years. The results, presented in Figure 3-5, showed a much more rapid rise in the groundwater pressure in filter 4 than in filters 2 and 3 which, it was suggested, tended to confirm that the rock surrounding filter 4 was more water bearing than that around the other filters. The lack of response in the water pressures when the backfill in the BMT drift was removed indicates that the water bearing features were not well connected to the BMT drift. The maximum pressures measured in the filters fit well with the heads recorded in the rock during the SAC macropermeability experiment (see Figure 2-18) and further endorse the concept of an excavation response zone around the drift with a lower average radial conductivity than that of the undisturbed rock.

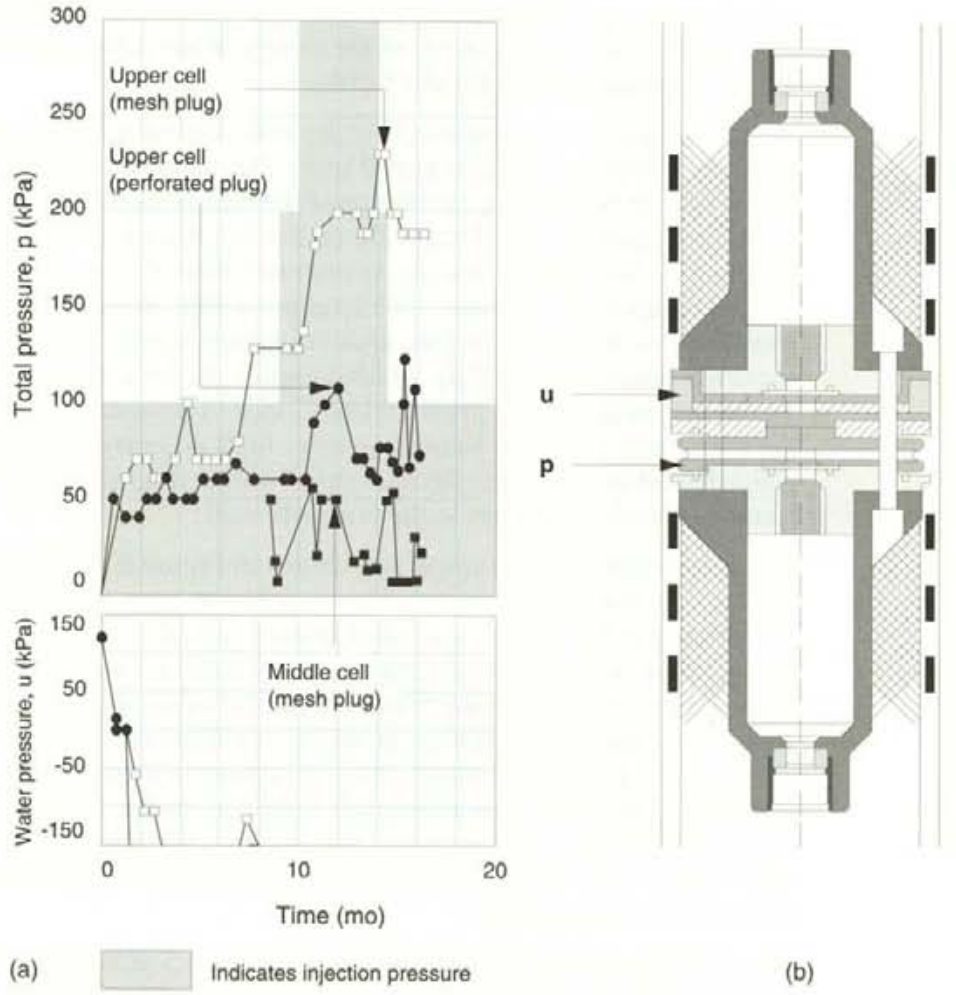

Figure 3-6 (a) Changes in total and pore water pressure with time and changing pressures in the upper chambers in the vertical borehole plugging tests; and (b) details of the design of the instrument used to measure total and pore water pressures in the maturing HCB plugs.

Simple porous medium radial flow modelling of the borehole and the surrounding rock mass, which was ascribed an hydraulic conductivity of 10^{-13} m/s, showed that the total flow rate into an open borehole would be approximately 8 ml/d. This was more than sufficient to completely saturate the HCB

plug within the period of the test. In contrast, a discrete fracture flow model, allowing for the observed distribution of natural fractures intersecting the borehole and diffusive water flux into the HCB at a rate prescribed by the laboratory measured diffusion coefficient of 4.10^{-10} m^2/s, indicated heterogeneous wetting of the HCB and incomplete saturation in the period of the test. Examination of the recovered plug showed that it was saturated.

Figure 3-6(a) shows the total and pore water pressures measured during the hydraulic testing of the vertical borehole plugs. The recorded total pressures are consistently less than the pressures in the water chambers and, being lower in instrument number 5 than in instrument number 6, tend to show a decrease with increasing distance from the pressurized water chamber. Moreover, the measured pore water pressures rapidly decreased to values below atmospheric and never recovered from these low values despite increases in the chamber pressure. This is particularly significant for instruments 3 and 6 which were close to the upper water-filled pressure chambers. The responses can be understood through examination of the design of the instruments used. This is shown schematically in Figure 3-6(b).

Total pressure was measured using the components marked p in Figure 3-6(b), pore water pressure was measured using the components marked u. Both measuring systems relied on the transfer of pressure through a water filled chamber to electrical resistance fluid pressure transducers. The fluid filled cell for the total pressure measuring system was encased in a flexible, impermeable neoprene/rubber membrane. The total pressures acting on the outside of the membrane were transferred through the membrane to, within the range of expected pressures, virtually incompressible de-aired water in the cell and acted on the membrane of the pressure transducer. The water in the cell measuring the pore water pressure, through porous, high-air entry, stainless steel filters, was allowed to come into direct contact with and adopt the pressure in the water in the clay and next to the borehole wall.

The pore water pressure responses shown in Figure 3-6(b) show that high suctions existed in the system. This is common in unsaturated clay media and particularly in bentonite, is a manifestation of both low capillary (matrix) and, low osmotic potentials in the clay water. The free water in the test cell tended to be drawn out through the filters. When pressures reached about -85 kPa the water in the measuring system probably cavitated and was released to the bentonite. This desaturated the measuring system and rendered the instrument inoperable. The water pressures used in the test appear to have been insufficiently high to restore function to the system. The measured pore water pressure response thus followed the path expected from understanding of the behaviour of bentonite clays.

The responses in total pressure shown in Figure 3-6(a) indicate that the clay seal was able to sustain an hydraulic gradient of about 10 or more. In this context it is recalled that the minimum hydraulic gradient for piping recorded in the horizontal borehole plugging tests was about 40. Thus, the results from the vertical and horizontal borehole plugging tests are consistent with one another. It can be concluded that HCB borehole plugs are well able to sustain the water pressure gradients that may be expected in a repository setting such as that exemplified by the conditions in the Stripa mine.

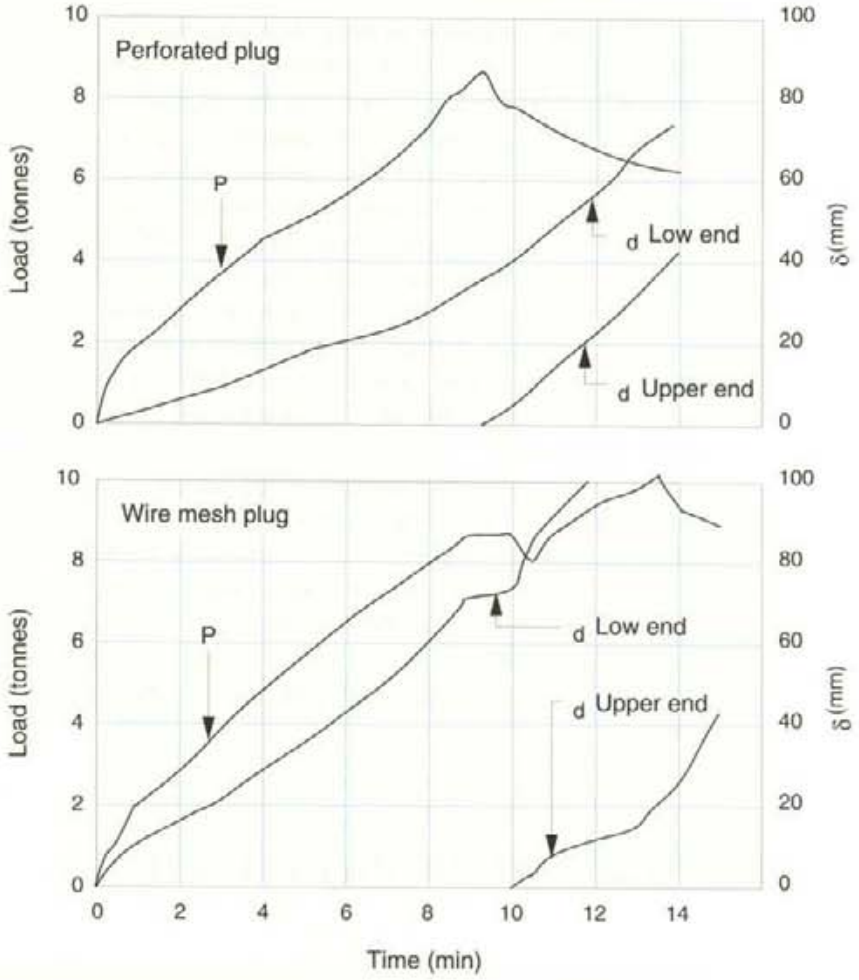

Figure 3-7 Load-time and deformation-time relationships measured during the extrusion of the two vertical borehole plugs.

The total pressures recorded in instrument numbers 3 and 5 were very much lower than the values of swelling pressure that could be predicted from Table 3-1 and Figure 2-15 to be thousands of kPa for the fully wetted and homogenized HCB plugs. Examination of the extruded plugs showed that while they were saturated with water, the outer skin of bentonite that had extruded through the copper exoskeleton to fill the gap between the emplaced plug and the borehole wall was significantly less dense than the inner part of the plug. The differences do not fully account for the low values of total pressure that were measured. In this regard it is noted that to act against the membrane of the pressure sensor the clay must not only have extruded radially outwards from the core of the plug, but also moved axially along the annular gap surrounding the plug and the sensors. It was shown in Chapter 2 that this process is controlled by the width of the gap. Thus, the total pressures measured in the vertical borehole plugging test are concluded not to represent the pressure of the clay against the borehole wall. This pressure, which effects the seal, is judged to have been about 1 MPa.

The forces required to extrude the two vertical borehole plugs and the corresponding deformations are shown in Figure 3-7. Prior to mobilization, the plug with the perforated copper tube exoskeleton exhibited less deformation than the plug contained within the wire mesh. Both plugs were fully mobilized

at a load of between 80 and 90 kN. After mobilization, continued increases in force were required to keep the wire mesh plug moving. In contrast, reflecting its more robust construction, the plug with the perforated copper tubing kept moving as force was decreased towards a residual value of about 60 kN. The tests were carried out sufficiently quickly to ensure no drainage of the clay. In these quick, undrained conditions the saturated clay has an apparent coefficient of internal friction of zero. With an operating length of 3.5 m and a wall pressure of 1 MPa the mobilized angle of friction (ϕ_{fric}) between the plug and the granite rock can be calculated to be between 4° and 7°. This is to be compared with a value of about 10° measured under similar quick undrained conditions in the laboratory between steel and bentonite. These data can be used to estimate the minimum length of a plug that is required to sustain significant differential hydraulic pressures between its ends. The length will depend on the diameter of the borehole. For a 76 mm diameter borehole, the pressure differential that can be restrained per metre length of an otherwise unrestrained plug is about 4.5 MPa (ϕ_{Fric} = 5°) which is equivalent to an hydraulic gradient of about 450. It is concluded that bentonite plugs like the ones tested at Stripa will fail hydraulically by piping before they fail mechanically by extrusion. Within the pressure range in which they are effective they can be estimated to seal the borehole to an effective hydraulic conductivity in the range 10^{-12} to 10^{-13} m/s.

3.3 SHAFT AND TUNNEL PLUG TESTS

Concrete and steel structures are commonly used in mining and civil engineering design and practice to limit and control water flow in excavated openings. Water leakage through and around these underground structures is normally concentrated at construction joints and at the interfaces between the structures and the rock. At construction joints, bitumastic, rubber, plastic or metal water stops are often used to limit flows. Interface flows are reduced by grouting, keying in the structure to the rock and scaling the rock surface prior to construction of the plugs. The use of bitumastic, plastic and rubber construction elements into a repository is generally considered to be undesirable as it increases the organic load in the facility. Metal corrosion produces gases. Moreover, the longevity of these materials in the repository environment is uncertain. The BMT and early experience from the borehole sealing experiments indicated that durable (see Chapter 5), inorganic, highly compacted bentonite (HCB), if used to fill excavated openings in the Stripa granite, would effectively limit flow at interfaces. Thus, the shaft and tunnel sealing experiments were carried out in Phase 2 of the Stripa Project to determine the practicality of using HCB to seal the interfaces between bulkheads and the rock and, by implication, to seal construction joints in bulkhead structures. The details of these experiments are provided by Pusch et al (1987b, 1987c). Essential elements of the experiments are discussed here.

3.3.1 Test configurations

The shaft and tunnel plugging tests were configured to determine the efficiency with which the swelling clay could limit flow at the interfaces between bulkheads, backfills and the excavated rock surfaces. The layouts of the tests are shown in Figures 3-8 and 3-11. In both the shaft and tunnel plugging tests two bulkheads were constructed within the excavations to form a test cell. The inner surfaces of the bulkheads were lined with HCB and the enclosed volume was filled with sand. The outer bulkheads, the inner, sand-filled part of the test cell and the rock acted as constraints to resist bentonite swelling. The inner sand filled chamber could be filled with water and pressurized and the hydraulic competence of the complete bulkhead and HCB gaskets could be tested.

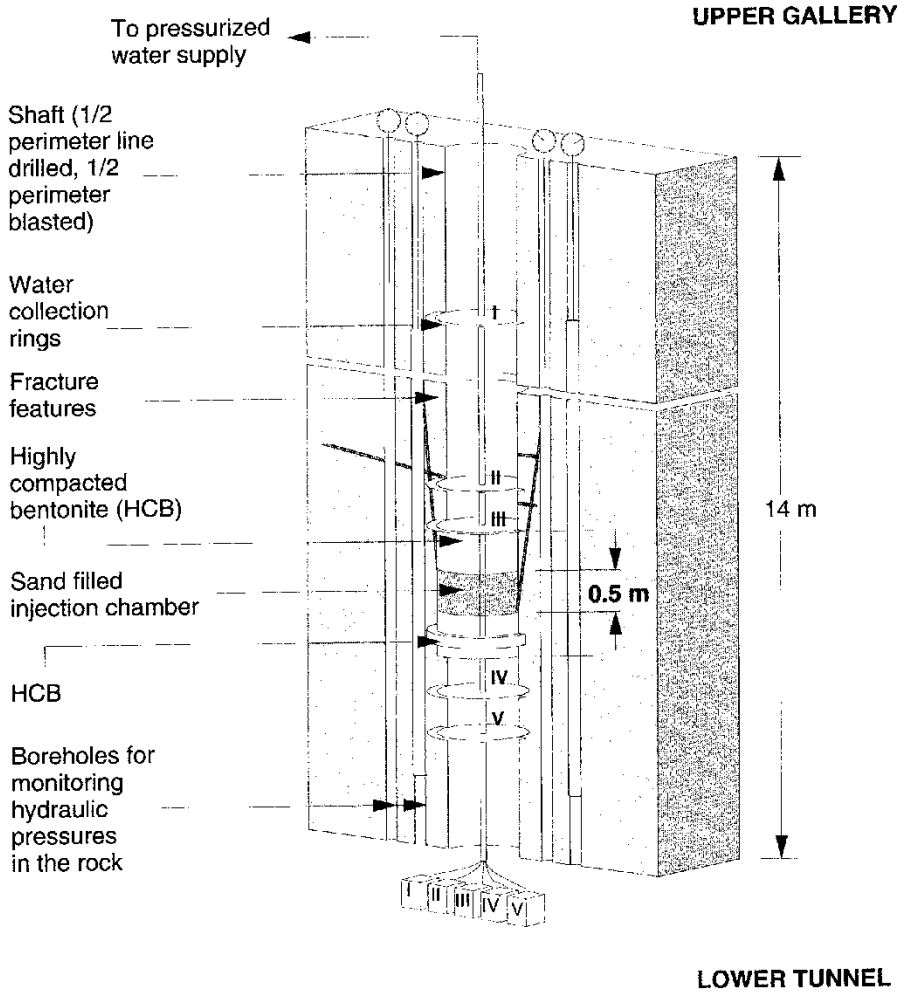

Figure 3-8 The layout of the shaft plugging test.

The shaft plugging experiment (Figure 3-8) was conducted near the vertical borehole plugging experiments (see Figure 3-1) in a 14 m deep vertical, tapered shaft that had been excavated to a diameter of between 1 m (top) and 1.3 m (bottom) between two vertically separated virtually horizontal tunnels. Excavation had been completed during the period of the SAC agreement to test different technologies for excavating large diameter

boreholes. The eastern half of the perimeter of the shaft had been formed by line drilling; the western half of the perimeter had been created as careful blasting techniques were used to remove the rock and form the shaft. Thus, the opportunity was provided to examine the effectiveness of HCB to seal against surfaces of different roughness and, maybe, examine the effects of excavation technique on the flows in the rock immediately adjacent to the excavation.

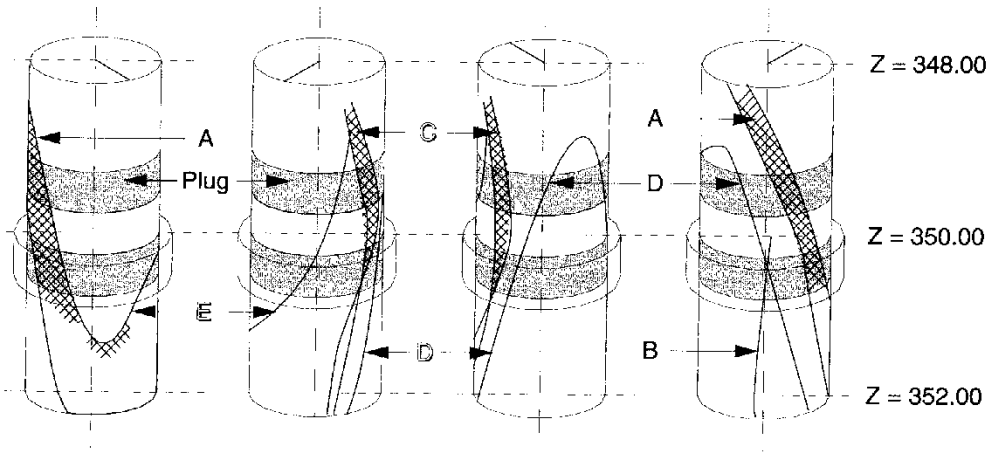

Legend:

Label	Description	Dip, degrees	Strike
A	Crushed rock zone	60	WNW/ESE
B	Large open joint	90	W/E
C	Crushed rock zone	70-90	NW/SE
D	Planar joint	65	NW/SE
E	Planar joint	60	WNW/ESE

Figure 3-9 Geometry of the major water bearing features intersected by the shaft at the elevations of the plug installation.

Inspection of the surfaces of the shaft, combined with observations of water inflows occuring into the shaft as water pressures were successively changed in 2 m long packed-off sections in an inner ring of 8 vertical boreholes symmetrically arranged around the axis of the shaft, revealed the major hydraulic features in the rock mass intersected by the shaft. Pressure reactions and water flows in an outer ring of 8 boreholes as conditions were changed in the inner ring of boreholes also aided understanding of the geometry of the connected water flow paths in the rock. Figure 3-9 shows the features of interest in the shaft section in which the test cell was built.

The test section was selected to allow for the evaluation of the effectiveness of two plug configurations to be determined. Shown in Figure 3-8 and, more clearly, in Figure 3-10(b), the upper bentonite plug merely filled the shaft opening and interface flows were to be restricted. The lower bentonite plug was extended into a 254 mm thick slot that was sawn circumferentially into the shaft wall to an arbitrarily chosen depth of 250 mm. This was intended to cut off flows axially down the shaft from the injection chamber through a possible excavation disturbed zone and through the hydraulic features shown in Figure 3-9.

Before the test of the bentonite plugs (the main test) was undertaken and the slot for the lower bentonite plug was sawn, a reference test, configured as shown in Figure 3-10(a) was carried out. Consisting of two plain concrete plugs, this test was intended to provide a baseline against which the effectiveness of the bentonite plugging systems could be appraised. In this context it is noted that the concrete plugs used in the reference test were only 0.5 m thick (less than half of the shaft diameter). This is much less than the thickness of concrete plugs that may be used to seal repositories and, thus, it is concluded here that the results of the reference test should not be taken to represent the sealing function of concrete plugs incorporated in repository designs. Other than noting that expanding cements were used, details of the concrete mix designs used in the reference and the main tests are not documented.

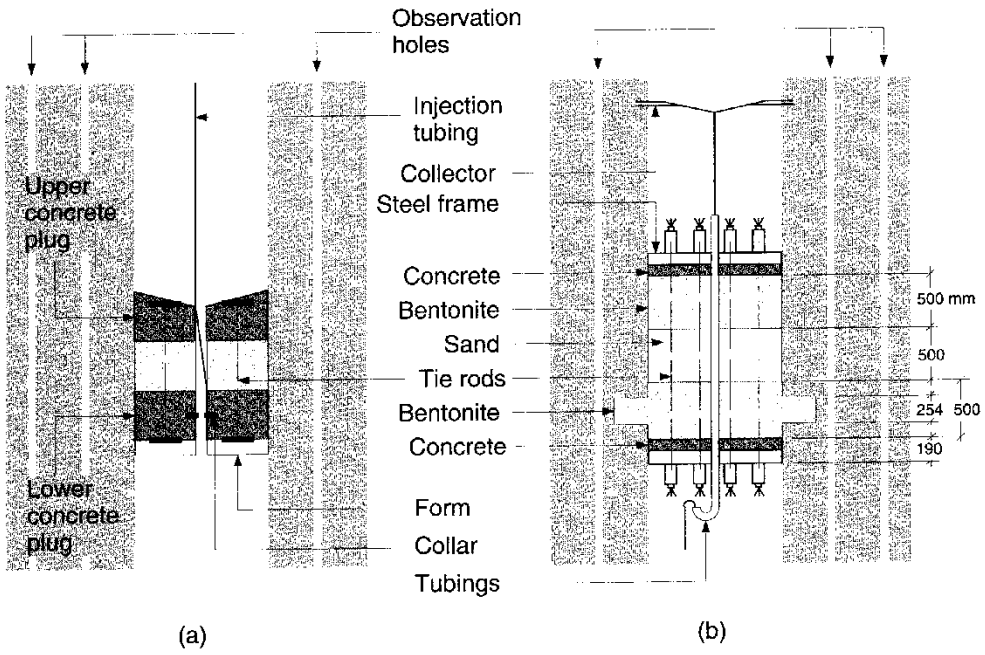

Figure 3-10 Longitudinal cross sections of (a) the concrete , and (b) the bentonite haft plugging tests.

Water flows into sections of the shaft were measured both above and below the test cell using five water collection rings (labelled I to V in Figure 3-8). The collectors extended in slots sawn into the shaft wall to a depth of about 75 mm. The uppermost collector (I) prevented water flowing down the shaft into the test area. The other four collectors were strategically located according to the determined connectivity of the natural water bearing features. These locations were kept the same for both the reference and the main tests.

The tunnel plugging experiment was carried out in a specially excavated, 35 m long, W-E orientated, dead-ended tunnel. The tunnel was excavated by careful blasting to a cross-sectional area of about 11 m^2 (compared with about 1 m^2 for the shaft plugging test) at the 380 m level of the mine located near the Buffer Mass Test tunnel as shown in Figure 3-1. To permit drainage, the tunnel was slightly inclined downwards towards the open end.

The test cell shown in Figure 3-11 was built in the tunnel. The inner 1.5 m diameter tube allowed personnel to access the inner end of the tunnel. It was considered that such systems may also be required during the construction and operation phases of repositories to allow for access of equipment and personnel to the emplacement levels of a repository through tunnel sections passing through water bearing zones in the rock. In contrast with the shaft plugging experiment, in which the HCB filled the entire cross-section of the excavation, in the tunnel plugging experiment the HCB was used to form a gasket (or "O" ring) on the perimeter of the inner surfaces of the concrete bulkheads at the bulkhead/rock interface. Moreover, only one tunnel plugging test was carried out in which the hydraulic competence of the total concrete/HCB sealing system was measured.

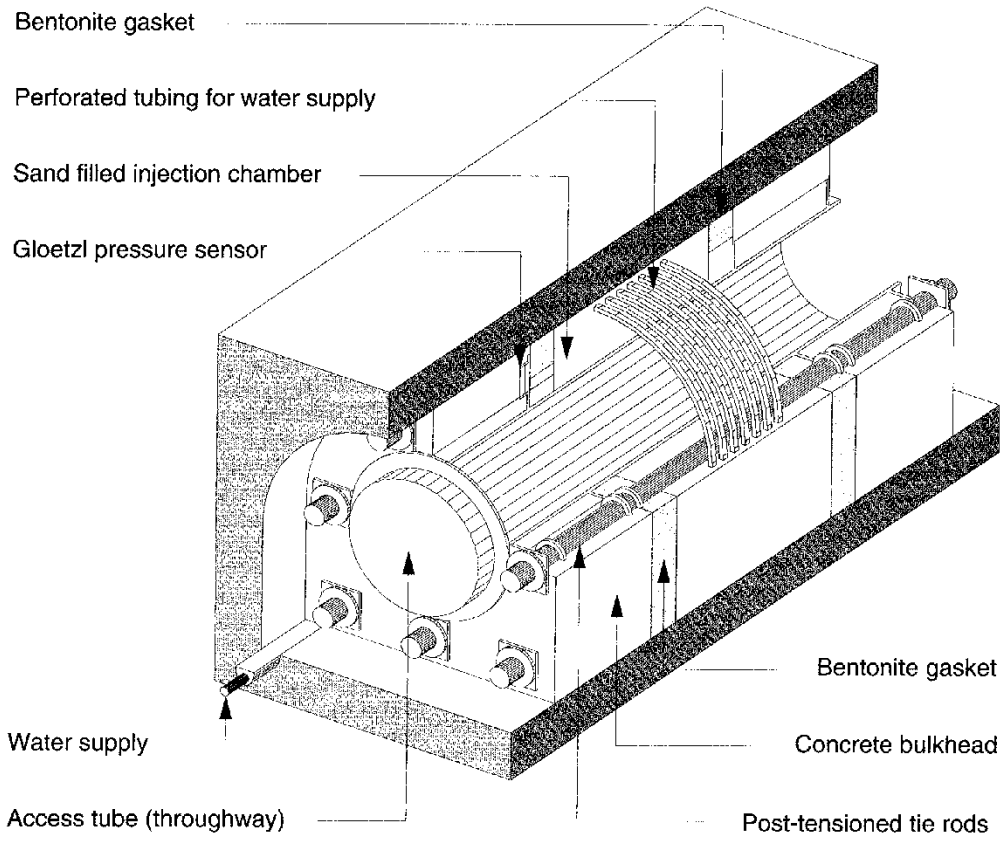

Figure 3-11 The layout of the tunnel plugging test.

Measurements of the hydraulic and rock stress regimes in the rock near the tunnel were not made. Based on the results of the SAC measurements and the observations made in the BMT, it was assumed that water pressures could be as high as 1 to 1.5 MPa within a distance of 3 to 5 m from the tunnel surfaces and that the principal stresses and magnitudes were σ_1 ~ 20 MPa (W/E), σ_2 ~ 10 MPa (N/S) and σ_3 ~ 4 MPa (vertical). Inspection and geological characterization of the surfaces of the tunnel revealed that the rock was inhomogeneous.

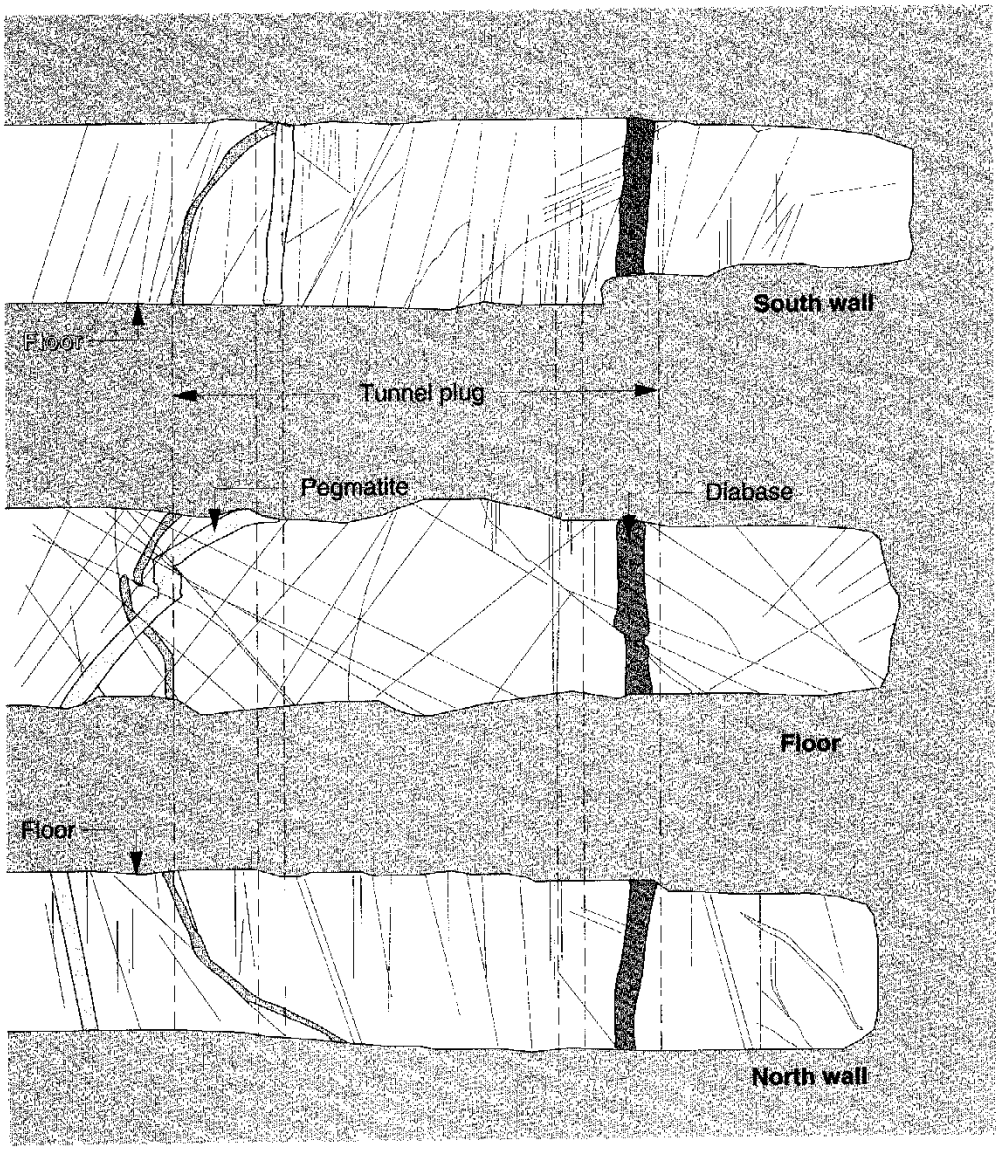

Figure 3-12 Surface map of the exposed rock surfaces showing major fractures and hydraulic features with respect to the location of the tunnel plugging test cell.

Diabase intrusions and pegmatite dykes were observed as discontinuities in the fine-grained grey/reddish matrix of the granite country rock. Along with natural fractures in the country rock, interfaces between the country rock and the intrusive features appeared to provide the major natural water flow paths. Moreover, the pegmatite was clearly more pervious and water bearing than the surrounding matrix. A map of the observed fractures and water bearing features is given in Figure 3-12. The selected location of the test cell is also shown. The outer concrete bulkhead is seen to coincide with the pegmatite dyke. The inner concrete plug covers the diabase intrusion. With a SW-NE strike, the pegmatite dyke provided a conduit for water flow from the inner sand filled chamber of the test cell around the outer bulkhead to the outer part of the tunnel. This channel was supplemented by a series of natural discrete fractures identified in both the walls and the floor of the tunnel. The water bearing features in the rock around the inner bulkhead were not as evident as those at the outer bulkhead. Thus, it was judged that

70 to 80 per cent of the flow from the inner pressurized, saturated, sand-filled injection chamber would occur in the rock around the outer bulkhead. In this context it is noted that, as with the arrangement of the shaft plugging experiment, the thickness of the concrete bulkhead was less (by a factor of about 2) than the maximum dimension of the excavation. Such structures are unlikely to be used in isolation in repository sealing. Much more massive concrete structures, with thickness of 2 or more times the maximum excavation dimension, are more likely to be considered. Thus, here, like that for the shaft plugging test, discussions of the tunnel plugging test are limited to an appraisal of the sealing effects of HCB. No comparison between the efficacy of concrete and HCB sealing systems is considered appropriate.

In both the shaft and tunnel plugging experiments, shaped HCB blocks using MX-80 bentonite with densities and, thus, properties similar to the buffer material used in the BMT, were used and tested. Allowing for swelling into spaces left at the irregular rock surfaces the final saturated bulk density of the bentonite in the gasket in the tunnel plug test was judged to be about 2.0 Mg/m^3. Thus, swelling pressures in the confined clay could be expected to rise to a maximum of about 7 MPa (see Figure 2-15). In both the tunnel and shaft plugging tests, Glöetzl total pressure transducers, similar to those used in the BMT (see Table 2-6) were emplaced in the test systems to measure swelling pressure development. In the tunnel plugging experiment 46 transducers were located strategically at the interfaces between the concrete bulkhead and the bentonite, the rock and the bentonite, and the sand and the bentonite. In the main shaft plugging test, transducers were placed centrally in the upper and lower bentonite plugs (1 in each) to record vertical total pressures. Two transducers, placed at diametrically opposed locations on the interface between the rock and the bentonite, were used to record the horizontal pressures acting on these surfaces in the lower shaft plug.

The full swelling pressure of 7 MPa combined with the maximum water pressures in the sand filled chambers (200 kPa in the shaft plugging tests; 3 MPa in the tunnel plugging test) would result in forces of approximately 8 MN and 65 MN acting axially on the bulkheads, respectively, in the shaft and tunnel plugging experiments. These large forces were restrained by tying the bulkheads together. Four steel tie rods (ϕ = 25 mm) passing through the bentonite plugs were used to restrain the steel end-plates in the main shaft plugging test. Reflecting the much higher forces acting, the central steel casing (with a diameter of 1.5 m and a wall thickness of 35 mm) was used in the tunnel plugging experiment to tie the bulkheads together. The casing was post-stressed to control expansive strain during the progress of the test. Prior to increasing pressure in the chamber, seven post-stressing cables (each consisting of 37, 15 mm cable units) were each tensioned to a maximum force of 2.0 MN, giving a total restraint of 14 MN. This was approximately equal to the forces exerted by a chamber pressure of 1 MPa. Later in the test, to limit displacements in the system as swelling pressures came to bear and water pressures were further increased, the cables were further tensioned to give a total restraint of 31.5 MN. Assuming the system to be rigid and slip to occur at the bulkhead/rock interface it was estimated that the maximum displacement of the outer end of the casing would be +/- 4.5 mm (sign denotes compressive or tensile strain).

Displacements at the bulkhead/rock interfaces and change in the length of the casing were monitored throughout the progress of the test.

Other than noting that concrete with a minimum unconfined compressive strength of 40 MPa was used, no other details on mix design and proportioning are available. The concrete was heavily reinforced to limit strain and deformation. Special detailing was included to limit leakage at interfaces in the structure.

In both the shaft and tunnel plugging tests, the swelling pressures from the bentonite were expected to deform the interface between the bentonite and the sand layer. Moreover, there was some concern that the bentonite may penetrate the voids in the sand. In the tunnel plugging test, plexiglass tubes passing through the bentonite to the sand filled chamber were installed in the outer bulkhead. Borehole viewing equipment was used in these to monitor the displacement of the bentonite/sand interface with time and test conditions. The derived results were compared with direct observations of movement of the interface made during the final disassembly of the experiment.

3.3.2 Schedule, installation and sequencing

The schedule for the main activities undertaken in the shaft plugging experiment is shown in Tables 3-4 .

Table 3-4 The schedule of activities for the shaft plugging experiment.

Period	Test	Activity	Chamber pressures (kPa)
Jan-Jun, 1984	REFERENCE	Construction	
Jul-Aug, 1984	TEST	Flow test	100
Aug-Sep,1984	Concrete plugs	Tracer test	100
		Disassembly	
Oct-Dec, 1984	MAIN TEST	Construction	
Jan-Feb, 1985	Bentonite plugs	Flow test	100
Mar-Jun, 1985		Tracer test (1)	100
Jul-Oct, 1985		Tracer test (2)	100
Oct, 1985 to Jan, 1986		Combined flow and tracer test	100 and 200
Feb-Mar 1986		Disassembly and clay sampling	

The table shows that the test took approximately two years to complete. The major part of this period was taken for the main test. Both the reference and the main tests consisted of injecting water into the saturated sand filled chamber, measuring the rate of flow into the chamber and measuring the flow rates into the water collection rings above and below the test chamber. Plain water was first injected into the chamber. At later times, in an attempt to identify the dominating water flow paths, non-sorbing tracers were mixed with the injected water. Water stained with 100 mg/l uranine solution was injected during the reference test. In the main test, solutions containing 1000 mg/l uranine or 1000 mg/l phloxine B were injected sequentially under chamber pressures of 100 kPa. Subsequently,

under a chamber pressure of 200 kPa, the uranine solution with a concentration of 1000 mg/l was used again. Signs of the tracers were sought both in the samples recovered from the water collection rings and in samples taken from the observation boreholes. Both colorimetry and chemical analyses were used to identify the presence and concentration of the tracers. With completion of the flow tests the cell was completely disassembled and the bentonite sampled and tested for water content (by the gravimetric method using oven drying at 105°C) and distribution. Visual evidence of tracer migration was sought during the disassembly of the test.

Table 3-5 Schedule of activities and events for the tunnel plugging experiment.

Period	Activity	Chamber pressure kPa
Nov 1982 to May 1983	Planning, site assessment and excavation of the tunnel	
Nov 1983 to Apr 1984	Construction	
Apr 1984	Compression of the casing under 14 MN	
1984,	HYDRAULIC TESTING	
Apr 10	Increase chamber pressure	100
Apr 15	Increase chamber pressure	200
May 15	Increase chamber pressure	500
May 31	Increase chamber pressure	750
Oct 1984	Compression of the casing under 31.5 MN	
1984,	HYDRAULIC TESTING	
Oct 20	Increase chamber pressure	2000
Nov 5	Increase chamber pressure	3000
1985,		
Aug 31	Decrease chamber pressure	250
Sept 10	Increase chamber pressure	1000
Sept 20	Increase chamber pressure	2000
Oct 1	Increase chamber pressure	3000
Oct 15	Decrease chamber pressure	250
Nov 1	Increase chamber pressure	1000
Nov 10	Increase chamber pressure	2000
Nov 20	Increase chamber pressure	3000
Dec 1	Decrease chamber pressure	250
Dec 31	Decrease chamber pressure	0
1986, Jan 10 to Jan 30	Unloading of the casing	
1986, Feb 10 to Apr 30	Breaking of the casing, excavating the sand and sampling the bentonite	

The timing of events for the tunnel plugging experiment is shown in Table 3-5. The experiment took about 4 years to complete. During the testing period the internal pressure in the sand filled chamber was cycled three times to a maximum value of 3 MPa. Cycling was done to determine the repeatability of the results. Rates of inflow into the chamber were measured using flow meters on the water supply lines. These rates were compared with rates calculated from the quantities of water collected at known intervals from sumps located outside the inner and outer bulkheads.

In addition to the flow measurements, the changes in total pressure recorded by the Glöetzl pressure sensors and the deformations occurring in the casing and at the bentonite-sand interface were recorded. Noted as the final event in Table 3-5, after the hydraulic testing was completed, an access hole was burned through the casing, the sand infill was removed and the bentonite was sampled for water content determination.

In both the shaft and tunnel sealing tests, during dissassembly, evidence for penetration of the swelling bentonite into neighbouring rock fissures and the sand infill was sought.

3.3.3 Results and discussion

The changes in the rates of water flow into the test chambers with time and applied chamber pressure are shown for the shaft and tunnel plugging tests in Figure 3-13(a) and 3-13(b), respectively.

The data show that for all tests at all chamber pressures the inflow rate decreased with time tending towards a steady value. In the main shaft plugging test the steady value was not significantly changed by increasing the chamber pressure from 100 to 200 kPa. The results for the tunnel plugging experiment show that the steady values tended to increase with increasing pressures up to 3 MPa. The steady values are plotted against chamber pressure in Figure 3-14. The line is the result of a simple linear regression analysis of the data and has a coefficient of determination of 0.97. The small variance can be attributed to a number of possible causes including air in the system and changes in the balance between the chamber pressure and the hydraulic pressures in the rock mass near the chamber.

The apparent decrease in flow with time in the reference shaft plugging test may have resulted from a malfunction in the testing system and not have reflected changing conditions in the test cell. Pusch et al (1987b) state that filters in the main water supply line became blocked with time. Using an auxiliary water supply line gave an estimated steady state flow rate of about 192 l/d for the reference shaft plugging test.

The tracer testing in the reference shaft plugging test identified joint B, shown in Figure 3-9, as the major source of leakage from the test chamber. Some leakage also occurred through crushed zone A and joint E. No upward flow from the chamber was identified. Results from the tracer tests carried out for the main shaft plugging experiment showed that the keyed cutoff in the lower bentonite plug eliminated flow from the test chamber through structure B into the collection rings below the plug. Structures A and E remained as the major flow paths from the test chamber around the bentonite plugs. Tracer testing in both the reference and main shaft plugging tests show no apparent connections between the chamber and the monitoring boreholes. Lack of knowledge of the hydraulic potential field in the rock near the shaft renders uncertain any analyses of this result. In this context it is significant that the inflow rates measured in the shaft plugging tests were significantly higher than the flow rates measured into the shaft through the use of the collectors, with the total volume of water provided in the main test being about 7 times the void volume in the bentonite plugs. It is concluded here that most of the injected water escaped from the test chamber into the rock mass through undefined flow paths.

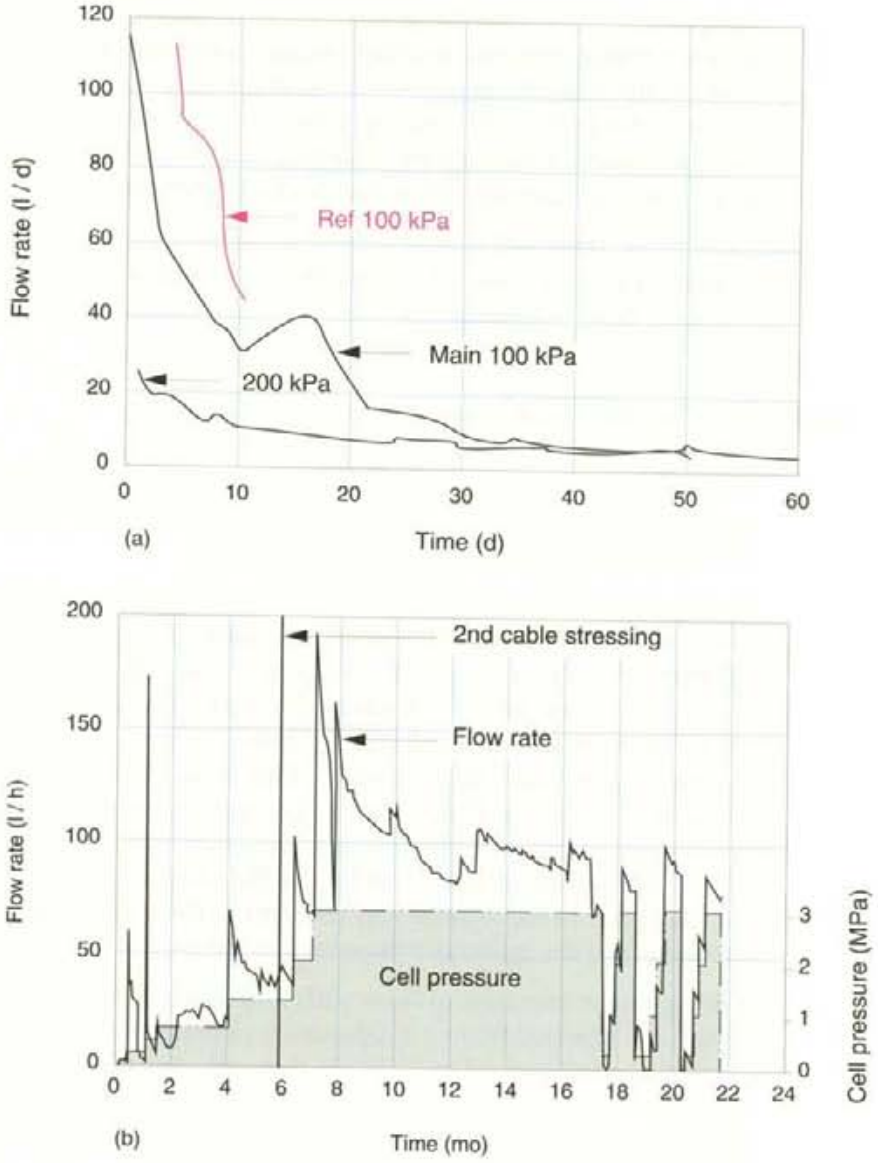

Figure 3-13 Flow rate/time/pressure relationships for (a) the shaft plugging test, and (b) the tunnel plugging test.

In contrast with the results from the shaft plugging test, the inflow rates recorded in the tunnel plugging experiment were, within practical limitations, the same as the outflow rates calculated from the water volumes recovered from the sumps in the tunnel outside the test cell. In accordance with expectations, at the steady flow rate conditions, 90 to 95 percent of the water escaped around the outer plug. It was concluded that the pegmatite zone and a series of discrete, steeply dipping, connected fractures in the floor of the tunnel allowed the water to circumvent the outer plug.

The flow data shown in Figure 3-13(b) characteristically show a rapid increase as the chamber pressure was incremented. At constant pressure the flows subsequently decreased gradually to the steady values. The rapid increases arose from changes in the dimensions of the chamber and compression of any air that remained in the system. According to Pusch et

al (1987c), at the lower chamber pressure of 100 kPa in the first stage of the tunnel plugging test, when, presumably, the bentonite had not significantly wetted and swelled, aerated water bubbled from the interface between the concrete plug and the rock. There is no record of these occurences at the higher pressures. The decrease in flux with time at constant pressure observed in both the tunnel and shaft plugging experiments is considered to be a consequence of the increasing sealing effects of the bentonite as the clay matured (wet and swelled) to accomodate the new conditions caused by the pressure change. Pusch et al (1987c) suggest that the bentonite gasket in the tunnel plug reduced the flow rate from 1000 to 200 l/h. In common with the results from the shaft plugging test, due to uncertainties in knowledge of the hydraulic potentials in the rock near the tunnel, it is not possible to fully evaluate the water flow paths in the tunnel plugging experiment. However, from both the shaft and tunnel plugging tests it is clear that, if necessary in a repository, plugs can be built to decrease water flows in excavated openings to lesser levels than those in the Stripa granite. Moreover, the flows in the granite are concentrated in major water bearing features which can be discriminated on a scale of metres. Phase 3 of the Stripa Project focussed on sealing these local features as well as the larger water bearing features identified in the studies of the natural barriers.

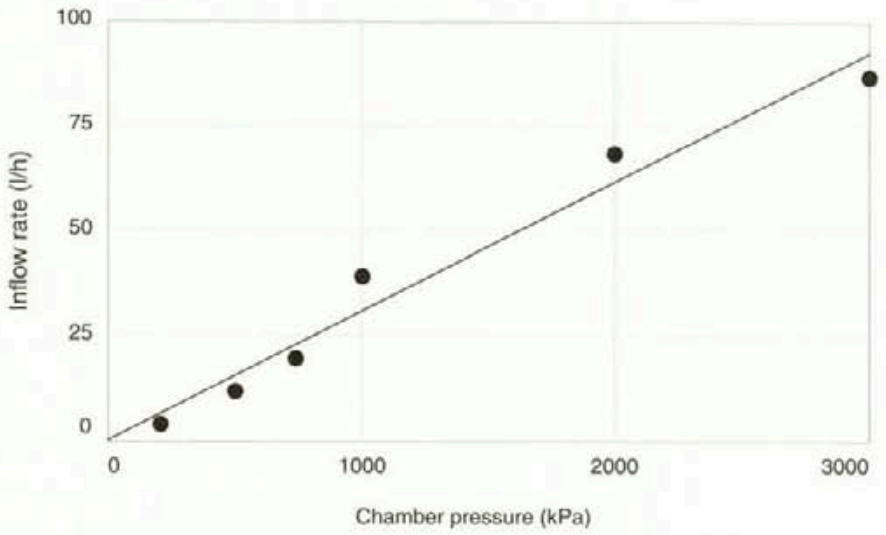

Figure 3-14 Steady state inflow rates versus chamber pressure from the tunnel plug test data.

The total pressures measured by the Gloetzl cells located on the bentonite/rock interface of the inner tunnel bulkhead are given in Figure 3-15. The pressures tended to increase with time and tended towards steady values towards the end of the test under a constant water chamber pressure of 3 MPa. Decreasing the chamber pressure towards the end of the test caused corresponding decreases in the measured total pressures at the bentonite/rock interface. The converse was also true. Thus, Pusch et al (1987c) suggest that the swelling pressure should be treated as an effective stress and calculated as the difference between the measured total pressure and the applied water pressure. This viewpoint has been confirmed for dense bentonite-sand mixtures by Graham et al (1989). Thus, the measured longer term values of swelling pressure exerted in the tunnel plugging experiment varied from as little as 0.1 MPa to as high as 5.2 MPa. The

higher values tended to be measured at the HCB/rock interface; swelling pressures measured at the HCB/sand interface were all below about 0.5 MPa. It is possible that these clear differences reflect decreases in the density of the bentonite at the sand/HCB interface. However, as noted in Table 2-6, the instruments and the materials in which they were embedded may not have been in compliance. The trends shown in the swelling pressure/time relationships measured at the HCB/concrete and HCB/rock interfaces were not entirely systematic. The HCB blocks were not closely fitting when placed. Thus, it was suggested (Pusch et al, 1987c) that differential wetting of the HCB occurred as water penetrated the material along the construction joints. This caused the opening and closing of pathways for water flow and, hence, the erratic responses in the pressure transducers.

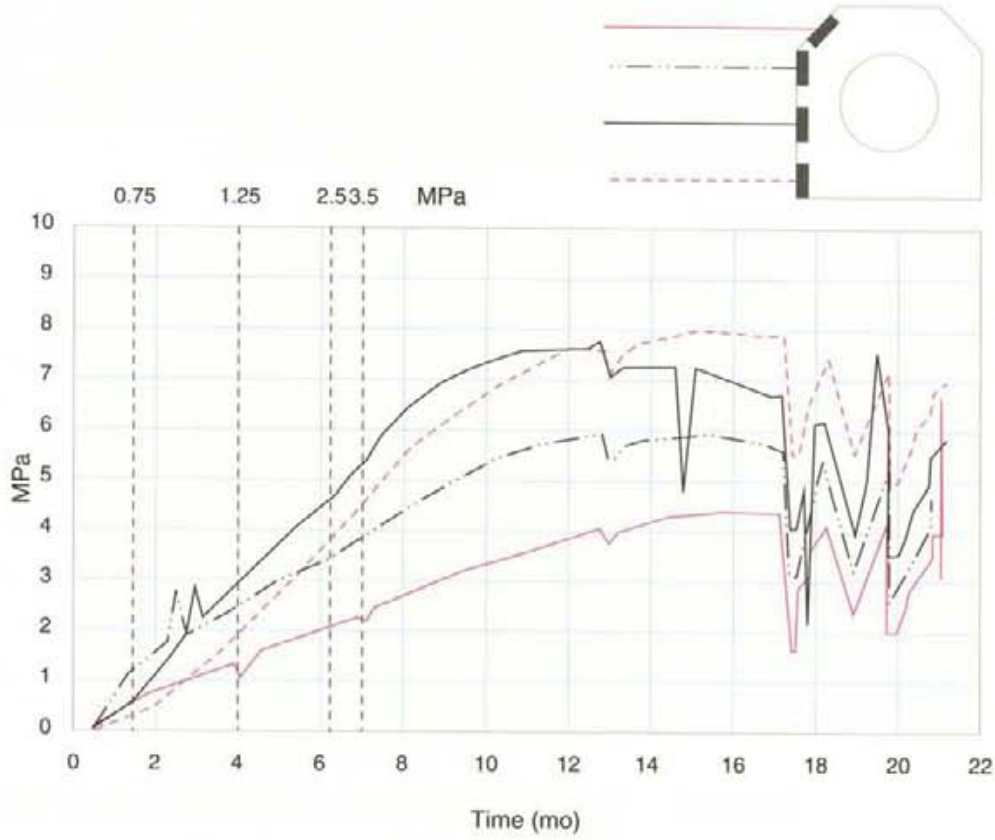

Figure 3-15 Total pressures measured at the HCB/rock interface of the inner bulkead wall of the tunnel plugging experiment.

The responses of the total pressure sensors installed in the shaft plugging experiment are shown in Figure 3-16. As expected, the pressures tended to increase with time. Insufficient data were available to discriminate orientation effects. The vertical pressures measured in the HCB masses (cells 2 and 4) were more internally consistent than the horizontal pressures measured at the HCB/rock interfaces(cells 1 and 3). The differences between the measured horizontal pressures could not be related with the hydrogeological features intersected by the shaft and were attributed by Pusch et al (1987b) to inhomogeneities in the HCB structures caused by lack of fit between the blocks. This is not entirely consistent with the

observations made during the disassembly of the shaft plugging experiment which showed a reasonably homogeneous clay mass that conformed well with the rock boundary and, internally, had regular patterns of water content distribution.

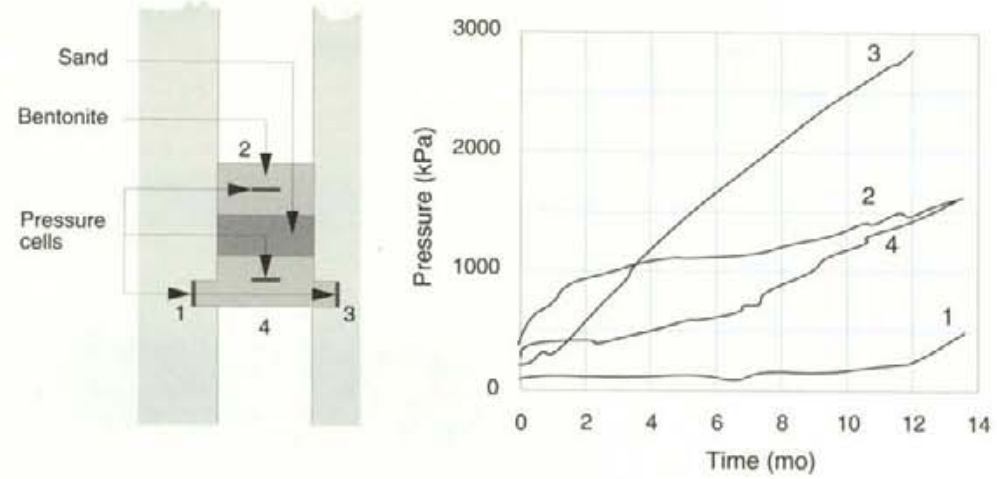

Figure 3-16 Total pressure build-up in the HCB of the shaft plugging main test.

The measured water content distributions in the lower HCB shaft plug are shown as interpreted iso-moisture lines in Figure 3-17. The values measured for the N/S section (on which the vertical swelling pressures were measured) are shown. Patterns across other sections were similar. The figure shows that at the end of the shaft plugging test the inner core of the HCB was not saturated.

Figure 3-18 presents a comparison between the measured and the predicted water contents in a half vertical section of the lower HCB shaft plug. The predictions were made using the simple isothermal diffusion equation (Eq. 2.12) that was developed for water flux in Phase 1 of the Stripa Project. A single diffusion coefficient of $4 \cdot 10^{-10}$ m^2/s was used for the calculations and water was assumed to be infinitely supplied at the upper and lateral surfaces of the plug. The comparisons indicate that water moved as predicted from the upper and side surfaces of the clay plug. Unexpectedly, in practice, water was also taken up from the lower surface of the plug. By inspection, it appears that, had a water supply been assumed at the base of the lower plug, solution of the isothermal diffusion equation could have provided a reasonably accurate description of the water contents in the plug at the end of the test. By inference, the time dependent changes in the water contents of the plug under isothermal conditions can be predicted with reasonable precision. It appears that, through the interactions between the bentonite and the rock surface, discrete fractures were effectively sealed as a boundary acting on the clay and that water was drawn at a regular rate into the clay plug over the whole surface of the body. This result is consistent with the findings of the BMT.

Reasonably, the isothermal moisture diffusion model involves approximations and can only be applied if the clay is virtually constrained. Expansion (density decrease) causes the moisture diffusion coefficient to increase and a more complex model is needed (see Yong and Warkentin, 1975). It was predicted that the interface between the clay gasket and the sand in the

tunnel plug would displace by as much as 120 mm. The measured displacements of 80 and 120 mm were well within the expected margin of error in the displacement calculations and, being commensurate with up to 25 per cent volume increase in the bentonite, rendered the water migration model too uncertain for application. Thus, in the tunnel plugging experiment, the rates of water migration in, swelling pressure development and sealing effectiveness of the HCB gasket were based solely on the observations made in the *in situ* tests.

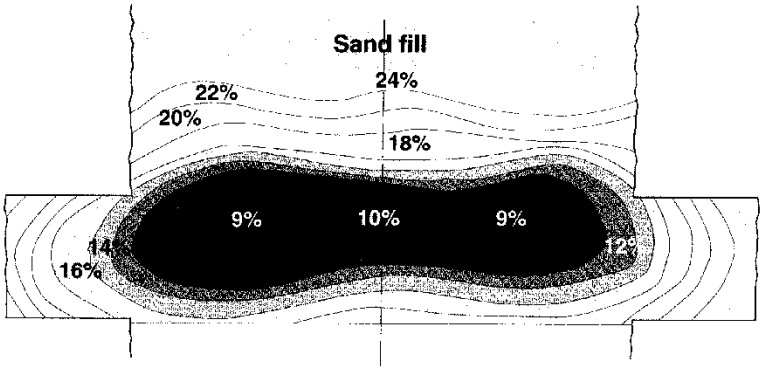

Figure 3-17 Measured water content distribution across a N/S section of the lower HCB shaft plug.

Typical moisture content profiles in the HCB gasket at the end of the tunnel plug test showed that moisture contents tended to be higher at the concrete/HCB and rock/HCB interfaces than in the centre of the clay mass. Similarly, as expected due to expansion, the water contents in the clay next to the sand layer were significantly higher than those deeper in the clay mass. Deep in the clay mass the moisture content typically varied from about 30 per cent at the concrete and rock surfaces to values of about 20 percent at the mid-section. At the sand/clay interface water contents as high as 90 per cent were recorded. Similar water contents at the rock/HCB and the concrete/HCB interfaces indicated that both surfaces acted as water supplies to the clay. Moreover, in common with the results from the borehole plugging and the shaft plugging experiments, the variations in moisture content through the clay showed that the HCB was not homogenized in the period of the test. Differential stresses were sustained. An eventual equalization of the stresses within and densities of the clay in the very long term remains questionable.

The displaced interface between the sand and the HCB at the end of the tunnel plugging test is shown in Figure 3-19. The figure also shows the close conformity between the expanded bentonite and the faces and edges of the inside of the concrete bulkhead. Similar views taken during the disassembly of the shaft plugging experiment show that the matured HCB closely conformed with both the line drilled and blasted faces of the shaft wall. This visual evidence adds support to the conclusion that the swelling HCB effectively sealed the interface between the engineered barriers and the rock surface. Moreover, limited penetration of the swelling HCB into the discrete fractures exposed at the rock surface could be clearly seen. Views similar to that shown in Figure 2-26 showed that in both the shaft

and tunnel plugging experiments the clay had self extruded into fractures to block the openings to effectively limit water access to the bentonite and divert water around the sealing system. Although the clay had penetrated outwards from the seal into the fractures the outward movement was clearly limited in extent and there was no evidence of erosion of the clay under the high pressure gradients imposed on the groundwater.

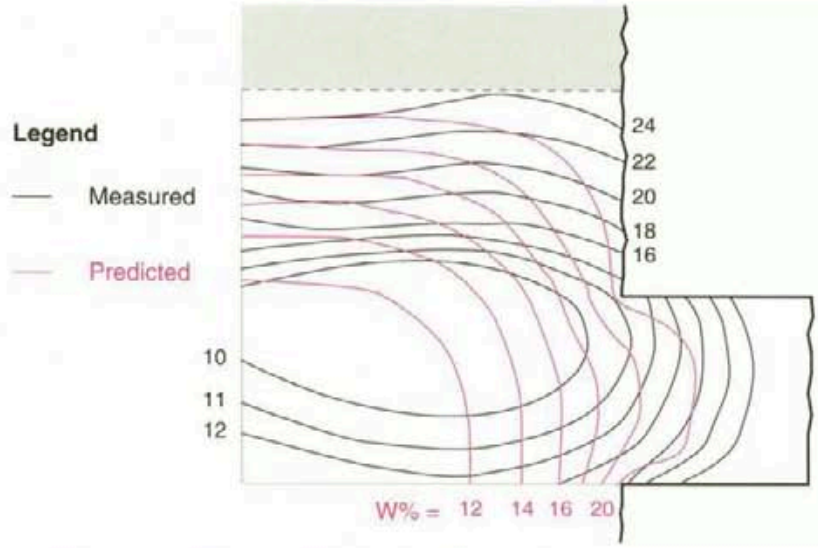

Figure 3-18 Measured and predicted moisture content distributions in the lower HCB shaft plug.

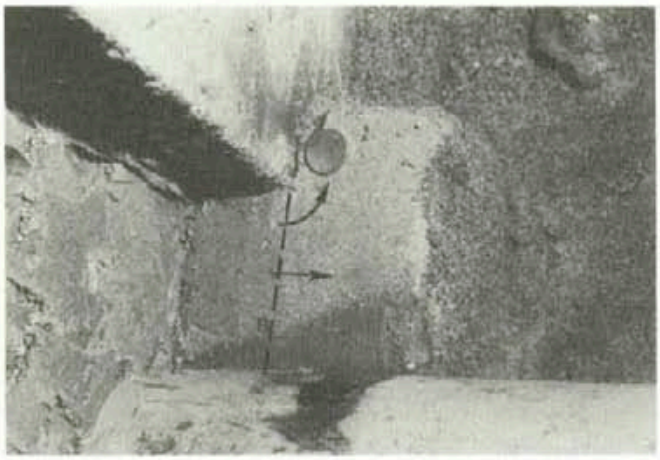

Figure 3-19 View of the HCB/sand and HCB/concrete interfaces after the test. The clay has compressed the sand, expanded outwards and around the corner of the concrete bulkhead and conforms to the geometry of the bulkhead.

The sand used to fill the chambers in the shaft and tunnel plugging tests had been specially selected and graded to provide a pore size distribution such that penetration by the clay would be limited. Sections of the sand/HCB interfaces obtained from samples removed from both the shaft and tunnel plugging tests were examined using optical and scanning electron

microscopy. The examinations showed that the clay had only moved 1 to 2 mm into the sand. This not only confirmed that the particle size distribution of the sand had been correctly chosen but further showed that earthen materials, such as the backfill used in the BMT, can be designed and used to confine HCB and maintain the long-term sealing functions of the clay.

4 PHASE 3 - 1986 TO 1992 *IN SITU* STUDIES OF GROUTS AND GROUTING

4.1 BACKGROUND AND SCOPE

By 1985, underground laboratories had been established in Canada (the Underground Research Laboratory), Sweden (the Stripa mine) and Switzerland (Grimsel test site) to investigate *in situ* the isolation properties of engineered granitic rock masses with specific regard to disposal of heat-generating radioactive wastes. Observations were also being made at other non-dedicated granite sites such as those at Fanay Augères in France, the Kasama quarry in Japan and the Harwell research site in the United Kingdom. The investigations had confirmed common experience that water flows in granite rock are concentrated in major fracture zones, in lesser fracture sets and within discrete fractures. The international scientific community through progress in the natural barrier studies of the Stripa Project and within national programmes was focussing attention on the characterization of these water flow paths and on the development of methodologies for the prediction of flows over time periods relevant to repository system performance assessment.

The engineered barrier studies of Phases 1 and 2 of the Stripa Project had provided confidence that excavations in rock bodies similar to the Stripa granite can be plugged with clay materials: these plugs were shown to have hydraulic conductivities that were as low or lower than average equivalent porous medium values measured for the undisturbed rock masses at proposed repository depths inside boundaries defined by the major fracture zones. Combined with the results of the shaft and the tunnel plugging experiments, data from the SAC macropermeability experiment and the BMT in the Stripa mine indicated that the zone of rock around the excavations had different hydraulic properties than the undisturbed rock mass. As shown in Figure 4-1, by meeting with the major fracture zones and the disturbed zones around sealed shafts, the excavation disturbed zones (EDZ) around tunnels may link the waste horizon with the surface of the earth. Without a more definitive understanding of the characteristics of the EDZ it could be necessary to assume that the connections through the EDZ would adversely affect total repository system performance. Thus, studies were undertaken within the engineered barriers research programme for Phase 3 of the Stripa Project to provide a more detailed characterization of the hydraulic properties of the EDZ around tunnels in granite. Given the possibility that the EDZ were characterized by higher hydraulic conductivity than that of the host rock, pragmatism required that studies were also undertaken to appraise materials and methods for sealing the pathways and to define the limits of these technologies.

Theoretical appraisals supported by the results of the SAC, Phase 1 and Phase 2 studies suggest that if amelioration of the properties of the EDZ is required, the zone will be sufficiently small to be readily accessed from the inside of repository excavations. Significant disturbance of the stress field around ex-

cavations will be limited to about three times the mean dimension of the cross section of the excavation (Kelsall and Shukla, 1980). This limits the volume of rock in which remedial operations may have to be effected and, thus, allows for quality control and assurance programmes to be implemented. The latter will be needed for the development of the repository construction, operation and licensing procedures which will permit the benefits gained by engineering measures to be included in assessments of repository performance and safety. Clearly it would not be easy or, in all likelihood, possible to provide these assurances for work remotely carried out in the rock mass. Specifically, it is not practicable to consider engineering works to improve the hydraulic performance of the major fracture zones *en masse* : the zones extend for hundreds to thousands of metres. However, where these zones or their subordinates are intersected by the excavations, work could be undertaken in the accessible volume of rock to enhance, locally and tactically, the function of sealing systems and still provide the information needed for performance appraisal and licensing. The engineered barriers programme for Phase 3 of the Stripa Project included *in situ* experimentation focussed on this latter objective.

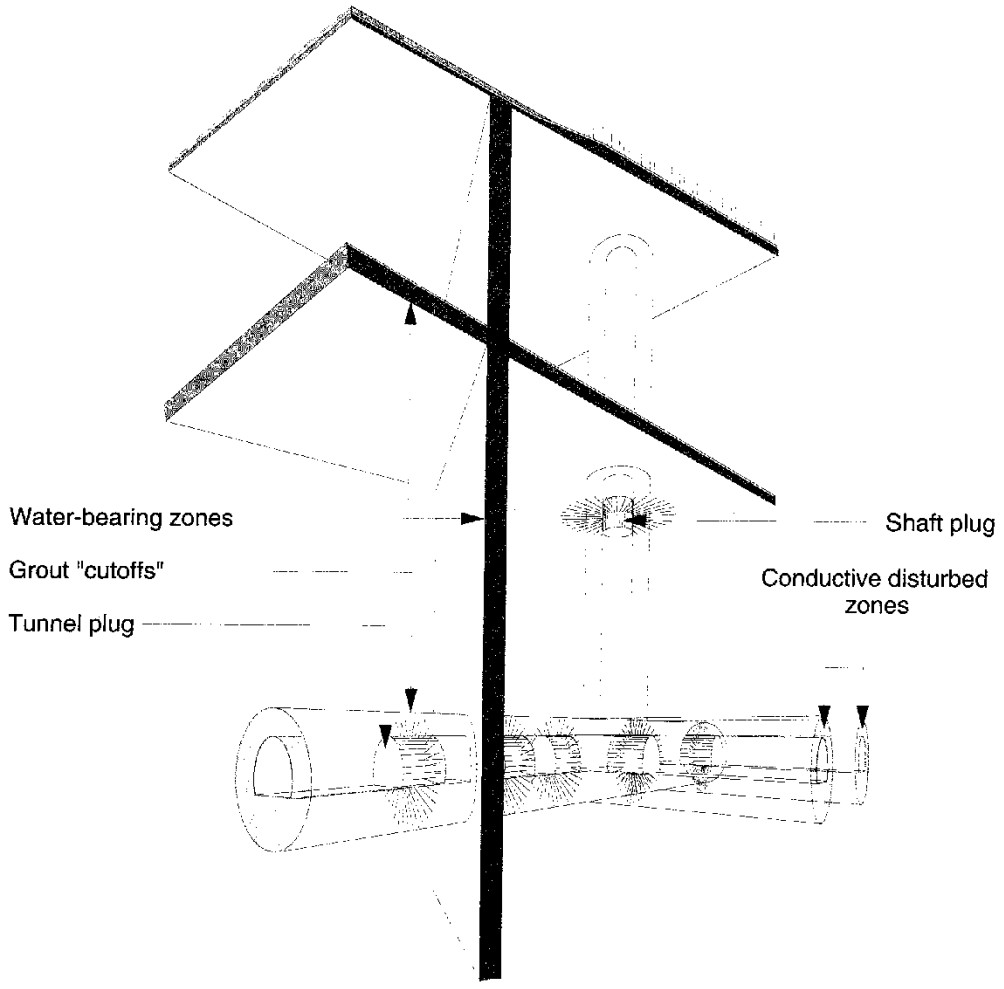

Figure 4-1 A concept for the major water flow paths in a sealed repository.

Results from the BMT had shown that discrete water bearing fractures were the primary source of water supply to the open heater holes; in the EDZ around the test tunnel, open discrete fractures in the floor appeared to carry water flows

that were higher than those in the surrounding rock mass. The results from the tunnel and shaft plugging experiments had shown that discrete single fractures and hydraulic features at the scale of metres in the rock could significantly influence the effectiveness of sealing operations. Specifically, discrete fractures in the floor beneath the tunnel plug and a pegmatite zone cut through by the tunnel proved to be the major sources of leaks in the tunnel plugging experiment. Initiated during Phase 2 of the project, *in situ* grouting experiments to evaluate measures to seal discrete fractures were expanded and completed in Phase 3.

Table 4-1 Members of the Task Force on Sealing Materials and Techniques.

Country	Name	Affiliation
	STRIPA PROJECT MANAGER	
Sweden	B. Stillborg	SKB, Stockholm.
	TASK FORCE CHAIRMAN	
United States of America	P. Gnirk	RE/SPEC Inc., Rapid City, S.D.
	PRINCIPAL INVESTIGATORS	
Canada	M. Onofrei	AECL Research, Pinawa, MB.
Sweden	R. Pusch	Clay Technology AB, Lund.
Sweden	L. Börgesson	Clay Technology AB, Lund.
United States of America	S. Alcorn	RE/SPEC Inc., Albuquerque, NM.
	REPRESENTATIVES	
Canada	M.N. Gray	AECL Research, Pinawa, MB.
Finland	M. Vaajasaari (1985-6) R. Riekkola (1986-8) Y-P. Salo (1988-91)	Technical Research Centre, Espoo. Saanio and Riekkola, Helsinki. Teillisunden Voima Oy, Helsinki.
Japan	M. Tokonami K. Toyoda	Tokyo University. Tokyo University.
Sweden	A. Bergström	SKB, Stockholm.
Switzerland	B. Knecht	NAGRA, Wettingen.
United Kingdom	J. Steadman	Building Research Establishment, Watford, Beds.
United States of America	W.E. Coons	RE/SPEC Inc., Albuquerque, NM.

Sections 4.3 (Discrete fracture grouting), 4.4 (Fracture zone grouting) and 4.5 (The excavation disturbed zone) summarize and review the activities and results of the *in situ* experiments. It is noted that Phases 2 and 3 of the project overlapped between 1986 and 1988. The interest of the member countries in the *in situ* preliminary discrete fracture grouting experiments carried out in the Phase 2 investigations of tunnel plugging (Pusch et al, 1987c) arose from the programmes pursued in Phase 3. For completeness, these preliminary experiments are described in section 4.3.

At the outset of Phase 3 it was recognized that investigations of grouts and grouting were largely new ventures for the programme. It was clear that highly compacted bentonite was not suitable for the Phase 3 investigations and that the state-of-the art in grouting technology was not adequately understood. It is noted in Volume 1 (Executive Summary) of this overview report that in 1985 a Task Force on Sealing Materials and Techniques, comprised of representatives of each of the member countries, was established by the Technical Sub-Group to guide the engineered barriers studies. The names and affiliations of the members of the task force along with those of the principal investigators are given in Table 4-1.

For the first two years of Phase 3, the task force members worked with the principal investigators to determine the state of the art in grouting technology and to determine the feasibility of experiments being planned. This led to the selection of grouting materials and methods to be investigated and to the definition of the *in situ*, laboratory and theoretical studies that formed the body of work that was carried out. It was established that the member countries were as much interested in determining the long-term performance properties of sealing materials as in the evaluation of technologies within the site specific arena of the Stripa mine. Thus, the task force strove for a balance between the work carried out to effect the *in situ* investigations and the activities undertaken to establish the longevity of sealing materials.

Section 4.2 of this chapter presents the rationale for selecting the materials and methods that provided the focus for the *in situ* and ancillary investigations: data, that both allowed for the *in situ* investigations and assist in the interpretation of the results, are provided.

In view of perceived importance by the member countries, presentation and discussion of the work on longevity is assigned to Chapter 5 of this report.

4.2 GROUTING MATERIALS

The task force (Coons et al, 1987) recognized that, prior to application at specific sites and in view of the different repository design concepts being developed in the countries that were subscribing to the Stripa Project, it was necessary to define performance objectives for grouts and grouting in a general sense. These general performance factors, which included an ability for materials to restrict water flow through the repository, work compatibly with the *in situ* environment and other engineered barriers components and maintain performance over very long periods of time (many thousands to perhaps millions of years), allowed for an appraisal of the wide range of possible

Table 4-2 Screen of candidate grouting materials.

WEIGHTING OF FACTOR	VERY IMPORTANT		IMPORTANT			DESIRABLE			OVERALL APPRAISAL
FACTOR / MATERIAL	Ability to perform as an hydraulic barrier	Emplace-ability	Long-term stability	Effects on radionuclide mobility	Availability	History of usage in engineering practice	Data-base available on chemistry and performance	Cost	
Cementitious materials	✓	✓	◆	✓	✓	✓	✓	✓	HIGHER PRIORITY
Clays (bentonite)	✓	✓	◆	✓	✓	✓	✓	✓	
Cement-clay mixtures	◆	✓	?	✓	✓	✓	?	✓	LOWER PRIORITY
Chemical grouts	✓	✓	◆	?	◆	◆	◆	◆	
Bitumen	✓	✓	◆	?	✓	◆	◆	✓	
Ceramics	✓	¿	◆	✓	✓	?	◆	¿	EXCLUDED FROM STUDY
Metals	✓	¿	◆	✓	✓	◆	◆	◆	
Synthetic	¿	?	?	◆	✓	?	?	?	

Legend: ✓ acceptable performance, ◆ acceptable performance likely, ? performance uncertain, ¿ performance probably unacceptable (exclusion from study).

grouting materials being investigated by the member countries and the selection of a small number of materials for study within the Stripa Project. Practical constraints, such as an ability to emplace the materials as grouts, a history of successful use, availability and cost, and the desire to use non-toxic materials further helped to define the materials ultimately chosen for priority study within the project. The materials and factors are shown in Table 4-2. Expert judgement and the review resulted in the development of the classifications shown in the table.

Initially, cementitious materials, ceramics, chemical grouts, clay materials, cement/clay mixtures, metals, and organic substances, such as bitumen and tars, were all considered as candidate grouting materials. Cementitious and clay materials were recommended as priority materials because they can be designed to meet all of the desired performance characteristics, there is a considerable history of successful use in similar engineering applications and there is indirect evidence that they will continue to perform for long periods of time. Chemical grouts were identified as a promising class of materials that could be very useful for specialty applications. Chemical grouts were not selected as a priority material because of their relatively higher costs, evidence for long-term performance was lacking and concerns existed with the toxicity of the materials both during and after injection. Cement/clay mixtures and bituminous materials may possess important performance characteristics but have uncertain long-term performance. Moreover, it was considered that, because they introduce organic substances, the effects of chemical grouts and bituminous materials on radionuclide mobility within a repository system were less certain than those of the two priority materials. Practical constraints, such as an inability to emplace the materials as grouts in fine fractures or an apparent lack of ability for materials to function as a low conductivity grout, led to synthetic materials simulating natural fracture infills, ceramics, and metals being excluded from further consideration within the Stripa Project. In this latter respect, due to normal project constraints, the Phase 3 engineered barriers investigations were ultimately dedicated only to the two priority materials, cement- and clay-based grouts. Within these two groups, studies focussed, respectively, on a modern class of cement grouts which has more recently become known as high-performance cements and, building on the experience gained in Phases 1 and 2, on bentonite-based clay.

Grouts can be made to penetrate rock fractures by a number of different methods which, among others, include static pressure injection, dynamic injection (pressure injection with the grout being subjected to vibrations), vacuum intrusion and electrophoresis. Conforming with a requirement to use common technologies that do not require significant development and are easy to transfer to contractors engaged for repository construction, static and pulsed (dynamic) pressure grout injection techniques became the focus for the Phase 3 studies. A working prototype dynamic grout injection pump had been developed under the auspices of SKB of Sweden with particular emphasis on the liquefaction and injection of thixotropic bentonite gel grouts (Pusch et al, 1985c). There were strong indications that high-performance cement-based grouts could also behave thixotropically and be better injected using techniques which included the vibration and liquefaction of the materials during injection. Thus, the prototype was further developed through the Stripa Project to permit its use with both clay- and cement-based grouts. These developments required increased understanding of the rheological properties of the selected materials during injection and refinements to the mechanical design of the injection pump and

auxiliary equipment to conform to the properties of the grouts. Significant laboratory work was undertaken to refine knowledge of pertinent grout properties and to allow for selection of materials and methods for use in the proposed *in situ* grouting experiments. The remainder of this section describes the results of this work.

4.2.1 Rheology

Broadly, according to their flow properties, fluids can be classified as newtonian, bingham and pseudo-plastic. The general equation for flow is:

$$\tau = \tau_o + m \left(\frac{\gamma}{\gamma_o}\right)^n \qquad (4.1)$$

where, τ is the shearing resistance (Pa), τ_o is the shearing resistance (Pa) at $\gamma = 0$, γ is the rate of shearing (s^{-1}), γ_o is the normalised rate of shearing, and m and n are material parameters. Newtonian flow is defined by n =1 and $\tau_o = 0$; Bingham materials are defined by n = 1. For newtonian and bingham materials, m is related to the dynamic viscosity (μ).

Both clay slurries and freshly mixed portland cement grouts can exhibit all three types of behaviour according to the proportioning of the mixtures. The main factors controlling the flow behaviour of clay-based grouts are the composition of the solids, temperature, the water to solids ratio, the predominant exchangeable cation on the clay, and the ionic concentrations in the mixing water. These same factors control the properties of freshly mixed cement grouts. In addition, special organic admixtures (superplasticizers) are included in cement grouts to modify their properties (Aïtcin et al, 1989). Inorganic salts (e.g. NaCl) can serve a similar function in clay based-grouts (Yong and Warkentin, 1975). The effects of these variables on the rheological properties of selected groups of both clay and high-performance cement grouts were studied. Moreover, the effects of vibrations on the properties of targeted subsets of the selected groups was examined. Subsets were selected based on an appraisal of the static flow properties of materials and preliminary tests on their response to vibration.

Clay grout

The principal component of the clay grout tested both in the laboratory and *in situ* experiments was a bentonite clay product with the trade name "Tixoton" supplied by "Süd-Chemie AG" of Germany. Unlike the MX-80 bentonite used in Phases 1 and 2 of the project, the exchange sites of which were naturally predominantly saturated with Na^+, Tixoton is a Na-bentonite resulting from the chemical and physical processing of a natural Ca-bentonite clay. The rheological properties of water based slurries of the clay mixed with quartz powder were measured.

Quartz powder, with a maximum particle size of 5 μm, was mixed in proportions of 0 to 75 per cent of the total dry mass of the mixture (the air-dry mass of the clay, which includes the hygroscopic moisture content of the clay, was used in proportioning the mixtures; thus, equivalent mixtures made at different times may have had slightly different compositions). Quartz was added to the clay in an attempt to increase the resistance of the grout to the erosional forces of moving groundwater. Tests to determine the effectiveness

of this treatment along with an assessment of the effects of silica addition on the longevity of the material are described by Pusch et al (1991b). The results lead to the general conclusion that the addition of quartz powders can be detrimental to the performance of clay grouts in repository environments. This information, which is discussed in more detail in Chapter 5 of this report, was not available prior to the execution of the *in situ* experiments with the clay grouts at the Stripa mine, where quartz-bentonite mixtures, along with other materials were injected into the rock.

Both simple classification tests and measurements of the fundamental rheological properties were carried out on the clay-based grouts (Börgesson et al, 1991). The classification tests allowed for a quick and ready appraisal of the relative effects of different grout mix variables on the material properties and a judgement on effects. The latter provided basic parameters for input into models for predicting the performance of the grout and the injection systems. It is pertinent to note that in grouting practice it is necessary to be able to quickly assure the suitability of a mix for injection and the correctness of its formulation. Requiring less expertise, time and equipment, the engineering classification tests tend to be more suitable for these field control activities.

The liquid limit test, carried out using the fall-cone method generally as specified in BS 1377 - Test 2(A) (1975), was applied as the engineering classification test. This test is a development of the original Casagrande method (BS 1377 - Test 2(B), 1975) and, according to Atkinson and Bransby (1978), gives a measure of the water content of clay-water mixtures at which the undrained shear strength equals approximately 1 kPa. In common parlance this corresponds to a transitional water content below which the material behaves like a malleable solid (e.g. plasticine) and above which it behaves like a liquid (e.g. thick cream). Vane shear tests (BS 1377 Test 18 (modified), 1975) were also used to measure the undrained shear strength of the grout.

The Bohlin VOR rheometer was used to measure the effects of shear rate on the shearing resistance (shear stress) of different clay grout mixtures. The principles of this device are shown in Figure 4-2. The grout fills the 1 mm wide annular space between the rotating cup and the static bob, the top and bottom of which also apply shear to the slurry. The torque bar measures the shear resistance as the cup is rotated at different rates.

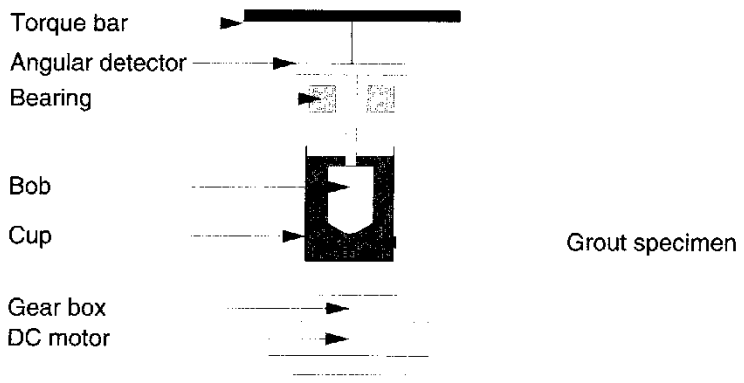

Figure 4-2 The general arrangement of the Bohlin VOR rheometer.

The Brookfield viscometer was used to measure the rheological properties of the grouts as they were vibrated to simulate the dynamic injection conditions that they may experience during injection. In principle the Brookfield viscometer is similar to the Bohlin rheometer. The grout is held in a cup and surrounds a bob which allows the rheological parameters of the fluid to be measured. The annular gap between the bob and the inner wall of the cup was 3 mm. In contrast with the Bohlin rheometer, the cup in the Brookfield viscometer is static and the bob rotates. This allowed for vertical vibrations of frequencies ranging from 2 to 10,000 Hz to be applied to the cup and its contents. The vibrations were applied vertically at amplitudes from 0.1 to 2.5 mm.

The effects of quartz and salt (NaCl) content on the liquid limit (w_L) of Tixoton are shown in Figure 4-3. Results from two separate batches of Tixoton supplied to the project are shown. The data show that, as expected (Lambe and Whitman, 1969), for each of the batches w_L decreases with quartz and NaCl content and that the decrease in w_L is virtually linear and inversely proportional to quartz content. The difference between the batches shows the expected variability in bentonite clay products that has been found elsewhere (Dixon et al, 1992a). Dilution of the clay with quartz diminishes variability. Quality control procedures applied during repository construction should allow for these variations. Designs for repository seals should accommodate these variations through appropriate safety factors and procedures. The measured batch variability may be significant. This was not examined in the Stripa Project and may need to be investigated further through appropriately applied statistically-based quality control and assurance methodologies (e.g. Taguchi, 1978).

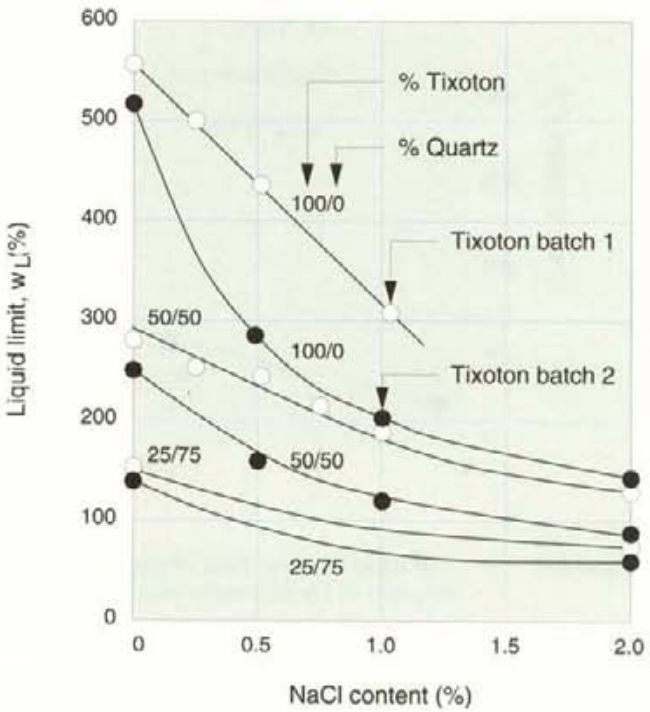

Figure 4-3 Measured liquid limits (w_L %) of different batches of Tixoton clay grouts with a range of quartz and salt contents.

From the test results shown in Figure 4-3 it was hypothesized (Börgesson et al, 1991) that, with time, a grout containing relatively high proportions of NaCl would lose the salt, through diffusion into the groundwater and rock with which it would be in contact. Thereby, the shear resistance of the grout should increase and, as shown in section 4.2.2, its hydraulic conductivity should decrease. Thus, it was concluded that it would be preferable to inject bentonite clay grouts with relatively high salt contents, which at minumum should be equal to or greater than that of the groundwater. Thereby, these materials became the focus for further detailed study through the laboratory studies and the *in situ* investigations. Materials containing no salt were investigated for the purposes of comparison.

Figure 4-4 presents the results of different methods used to measure the undrained shear strength of Tixoton at 150 per cent of its liquid limit ($w \approx 840\%$) at different times after mixing. The data show that shear strength increases with time and illustrates that the bentonite clay slurries, as expected, were thixotropic. Other measurements demonstrating the same phenomenon are provided by Börgesson et al (1991). These data confirmed that grouts liquefied, prior to injection, by mechanical processes could be expected to regain strength and become increasingly resistant to mechanical disturbance with time. According to Atkinson and Bransby (1978), and as shown in Figure 4-4, injected at a water content that is higher than the liquid limit (as proposed and as effected in the *in situ* experiments) the clay slurry will have a strength that is less than 1 kPa immediately after injection . Injected with high salt contents, subsequent decreases in the salinity of the pore waters and the thixotropic properties of the material will lead to strengths above 1 kPa.

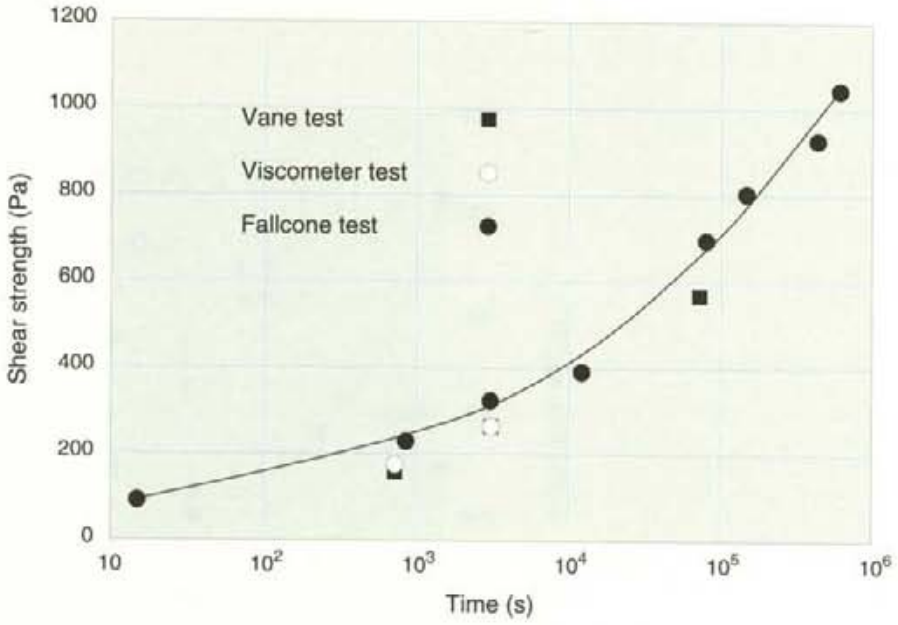

Figure 4-4 The effects of time after mixing and disturbance on the undrained shear strength of Tixoton-water slurries at $1.5 \cdot w_L$.

The results from tests using the Bohlin rheometer showed that at the water contents being considered ($1.0 \leq w/w_L \leq 2.0$) the clay slurries were pseudo-plastic with $n \neq 1$ (see Eq. 4.1). Typical results from the tests with the Brookfield viscometer in which the grout was subjected to vibrations are presented in

Figure 4-5. The abscissa, the shear strain amplitude (γ_A), is the ratio of the absolute applied amplitude to the annular gap between the cup and the bob expressed as a percentage. With a gap of 3 mm the maximum applied amplitude of 2.5 mm gives a maximum shear strain amplitude of 83 per cent. The data show that both the amplitude and the frequency of the vibrations decreased the viscous resistance of the grout. The parameter n was increased and approached a value of 1 (the value for a newtonian or bingham fluid) at frequencies above about 50 Hz with γ_A at 8 to 10% or higher. The effects of amplitude were more significant than those of frequency. At amplitudes greater than about 10% and frequencies of 50 Hz or higher, the materials behaved as a newtonian fluid with m, the viscosity parameter, equal to about 3 Pa and $\tau_o = 0$.

The results for quartz/bentonite mixtures showed similar trends. The effects of increasing γ_A on the m value for 50% quartz/50% bentonite mixtures are shown in Figure 4-6. The patterns in the data and the magnitude of the m values are similar to those shown in Figure 4-5 for the 100 % clay-water systems. The m values determined for mixtures with different NaCl contents at a constant w/w_L value of 1.7 are shown in Figure 4-6(a). Ideally, the curves should be congruent. The differences probably arise from the imprecision inherent in the measurement of w_L. The effects of increasing water content while holding all other mix parameters constant are shown in Figure 4-6(b). The trends in the results are consistent with those shown by other mixtures and, logically, show that the material becomes less viscous with increasing water content.

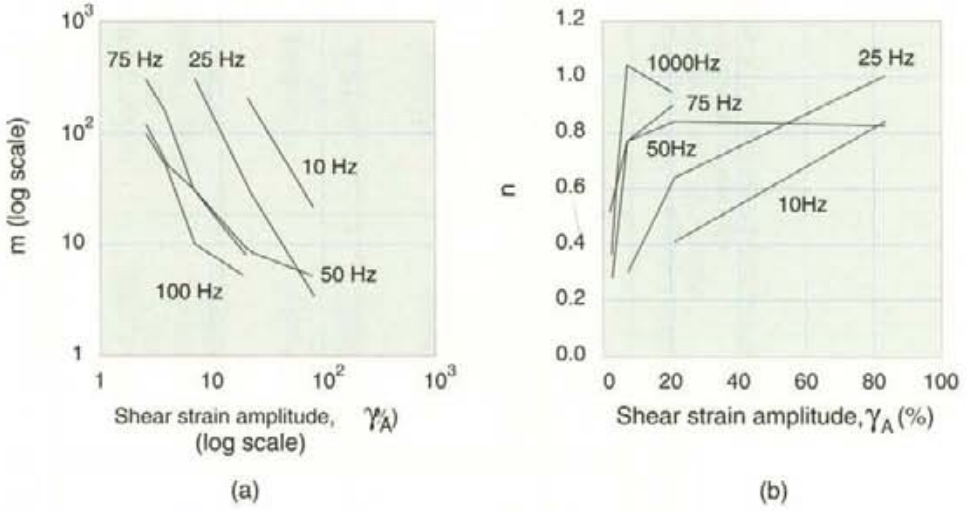

Figure 4-5 The effects of shear strain amplitude and vibration frequency on the viscosity parameters m and n for Tixoton-fresh water mixtures at w/w_L = 1.2.

Thus, in synthesis, the tests on the rheological properties of the clay/quartz/water mixtures showed that adding salt to and vibrating clay slurries during injection would reduce their viscosity. This, in turn, should help the grouts to penetrate fissures in the rock or, otherwise, improve the effectiveness of the clay grout. The water contents of the grouts should be about 150 per cent of w_L, at which the shear strength of the material at injection would be less than 1 kPa and the clay dry density (see note 9, Chapter 2) of the grout would be

Table 4-3 Cement-based grout materials used in the laboratory and *in situ* tests.

MATERIALS	LABORATORY STUDIES		*IN SITU* TESTS			
			PILOT TESTS		EDZ GROUTING	FRACTURE ZONE GROUTING
			Stage 1	Stage 2		
CEMENT: Type [1] Content [2], % Supplier	SRPC/50/V/R 100 to 90 Ciment Canada Lafarge	ALOFIX (MC-500) 100 to 90 Onoda Corp., Japan	SRPC/50/V/R 90 Ciment Canada Lafarge	SRPC/50/V/R 90 Cementa, Sweden	ALOFIX 100 Onoda Corp., Japan	ALOFIX 100 Onoda Corp., Japan
POZZOLANA: Type Content[2], % Country of origin	Silica fume 0 to 10 Canada	Silica fume 0 to 10 Canada	Silica fume 10 Canada	Silica fume 10 Sweden	- - -	- - -
WATER REDUCER: Type [3] Content [4], % Trade name Supplier	Na-SNFC 0 to 3 Disal Handy Chemicals PQ, Canada	Na-SNFC 0 to 3 Disal Handy Chemicals PQ, Canada	Na-SNFC 1.1 Disal Handy Chemicals PQ, Canada	Na-SNFC 1.3 Disal Handy Chemicals PQ, Canada	Na-SNFC 1.4 Mighty 100 Onoda Corp., Japan	Na-SNFC 1.4 Mighty 100 Onoda Corp., Japan
W/CM [5]	0.4 to 0.7	0.7	0.425	0.36	various	0.4 to 0.45

NOTES:
1 Sulphate Resistant Portland Cement, Canadian Type 50, US Type V, R = reground to Blaine fineness of 600 m^2/kg.
2 Based on total mass of cement plus pozzolana. Values expressed as a percentage.
3 Na-SNFC = sodium salt of sulphonated naphthalene formaldehyde condensate.
4 Mass of solid water reducer/ total mass of cement plus pozzolana, expressed as a percentage.
5 Mass of water/ total mass of cement plus pozzolana.

about 0.25 Mg/m^3 or less. At its maximum value, the density of the grout is about 60% of that in the upper backfill material applied and tested in the BMT as part of Phase 1 of the Stripa Project. The strength should increase with time to values above 1kPa. To optimize the workability of the clay grout, the pumps should be designed to provide vibrations at a minimum frequency of about 40 Hz with a large strain amplitude.

Cement grouts

The rheological properties of a number of different cement types and mixtures of the materials with pozzolanas [12] and water reducing agents [13] were determined during the Phase 3 studies for the project. Table 4-3 presents a summary of the materials on which the laboratory studies were ultimately focussed and identifies the materials that were injected into the Stripa rock for the *in situ* experiments.

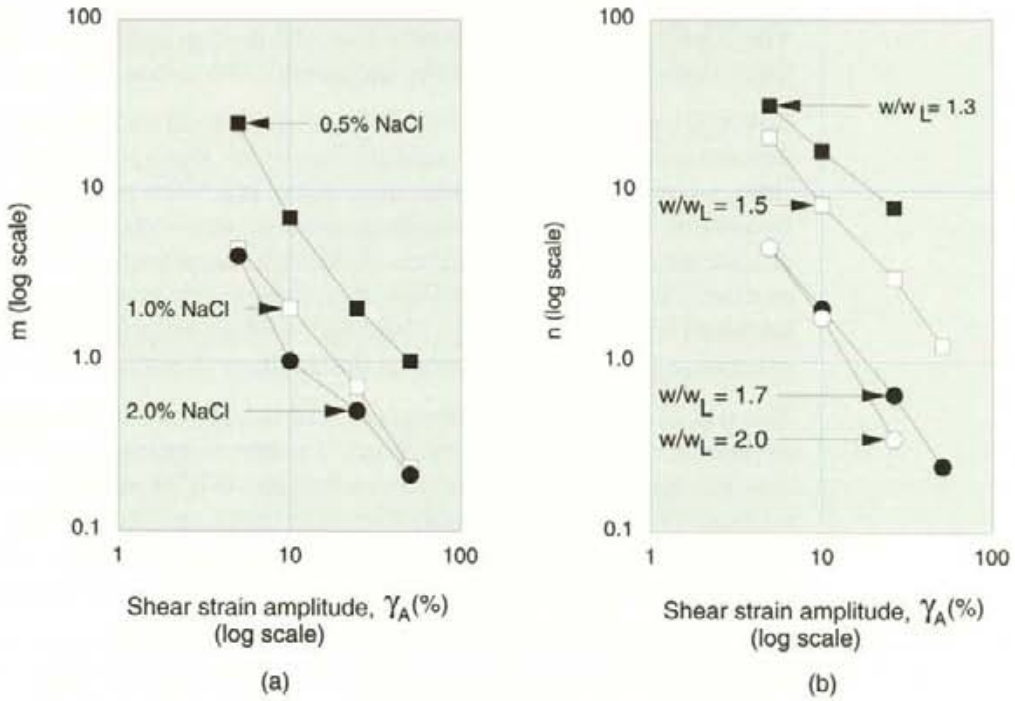

Figure 4-6 The effects of shear strain amplitude at f = 40Hz on the viscosity, m, of 50% quartz/50% Tixoton - water mixtures showing (a) the effects of salt content at w/w$_L$ = 1.7, and (b) the effects of water content with 2% NaCl. Note from Figure 4-5 that at f≥ 50 Hz, n → 1 with γ_A > 10%.

---

12 Pozzolanas are Siliceous and aluminious materials which, though not cementitous themselves, in the presence of water at normal temperatures combine with lime (Ca(OH)$_2$) to form compounds which have low solubliities and possess cementing properties.

13 Water reducing agents are also known as plasticizers and superplasticizers. They are addes to cementitous materials to allow for the rediction of water content while maintaining high fluidity in freshly mixed cement pastes.

A wide range of portland cement types is commercially available in the member countries. For practical reasons, it was necessary to restrict the number of materials studied within the project. This was achieved by reference to the results of grouting studies undertaken between 1984 and 1987 as part of a bilateral international agreement between AECL Research (Canada) and the Department of Energy (United States of America). For completeness the activities undertaken for these studies are briefly described here.

Sulphate Resistant Portland Cement (SRPC, Canadian Type-50), expansive cement (Canadian Type K) and Alofix (MC-500), a commercially available slag cement designed for rock-grouting applications, were examined in the AECL/USDOE investigations (Gray and Keil, 1989). SRPC was considered as being appropriate for use in granitic rock, where some groundwaters contain sufficient quantities of sulphates to be considered aggressive to cementitious materials. While portland cement grouts injected into saturated fracture zones should not significantly shrink during setting and hardening, the use of expanding cements (Canadian Type K) could be advantageous in some sealing applications and were studied.

Since the penetration of very fine fractures was of interest, both the SRPC and Type K cements were investigated at their normal fineness and after regrinding. The Alofix cement is extremely fine and no regrinding was necessary. The three cement types were tested alone and with silica fume admixed.

Silica fume (a pozzolana) was incorporated in all mixes to minimize the amount of readily soluble residual lime ($Ca(OH)_2$) in the hardened grout. The lime, which is formed as a product of the reactions occurring during cement hydration, is converted through pozzolanic reactions to less soluble calcium silicate and aluminate hydrates. While the supposed prime benefit of these reactions is enhanced durability, the studies showed that grouts with silica fume admixed also exhibited less bleeding[14] and segregation than that observed in otherwise similar grouts without the additive (Onofrei et al, 1992).

The use of low *W/CM* [15] in a grout will tend to maximize density and, inversely, minimize porosity. Thus, a water reducing agent (superplasticizer) was incorporated in all mixes to reduce the *W/CM* of the grout while achieving a viscosity that is low enough to permit injection into the rock (Aïtcin et al, 1989). The superplasticizer used was a proprietary sodium salt of sulphonated naphthalene formaldehyde condensate (Na-SNFC) - see Figure 5-23.

The AECL/USDOE studies showed that low viscosity, non-segregating grouts could be prepared using any of the three basic cement types investigated. The quantity of superplasticizer could be varied to achieve a grout with characteristics suitable for pressure injection into the rock. The reground SRPC cement with 10% silica fume appeared to require slightly less water than either the Type K with 10% silica fume, or the MC-500, for the equivalent viscosity. Moreover, SRPC cement is a widely available material, with its properties well

---

[14] Bleeding is the separation of the solid particles from the liquid phases of a freshly mixed grout. It can occur after injection, by simple settlement or, during injection, by consolidation of the solids under pressure gradients. Bleeding can cause larger voids or other inhomogeneities to be formed in the material structure. These inhomogeneities may be detrimental to the performance of the grout and are to be avoided.

[15] *W/CM* is the ratio of the mass of water to the combined mass of cement plus silica fume (cementitious materials). This corresponds to the water to cement ratio used in conventional cement and concrete technology.

documented in the open literature and, thereby, fulfilled the requirements of a generic research programme meeting international needs.

Thus, a reference grout mixture was adopted for further use in *in situ* investigations undertaken as part of the AECL/USDOE agreement. The grout had the following composition:

- 90% [16] sulphate resistant portland cement (Canadian Type-50), reground to a Blaine fineness of 600 m^2/kg,
- 10% [16] silica fume,
- 1% [16] superplasticizer (sodium salt of sulphonated naphthalene formaldehyde condensate), by the total mass of cement plus silica fume, and
- water (*W/CM* between 0.4 and 0.6 by mass).

These materials were successfully introduced by pressure injection into an hydraulically active fracture zone at the Underground Research Laboratory in Canada (Gray and Keil, 1989). Fractures as narrow as 20 mm were penetrated and sealed (Onofrei et al, 1988).

As noted above, the Stripa Project, Phase 3, built on these data and experiences and the task force selected the above mix composition as the base of its laboratory and some *in situ* investigations. Recognizing the possible benefits of the fine particle size of Alofix and silica fume, mixtures containing these materials were also investigated. Later in the investigations SRPC cements and finely ground cement grouting materials produced in Sweden were also studied.

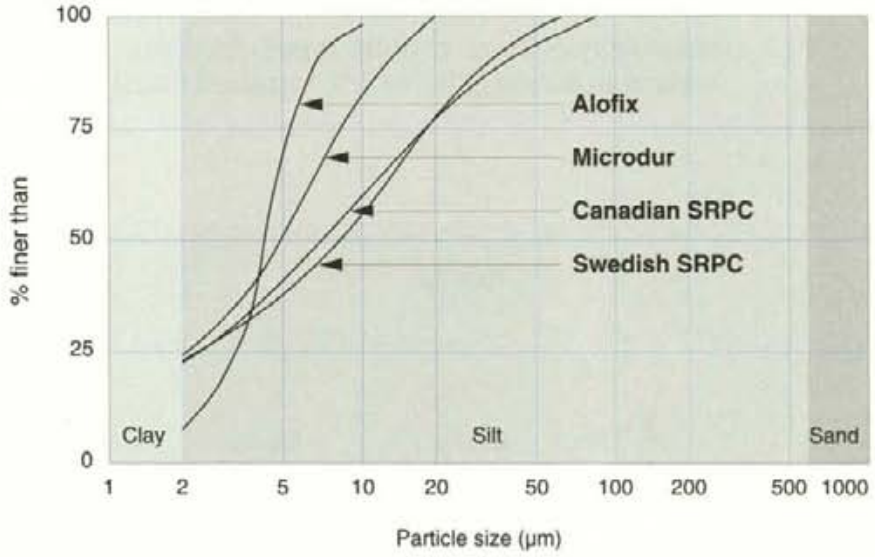

Figure 4-7 The particle size distributions of the different cement types investigated.

The viscous flow properties of the cement grouts were determined using the Bohlin VOR rheometer and the Brookfield viscometer used for the tests on the clay materials. In addition, a simple efflux viscometer (a variation on the Marsh Cone, IAEA, 1990) was used. In common with the liquid limit tests

[16] Percentages based on the total mass of cementitious materials (*CM*) = cement plus pozzolana.

applied to the clay grouts, the efflux viscometer tests allowed for rapid assessments of mix variables on material properties and, ultimately, could be used for quality control tests to be conducted on the materials during *in situ* applications. These tests were supplemented by standard setting time tests and measurements of the unconfined and confined compressive strengths of selected mixtures after hardening and with time. In addition to allowing for quality control of the mixtures, the strength tests provided information on the possible performance of the cement grouts after injection and hardening. The setting time tests were needed to ensure that the mixtures selected for the *in situ* studies were workable over the time available for grout injection.

The cements tested varied one from another both in chemical composition and in particle size distribution. Figure 4-7 shows the differences in particle size distribution. The differences in chemical composition are discussed in Chapter 5. Reflecting the physical and chemical differences, the rheological properties of fresh cement/water mixtures differed between the cement types. Moreover, the changes in the rheological properties resulting from admixing silica fume and superplasticizer with each of the cements were not identical (Börgesson et al, 1991). However, the following common trends were observed in the results from the viscometer tests on freshly mixed materials.

The materials of interest were pseudo-plastic. Their rheological behaviour, like that of the clay grouts, could be described by Equation 4.2.

$$\tau = m \left(\frac{\gamma}{\gamma_o}\right)^n \qquad (4.2)$$

where τ, γ, γ_o, m and n have the same meaning as in Equation 4.1.

As expected, increasing the *W/CM* increased the fluidity (decreased the shearing resistance, τ) of the grout. Similarly, increasing the superplasticizer content in the range 0.5 to 2 % increased fluidity.

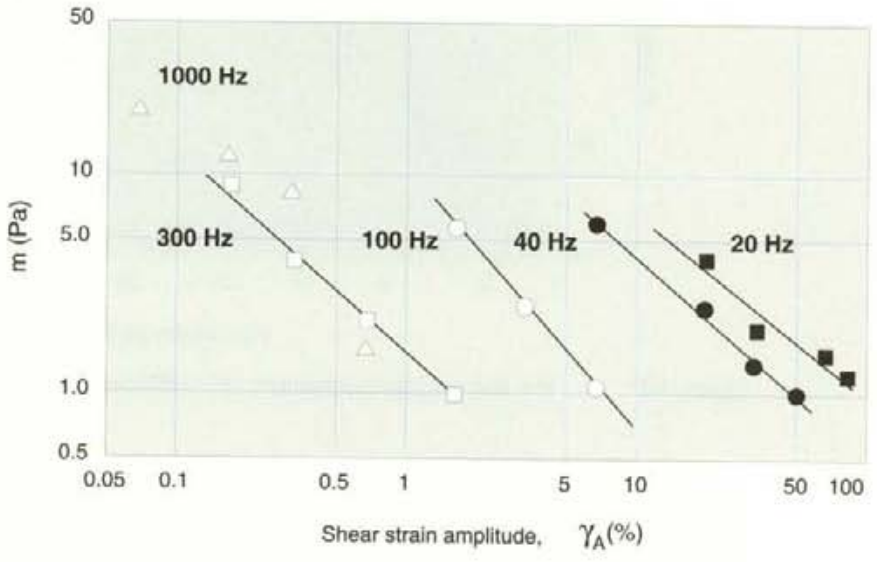

Figure 4-8 The effects of frequency and amplitude of vibrations on the viscosity parameter m of mixtures of SRPC cement (Swedish), 10% silica fume, 0.75% Disal superplasticizer at *W/CM* = 0.35.

Vibrating the cement grouts decreased τ. Other test variables being maintained constant, increasing the frequency and the amplitude of the applied shear strain decreased τ , with n tending towards a value of 1 (i.e. with increasing vibration frequency and amplitude, material behaviour tended towards newtonian). Typical results are shown in Figure 4-8. The data show that at lower frequency, higher amplitude vibrations were needed to achieve the same viscosity, m, as that attained with higher frequency, lower amplitude vibrations. It was concluded that an injection pump capable of delivering either high frequency, low amplitude or lower frequency, higher amplitude vibrations could assist injection of the high-performance low *W/CM* cement grouts being considered in the programme. Furthermore, the general expectation, that the viscous properties of the grouts could be adjusted to within appropriate limits by varying the *W/CM* and the superplasticizer content without adversely influencing other important properties such as bleeding and setting time, was confirmed.

Cement-based grouts differ from clay materials in that, following a dormant period after mixing with water, new hydrated minerals are formed and the grouts set and harden. These processes limit the period through which the cement grouts remain workable and can be injected into the rock. Setting time tests, carried out in accordance with ASTM-C-191 (1984) or similar national standards, are used in engineering practice to provide a general guide to the period of workability. Tests carried out with the Bohlin rheometer provided a more precise indication of the effects of setting processes on the viscosity of the grouts. The effects of time and temperature on the shearing resistance of a grout mixture based on Alofix cement are presented in Figure 4-9 (a). Similar trends were shown by other cement grouts studied.

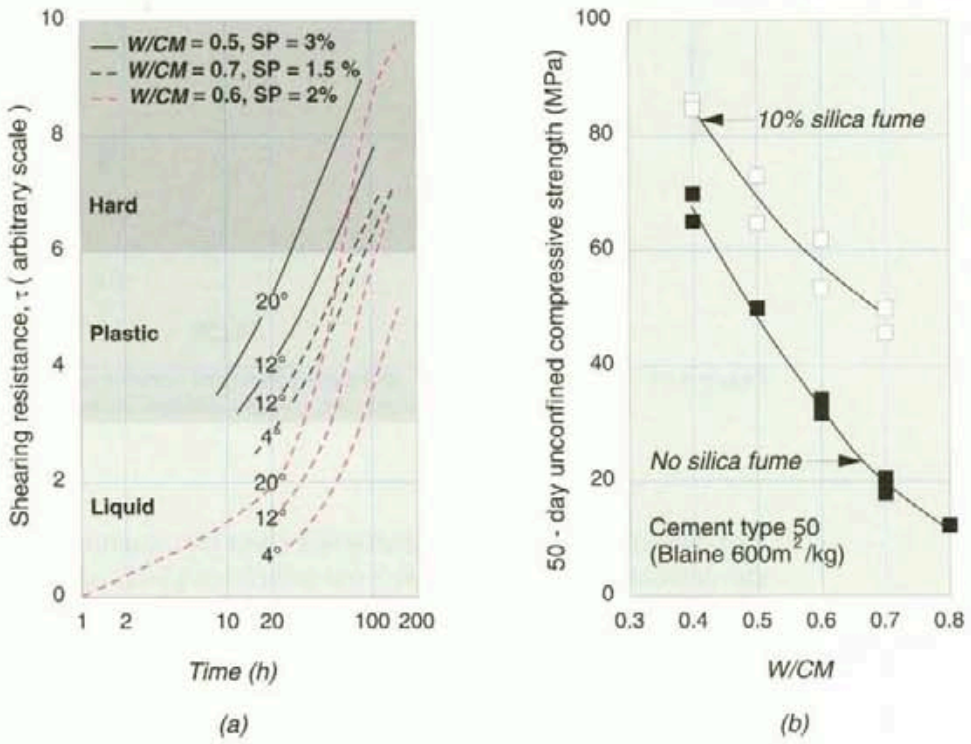

Figure 4-9 (a) The effects of time, temperature, *W/CM* and superplasticizer content on the shearing resistance of setting Alofix cement, and (b) the influence of silica fume content and W/CM on the unconfined compressive strength of hardened SRPC grout.

The data in Figure 4-9(a) show that decreasing the temperature and increasing the *W/CM* delay the onset of hardening of the mixtures. This can be identified in the figure by the change in slope of the τ-time curve. This occurs at a value of τ between 1 and 2 on an arbitrary scale. Shearing resitance was probably about 1 kPa which is the value for clay-water mixtures at their liquid limit (w_L) and at or below which it was concluded the the clay grouts were workable. During injection the grouts will vary in temperature due to the effects of friction during mixing and pumping, the liberation of heats of hydration and the differences between the tunnel temperature and that of the rock mass. These factors need to be accommodated during the application of the materials. For example, the generally lower temperature of the rock mass will delay setting of the cement grouts and may make them vulnerable to erosion if they are subjected to high groundwater pressure gradients. This is discussed further in sections 4.2.3 and 4.4. The setting time results combined with the τ-t data presented in Figure 4-9(a) showed that the mixtures would remain workable for periods of four or more hours, which was considered adequate for both the *in situ* testing conducted for the Stripa programme and the use of the materials in repository sealing.

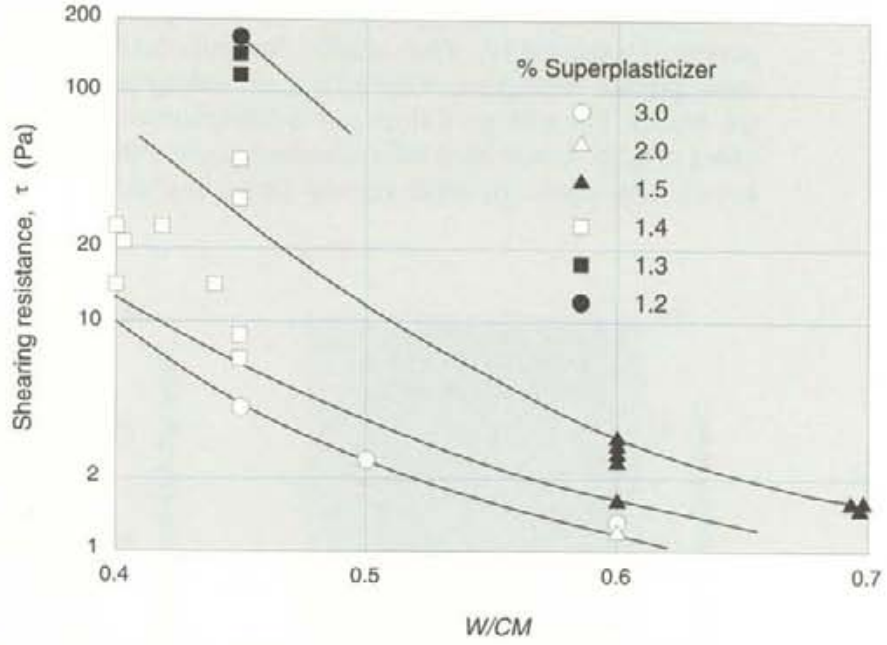

Figure 4-10 Effect of *W/CM* and superplasticizer content on the shearing resistance (τ) of freshly mixed batches of Alofix cement delivered at different times to the project.

The data in Figure 4-9(a) (abstracted from Börgesson et al, 1992b) indicate that the cement grouts were considered to behave plastically within the range on an arbitrary scale of $3 < \tau < 6$. This probably corresponds to the range 1 kPa $< \tau <$ 100 kPa which has been measured for clays in the range $w_P < w < w_L$ (Atkinson and Bransby, 1978). Figure 4-9 (b) shows the effects of *W/CM* on the unconfined compressive strengths (cured in water for 50 days after mixing) of the SRPC based reference grout with and without the addition of silica fume. The data show that, after hardening, cement grouts gain strength to achieve high values that depend on the mix composition. Both decreasing the *W/CM* and admixing silica fume increase strength. Superplasticizers (water reducing

agents) of the type examined in the Stripa programme allow for low *W/CM*, non-bleeding, workable mixtures to be used and are an essential constituent of the high-performance cement grout materials investigated. The term "high-performance" not only relates to high strength but also reflects the low hydraulic conductivity (section 4.2.2) and the high durability (Chapter 5) expected of these low *W/CM* mixtures.

In common with the bentonite clay grouts, the viscosity of freshly mixed cement-water grouts varied within batches and between batches. A measure of this variability in Alofix is presented in Figure 4-10. The differences arise from inherent variability in the industrial product, variabilities in the sampling and mixing processes and the age of the product. Both cement and silica fume are particularly subject to change with age in both laboratory and, perhaps more, industrial settings. A phenomenon known as "pack-setting" causes aggregations of particles in both cement and silica fume. The high efficiency mixers used for grout preparation are not able to completely disaggregate the compacted particles. The resulting larger maximum particle size may limit the ability of the grouts to penetrate finer fissures. This may render the materials less useful as grouts with time and affected the selection of the grouts for use in the *in situ* experiments.

The cement used as a component of the AECL/USDOE reference grout was a special product that had been processed (reground) in 1986 and dry-stored in sealed containers since then. The material was successfully used in the *in situ* experiments in Canada and in preliminary *in situ* trials for the Stripa Project. The full scale grouting experiments were carried out in the Stripa mine during 1990 and 1991. At this time it was concluded that "pack setting" had occurred in the reference materials to a degree sufficient to limit the success of the experiments: thus, shown in Table 4-3, freshly manufactured Alofix was selected for use in the experiments. With this experience it can be noted that if used in repository sealing, the inherent variability in cement-based grouts has to be accommodated through appropriate quality control procedures. Particular attention has to be placed on the natural variability in the cement and silica fume products and the effects of age on the particle size distribution of these materials: the viscous properties are less affected by the small but, possibly, significant changes in particle size distribution that occur through time. Even with adequate quality control procedures in place, it can be inferred from the test results shown in Figure 4-10 that inherent material variability will require adjustment of mix proportions as the field activities are undertaken. In this latter respect it is noted (Onofrei et al, 1992) that industrial scale grout mixers tend to be more efficient than laboratory equipment. Thus, in addition to variability in the constituent materials, the effects of mixing and handling processes can affect the injection and, ultimately, the sealing properties of the grout. All these factors can influence the success of a grouting process and will require control during repository sealing operations. Experienced and trained personnel will be required to effect the control procedures and make the field adjustments to mix design, which in final form will be effected through the application of understanding gained from observations made during the progress of the *in situ* grouting operations. This latter comment also applies to grouting with clay-based materials.

4.2.2 Hydraulic conductivity

The laws and field equations governing mass transport through porous media were discussed in Chapter 2. Generally, it was shown that water flux, J_W, can be described by Equation 4.3.

$$J_W = L_{HH}.\nabla(-H) + L_{HT}.\nabla(-T) + L_{HC}.\nabla(-C) + L_{HE}.\nabla(-E) \qquad (4.3)$$

where, L is the transfer coefficient under gradients of temperature (T), electrical potential (E), hydraulic head (H) and chemical concentration (C). The two subscripts on L denote first the flow type and second the driving gradient. The element $L_{HH}\nabla(-H)$ represents Darcy's law. The hydraulic conductivity L_{HH} - k - of the clay and cement grouts were determined. Moreover, some aspects of the effects of mechanical disturbance on the hydraulic conductivity of these materials were evaluated.

Clay grouts

It was shown in Chapter 2 that the hydraulic conductivity of highly compacted bentonite (HCB) and bentonite/sand mixtures decreases with increasing clay dry density. Similarly, it has long been established that the hydraulic conductivity of loose clays, such as the clay grouts proposed for testing in the *in situ* experiments, increases with decreasing clay dry density (Lambe and Whitman, 1969). Due to more pronounced colloidal behaviour with decreasing clay dry density, the effects of increasing ionic concentration in the permeating pore water, temperature and dielectric constant could be expected to be more evident in the proposed, low density, clay grouts than in the HCB. Moreover, the clay grouts had low mechanical strength and, at elevated levels, hydraulic pressure gradients could mechanically disturb the fabric of the soft materials. It is likely that the resulting changes in the connected porosity and pore size distribution of the clay grouts would increase the apparent hydraulic conductivity of the clay media. The extreme expression of this process is the generation of enlarged pathways for water flow through the clay. This is commonly known as "piping". These aspects of the hydraulic properties of the proposed clay grouts were studied using laboratory devices specially designed and built for the Stripa Project.

The hydraulic properties of loose clays in bulk are well established (Lambe and Whitman, 1969). However, injected as grouts, the materials will generally be in the form af thin films, the properties of which are less well understood. Thus, the two devices shown in Figure 4-11were built and used to investigate the properties of thin films of the clay grouts.

Both of the devices allowed for the hydraulic conductivity of the thin grout films to be measured. By moving the inner cone relative to the outer housing, the cone-in-cone apparatus allowed for the aperture holding the film to be varied during the progress of the tests and the hydraulic response of the clay to the adjustment to be measured. The piping test equipment allowed for the effects of hydraulic lengths longer than those in the cone-in-cone apparatus on the piping resistance of the clay to be studied. In both test systems the hydraulic aperture was set at 1 mm. A maximum variation of 300 μm (30%) was applied in the width of the aperture in the cone-in cone apparatus. To set up the tests the clay or clay/quartz grout slurries were smeared in excess on the aperture surfaces and the test cells were assembled, the excess grout removed

and the completed system connected to water supplies and flow measuring systems.

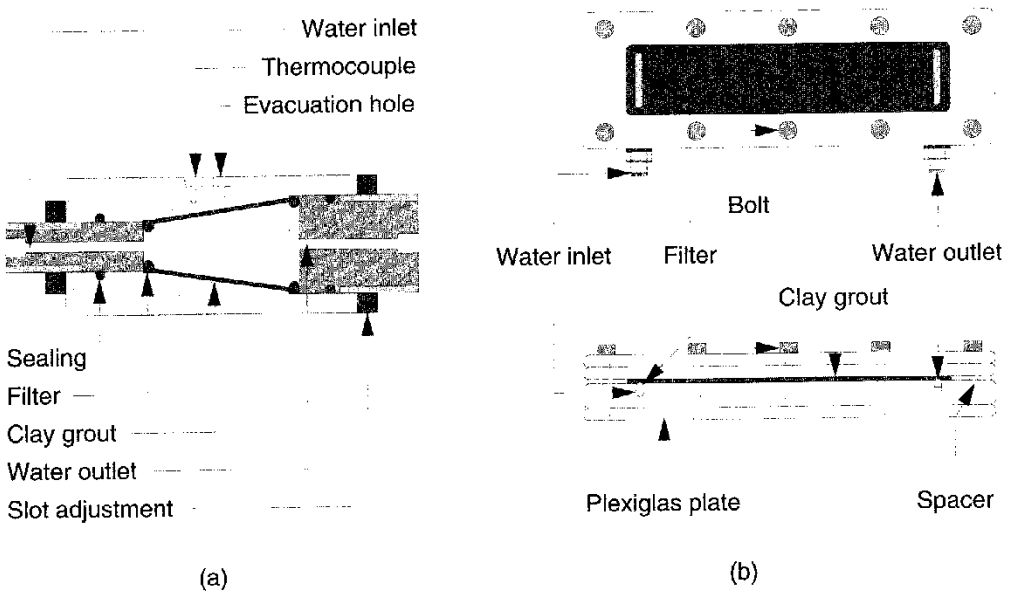

Figure 4-11 (a) the cone-in-cone apparatus, and (b) the piping test equipment used to measure the hydraulic conductivities of thin films of grout.

For the cone-in-cone tests, seven days after the cell had been assembled an hydraulic gradient of 14 was applied to the clay grout. Once flow through the cell had stabilized and the hydraulic conductivity of the undisturbed grout was known, the aperture was expanded by 30% and, simultaneously, the cell was heated to a temperature of 90°C. The systems were allowed to come into equilibrium under these new conditions after which the temperature was returned to its original value of 20° $^{+}/_{-}$ 1°C.

For the piping tests, after the equipment including the test specimen were readied, at 15 minute intervals the hydraulic gradient was incremented by appropriate values until piping occurred. Piping was recognized by a sudden increase in flux through the specimen.

Based on the rheological tests results and the proposal that NaCl rich grouts should be injected in the *in situ* experiments, the cone-in-cone tests focussed on Tixoton or Tixoton/quartz clay grouts mixed with 1% NaCl solution at w/w_L = 1.6 ($\gamma_c \leq 0.19$ Mg/m^3)[17]. In some cases a Ca-bentonite clay was tested: the effects of w/w_L were also determined. Materials mixed at w/w_L = 1.3 were used for the piping tests.

Three permeants were used in both the cone-in-cone and the piping tests; the permeants were distilled water and two $CaCl_2$/NaCl solutions with total dissolved solid contents of 1.2 and 1.5 % and Ca^{2+} and Na^{+} in the ratios of 1.3:1 and 1:26, respectively. The Na^{+} rich solution was considered to represent sea water, the Ca^{2+} rich solution was similar in composition to the waters found in granic rocks housing the repository for intermediate and low-level radioactive wastes near Forsmark in Sweden (Pusch et al, 1991b).

---

17 The clay dry density , ρ_c, is used here. Generally, bulk density, ρ_b, is reported by Pusch et al . See footnote 10 (Chapter 2) for the relationship between these parameters.

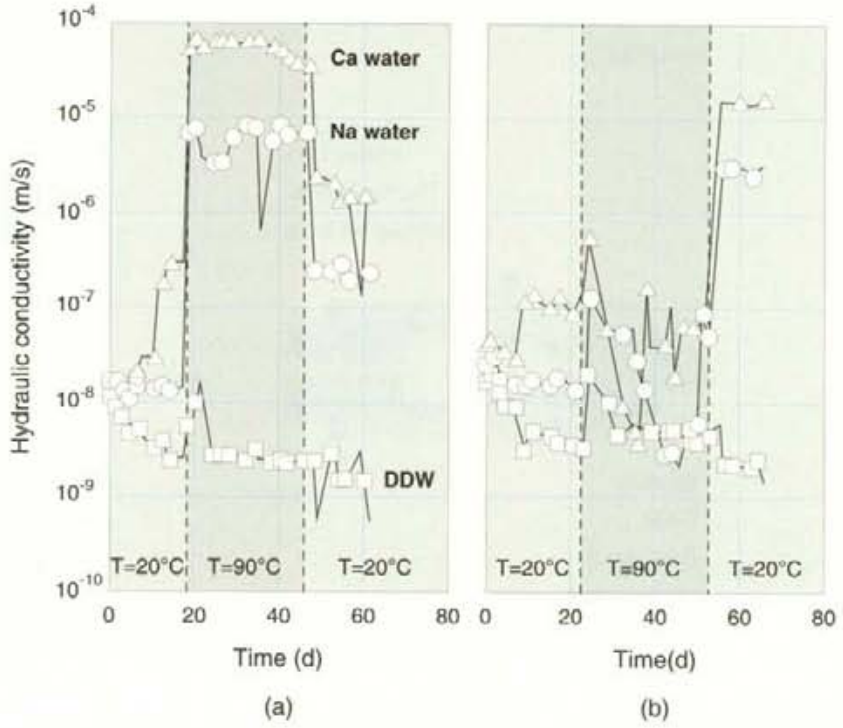

Figure 4-12 The results of the cone-in-cone tests on (a) 100 % Tixoton, and (b) 50% Tixoton/50% quartz mixtures mixed with 1% NaCl solution and permeated with three waters with different dissolved solids.

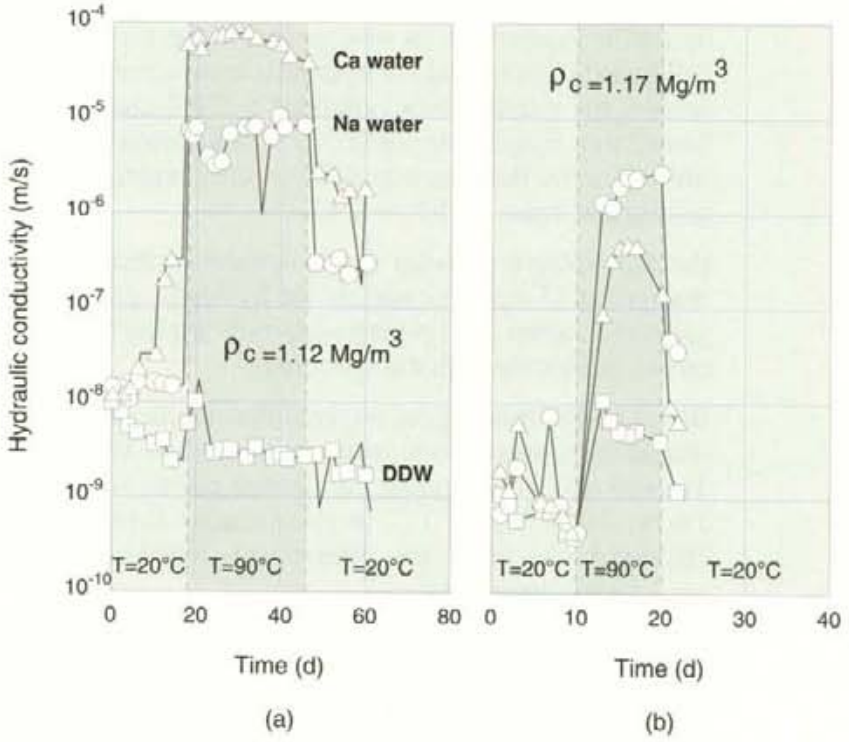

Figure 4-13 The effects of (a) the salinity of the permeant, and (b) the initial density of the clay and the salinity of the permeant on the response of Tixoton grout in the cone-in-cone tests.

Results from cone-in-cone tests on 100% Tixoton and 50% Tixoton, 50% quartz mixtures are presented in Figure 4-12(a) and 4-12(b), respectively. The

values and responses of 75% Tixoton, 25 % quartz mixtures were similar to those of the 100% Tixoton grout. The minimum hydraulic conductivity of the clay grouts is approximately 10^{-9} m/s and is achieved by the materials permeated with fresh water. At the start of the test, the hydraulic conductivity of both the clay and the 50-50 clay-quartz mixtures lay in the range $2.10^{-8} < k < 5.10^{-8}$ m/s, with the clay being slightly less conductive than the mixture. In this latter respect it is noted that the porosity of the mixture is lower (~89%) than that of the clay (~93%) yet the latter has a higher clay density (0.19 Mg/m^3 as compared with 0.16 Mg/m^3). This finding continues to support the general suggestion, noted in Chapter 2, that the clay dry density (clay porosity), not the total porosity of bentonite clay/aggregate mixtures is a major determinant in the control of the mass transport characteristics of the materials.

During the initial stages of the tests, with time the hydraulic conductivities of the materials permeated with fresh water tended to decrease and the hydraulic conductivities of the materials permeated with the salt waters tended to increase. Permeation with the Ca-rich water caused a greater increase in k than permeation with the Na-rich water. This reflects changes in the microstructure of the materials which can be explained by recourse to the theories of colloids (van Olphen, 1963). The salt solutions tend to flocculate the clay particles and cause an adjustment in the pore size distribution in the clays. At similar concentrations bivalent cations will have greater effect in this regard than monovalent cations. It is noted that the total porosity (n) of the system was not changed during the first stage of the cone-in-cone tests. Moreover, with $k \sim 10^{-8}$ m/s and $n \sim 90\%$, it would take approximately 74 days for the pore water in a single pore volume to be displaced by the permeant - assuming slug action. Other processes, such as diffusion, osmosis and channeling of flow in major conduits appear to have enhanced the rate at which the clay microstructures were changed by the permeating solutions. The general hypothesis that injecting salt-laden clay grouts should enhance the long term sealing effects seems to have been sustained. With time after injection the clays will tend to lose salt and become less permeable.

The results of cone-in-cone tests on 100% Tixoton grouts prepared at $1.1w_L$ ($\rho_c \cong 0.26$ Mg/m^3) and 1.3 w_L ($\rho_c \cong 0.23$ Mg/m^3) are shown in Figure 4-13(b) and compared with those of grouts mixed at 1.6 w_L ($\rho_c \cong 0.19 Mg/m^3$) in Figure 4-13(a). The results are consistent with previous findings and show that k tends to decrease with increasing ρ_c. The responses of the grouts to changes in total porosity and temperature are similar but tend to become less pronounced with increasing density. The decreases in k with increasing density were not sufficient to warrant the use of the denser, more viscous and less workable materials in the *in situ* experiments.

The results of the piping tests reported by Pusch et al (1991b) showed that, depending on the composition of the grout and its density, the films of clay and clay/quartz grouts prepared at 1.6 w_L could sustain hydraulic gradients of 20 to 50 before failure due to piping. No clear relationship between density, quartz content and critical hydraulic gradient could be established. There was some indication that, with time, cation exchange, as may occur *in situ* as grouts are permeated by groundwater, may increase the piping resistance of thin clay grout films.

Cement grouts

Tests were carried out in the cone-in-cone apparatus to determine the hydraulic properties of thin films of hardened cement grouts and the effects of mechanical and thermal perturbations on these properties. Moreover, the hydraulic conductivies of bulk specimens of cement grouts were measured. These latter tests were focussed to provide information for the evaluation of the longevity of the materials and are discussed in greater detail in Chapter 5 and by Onofrei et al (1992). Pertinent details are included here.

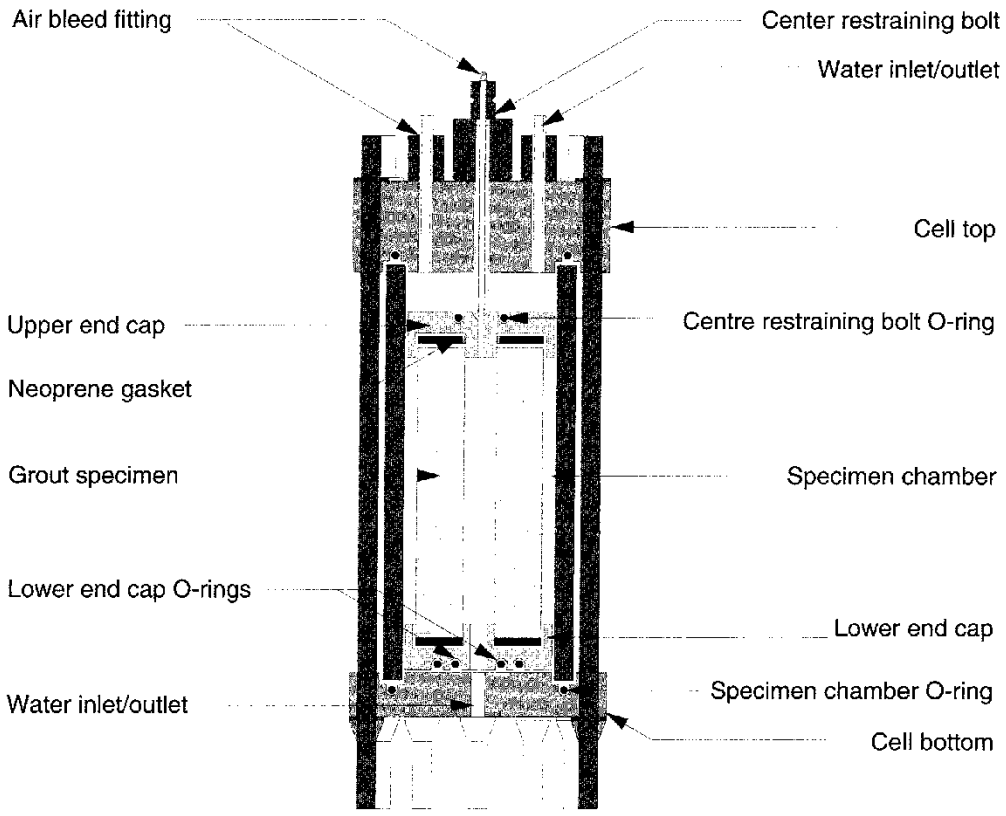

Figure 4-14 The test cell built to measure the hydraulic conductivity of hardened bulk cement grout.

The hydraulic conductivity (k) of hardened bulk specimens of the high-performance cement grouts based on SRPC were determined for $0.4 \leq W/CM \leq 0.8$ with specimens subjected to compressive or tensile stress in specially designed radial flow permeameters (Figure 4-14). The apparatus was designed to withstand hydraulic pressures of up to 10 MPa. Thus, hydraulic gradients of up to 40,000 could be and were applied radially across the 25 mm thick wall of the hollow cylindrical grout specimens. The pressurized oil-water interface flow measuring systems to which the inlet and outlet ports were connected had a resolution of 0.01 ml. This allowed for measurements of k of less than 10^{-14} m/s with an accuracy of $5 \cdot 10^{-15}$ m/s.

Results from the compressive test series for grouts with no silica fume and those containing 10% silica fume showed that both of the grouts tended to store some water over the range of time and pressures investigated (Figure 4-15). Under hydraulic pressure differences > 4,000 kPa (i $\cong$ 16,500) grouts with no

silica fume transmitted water in the direction of i. Hydraulic pressure differences equal to or greater than 8600 kPa (i ≅ 35,000) were needed to obtain measurable through-flow of water with specimens containing silica fume.

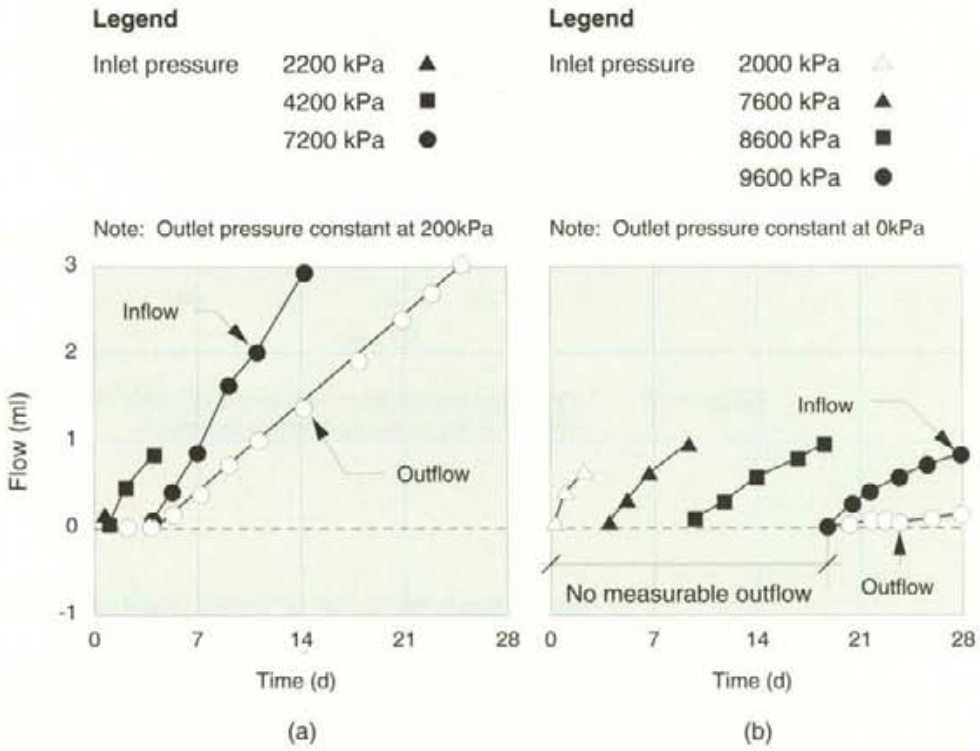

Figure 4-15 Flow-time curves from hydraulic conductivity tests on bulk specimens of (a) SRPC-600 (reground to Blaine fineness = 600 m^2/kg) at *W/CM* = 0.4, and (b) SRPC-600/10% silica fume mixtures at *W/CM* = 0.4. Specimens were under compression.

Flow data for the grout containing silica fume at *W/CM* = 0.4 with the specimen in tension and hydraulic pressure differences of up to 2,000 kPa (i ≅ 8000) are presented in Figure 4-16. The results show that there was no measurable through-flow of water. The grout had very low hydraulic conductivity (i.e., $< 10^{-14}$ m/s). In fact, water was taken up by the grout at both the low and high pressure sides of the specimens.

Thus, it was observed that under both compressive and tensile stress conditions water flow could not be described by the Darcy equation. Under very high hydraulic gradients, which could only be tolerated by the specimens under compressive stress, water tended to flow through the specimens, with some storage. Figure 4-17 presents the k values for these mixtures calculated on the assumption that Darcy's law could be applied to the inflow and outflow rates.

The data show that adding silica fume decreased the apparent hydraulic conductivity of the grout which, for the grout containing silica fume, was approximately 10^{-15} m/s and was influenced little by *W/CM* . For the mixtures without silica fume, k increased with *W/CM* for *W/CM* > 0.6. Below this value, k was in the order of 10^{-14} m/s and was not significantly influenced by *W/CM*.

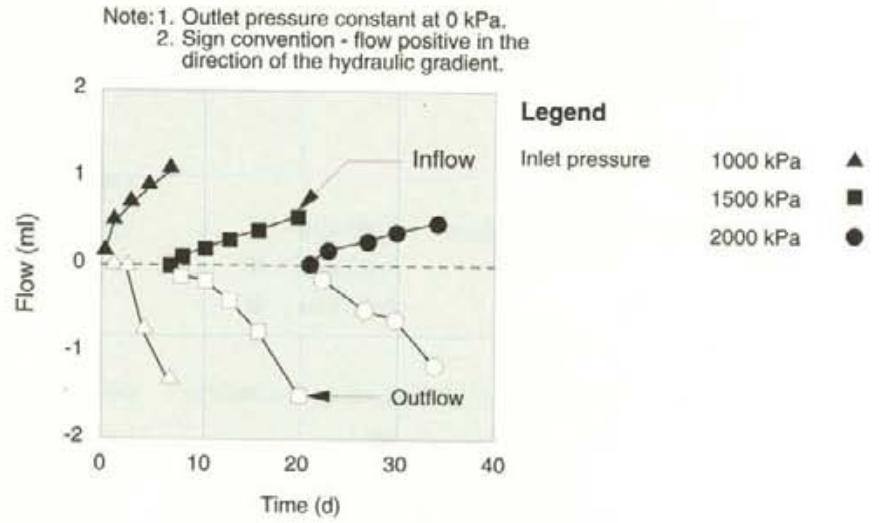

Figure 4-16 Flow-time curves from tests on SRPC-600/10% silica fume mixtures at W/CM =0.4 with the specimens in tension.

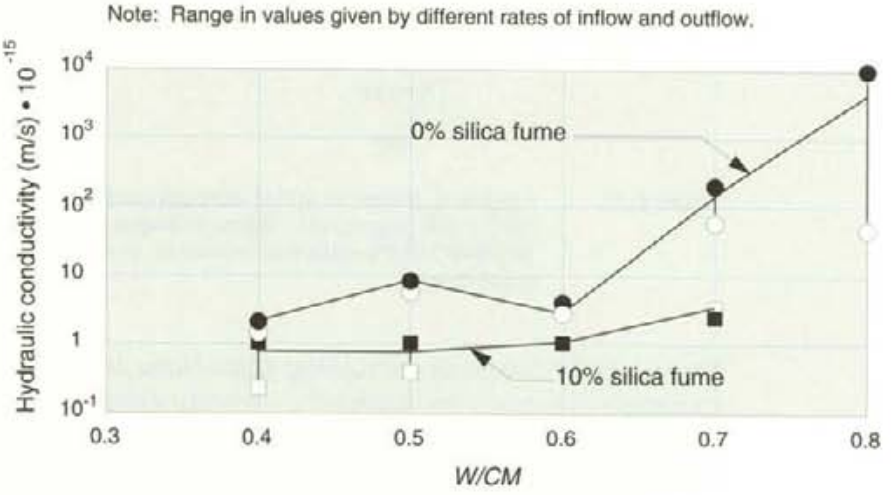

Figure 4-17 The influence of silica fume (SF) content and *W/CM* on the hydraulic conductivity of hardened cement grout ($i > 28500$ for SF = 0% and $i > 35000$ for SF =10%)

Thereby, it was concluded that, in bulk and when intact, high-performance cement grouts are practically impermeable under hydraulic gradients that are very much higher than those expected in a repository where i may be as low as 10^{-2} (Chan, 1987). At these low gradients water does not pass through the materials which have a tendency to take up and store water.

A number of possible explanations could account for the total resistance to the through flow of water at lower gradients. These include the presence of entrained air in the pore spaces, continued hydration reactions, and morphological transformation of hydrated cement minerals. A series of tests were carried out to evaluate the effects of air in the permeant and in the specimens. The effects

of morphological transformation and continuing hydration were also examined (Onofrei et al, 1992). The results of the latter work are discussed in Chapter 5. Figure 4-18 compares hydraulic conductivity test results from specimens that were allowed to set and harden *in vacuo* and permeated with deaired water with those obtained using normal specimen preparation and testing procedures. The data show that air entrapment in the specimen and the presence of air in the permeant did not significantly influence the flow properties of the material.

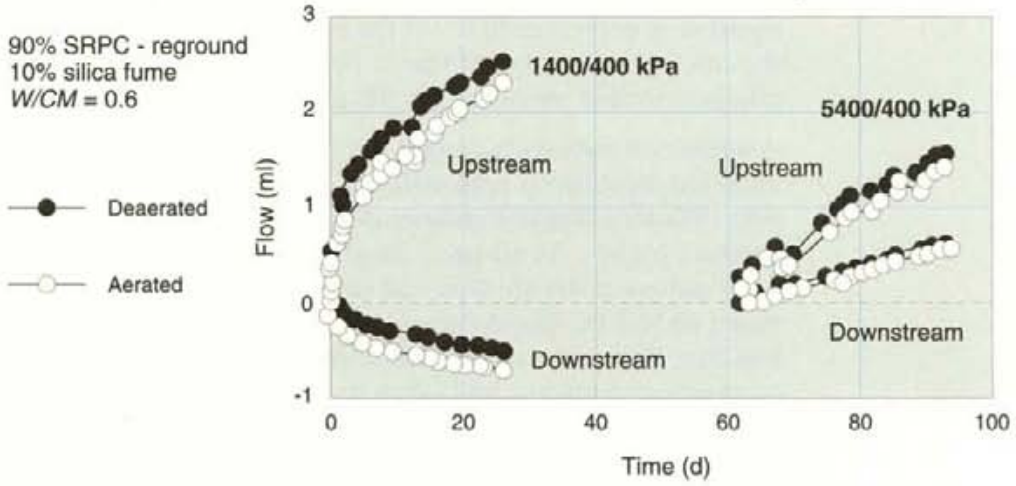

Figure 4-18 The effects of hydraulic pressure gradient on the time-dependent flow through hardened SRPC-600/10% SF grout at W/CM = 0.6. The effects of deairing the permeant are shown.

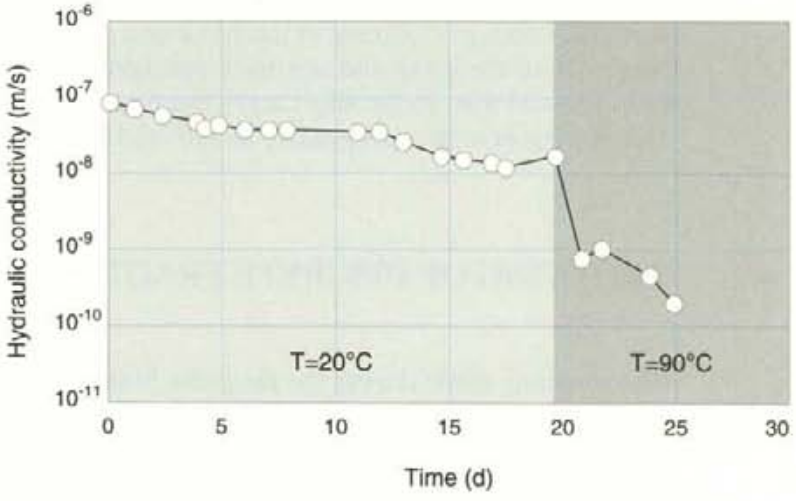

Figure 4-19 Results of cone-in-cone tests on SRPC-600/10% SF at *W/CM* = 0.41.

Cone-in-cone tests were carried out to determine the effects of fracture dilation and temperature increase on the hydraulic properties of hardened cement grouts. Materials based on reground SRPC and Alofix at low *W/CM*, cured for one month before beginning the tests, were studied. Results from a test on an SRPC-based grout containing 10% silica fume and mixed at W/CM = 0.6 are presented in Figure 4-19. In this test the grout film was initially 1 mm thick. After permeation with deaired, distilled water in the undisturbed state, the

aperture width was increased to 1.1 mm and the flow properties of the cracked grout film were measured at different times. In a third stage, the effects of heating the cracked cement to 90°C were measured. The following important details are noted. The flow measuring systems used could measure hydraulic conductivities down to 10^{-11} m/s. They were not sufficiently sensitive to give a measure of the conductivity of the intact cement film which is presumed to have had conductivity properties similar to those measured for the bulk specimens (i.e. $k \leq 10^{-15}$ m/s). The data in Figure 4-19 show that the freshly cracked film had an overall conductivity of $< 10^{-7}$ m/s which tended to decrease with percolation and time. Heating the cracked specimen resulted in further significant decreases in k. At the end of the test the hydraulic conductivity of the cracked cement grout was $< 10^{-9}$ m/s. This is similar in magnitude to the minimum value measured for the expanded and heated clay grout films.

A variety of tests were carried out (Onofrei et al, 1992). Test variables included percolation with different water types, materials of different composition, different film thicknesses and different sequencing of the stress and temperature probes. In all cases the results were similar to those shown in Figure 4-19 and generally showed that the hydraulic conductivity of intact Alofix-based and SRPC-based cement grout films could not be measured and were less than 10^{-11} m/s. At the end of the tests the hydraulic conductivities of the cracked cement films had fallen to values in the order of 10^{-9} m/s or less. Moreover, adding silica fume tended to decrease the final hydraulic conductivity of the grout, whereas the chemical composition of the permeant did not significantly influence the measured k. A number of factors account for the decreasing hydraulic conductivity with time and percolation. These include the presence of unhydrated material in the hardened grouts which, when exposed on the cracked surface, hydrates to form solids with increased volume, the formation and deposition of new minerals on the surface of the cracks through leaching reactions operating at the water/crack surfaces and inherent thermodynamic changes occuring in the hardened pastes. These processes affect the longevity of the grout and are discussed further in Chapter 5. The cone-in-cone tests showed that, in the short term, the processes are beneficial since they provide the grout with a propensity to self-seal any disruption.

4.3 GROUTING OF DISCRETE FRACTURES

Observations made during the progress of the Stripa investigations showed that discrete fractures provide the primary pathways for water flow in the Stripa rock mass within boundaries defined by the major fracture zones. Experiments carried out for the investigations into the natural barriers (Abelin et al, 1985; 1990a; 1990b) showed that water did not flow uniformly across the fractures but was channelled at a scale of tens of centimetres. A conceptual model of this channelling is shown in Figure 4-20. A number of different reasons can account for channelling. These include the uneven presence of mineral infills, the irregularity of the surfaces in contact and the magnitude and distribution of stresses across the fracture. All of these factors are subject to change with time, and the channel geometries and flow capacities can be perceived as dynamic within the long periods over which the performance of a repository may need to be predicted. The lack of ability to evaluate deterministically the complex channelling processes and associated parameters,

combined with the uncertainties regarding possible time-dependent changes in the flow channels, led the Stripa studies on natural barriers to attempt to model flows in rock fractures generically and stochastically. The generic flow models were tested through observations in a specific rock volume within the Stripa site. The studies provided a focus for the Phase 3 investigations on natural barriers and are described in Volume II of this overview report and the associated documentation.

To function effectively grouts must be able to penetrate and block the channels. The ability to achieve this result depends on the characteristics of the fracture (aperture, channelling, etc.), the grout properties and the methodologies used during the grouting operations. With regard to the latter, among other factors, the pumping equipment, the method of drilling the holes through which the grout is injected, the hole sizes, the pattern (spacing) and length of the holes, the "down-hole" equipment, the injection pressures, special operations (such as flushing the grout hole or between grout-holes with water prior to injection) and the sequencing of operations all bear on the eventual success and, in practical circumstances, cost of the operations. With these imponderables, designs for grouting operations are conventionally based on experience in similar ground conditions and situations. Moreover, the designs are "living documents" which allow for changes as increasing knowledge of the rock and its response to the grouting is gained as *in situ* works proceed.

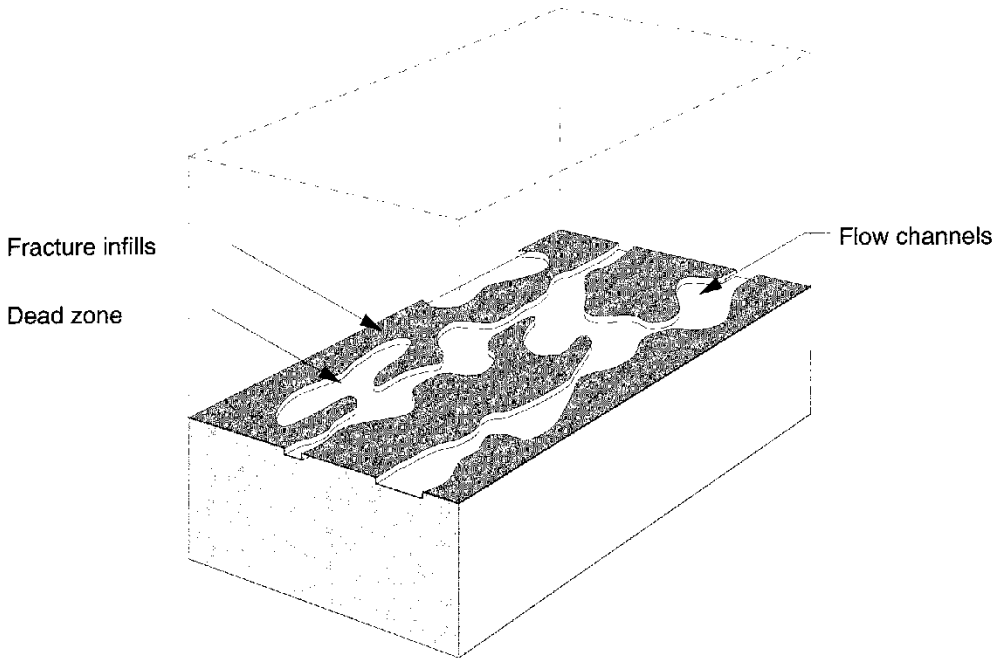

Figure 4-20 An impression of channelled water flow in fractures in granite.

The permeability of the undisturbed Stripa granite at the depth at which the experiments were undertaken was in the order of 10^{-17} m^2 (i.e. considered as a porous medium, the rock has an equivalent hydraulic conductivity of $< 10^{-10}$ m/s). This is considered virtually impermeable in normal engineering design for water retaining and control structures in which grouting is not generally considered necessary or practised if the apparent hydraulic conductivity is less than 10^{-8} to 10^{-7} m/s. Apart from experiments carried out in Canada in connection with repository design and construction where granite rock with an

apparent hydraulic conductivity as low as 10^{-8} m/s was grouted (Gray and Keil, 1989), there was no direct experience on which to draw to configure the Stripa grouting experiments. Thus, in addition to the experiments investigating the ability to grout discrete fractures described in this section, the work on grouting fracture zones (section 4.4) and the excavation disturbed zone (section 4.5), were novel and can only be considered as first developments towards the grouting practices that may be required for repository sealing. Due to normal programme restrictions many of the variables controlling the success of grouting operations noted in the previous paragraph, could not and were not investigated. Attempt is made here to take these factors into account in an analysis of the work that was undertaken.

One major test (Börgesson et al, 1991) was undertaken during Phase 3 of the project to investigate the feasibility of grouting discrete fractures. However, prior to its conduct, important preliminary work was carried out. The preliminary activities are described in section 4.3.1. Section 4.3.2 presents an overview of the main test.

4.3.1 Development and modelling activities

To assist with the conceptualization of the main test three distinct series of activities were undertaken. These are listed as follows:

- The discrete fractures creating leakage around the outer bulkhead of the tunnel plugging test (see Figure 3-11) were penetrated by boreholes and sealed using clay grouts and a prototype dynamic injection pump. The sealing effects were measured and the extent of grout penetration was determined. This work is reported in detail by Pusch et al (1985c).
- Assuming fractures to be planar elements with uniform apertures, a numerical model was developed to predict the depth of penetration of grout from a borehole in which grout was injected under vibration and pressure. The predictions of the model were compared with results obtained from surface laboratory tests in which, using a final version of the vibratory injection pump, clay and cement grouts with known rheological properties were injected into a narrow slot of regular small aperture created between two confining and confined steel plates (Pusch et al, 1988; Börgesson et al, 1991).
- Using the vibratory injection pump, cement grout was injected into a series of fractures in the rock forming the floor of a room near the BMT drift (the room previously used for the LBL Time-Scale experiment was used - see Figure 2-2). After grouting, the floor of the room was broken out and the extent of grout penetration was evaluated (Pusch et al, 1988).

The main elements and results of these activities are examined below.

Grouting around the tunnel plug bulkhead

The major discrete fractures around the outer bulkhead of the tunnel plug construction are shown in Figure 4-21(b), labelled I to V. Each of these features was intersected by one diamond drilled borehole (ϕ = 56 mm), labelled 1 to 5 in Figure 4-21, and the recovered core provided information on the frequency and distribution of the fractures in the rock near the tunnel surface. The rock was grouted through each of the holes in sequence. Initially, a packer was set low in each hole, the enclosed space was filled with clay grout

and connected to the prototype dynamic injection device, which, once filled and locked off, applied static pressures of 1.5 MPa with a dynamic variance of approximately + 2 MPa and - 0.5 MPa at a frequency of 20 Hz to a Tixoton-based grout. The process was repeated as the packer was incrementally withdrawn from the hole and reset. It is not clear and is presumed here that as the final step the packer was locked in to retain the clay grout. The high grouting pressures close to the rock surface were permitted by the presence of the robust concrete bulkhead construction which resisted rock movement.

Prior to use as the grout, the predominant exchangeable cation on the Tixoton clay product was changed from Na^+ to Li^+. Correspondingly, w_L increased from about 425% to about 500% at which water content the clay was injected as a grout. Thus in this preliminary test the grout was less fluid than the grouts proposed for and used in the main test. Moreover, the frequency of the large shear vibrations applied to the grout was about half of the value seen to be required by the subsequently conducted laboratory work (see section 4.2). In addition, methylene blue dye was added to the mixing water at a concentration of 0.2 g/l. Subsequent testing showed that this dye did not significantly change the rheological properties of Tixoton grout (Börgesson et al, 1991).

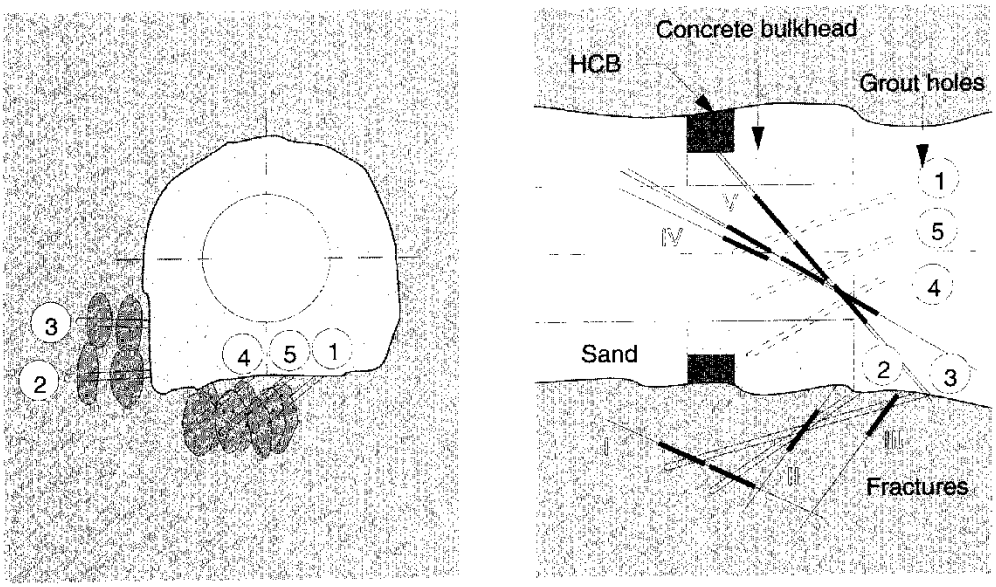

(a) Section (b) Plan

Figure 4-21 The configuration of the fracture features and the grouting arrangements to seal the rock around the outer bulkhead of the tunnel plug.

The grouting was completed before the final disassembly of the tunnel plug. Thus, hydraulic testing of the effectiveness of the grout injection was possible. This was made by incrementing the internal water pressure in the tunnel plug assembly and monitoring the water flow out of the vessel. Pressures of 0.25, 1, 2 and 3 MPa were applied to the water in the tunnel plug. Outflow from the system was monitored for seven days at each value of water pressure. The results from tests with water pressures of 1 and 2 MPa are presented in Figure 4-22. They show that the grouting effectively reduced the outflow from the test chamber and that the effectiveness of the grouting tended to decrease with in-

creasing hydraulic gradient across the grout. At 3 MPa the outflow after grouting was the same as that before grouting and erosion of the injected grout was observed. Blue clay grout was seen to extrude from the points of intersection of the fractures with the tunnel surface.

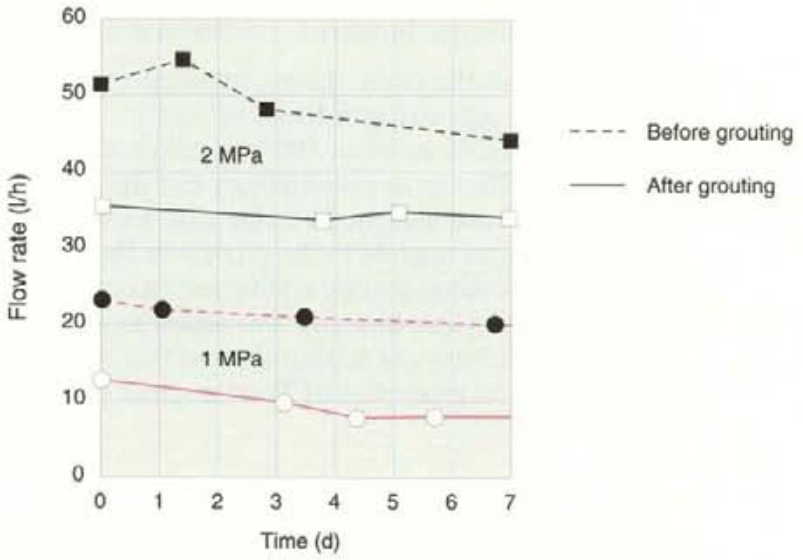

Figure 4-22 Water flow rates from the tunnel plug with internal pressures of 1 MPa and 2 MPa.

The test confirmed that dynamic injection could effectively introduce thick (low water content) clay grouts into water bearing fissures in rock and indicated that further development of this technology was appropriate for the Stripa programme. Moreover, the positive sealing effects achieved through the preliminary grouting activities justified more detailed investigation of the proposed dynamic grouting methodology through the developing concept for the main test. In this latter context it is noted that in this preliminary test the grouts were injected within approximately 2 m of the surface of the tunnel floor and wall. This is within the zone that was expected to be disturbed by excavation processes and stress relief. Thus, this preliminary trial also gave promise for success of grouting operations in the EDZ around the excavations at the Stripa site.

Pump development, injection modelling and slot tests

The modelling and equipment development activities were undertaken concurrently. With the known boundaries on the performance characteristics of the pump, the models were then used to predict the results of tests in which clay and cement grouts with known rheological properties were injected into slots of known dimensions.

In its final form, shown in Figure 4-23, the dynamic injection pump consisted of a cylinder, A, which could be filled with grout. A dynamic load could be exerted on the confined grout through the actuator, B, to which a sinusoidal load could be applied longitudinally from the sliding percussion device, C. An ability to slide was needed to accommodate the reducing volume of grout as it extruded from the pump. The dynamic load could be applied at a frequency of

up to 50 Hz, with a maximum positive amplitude of 10 MPa. This latter value cannot be readily translated to the shear strain amplitude, γ_A, which was shown through the laboratory work to control the viscosity of the grout. A static pressure of up to 3 MPa could be applied to the grout in the cylinder through a pneumatic pressure pump which was located beneath the percussor. Valve gear allowed the cylinder to be connected alternatively to the grout supply and the borehole.

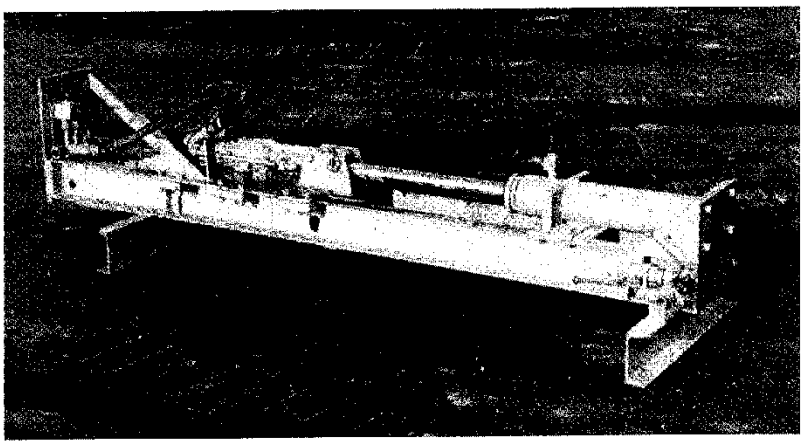

Figure 4-23 The final configuration of the dynamic injection pump.

Measurements showed that the sinusoidal character of the applied waveform from the pump was translated in practice to the grout to a complex, largely positive (over the static pressure), spiked configuration. Among other factors, reflection waves, the length and diameter of the borehole, the diameter and length of the connecting tubing, the effects of friction along the tubing and the borehole wall, the restricting effects of junctions in the flow paths, the stress-strain characteristics of the rock and the complex geometry of the fractures intersecting the borehole could all be expected to have influenced the waveform. In addition, the amplitude and background pressure acting on the grout could be expected to decay with distance from the pump to the advancing grout front. Thus, the shearing resistance of the grout could be expected to increase with increasing distance from the pump. It was not possible to accommodate all of these variables into deterministic mathematical descriptions of the grouting process. The simplified models which were developed are detailed by Pusch et al (1988) and Börgesson et al (1991).

Assumptions used for the development and use of the simple model were as follows:

- the rheology of the grout during injection can be described using the m and n parameters derived from the laboratory tests;
- the densities of the grouts can be determined from the mix proportions and the known relative densities of the mix components;
- the elastic properties of the fresh grout are similar to those of water; those of the rock can be estimated from laboratory tests and applied engineering judgement;

- the pump applies vibrations sinusoidally at a frequency of 40 Hz and creates an amplitude in the pressure wave of 2.5 MPa over a baseline static pressure of 2 or 3 MPa;
- the pump, connecting tubing and borehole can each be considered as long cylinders with known dimensions;
- natural fractures can be considered as slots of regular aperture and grout advances along the slot radially from the borehole without segregation or dilution;
- the aperture of natural fractures can be estimated from tests in which water is injected under pressure over defined intervals of the borehole drilled for grout injection.

Hence, calculations could be made to estimate the rate of advance of the grout front and the final distance of penetration of the grout from the borehole.

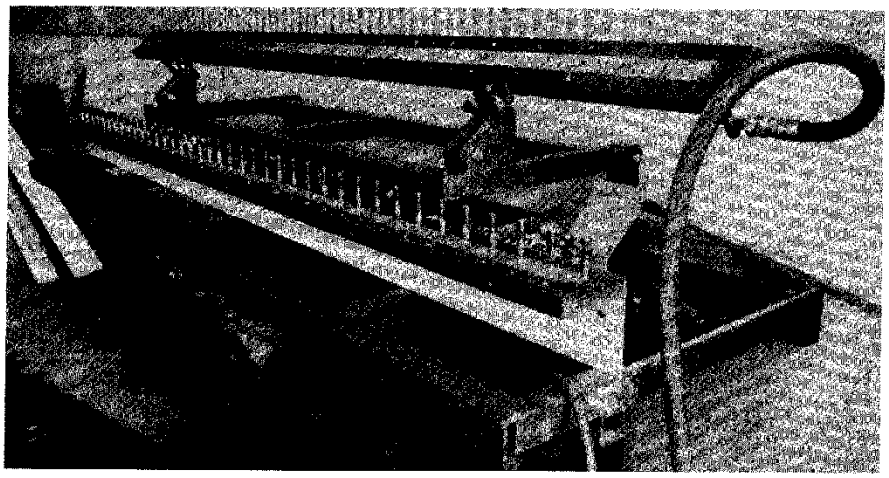

Figure 4-24 The general arrangement of the test cell forming the artificial slot into which grout was injected for qualification of the simplified mathematical model.

As shown in Figure 4-24, two parallel steel plates with faces separated at the edges by 0.1 mm thick copper foil defined the 3 m long, 50 mm wide, regular 0.1 mm thick slot into which grouts were injected. In an alternative configuration, a slot with a triangular cross-section with a maximum aperture of 0.1 mm and a width of 100 mm was formed by omitting the copper foil along one long edge of the device. In all cases, across the width of the slot the steel surfaces were roughened by parallel, transverse, 0.1 mm deep scratches with a separation of 2 mm. Pressure transducers were flush-mounted in the base plate at intervals of 30 cm. Windows in the upper plate allowed for visual examination of the advance of the grout front from the injection point. The injection point was located at one end of the device and connected to the dynamic injection pump; at the other end of the device, the water filled slot was allowed to drain against a back pressure.

The measured depths of penetration of different Tixoton clay grouts are compared with the predicted values in Figure 4-25. Grouts with different liquidity ratios, quartz contents and salt contents ranging from 0 to 2 per cent were tested. The ranges in the predicted values arise from the batch variability in the grout noted in section 4.2. It can be seen in Figure 4-25(a) that the measured values tended to be higher than the calculated penetrations when the frequencies

of the vibrations were assumed to be the same as those which were directly applied (i.e. 40 Hz). Pressure measurements indicated that, due to reflection waves within the test system and the generation of overtones, the actual frequency of vibration of the grout was about 100 Hz. Using a frequency of 100 Hz, the predictions made for the test series with the triangular slot proved to be a reasonable mean of the measured penetrations (Figure 4-25(b)). Similar results to those for the Tixoton clay grouts were obtained when cement grout consisting of 90% reground SRPC, 10% silica fume, superplasticizer and water, at $W/CM = 0.42$, were injected into the slot.

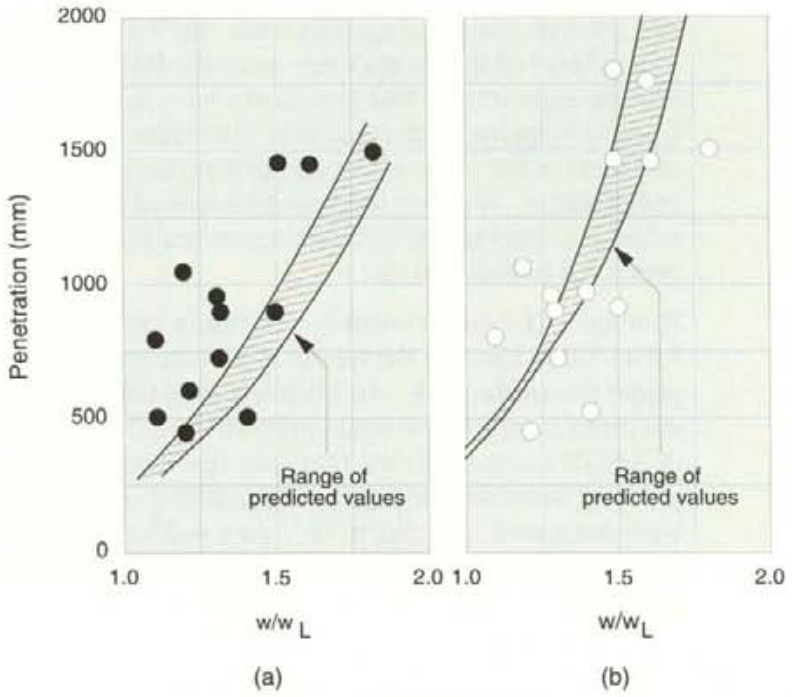

Figure 4-25 Predicted versus measured penetration of the clay grout front for (a) a regular slot with an assumed frequncy of vibrations of 40Hz, and (b) a triangular slot with an assumed frequncy of vibrations of 100 Hz (after Börgesson et al, 1991).

In addition to penetration, the spread of the grouts into the narrower parts of the triangular slot were measured and the homogeneity of the injected grout was assessed. Using static injection, the clay grouts did not penetrate those parts of the triangular slot with apertures less than about 40 µm. This aperture limit was decreased to 20 µm when dynamic injection was used. This latter value corresponds well with values measured *in situ* for cement-based grout (Gray and Keil, 1989). Examined visually and under the microscope, grouts recovered from the tests in the regular slot was determined to be homogeneous and free from separation and dilution (Pusch et al, 1988). This was also true for grouts recovered from the wider parts of the triangular slot. There was some evidence of increased porosity (dilution and separation) in the thinner grout elements. The bearing that this latter observation may have on the long term performance of the grouts is discussed in Chapter 5.

The modelling, equipment development and slot testing work had tangible results. The dynamic injection device was built and experience was gained in

its use. It was shown through theoretical appraisal and associated testing that, as expected, the application of vibrations during the pressure injection of the high-performance, low water content, clay and cement grouts assisted the penetration of these materials into narrow aperture fractures. Moreover the ability of these materials to penetrate fractures as narrow as 20 μm was confirmed. The simplifying assumptions used in the theoretical models for grout penetration led to deviations between predicted and measured values. The parameters used in the calculations needed to be adjusted as more experience was gained and measurements were made.

In situ pilot tests

The pilot *in situ* grouting tests were carried out in the floor of the drift at the 335 m level of the Stripa mine, near the BMT room, where the Time-Scale heating experiments had previously been carried out under the SAC agreement. Careful mapping of the fractures intersected by the excavations (Thorpe, 1979) allowed for the selection of an appropriate location for the pilot grouting experiments. A major fracture set exposed by the excavations was grouted. A schematic drawing of the fracture set and the layout of the grouting holes are presented in Figure 4-26.

Boreholes (I-1 to I-6) with ϕ = 76 mm were diamond drilled to depths from 1.5 to 7.0 m through the fractures and the core was logged to define the properties of the rock. To limit heave of the rock surface during the injection of the grout (a maximum static pressure of 3.5 MPa with a dynamic over pressure of 3.5 MPa was used) the rock was tied back using carbon steel dowels. The grouting induced displacements occurring at the exposed ends of these dowels were measured. As shown in Figure 4-26, two long boreholes, S_1 and S_2, which had been drilled for the Time-Scale experiment were also tested and grouted.

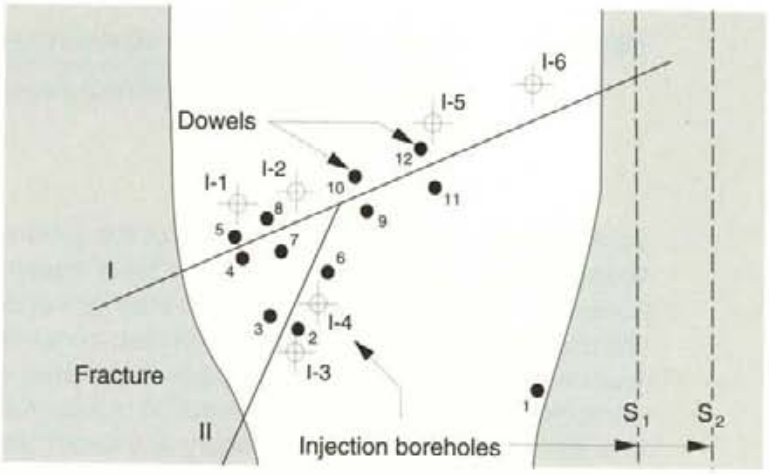

Figure 4-26 Location of the grout injection boreholes (I and S), major fracture features intersecting the test room (I and II) and the dowels used to limit uplift of the floor of the room during grout injection in the LBL Time-Scale drift.

The core logging showed that the rock was richly fractured (107 fractures were identified in the cores from the 6 grouting boreholes) and, specifically, it was

noted that the rock intersected by the upper 400 mm of each of the grout holes was intensely fractured. This was interpreted as a direct effect of blasting.

Pressurized water injection tests were carried out in each of the holes through which the rock was to be grouted. The rock was grouted and, after reaming the grout from the holes, the hydraulic testing was repeated. Due to the need to pack-off the holes during the tests, the hydraulic properties of the upper 0.5 m of the holes could not be determined. Several methods were used to interpret the results from the hydraulic conductivity tests and obtain a measure of the hydraulic conduction properties of the rock. Each of the methods rested on simplifying assumptions and, thus, the values obtained cannot be considered absolute. However, a measure of the effects of grouting was obtained.

The dynamic injection device was used to inject either clay- or cement-based grout into the holes. Details of the grout type used and the effects on the hydraulic conductivity of the rock are provided in Table 4-4. The data show that both grout types were able to reduce the hydraulic conductivity of rock with ungrouted values greater than 10^{-9} m/s giving conductivities for the grouted rock of 10^{-10} to 10^{-9} m/s. Displacement was within the accuracy of measurement (i.e. less than 0.1 mm and not significant) on all but dowels Nos. 9 and 12 where the grouting caused permanent heave of the floor of the room of 2.62 and 1.26 mm, respectively. It is noted here that these dowels are distant from the restraining effects of the walls of the room.

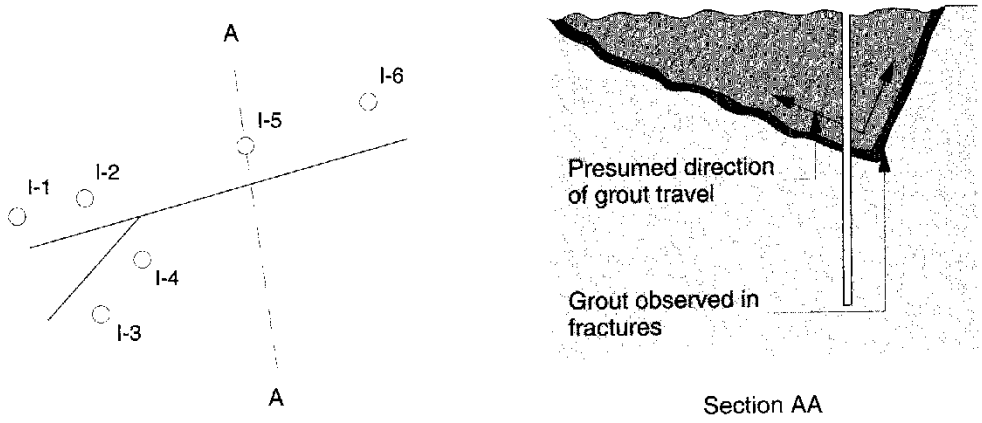

Figure 4-27 Extent of grout movement traced after the careful excavation of the rock around injection hole I-5.

During the injections the grout was observed to emanate from both major and minor fractures in the floor of the room. This was particularly evident during injections into I-4 and I-5. The cement grout was dyed yellow and the clay grout was blue. This assisted in the identification of the grout flow paths when, on completion of the hydraulic testing, the floor of the room was carefully excavated and the fracture surfaces were exposed. As shown in Figure 4-27, cement grout was identified along two intersecting fractures that were grouted through hole No. I-5. It may be significant that the greatest displacement of the floor of the room was observed in this area. Irrespectively, both blue (clay) and yellow (cement) grouts were identified on the surfaces of fractures exposed near the other grout holes.

Table 4-4 The effects of grout injection on the estimated hydraulic conductivity of the rock around each of the injection boreholes at a depth of 0.5 to 1.5 m.

Hole No.	Depth	Grout * type	Grout volume injected	Water uptake during hydraulic testing		Estimated hydraulic conductivity	
				Pre-grouting	Post-grouting	Pre-grouting	Post-grouting
	(m)		(ml)	(l/h)	(l/h)	(l/h)	(l/h)
I-1	1.5	Clay	5-25	0	0	$<5.10^{-12}$	$<5.10^{-12}$
I-2	1.5	Clay - quartz	5-25	0.312	0.132	$3.6.10^{-9}$	$9.8.10^{-10}$
I-3	1.5	Cement	40-70	0.258	0.012	$2.1.10^{-9}$	$8.2.10^{-11}$
I-4	1.5	Cement	>500	17.640	ND	$>10^{-5}$	ND
I-5	7.0	Cement	>650	15.66	0.300	$8.4.10^{-7}$	$3.6.10^{-10}$
I-6	7.0	Clay - quartz	70-100	0.204	0.012	$5.9.10^{-9}$	$1.4.10^{-10}$
S_1	40	Cement	50-200	0.396	0.347	-	-
S_2	40	Clay - quartz	ND	0.502	0.520	-	-

* Clay (Tixoton at $w/w_L = 1.5$); clay-quartz(50% Tixoton + 50% quartz at $w/w_L = 1.6$); cement (90% SRPC +10% silica fume at $W/CM = 0.36$ with 1% superplasticizer) .

ND - not determined.

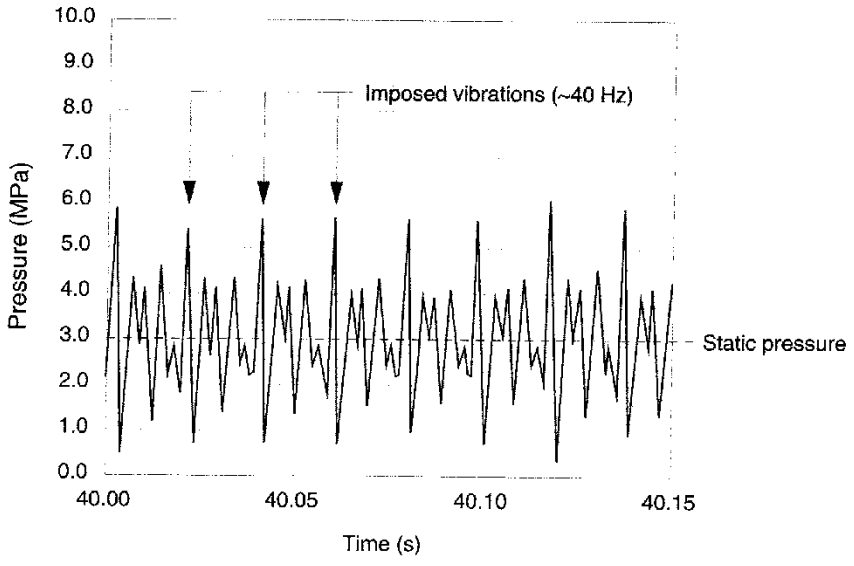

Figure 4-28 Pressure transients in the grout recorded during the injection of hole I-1.

In addition to the observations on the effectiveness of the grout to penetrate and seal the rock, assessments were made on the general performance charac-

teristics of the injection pump. Figure 4-28 shows the pressures experienced by the grout during injections into hole No. I-1. The data show that, during grouting, reflection waves within the grouting system compounded with the applied waveform to give a vibration frequency - at the resolution shown - of 100 to 120 Hz. These results generally confirm the findings of the slot injection tests carried out in the laboratory.

The *in situ* pilot tests provided continuing support to the suggestion that high-performance clay- and cement-based grouts could be successfully introduced into disturbed zones around excavations in the Stripa granite. The injections successfully decreased the hydraulic conductivity of the zones, which were tied back with dowels, and experience was gained with the use of the newly developed grouting equipment. Data were provided on the performance characteristics of the grouting pump which could be used in the design of the equipment to be used in the main grouting experiments to be undertaken in Phase 3 of the Stripa Project. The positive results of the pilot tests and the other preliminary activities all supported the decision to proceed with the works for the main grouting experiment.

4.3.2 Main test (grouting around deposition holes)

Configuration and sequencing

The concept for the main *in situ* test of grouting discrete fractures is described by Börgesson et al (1991) and shown schematically here in Figure 4-29. The test was carried out in the rock beneath the floor around holes 1 and 2 of the BMT room. The intentions were to determine the extent to which discrete fractures in the floor of the BMT room could be sealed using the high-performance grouts and, further, to measure the effects of a temperature excursion, such as may be experienced around disposal holes in a repository, on the hydraulic properties of the grouted rock.

The pilot test had shown that it was possible to grout the floors of excavations in the Stripa granite through small diameter, diamond drilled boreholes. This method was considered for the main experiment but was eventually abandoned in favour of injection from the 760 mm diameter boreholes used for the BMT. The loci of fracture planes intersected by the large diameter borehole were sufficiently long to ensure that open channels in the fractures were exposed and available to receive grout. Moreover, the large diameter boreholes in the floor of the BMT room had been open since 1985, when the BMT had been completed, and the grouting test was carried out in 1989. In the intervening four year period natural water flows had removed clay that had self injected into the fractures during the BMT and the rock surfaces had been washed.

The large diameter of the boreholes necessitated the development of the special packer and injection system shown in Figure 4-30. This was to be connected to the dynamic grout injection pump which had been developed through the preliminary activities. The design of the large, down-hole, injection system took advantage of the smooth walls of the diamond drilled heater holes and was configured largely on the basis of flow calculations made using the flow models which, as described in section 4.3.1, had also been developed through the preliminary activities. The models were used for sensitivity analyses on the predicted performance of the pump, grout, and injection system. These analyses allowed for the refinement of the geometry of the design of the injection

chamber and led to the specification for the width of the annulus (4 mm) between the injection tool and the borehole wall and the flattened geometry of the grout trumpet.

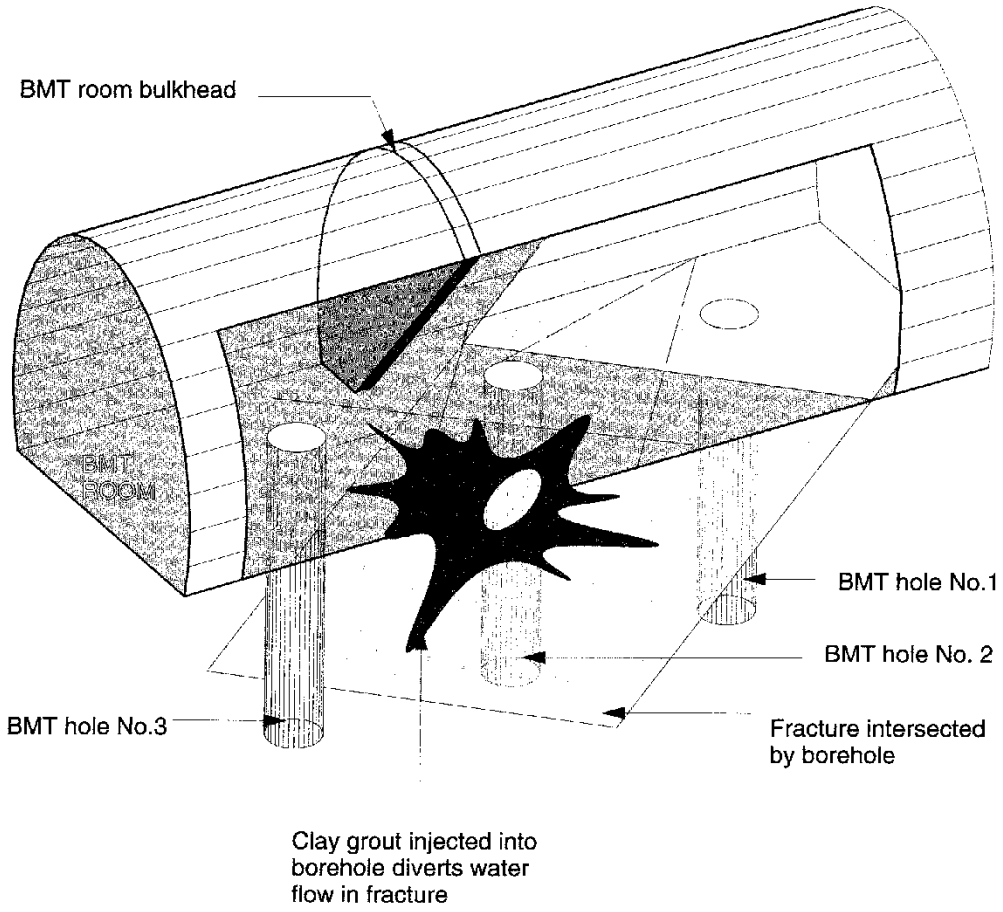

Figure 4-29 The general concept for the main discrete fracture grouting experiment.

Tests were carried out in BMT boreholes 1 and 2. The tests were carried out in steps as follows:

1 the hydraulic conductivities of the rock intersected by the boreholes were measured by using the large injection device (LID) to inject water under static pressures of 100 or 200 kPa into the rock over approximately 0.5 m long sections. The packers were inflated to a pressure of 1000 kPa and water flow was monitored until steady rates of outflow were sustained. The large dimensions of the packer systems limited the lengths of the boreholes over which the pressure tests could be carried out. The upper 0.5 m of the rock could not be tested. The methods used to calculate the hydraulic conductivity are described in detail by Börgesson et al (1991) who recognize the values as uncertain and approximate. The uncertainties arise from indeterminate effects of fracture orientation, flow geometry and the squat dimensioning of the LID. Combined with instrument error and other factors, the apparent error of estimate may have been significantly higher than the factor of 3 suggested by Börgesson et al (1991). Insufficient information is available to provide precise accounting in this respect.

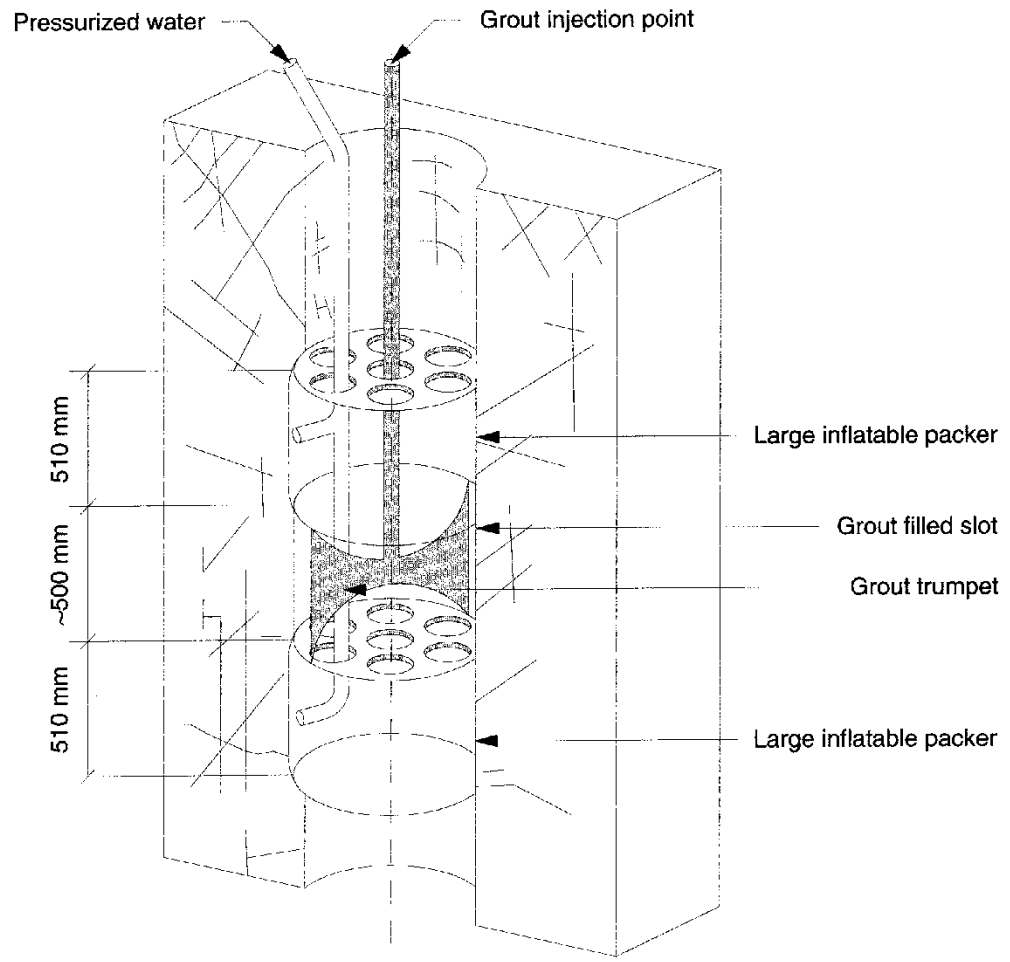

Figure 4-30 The packer and injection system developed for grouting around deposition boreholes.

2 Clay-based grouts were injected into the rock using the LID and associated systems. Injections were made as the LID was advanced in 0.5 m intervals down the holes. Tixoton/quartz grout was used in hole No. 1. In hole No. 2, after grouting the uppermost section with Tixoton/quartz grout, lower sections were first injected with Tixoton alone as the LID was advanced. Subsequently, during withdrawal, the two upper sections were grouted with a Tixoton/quartz mixture. The sequencing of the operations, the mixtures used, the pressures applied and other details are given in Table 4-5.

3 The hydraulic conductivities of the grouted rock were measured as described for step 1.

4 Heaters were installed in the holes and the grouted rock was heated to a maximum temperature of 98°C (on the borehole wall at central elevation). The maximum temperature was maintained for 80 to 100

Table 4-5 The details of the grouting activities undertaken in BMT holes 1 and 2.

Date (1989)	Section grouted (Elevations in m)	Grout used				P_s[1]	P_A[2]	Grouting time	Comments
		Quartz to Tixoton ratio	NaCl content (%)	w (%)	w/w_L	(MPa)	(MPa)	(s)	
	BMT heater hole No. 1								
20 April	336.74 to 337.29	1	1.0	290	1.6	0.4	0.25	-	Outflow on room floor
25 April	337.24 to 337.79	1	1.0	290	1.6	2.1	0.40	31	
26 April	337.74 to 338.29	1	1.0	290	1.6	2.1	0.40	-	Leakage around packer
10 May	338.24 to 338.79	1	1.0	290	1.6	2.9	0.40	15	Leakage around packer
11 May	338.62 to 339.17	1	1.0	290	1.6	2.7	0.40	22	
16 May	339.17 to 339.72	1	1.0	290	1.6	2.9	0.40	24	Bottom of hole grouted
	BMT heater hole No. 2								
30 May	337.12 to 337.67	1	0.25	400	1.6	1.0	0.40	-	Outflow on room floor
30 May	337.12 to 337.67	1	0.25	300	1.2	1.2	0.40	-	Outflow on room floor
1 June	337.62 to 338.17	0	0.25	800	1.6	2.3	0.30	27	
1 June	338.12 to 338.67	0	0.25	800	1.6	2.3	0.40	17	
1 June	338.62 to 339.17	0	0.25	800	1.6	2.3	0.40	17	
5 June	337.62 to 338.17	1	0.25	325	1.3	2.3	0.30	16	
6June	337.12 to 337.67	1	0.25	325	1.3	1.4	0.40	30	Outflow on room floor

NOTES: 1 Applied static backpressure on the grout.
2 Average amplitude of the dynamic loading on the grout measured at the slot between the LID and the rock. The measured patterns and frequencies of vibration were similar to those shown in Figure 4-28.

days after which the system was allowed to cool. It took approximately 20 days for the temperatures to return to approximately ambient values.

5 The hydraulic conductivities of the grouted rock after the temperature excursion were measured as described for steps 1 and 3.

At the start, end and between each of the above steps, precise levelling of points on the surface of the room was undertaken. In addition, before and after grouting and after the temperature excursion, visual observations on the surface of the borehole walls were made and the points at which water flowed into each of the boreholes were mapped. With all these activities completed and after the completion of the test decribed in section 4.5 the floor of the room was carefully excavated to reveal and map the extent to which the clay grout (which, as in the pilot tests, had been dyed with methylene blue) had travelled in the rock.

Results

With increasing experience gained in using the LID, dynamic injection pump and associated equipment, the grouting operations became more efficient. As recorded in Table 4-5, the time for operations in heater hole No. 2 was significantly less than that required for heater hole No. 1. Several adjustments were made during the operations to accommodate practical difficulties during the grouting work. The adjustments included changes in the packer pressures which, with higher grout injection pressures, were increased in some cases to as high as 5 MPa to limit leakage between the packer and the rock. The displacements of the rock with these high pressures exerted on the borehole wall are not recorded. However, Börgesson et al (1991) indicate that they were satisfied by the operation of the grouting system and indicate that, with minor modifications, the LID should be suitable for grouting around diamond drilled disposal holes in a repository in granite.

Due to leakage around the packers and, during grouting the uppermost sections of the boreholes, extrusion of the clay grouts through the fractures and on to the floor of the room, it was not possible to provide a reliable estimate of the quantities of grout injected into the rock. Volumes of 12 l and 5.7 l, respectively, in the uppermost sections of boreholes 1 and 2 are estimated by Börgesson et al (1991). The descriptions of the grouting carried out in lower sections show that the grout and packer pressures were higher and suggest that injection was more difficult as the operations proceeded deeper into the holes. This tends to agree with expectations arising from the results of the hydraulic conductivity meaurements.

The estimated hydraulic conductivity of the rock with depth before and after grouting and after the temperature excursion are shown in Figure 4-31. It was noted earlier that uncertainties exist in the estimated hydraulic conductivity values. For this reason, the hydraulic conductivity measurements were made using standardised packer and water injection pressures. Hence, despite the errors of estimate, the values shown in Figure 4-31 can be considered to provide a reasonable relative measure of the effects of grouting and the temperature excursion.

The results for the ungrouted rock show that hydraulic conductivity tended to decrease with increasing distance from the excavation surface. This was more pronounced for the rock around hole No. 2 than for that around hole No. 1.

Within 1 m of the floor of the room the hydraulic conductivity (k) around hole No. 2 reached reported values as high as $4 \cdot 10^{-7}$ m/s. At the same depth around hole No. 1, k was 1 to 2 orders of magnitude less. Around both boreholes, at depths of 1.5 m or more, k decreased to approximately 10^{-9} m/s or less. The higher hydraulic conductivity around borehole No. 2 was consistent with the water flow rates measured into each of the boreholes during the conduct of the BMT. Table 2-5 shows that the natural rate of water flow into the upper half of hole No. 2 was more than twice that into hole No. 1. The results increased support to the suggestion that an excavation disturbed zone (EDZ) existed around the excavations in the Stripa mine which, parallel to the tunnel axis, was more hydraulically conductive than the undisturbed rock.

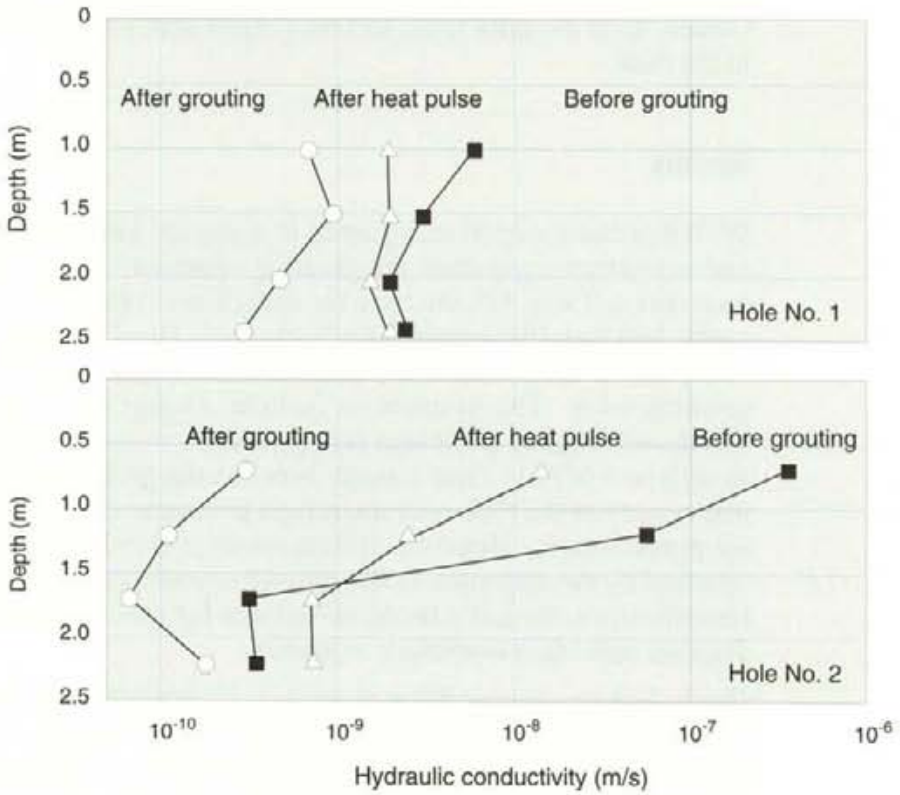

Figure 4-31 The effects of grouting and the heat pulse on the estimated hydraulic conductivity of the rock around deposition holes 1 and 2.

The grouting procedures and materials successfully decreased the hydraulic conductivity of the rock. The effects were more pronounced for the initially more highly conductive rock around hole No. 2 around the uppermost parts of which k was decreased by approximately 3 orders of magnitude to lie in the range $10^{-10} < k < 10^{-9}$ m/s.

The temperature excursion affected k. Close to the tunnel surface, the reported final values were intermediate between those of the ungrouted and grouted, but unheated, rock. The accuracy with which the measurements were made may account for the measured reported differences in k deeper than 1.5 m into the rock.

The results of the surveys of floor levels at different stages of the grouting tests are shown in Figure 4-32. Apart from some compression of the floor during the period over which the preliminary works were undertaken, the data are consistent and show that both the grouting operations and the heating step

caused permanent upward movement (heave) of the floor of the room. Numerical modelling of the rock mass showed that the heat pulse should result in residual heave. However, the results were not absoluteley precise because of, among other factors, lack of a clear appreciation of the complex geometry of the fractures and fracture sets involved, lack of good knowledge of the constitutive stress-strain-time properties of the fractures and the rock, lack of information on the *in situ* stress conditions and water pressures, and the complex boundary conditions acting on the rock boundaries which changed throughout the progress of the studies. Logic leads to the suggestion that, in both the grouting and heating steps, some shear displacement occurred along fractures and caused irrecoverable normal displacements. The shearing resistance of the grout (1 to 5 kPa) was not sufficient to support the normal loads imposed by the body of rock. The displacements measured during the heating step are opposite to those measured and predicted at several metres into the floor of the Time-Scale and Full-Scale heater tests carried out under the SAC agreement (Hood et al, 1979). Several suggestions can be made to explain this difference. However, it is sufficient to note here that the heave occurring in the floor of the BMT room may not be evident at other sites where local conditions will dictate the mechanical response of the rock to heating.

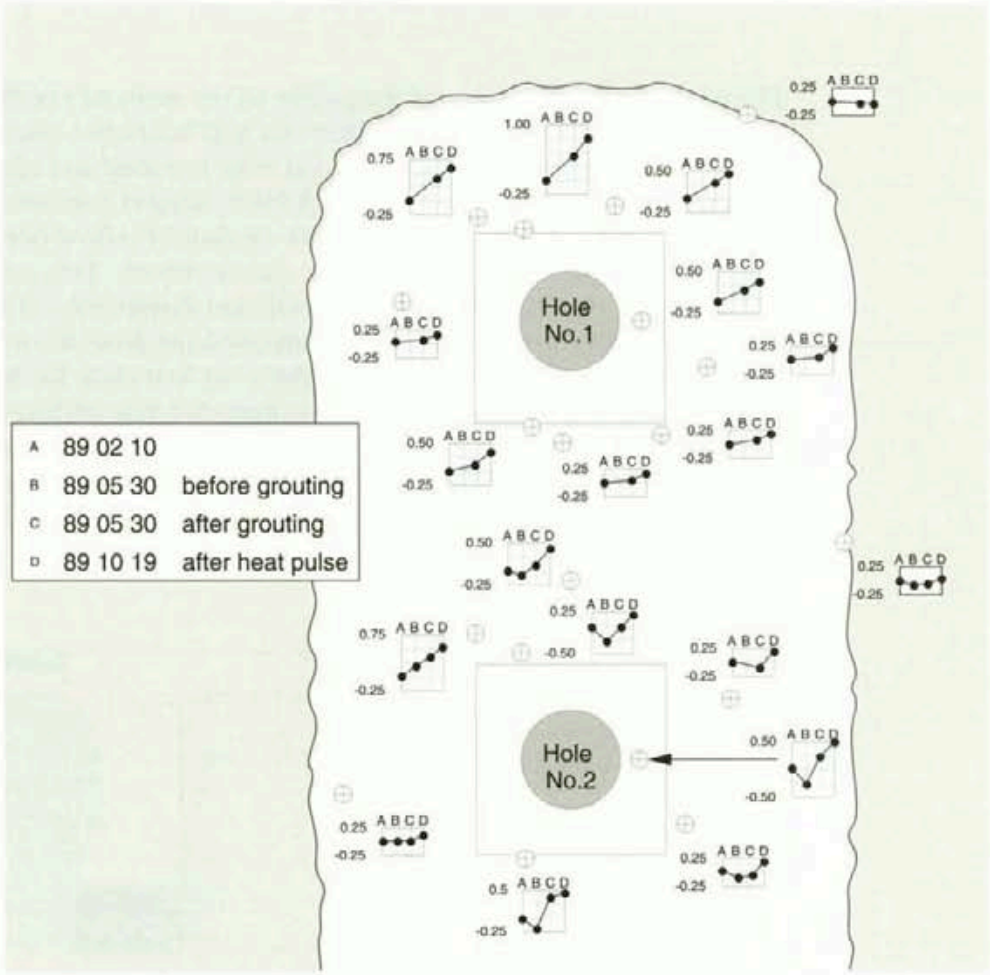

Figure 4-32 Results of precise level surveys of the floor of the BMT room at different stages of the grouting experiment.

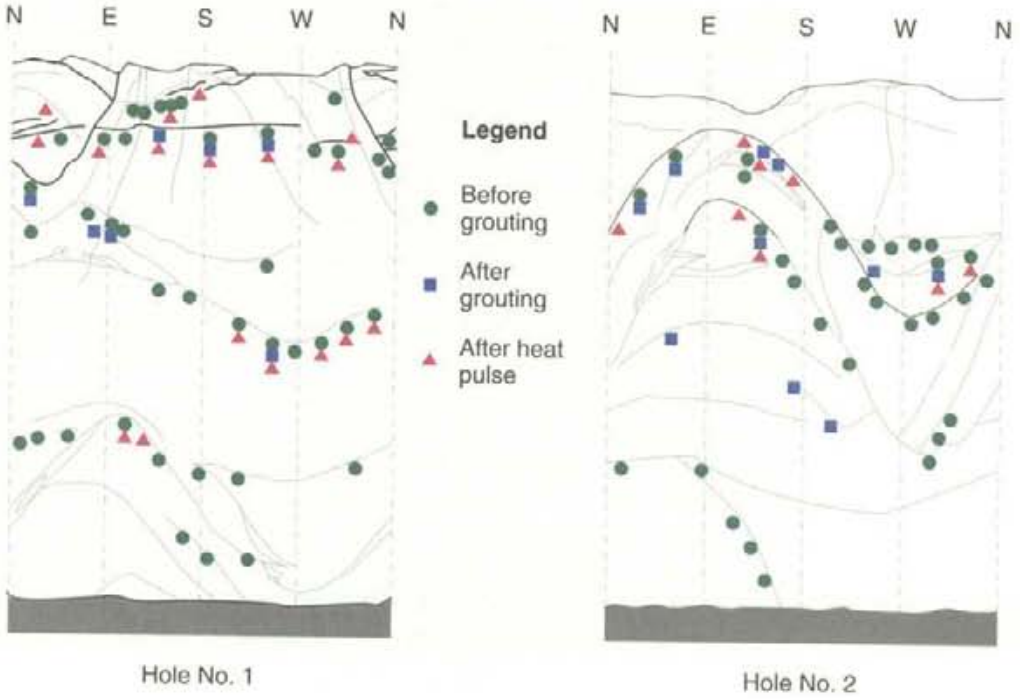

Figure 4-33 Points where water flowed into BMT holes 1 and 2 before grouting, after groutig and after heating.

Figure 4-33 presents maps of the points on the walls of boreholes 1 and 2 at which water was seen to flow within one half hour after towelling the rock surface dry. The inflow points before and after grouting and after the temperature excursion are shown. Consistent with the hydraulic conductivity test results the maps show that grouting decreased the number of inflow points. Some changes in the location of the inflows also occurred. This can be attributed to a change in the channels caused by mechanical disturbance of the fractures and may reflect the permanent deformations resulting from the grouting processes. Further confirming the hydraulic conductivity test data, the heat pulse appeared to re-open grouted pathways as well as generate new pathways for water flow. These qualitative results tend to support the quantitative measurements of hydraulic conductivity which were further supported by the findings made during careful excavation of the floor of the room around hole No. 2.

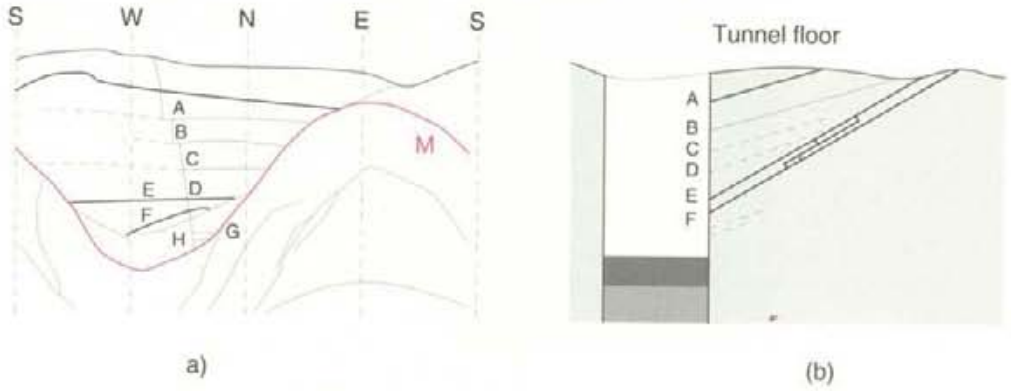

Figure 4-34 Locations of clay grout observed during the careful excavation of the rock around BMT hole No. 2.

The surfaces of major fractures intersecting borehole No. 2 at depths down to approximately 1.5 m were exposed by careful excavation of the rock mass. The extent of these excavations is shown in Figure 4-34 (a). Figure 4-34(b) presents a section of the locations along which blue grout was visually identified. Consistent with observations made when the uppermost section of the hole was grouted, during which grout was seen to extrude into the room from fractures intersecting the floor of the room to the north of the hole (see Table 4-5), the grout was observed to have penetrated distances of two or more metres along the wider fractures. These distances are similar to those which may be predicted using the penetration models developed during the preliminary activities (see section 4.3.1).

The results in Figure 4-33 indicate that fracture M was well sealed by the grouting operation. Very little grout was found on the surface of this feature which was coated in places with chlorite. It was suggested that this coating hindered penetration of the grout and that the decreased inflows into the hole caused by the grouting were caused by compression of the natural infills and filter packing in advance of the grout front (Börgesson et al, 1991). Significantly, the grout penetrated fractures that did not contain well developed natural infillings.

4.4 FRACTURE ZONE GROUTING

4.4.1 Test concept and sequencing

The 3-D migration experiment undertaken by the natural barrier research group during Phase 2 of the project provided the results shown in Figure 4-35 for natural water flows into the special cruciform shaped excavations created for the experiment (Abelin and Birgerson, 1987; Abelin et al, 1987a and 1987b; Andersson and Dverstorp, 1987). Measured on the roof and the walls of the excavations, water flows were seen to be concentrated at two main locations which, later, in Phase 3 of the investigations, were shown to be related to the major fracture sets existing within the Stripa site.

Figure 4-36 presents a plan view of the major fracture sets identified through the natural barrier investigations by the end of Phase 3 of the project. Zones J and K can be reasonably assumed to have been the major sources of flow into the 3-D migration experiment drift. It was estimated that these two hydraulically active features accounted for a total of approximately 90 per cent of the total flow of water into the excavation.

Based on the limited information available at the start of Phase 3, the experiment scheme shown in Figure 4-37 for testing the ability of high-performance grouts to penetrate and seal fracture zones in the Stripa granite was developed and pursued. In brief, the plan was to measure the rate of water flow into the eastern arm of the cruciform excavation using the ventilation techniques developed for the SAC "macropermeability" experiment. The quantities of water flowing into the room, which would be closed by a light timber wall, would be determined by measuring the change in humidity of the air used to ventilate the room. The effectiveness of the grouting could be assessed by performing the measurements before and after the water bearing zones were grouted with cement-based grout.

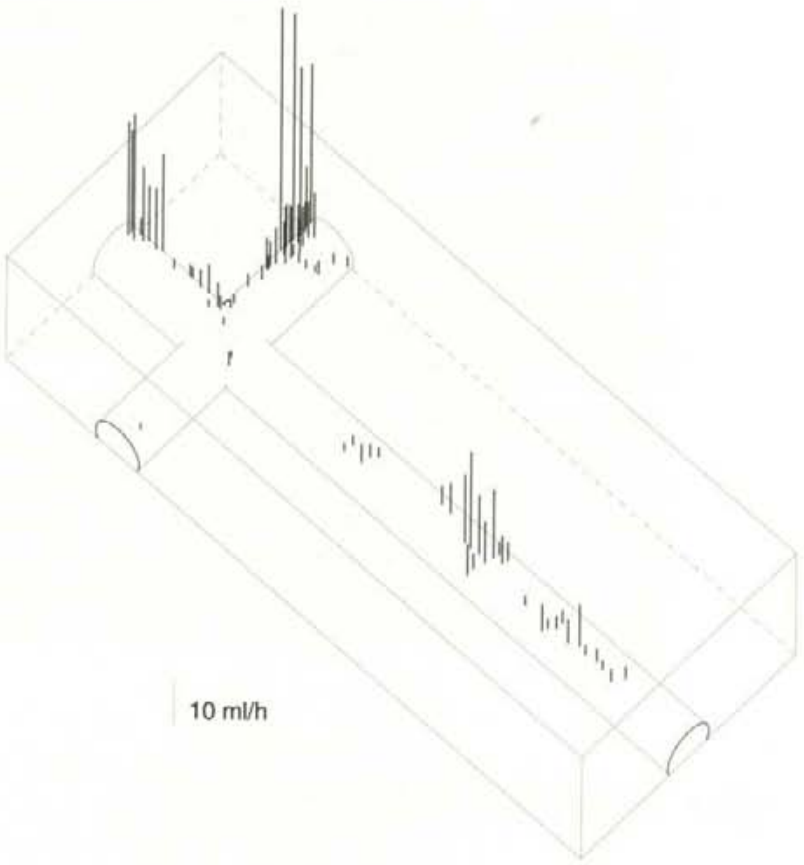

Figure 4-35 Water inflow rates measured in the walls and roof of the drift used for the 3-D tracer migration experiment in Phase 2 of the Stripa Project.

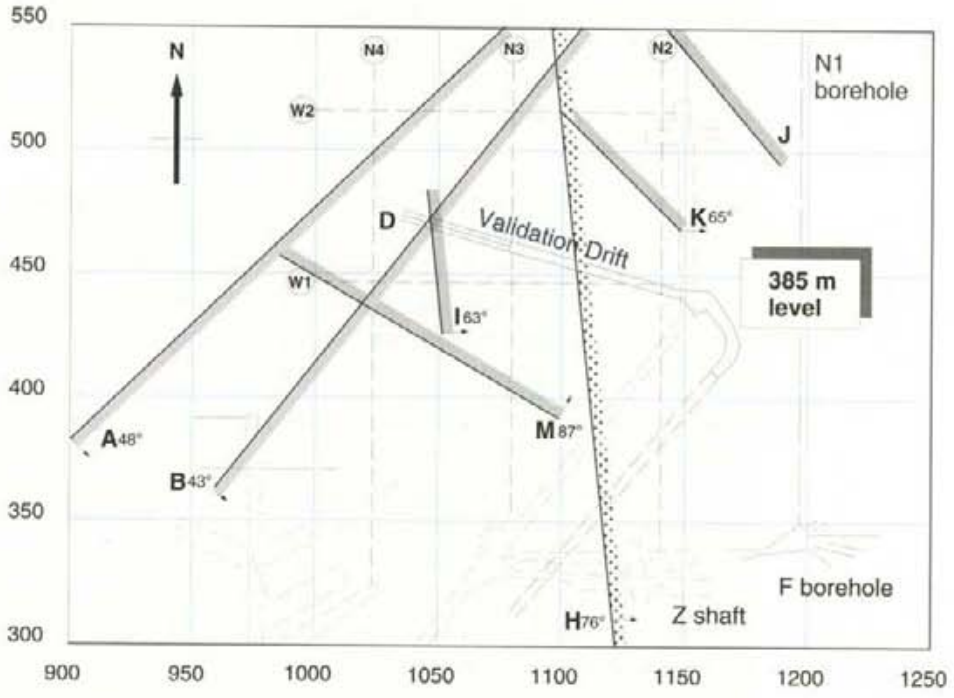

Figure 4-36 Plan of the major hydraulic features in the Stripa rock mass revealed through the Phase 3 studies into natural barriers.

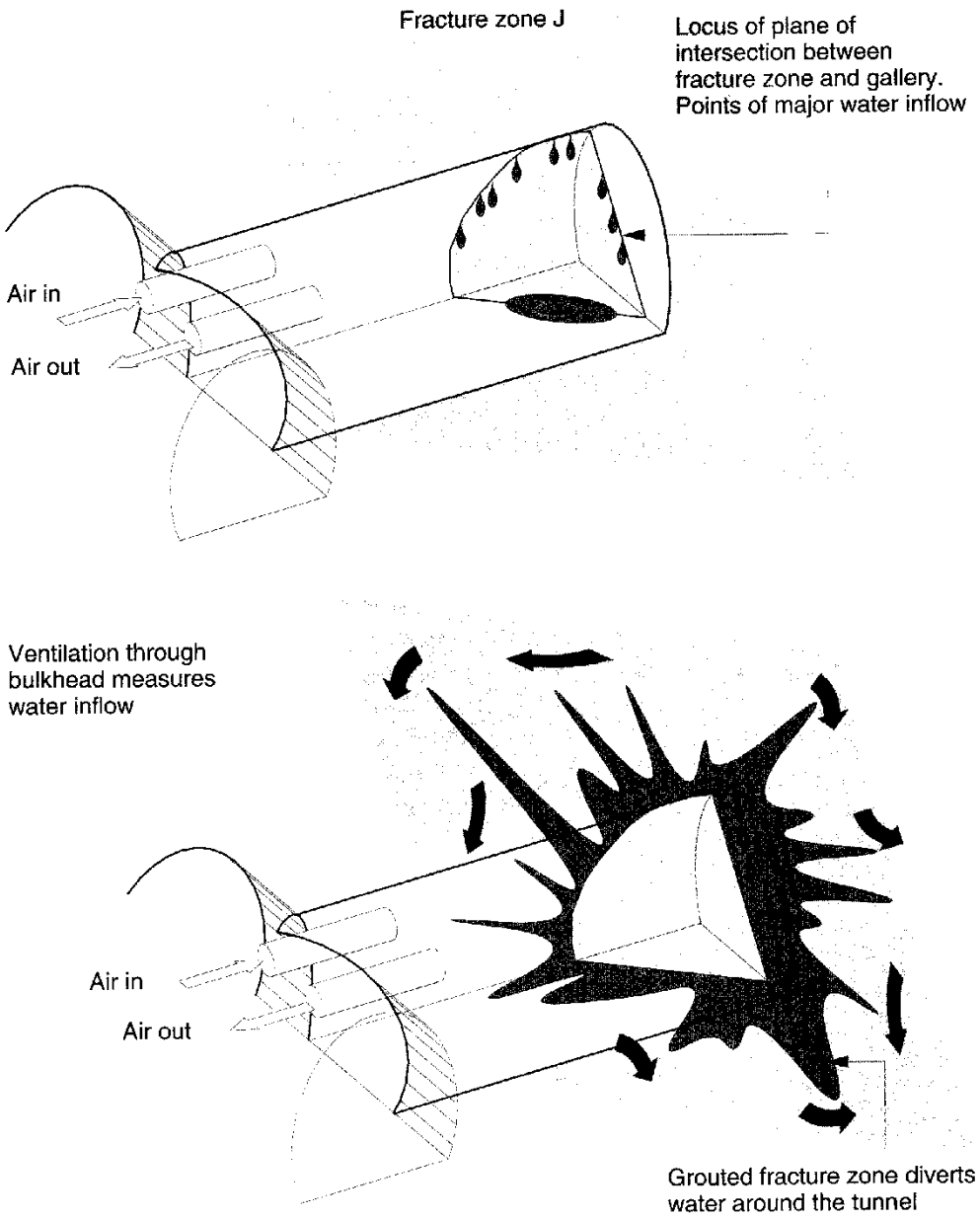

Figure 4-37 The concept for the fracture zone grouting experiment.

At the outset of the studies, little was known of the detailed hydrogeological characteristics of the rock volume in which the room had been excavated. Thus, the first activity was to acquire more detailed knowledge of the piezometric and flow conditions in the rock prior to the initiation of the grouting experiment. A comparison of these data with those obtained from measurements after grouting could also provide a measure of the effects of grouting. BAT piezometers, similar to the ones used in the BMT, were installed in the rock at

distances of up to 10 m from the surfaces of the excavation in the six percussion drilled boreholes located as shown in Figure 4-38. The pressures recorded in these instruments were monitored throughout the period of the experiment. In addition, at selected times, sections of the holes were packed off and, to attempt to identify water flow paths in the rock, were used to either inject coloured tracers or for "Lugeon" type tests in which the water flows into the rock that occurred with the water in the borehole maintained at a constant overpressure were measured. The latter gave approximate values for the equivalent hydraulic conductivity of the rock. In addition to the six BAT piezometer holes, shown in Figure 4-38, a ring of 52 mm diameter boreholes (the borehole screen) was percussion drilled around the perimeter of the enclosing wall prior to its construction.

Initially, the holes were sealed with packers at approximately 0.5 m from their entrance and pressure/flow (Lugeon type) tests were carried out to provide a measure of the approximate hydraulic conductivity of the rock over the length of the borehole. Subsequently, all the packers were removed and the inflows from the rock into the boreholes were measured throughout the period of the test. Thus, a clear hydraulic boundary for the experiment was defined.

Already supplemented by the tracer tests, the measurements by the ventilation technique of the volumes of water flowing into the room were also supported by attempts to map locally the variations of water inflow with area on the surfaces of the room. Initially this was done by visual inspection. Later a device developed by Watanabe et al (1989) was used to measure the rates at which water evaporated from selected areas of the walls of the room. The principles of operation, accuracy of measurement and methods of use of this instrument were provided by Watanabe (1991).

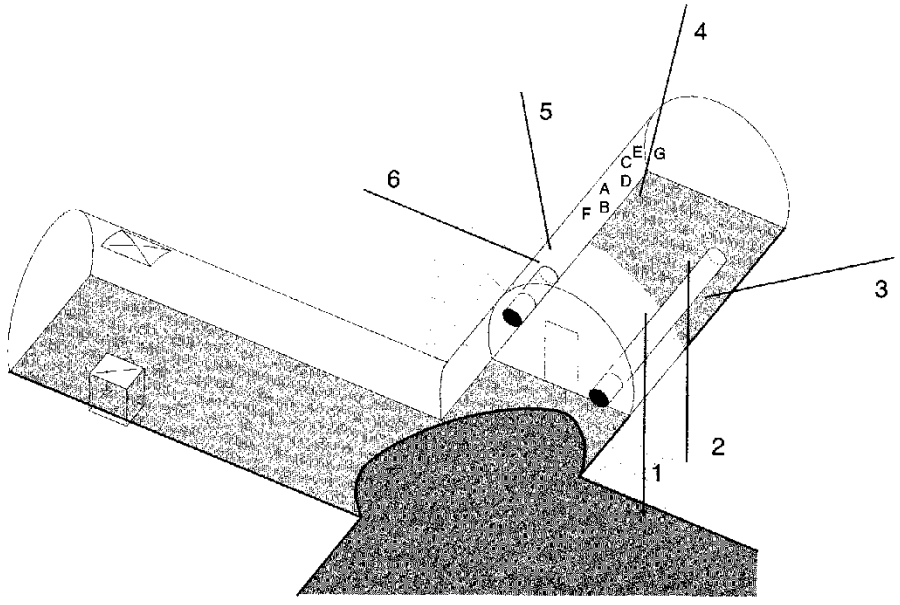

Figure 4-38 The layout of the boreholes used to measure and monitor water pressures and flows in the rock surrounding the experiment room.

The preliminary activities to characterize the water flow paths in the rock surrounding the test room led to a revised understanding of the structural geology of the site and the dominant hydraulic features. Grouting was undertaken in two stages to accommodate this expanded knowledge. Moreover, the understanding of the rock mass and the effects of grouting were further enhanced through the drilling activities and other probes made into the rock during the first grouting attempt. These observations allowed for continuing revision of the experiment plan as the work progressed. Such revisions are normally expected during full scale grouting work and can be expected during the construction and sealing of a repository for heat-generating radioactive waste. In this latter regard the experiment can be seen to have confirmed the approach conventionally used for the design and conduct of rock grouting operations. Furthermore, it is clear that, like the BMT, shaft and tunnel sealing experiments, the engineering works for this grouting experiment increased understanding of the details of the hydrogeological conditions in the Stripa rock mass. By similarity, the engineering activities associated with repository construction will provide more details of the rock than those available from initial site investigation activities. These details can be used to advantage in the layout of the repository and in the design of sealing systems. This has the consequence that the final detailed design of the repository cannot be defined until many of the development and engineering activities associated with construction and operation have been effected. Final detailed models of the performance of the repository will have to be generated when the "as-built" configuration of the repository system is available.

Insofar as the observations made during the progress of the experiment led to revisions of the experiment design, the design itself can be considered as a result of the experiment. Thus, in the following section, the activities undertaken for the experiment are described along with the observations. The information was drawn generally from Pusch et al (1991a).

4.4.2 Results

General characterization

The water pressure and flow measurements confirmed that a conductive element existed in the rock mass within decametres of the north wall of the room. Flow rates into holes 5 and 6 (see Figure 4-38) were 5 to 10 times higher than those into the other monitoring boreholes. The flow rates into the curtain of open boreholes around the wall were not measurable except for the values shown in Figure 4-39. These data support the findings from the monitoring holes. Flow/pressure measurements in the boreholes shown in Figure 4-39 indicated that the rock had a mean equivalent hydraulic conducitivity of 1.5 to $2.0 \cdot 10^{-11}$ m/s. This is similar to the value estimated from the macropermeability experiment. Hydraulic conductivity values at other orientations around the room were clearly less than 10^{-11} m/s.

Points A to G shown in Figure 4-38 were identified as the major points at which water flowed into the room and were associated with a series of vertical fractures which, almost normally, traversed the width of the room. Coloured tracers injected into monitoring borehole No. 5 appeared at points C, D and E within 24 hours after injection and later at point G in the floor and close to the

end of the room. Coloured tracers injected into holes 3 and 4 never appeared on the faces of the excavations.

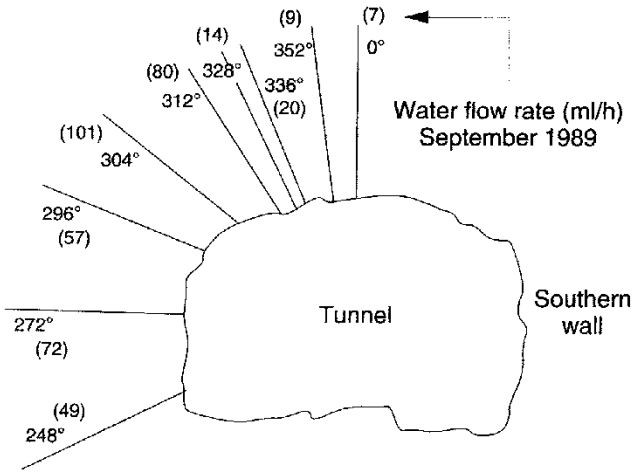

Figure 4-39 Rates and locations of major water flows into the open boreholes of the screen around the wall enclosing the room.

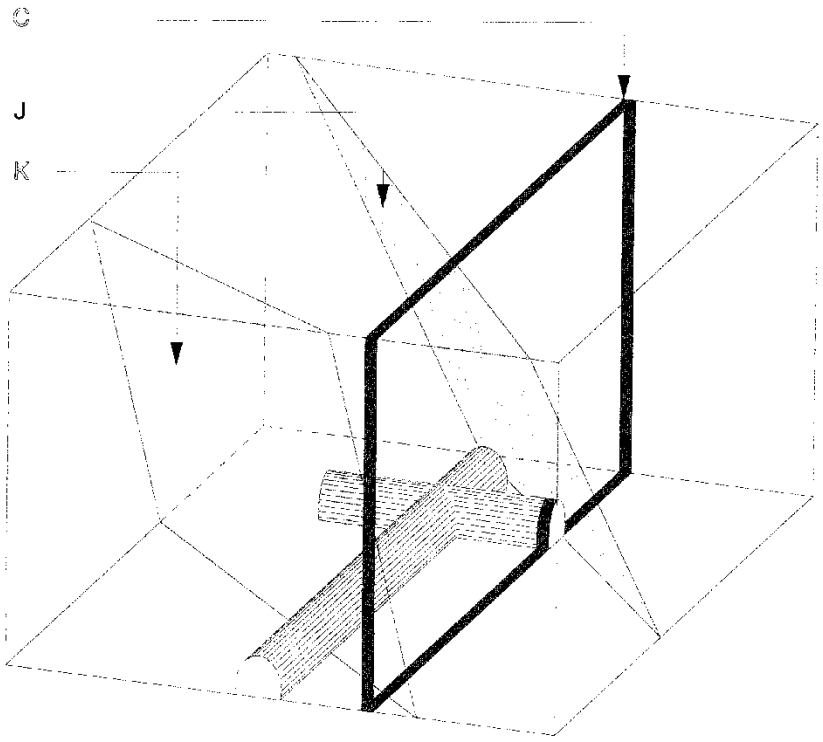

Figure 4-40 A revised model for the major water bearing structures controlling inflow into the 3-D migration experiment drift.

Combined with detailed maps of the fractures appearing on the surfaces of the room, the hydraulic conductivity data, the results of the tracer tests and the monitored values of natural water pressures in the rock led to the conclusion that fracture zone J did not intersect the room. The major flows of water into the room appeared to travel through fracture sets with a NW strike. This set was labelled the C zone. The tracer tests indicated that the C zone was hydraulically connected to the J zone. A revised view of the hydraulically active fracture sets controlling major water flows into the test room is shown in Figure 4-40.

The total rates of water flow into the room measured by the ventilation technique, supplemented by the regular removal and measurements of volumes of water collecting at lower points on the floor of the room, are shown in Figure 4-41. The total rates of inflow are remarkably regular and varied over a period of six months from approximately 1050 to 1375 ml/h with a mean of about 1200 ml/h. This is approximately 3 times the value that could be deduced from the data obtained from the 3-D migration experiment. This difference partly can be accounted for by the measurement of the volumes of water collecting on the floor of the room. These volumes were not measured during the 3-D migration experiment. The data in Figure 4-41 show that, while the total rate of water flowing into the room remained reasonably constant over the monitoring period, the fractional volumes collected from the floor of the room and in the ventilation system varied significantly. No accounting is presented for these variations. Insofar as the fractional volumes collected from the floor of the room tended to decrease with time, it is possible that the variations can be ascribed to an increasing efficiency in the operation of the ventilation measurement system associated with the continued elimination of ponding on the floor of the room.

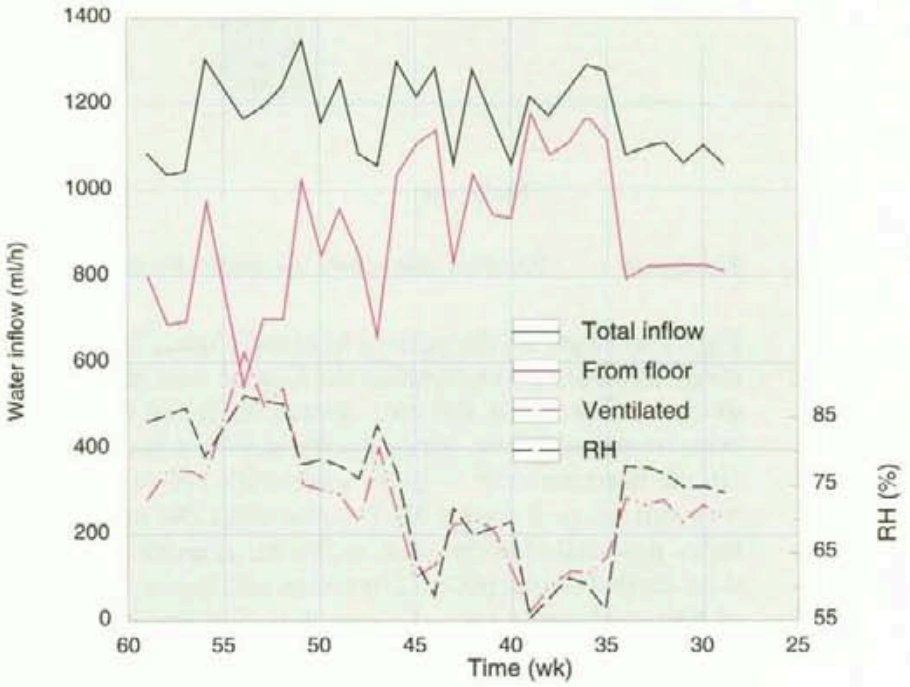

Figure 4-41 The rates of water flow into the experiment room measured before the grouting.

Grouting

The grouting was undertaken in two stages. In the first stage the effects of grouting selected volumes of the C zone were observed. In the second stage a volume of rock above and to the north of the room, where the C zone was presumed to intersect the J zone, was grouted. In both cases Alofix cement grout was injected using the dynamic injection equipment described in section 4.3.1. After each grouting stage, the total rates of water flowing into the room were measured using the ventilation and associated techniques described in the previous section. Local inflows were determined using the evaporation measurement device of Watanabe and tracer tests were conducted to determine changes in the water flow patterns.

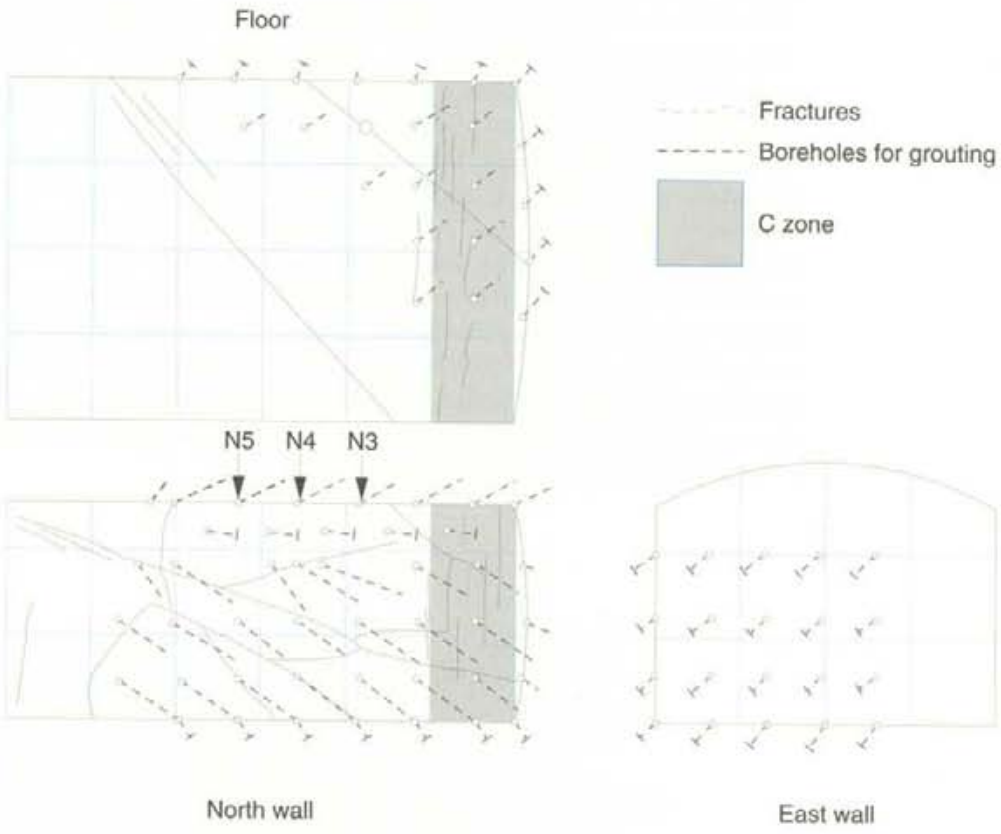

Figure 4-42 The grout hole pattern used in the first stage grouting of fracture zone C.

Figure 4-42 shows the pattern of closely spaced, percussion drilled, 52 mm diameter holes through which the C zone was grouted. Grouting was effected in the northern wall, the end (eastern wall) and the floor of the room, where, prior to grouting, the majority of water flow into the room visibly occurred. On the northern wall 20 holes were drilled in two lower rows to a distance of 5 m into the rock with a NNE strike and a dip of 15°. An upper row of 7 holes was drilled at the same strike but at an elevation of 15°. Twenty holes were drilled to a depth of 2 m on the end (eastern wall) of the room at a strike of ENE and dip of 15°. Twenty two, 5 m long holes were drilled in the floor with a WE strike at a dip of 75°. Not shown in the diagram, 7 additional holes were drilled at the intersection between the northern and eastern walls.

Hydraulic tests in the grout holes prior to injection identified three holes on the northern wall, marked as N3, N4 and N5 in Figure 4-42, as having intersected

water bearing fractures. The rock intersected by all the other holes was generally ascribed an hydraulic conductivity of 10^{-10} m/s or less. The C zone was estimated to have a marginally higher hydraulic conductivity of 10^{-10} to 10^{-9} m/s. Experience in the discrete fracture grouting experiments (section 4.3) indicated it may not be possible to effectively grout fractured Stripa granite with these low conductivities.

Cement grout comprised of Alofix at *W/CM* = 0.40 with a superplasticizer content of 1.4% was injected into the rock. The dynamic injection device shown in Figure 4-23 was used. In the longer (5 m) holes packers were set at two locations (i.e. at the end and 2 m into the hole) and grouting proceeded outwards in stages. Grouting through the shorter (2 m long) boreholes was effected in a single stage. In the outer 2 m a static pressure of 1 MPa was used; a static pressure of 1.5 MPa was used in the inner sections of the longer boreholes. In this regard, it is noted that the groundwater pressures recorded in boreholes 1 to 6 at depths of 7 to 10 m into the rock ranged from 0.8 to 1.8 MPa. The dynamic injection device is reported to have applied maximum pressures of approximately 6 MPa to the grout. Each injection step took between 20 and 30 s. The packers were left in place and the cement was allowed to set and hydrate overnight between grouting operations and, generally, for not more than 24 h.

Measurements of the rate of water flow into the room using the ventilation system showed that grouting had not significantly changed the total flux of water into the room. Water pressures measured in holes 5 and 6 remained virtually unchanged. However, it was suggested that tracer tests provided evidence of a redirection of the water flow in the rock behind the northern wall. With these limited results the second grouting phase was initiated, in which an attempt to cut off the water supply to the C zone at its intersection with the J zone or a hydraulically connected subordinate fracture set was attempted.

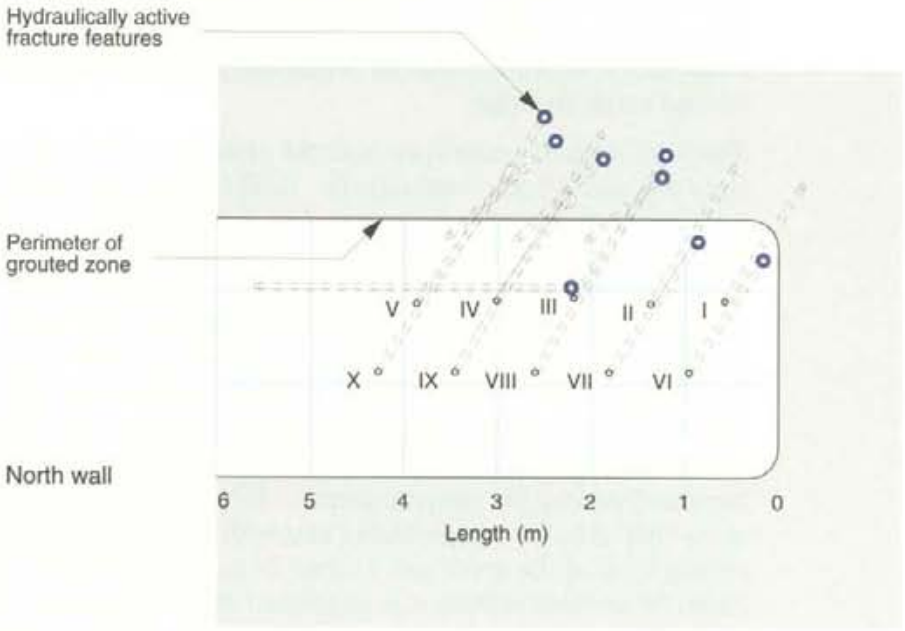

Figure 4-43 The pattern of holes diamond drilled from the northern wall of the test room and used to penetrate, test and grout the J zone.

Ten holes with a diameter of 56 mm were diamond drilled into the northern wall in the pattern shown in Figure 4-43 (holes labelled I to X). Observations on the recovered core, the results of hydraulic tests carried out in the holes and responses in the pressure monitoring system occurring as the holes were drilled indicated that the rock had a noticeably higher fracture frequency within 0.4 m of the wall of the room and an hydraulically active fracture set existed between 3 and 6 m distant from the wall.

The higher fracture frequency near the wall was considered to be the result of damage to the rock caused by the excavation and was similar in extent to that found during the grouting experiments carried out in the BMT room. The hydraulically conductive zone had a conductivity of 10^{-9} m/s or higher and was intercepted by holes VII to X. This zone was considered to be the source of supply of water to grout holes N3, N4 and N5 that had been drilled for the first grouting phase (see Figure 4-42).

Cement grout comprised of Alofix at $W/CM = 0.45$ with a superplasticizer content of 1.4% was injected through boreholes I to X into the rock using the dynamic injection device. The water content of the grout was higher than that used in the first grouting stage. This was needed to accommodate batch variability in the material. An injection time of 30 to 45 s, which was 10 to 20 s longer than that used in the first injection, was employed. It is not clear and is assumed here that grouting pressures were similar to those used in the first grouting stage. Two packer positions were used in most of the holes which were used to grout the rock in the sequence: VI, I, VII, III, VIII, II, IX, IV, X. Hole V was not grouted and was used to monitor the effects of grouting.

The rates at which water flowed naturally into boreholes I to X measured before and after grouting are shown in Table 4-6. The figures obtained after grouting were measured with the cement plug remaining in the drill hole. In addition to these flow measurements, coloured tracers were injected into borehole V before and after grouting to determine changes in the water flowpaths. Moreover, a week after grouting, 15 holes were percussion drilled parallel and close (~100 mm) to the injection boreholes. Natural inflows into these boreholes could be compared with those occurring in holes I to X. Observations from these activities combined with the results of the ventilation testing and the evaporation measurements of Watanabe gave measures of the effects of the second stage grouting.

The total rates of water flow into the grouting holes before and after grouting were 5.1 and 1.9 l/h, respectively. Both figures exceed the total rate of water inflow into the room before holes I to X were drilled (~ 1.2 l/h). Thus, the flow rate results further confirm that holes I to X intersected a volume of rock which was more hydraulically conductive than the C zone and the other rock volume exposed on the surface of the test room. The rate of water flow after grouting is somewhat surprising since the holes were filled with cement. This is accounted for by Pusch et al (1991a) by erosion and piping of the grout at the borehole/rock interface; the same authors also note that the packers were moved and removed within 24 h after grouting (left more than 24 h, the packers became fixed by the cement grout). The data presented in Figure 4-9(a), which show that at lower temperatures and with higher superplasticizer contents the setting time of the grout can exceed 24 h, tend to confirm that the grout eroded. From these observations it is suggested here that it might have been provident to use disposable packers that could be left in place for longer periods than

those used. Data on the changes in pressure with time in the setting grout are not available (as with the packers, pressure sensors would have been lost).

Table 4-6 Estimated volumes of injected grout.

Hole No.	Section grouted m	Injected volume * ml	Rates of water flow into drill holes Before grouting l/h	After grouting Inner section l/h	After grouting Outer section l/h
I	0.2 to 7.0	140	< 0.04	< 0.04	< 0.04
II	0.2 to 7.0	0	< 0.04	< 0.04	< 0.04
III	5.0 to 7.0	0	0.24	0.22	
III	0.2 to 5.0	180			< 0.04
IV	4.0 to 7.0	50	0.08	0.08	
IV	0.2 to 0.4	70			< 0.04
V	Not grouted		0.60	0.07	0.07
VI	1.4 to 7.0	50	< 0.04	< 0.04	
VI	0.2 to 1.4	70			< 0.04
VII	0.2 to 5.0	60	0.56	0.44	
VIII	2.0 to 7.0	210	1.37	1.38	
VIII	0.2 to 2.0	62			1.50
IX	5.0 to 7.0	70	1.78	0.52	
IX	0.2 to 5.0	-			0.37
X	5.0 to 7.0	0	0.44	0.08	
X	0.2 to 5.0	50			< 0.04

* These values are overestimates due to the presence of air in the measuring systems.

The flow figures for after grouting shown in Table 4-6 are from measurements made immediately after grouting. One week later, the total rate of water flowing into the boreholes had fallen from 1.9 l/h to 0.55 l/h. Further decreases with time were observed. It was clear that these changes were not associated with the effects of grouting on the groundwater pressures, which were not significantly influenced by the grouting activities. A number of possible explanations exist for the decreasing rates of water flow. These include continued hydration of the grout, redistribution of natural fracture infilling materials and precipitations in the fractures arising from locally modified hydro-geo-chemistry. The longer term consequences of these processes on water flow rates are not known.

The data from the ventilation measurements made after the grouting experiment are shown in Figure 4-44. The decrease in the measured total water flow into the drift (ignoring the flows into the grouted boreholes) during the first 15 to 18 days reflects lack of equilibrium in the system. Equilibrium between outflow and inflow was considered to be achieved over the last 15 days of the test. The average rate of water flowing into the room during this period was about 1.13 l/h. This is less than the average value measured before grouting. However, the decrease in the mean value is less than half of the range in values measured before grouting and, thus, no significant change in total inflow was induced by grouting.

Figures 4-45 and 4-46 present the results from the evaporation measurements made by Watanabe. Before and after grouting, scans were made of the rock surfaces exposed around the room along sections A and B and over the area of the northern wall shown in Figure 4-45. The evaporation rates along sections

A and B are shown in Figure 4-45. The evaporation rates from the wall are presented in Figure 4-46. Both sets of data indicate significant changes in the pattern of water flow into the room from before to after the second stage of grouting. These results were supported by those arising from the injection of coloured tracers into borehole V. The tracers appeared at fewer and different locations on the northern wall after grouting than before grouting and the colouration was less intense.

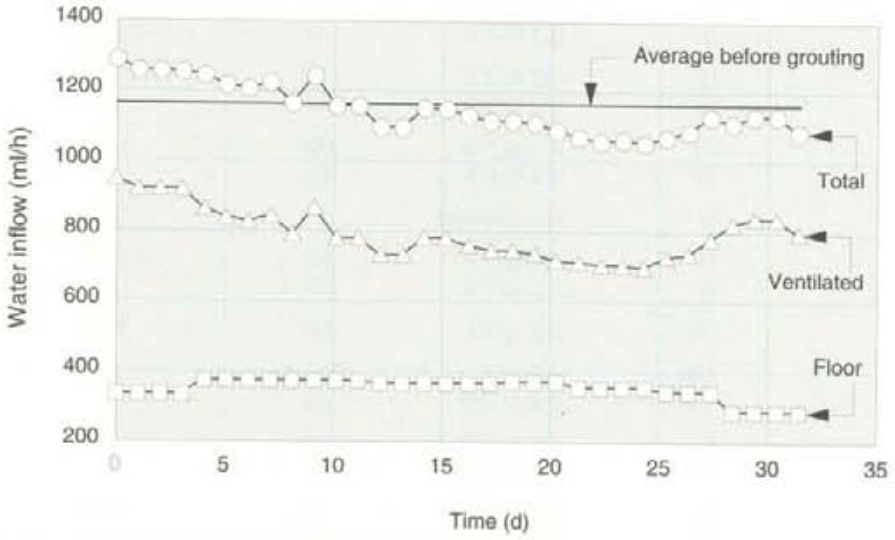

Figure 4-44 The effects of grouting on the rates of inflow into the experiment room.

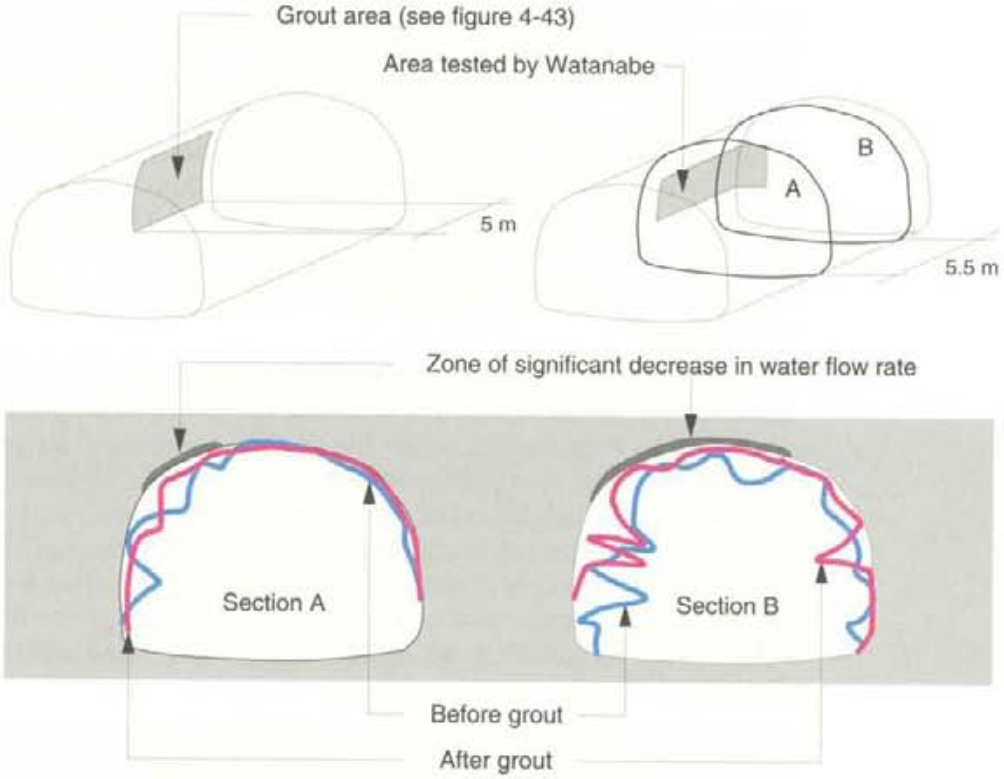

Figure 4-45 The effects of grouting on the distribution of water inflows over two sections of the experiment room.

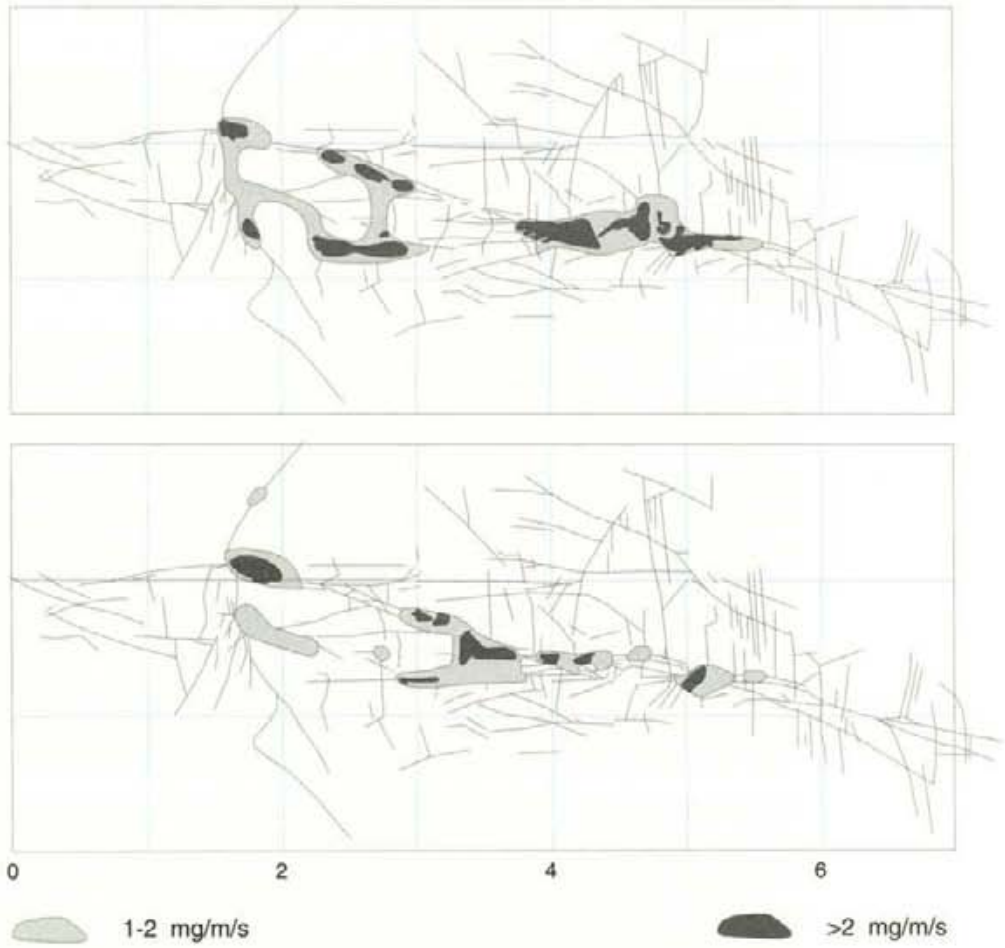

Figure 4-46 The effects of grouting on the water inflow over an area of the northern wall of the experiment room.

After all the *in situ* testing had been completed, four holes with diameters of 56 mm were diamond drilled approximately parallel, to the west and within 270 mm, of grout hole VIII. Cement grout was identified on natural fractures intersected by two drill holes passing within 150 mm of the hole through which grout was injected. The surfaces of the grouted fractures were examined using optical and scanning electron microscopy. These investigations confirmed that there was good bond between the cement and the fracture surfaces, which were usually covered with natural deposits of chlorite or epidote, and that the grout was present in fractures with apertures as narrow as 10 μm. Further results from these laboratory studies are evaluated in Chapter 5 in relation to the predicted longevity of the grout. It is sufficient to note here that the ability of high performance grouts to penetrate fine fissured was confirmed. However, to effectively seal the J or similar zones, the spacings of the holes used for grouting would have to be closer than the ones used in the second stage of this grouting experiment.

4.4.3 Evaluation

The natural barrier investigations provided background information on the hydrogeological characteristics of the rock mass that was to be grouted. This information was used to develop a conceptual plan for an experiment that was intended to determine the effectiveness with which high performance grouts could seal hydraulically active fracture zones in the rock mass. Effectiveness was to be evaluated by measuring the extent to which grouting decreased the rate of water flow into an excavation.

The background information on the hydrogeological characteristics of the rock proved to be insufficient for the level of understanding of the rock required for the grouting experiment. Additional probes to locally characterize the rock indicated more complex hydrogeological characteristics than those originally envisaged and led to a revised conceptual model of the hydrogeological conditions. The hydrogeological characterization activities associated with the experiment identified a subset of fracture features, providing local control (at the scale of tens of metres) on water flows. The subset does not seem to have been recognized by preceding, more globally orientated, natural barrier studies. Similar findings may be expected should grouting activities prove to be necessary to effect repository sealing. Such grouting activities will provide additional information on the detailed structural geology of the host rock and may be used to refine hydrogeological models used for site assessment.

Hydraulic testing of the rock locally around the test room provided estimates for the apparent hydraulic conductivities (k) of the different structures through which the excavation had been made. The structures included the following: a generally intact rock mass with $10^{-10} > k > 10^{-11}$ m/s; an excavation disturbed zone around the room approximately 0.4 m thick (considered to be the result of damage due to blasting) with $k \sim 10^{-8}$ m/s; and, a subset of fractures, approximately 0.75 m wide, intersecting the room (normally with the longitudinal axis) and with $k \sim 10^{-9}$ m/s. The subset connected with an hydraulically active fracture zone with $10^{-9} < k < 10^{-8}$ m/s between 5 to 10 m away from and almost parallel with the axis of the room. With this information it was possible to construct a simple axisymmetric finite element model of the flow paths. Using the known hydraulic pressures in the rock and assuming that the hydraulic conductivity of the more permeable zones was reduced to approximately 10^{-10} m/s by grouting an estimate was made for the effects of the limited grouting undertaken on the total inflow into the room (Pusch et al, 1991a). The total inflows could be expected to be decreased by less than 10 %. This is less than the natural fluctuations measured before grouting. While some measure of this decrease was observed in the test results, it is clear that, alone, the measurements of total inflow into the room were inappropriate to evaluate the effects of grouting. Grouting activities that were more extensive than the ones undertaken would have been required to significantly change the total rates of water flow into the room. In light of the hydrogeological conditions that will exist in a sealed repository after the major disturbances to the groundwater flow caused by repository construction are removed, the rate at which water flows into a room may not be the appropriate criterion by which to evaluate the effectiveness of grouting.

The physical presence of grout in the fractures, the results of the tracer experiments and the rates of evaporation from the rock surfaces before and after grouting, the measured rates of inflow from holes drilled into the ungrouted and grouted hydraulically active volumes of rock, along with hydraulic testing

of ungrouted and grouted rock, all indicate that the grouting activities changed the dominant water flow paths in the rock.

From these observations it was concluded that, using the techniques and cement-based grouting materials developed and used through the programme, it would be possible to decrease the apparent hydraulic conductivity of fracture zones, such as that exemplified by the J zone in the Stripa rock mass, from $10^{-8} > k > 10^{-9}$ m/s to $5 \cdot 10^{-10} > k > 10^{-10}$ m/s. To achieve this effect borehole spacings would have to be closer than the ones used in this experiment. Further improvements in grouting equipment, techniques and processes would add further confidence in an ability to achieve the result.

4.5 GROUTING THE EXCAVATION DISTURBED ZONE

4.5.1 Background and test concept

The major *in situ* investigations to evaluate the hydraulic properties of the excavation disturbed zone (EDZ) and the ability to grout and seal the zone were carried out in the enclosed section of the BMT room above heater holes 1 and 2 (see Figure 2-3). This was also the area where the main test on grouting discrete fractures described in section 4.3 was conducted. The investigations into the excavation disturbed zone were carried out after the grouting but before the final careful excavation of the rock was effected to determine the extent of grout penetration into the rock achieved during the discrete fracture grouting experiment.

The room had been excavated in 1978 and the SAC macropermeability test had been carried out in this part of the mine between 1978 and 1980. This had been followed by the BMT described in Chapter 2. The horizontal borehole sealing experiments described in Chapter 3 were also carried out close to the excavation. Subsequently, the discrete fracture grouting experiment was carried out between 1987 and 1989. Thus, the rock surrounding the excavations had been subjected to significant disturbances, which not only included the immediate responses to excavation but also two periods over which the rock had been heated to temperatures as high as 98°C in the floor of the room. The first heating cycle had lasted about two years: the second had lasted for about 100 days. During the first cycle, the excavations were sealed by the bentonite/sand backfills used in the BMT and, as shown in Figure 2-23, water pressures in the rock within 1 m of the surface of the excavations had been elevated to about 60 kPa. The excavations were left open during the second heating cycle. Thus, the conditions in the EDZ around the BMT may have differed significantly from those in the EDZ surrounding the "validation drift" examined in the natural barrier investigations during Phase 3. An appraisal of the effects of the disturbances is provided by Börgesson et al (1992a).

For the purposes of the Site Characterization and Validation (SCV) exercise undertaken for the the natural barrier studies - see Volume II - the total rate of water flow into a group of six boreholes was measured. Five of the boreholes were driven at approximately equal spacing around the circumference of the planned circular cross section of the "validation drift". The sixth hole was driven along the longitudinal axis of the future drift. The total rates at which water flowed into the six boreholes were between 100.2 and 105 l/h which

were about 8 times higher than the total rate of water flow into the "validation drift" within 3 months after it was blasted out (Hodgkinson, 1992). Less than 50 per cent of the difference between the rates at which water flowed into the boreholes and into the tunnel could be attributed to stress redistribution in the rock around the excavation. Other suggested explanations included changes in the water flow conditions in the rock near to the excavation surfaces due to the presence of gases and from pressure surges during blasting. It was suggested (Olsson,1992), qualitatively, that the gases could be derived from degassing of groundwater, as water pressure decreased closer to the excavation surface, or result from the combustion of the explosives. The gases from groundwater could be expected to persist as long as the excavations were open. The period through which the effects of gases introduced by the explosives lasted is not clear nor are the consequences of backfilling the BMT drift with bentonite/sand mixtures. The following descriptions of the results of the grouting experiment should be considered with these facts in view and with the perspective that the results of the Phase 3 studies into the natural barriers had not been obtained prior to the initiation of the EDZ sealing investigations.

Results from the SAC macropermeability test, the BMT, the preliminary and main experiments on discrete fracture grouting, and the experiment on grouting fracture zones had consistently shown that the fracture frequencies in the rock within about 0.5 to 1 m from the surface of the excavations in the Stripa granite were higher than those of the undisturbed host media. Also, there were strong reasons to suppose that there was a zone near tunnels in which the hydraulic conductivity parallel with the longitudinal axis was higher than that normal to the axis. *In situ* tests and associated analyses were undertaken to confirm these observations, to enhance knowledge of phenomena associated with the EDZ at the Stripa site and to determine the extent to which the advanced grouting technologies being investigated could be used to reduce the hydraulic conductivity of the zones.

The stress field around excavations in the Stripa granite was disturbed by the excavation. It was noted earlier that conventional wisdom (Kelsall and Shukla, 1980) indicated that this disturbance could be expected to extend radially into the rock by approximately 3 times the mean diameter of the cross section of tunnels. The effects of stress concentration and redistribution can be expected to be more pronounced closer to the surface of the excavation than further from it. Moreover, the effects of stress redistribution and concentration will depend on a number of factors which include the shape of the excavation, the magnitude of the stresses and the quality of the rock mass. It is generally supposed that the rock near the surfaces of tunnels which have been excavated by blasting will also be damaged from the blasting action. Immediately next to the face of the excavation it can be difficult to distinguish the effects of stress concentration from those due to blasting. With this recognition, for the purposes of the Stripa investigations the zone of disturbance immediately next to the surface of the excavation was termed "the blast damaged zone": the blast damaged zone was considered to be enveloped by a "stress disturbed zone" which extended to the undisturbed rock mass. The experiment was focussed on the hydraulic characterization of both the blast damaged and the stress disturbed zones. Before proceeding to a description of the experiment, it is important to recall that it is not clear that decreasing the hydraulic conductivity of the rock mass will always benefit the isolation capacity of a repository for heat-generating radioactive wastes. In some circumstances increased porosity can

decrease groundwater velocity and, thereby, decrease the rate of advective transport of radionuclides. Moreover, the sorption of radionuclides on exposed fracture surfaces and infilling materials from slowly moving groundwater may exceed the sorption from faster moving water and further delay radionuclide release to the biota (Chan and Stanchell, 1990). In this context the term "damaged" may be considered to be misleading. The term is retained here for consistency with the nomencalture used in the technical reports.

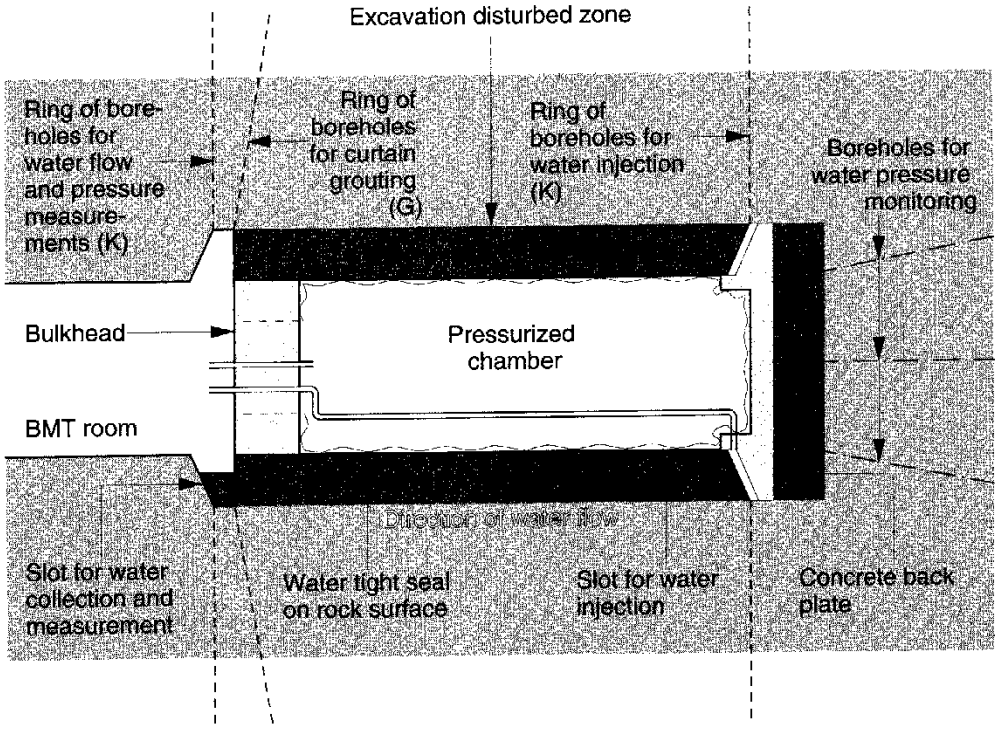

Figure 4-47 General layout of the experiment to characterize and grout the excavation disturbed zone around the inner BMT drift.

The general arrangement of the experiment is shown in longitudinal cross section in Figure 4-47. Slots were made into the rock through the supposed blast damaged zone around the circumference of the room at the end of the room and immediately outside the steel bulkhead that remained in place after the completion of the BMT. The bulkhead was designed to withstand internal pressures of up to 3 MPa. The inner slot was used for both water collection from and water injection into the blast damaged zone. The outer slot was used for water collection only. Continuous slots were cut by percussion drilling overlapping holes with diameters of 100 mm. The inner and outer slots were about 700 and 400 mm deep, respectively. The end of the room was fitted with a concrete backplate after a curtain of 7 m long boreholes with diameters of 48 mm had been percussion drilled in a fan-like array with 5° of separation (72 holes). A similar curtain was drilled and extended from the outer borehole. The boreholes in the inner and outer curtains were intended to be used to measure the hydraulic characteristics of the stress disturbed zone.

The BMT holes 1 and 2, which are not shown in Figure 4-47, were filled with a compacted bentonite/sand mixture. Details of the mixture and the com-

paction methods used are not reported - it is presumed here that at least 20% of the mixture was bentonite and that the material was placed to degrees of compaction that were comparable to those achieved in the backfills used in the BMT room (see Chapter 2). The water uptake characteristics and the effects of the high negative potentials (suction) in the clay on the groundwater flow characteristics locally in the floor of the room were not reported and the influence of the backfill on the results of the experiment is not fully discernable.

The original design for the experiment, shown in Figure 4-47, included an impermeable liner to cover the surface of the room. This would allow the room to be filled with water which could be pressurized to levels exceeding the water pressure in the rock outside the seal. Thereby, radial water flow into the room could be eliminated and longitudinal flows around the room in the disturbed zones and between the borehole screens and slots could be assured and measured.

Trials with different materials to seal the room led to the selection of a bituminous sealing material, with the trade name of Procoat, that, with thicknesses of 3 to 5 mm, was used to coat the surface of the room . Applied during the experiment, the seal was found to leak in spots. Filled with water and pressurized to 220 kPa, the rate of flow of water out of the "sealed" room into the rock was measured to be "several tens of litres per minute" with significant flows being observed at the interface between the outer bulkhead and the rock (Börgesson et al, 1992b). It was concluded that the lining could never be applied to achieve the seal needed for the experiment.

The decision was taken to pressurize the tunnel that had been lined with Procoat with a bentonite clay slurry. The properties of the slurry were similar to those of the grouts used in the test described in section 4.3.2. Under slightly higher pressure than that in the groundwater, the clay would extrude through the leakage points in the liner and seal the interface. A bentonite clay with the trade name Geko Q/I ($w_L \sim 275$) was used. To limit the volume of clay needed, the central volume of the room was equipped with a large rubber bladder that could be filled with water and pressurized. Inflated, the bladder occupied a volume of about 100 m^3. The total volume of the room exceeded 200 m^3. The space between the bladder and the rock was filled with the clay slurry. A clay slurry with w = 500% ($w/w_L \sim 1.8$) was used to fill all but the upper 10 m^3 of space. A slurry with w = 400 % ($w/w_L \sim 1.45$) filled the upper 10 m^3. The more liquid slurry was used in the bottom parts of the space to limit the effects of thixotropy and ensure an ability to pump out the slurry at different stages of the test. Significant practical difficulties, such as the careful balancing of pressures between the bladder and the slurry and removing the slurry between different stages of the test were successfully overcome (Börgesson et al, 1992b). Some settlement of the clay particles occurred in the clay slurry during the progress of the tests. Moreover, under pressure from the bladder the slurry consolidated to a denser mass. Logically, consolidation could only occur through the extrusion of water from the slurry into the rock. A special test was carried out to measure the leakage associated with consolidation. The pressure in the bladder was progressively increased to 10 bars (~ 1000 kPa) and the flows into the borehole curtains and associated slots were measured under natural background water pressure conditions. Analyses of the data indicated a leakage rate of 2.3 l/h with a bladder pressure of 10 bar. This rate of leakage was about one-thousandth of the rate at which water was lost when the chamber was filled only with water and pressurized to 220 kPa. At 2.3 l/h, the rate of water flowing from the slurry into the rock remained significant. It

is noted later (see Figure 4-54) that a need existed to measure changes in the rate of flow of water into the borehole screens of 8 l/h or less.

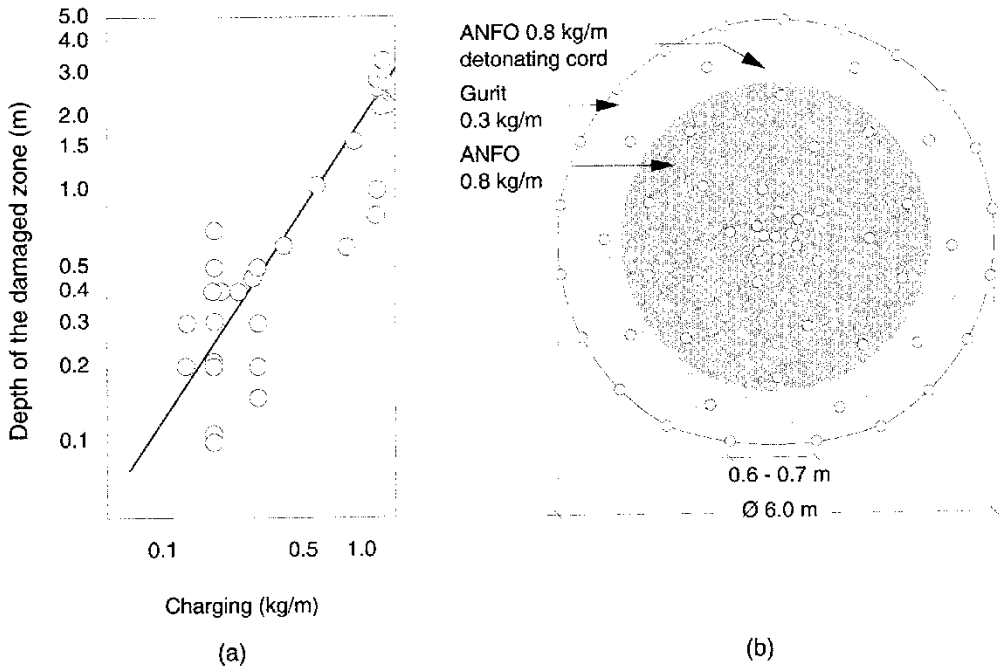

Figure 4-48 (a) the estimated extent of the blast damaged zone (after Riekkola, 1989), and (b) the charge pattern and loadings used to excavate the rooms at Stripa.

Before the liner was applied and the room was sealed with the clay slurry, the fractures exposed on the surfaces of the room were carefully mapped and in 50 places, where there was some possibility of significant rock movement during the injection of the grout, the rock was reinforced with steel rock anchors (ϕ = 20 mm) to a depth of 2 m. No tension was provided to the anchors, which were cemented in place.

The fracture mapping and a series of flow tests in the borehole screens and the slots before the grouting was carried out led to the following understanding of the rock mass and the disturbed zones.

4.5.2 Characterization of the rock mass and the disturbed zone

The pattern of holes in which the charges were placed to excavate the rooms in the Stripa mine is shown in Figure 4-48(b). The charging of the holes is also given. The sequence and timing used to fire the charges is provided by Andersson and Halén (1978). The BMT room was excavated using these patterns and methods. A review of the literature on the extent of blast induced damage around excavations in hard crystalline rocks was undertaken by Riekkola (1989). Results from this review are presented in Figure 4-48(a) which shows a correlation between the estimated thickness of the blast damaged zone (BDZ) and the charging used in the excavation. The results can be considered only in a general sense since factors such as stress levels, the morphology and strength characteristics of the rock, the shape of the excavation and the sequence of fir-

ing and mucking are not separated and, thus, cannot be evaluated. With these provisos the data in the figure indicate that, with the charging shown in Figure 4-48(b), the BDZ around the BMT room might be expected to extend between 0.5 and 1.5 m into the rock. This is thicker than the thicknesses estimated from observations in the Stripa mine where, for the BMT room, the BDZ was estimated to extend about 0.3 m into the rock forming the walls and roof of the excavation (Börgesson et al, 1992a) and to about 1.2 m into the floor. The differences between the thicknesses of the BDZ observed at Stripa and those seen elsewhere are ascribed by Börgesson et al (1992a), after Andersson and Halén (1978), to the sequencing of the excavation process. The inner, ANFO charged holes were first fired and the excavation was cleared of debris. Subsequently, the outer ring of holes was charged and fired. The open excavation within the outer ring of holes relieves the impact of the explosives on the rock and the procedure stripped fractured rock from the surface of the excavation and , thereby, thinned the BDZ.

Figure 4-48(b) is not correct in all respects. The floor of the room was not stripped and greater charging was applied near the floor to facilitate excavation and muck removal. This accounted for the observed greater thickness of the BDZ in the floor than in the walls and roof of the room.

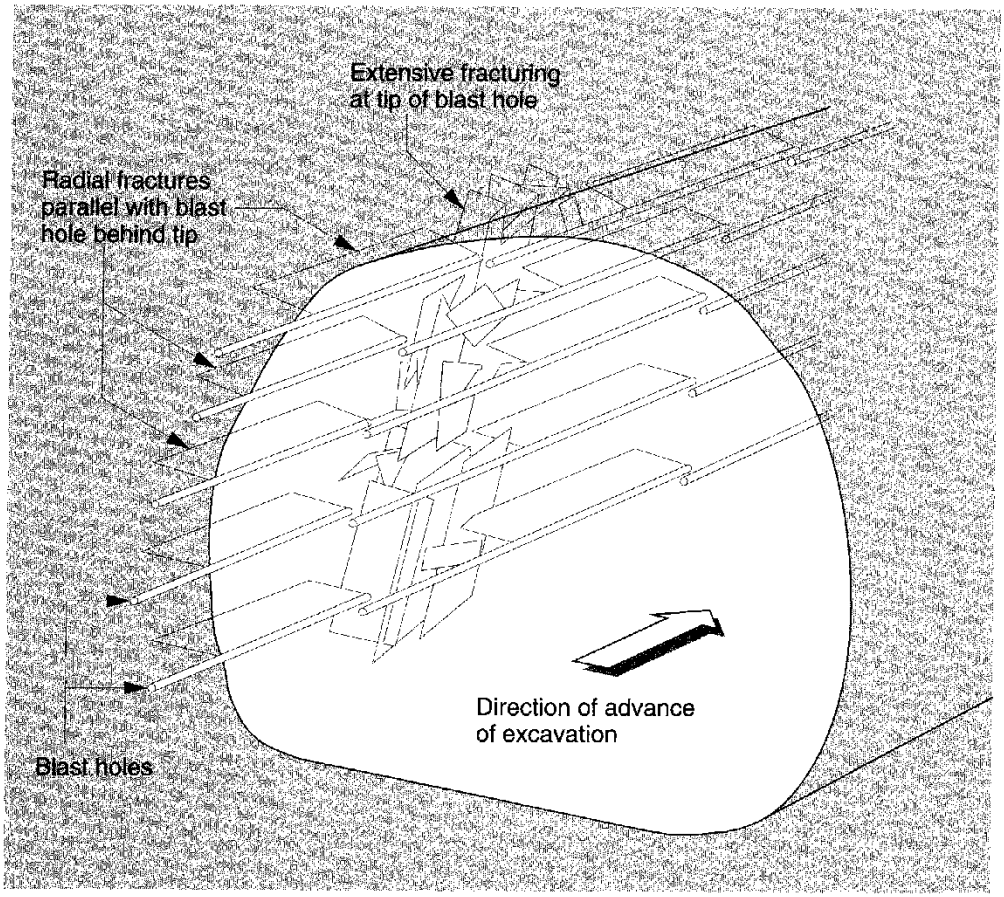

Figure 4-49 An impression of the fracture pattern in the blast damaged zone.

Fracture mapping, core logging and knowledge of the blasting process led to the impression shown in Figure 4-49 for the geometry and pattern of the

significant fractures in the BDZ in the walls and, possibly, the roof of the BMT room. It was suggested that the fractures running longitudinally along the axis of the room and in the same plane as the axis of the blast-holes provided the major pathways for water flow in the BDZ. Data from the BMT and the discrete fracture grouting experiment indicated that the BDZ was more conductive axially along the room than radially about it. Fracture patterns similar to those shown in Figure 4-49 can be observed also at the URL in Canada. Similar blasting patterns and techniques to those used at Stripa were employed in creating the excavations at the URL. The longitudinal fractures do not appear to be as extensive in the URL rock as at Stripa and tend to be observed in zones that can be estimated to be in extension under the redistribution of stresses caused by the creation of the opening. Higher stresses than those measured at Stripa in the vicinity of the BMT room were needed to create conditions of extension in the BDZ around the test room. It was noted in Chapter 2 that σ_1 and σ_2 were sub-horizontal and σ_3 was sub-vertical with values of, approximately, 20 MPa, 10 MPa and 4 MPa, respectively. The room was driven with the major axis parallel to σ_2.

To attempt to understand the characteristics of the stress disturbed zone it was necessary to develop a conceptual model of the geometry of the natural fractures in the rock. This model could then be applied in deterministic calculations of the effects of stress redistribution on the fracture apertures. Recently developed, commercially available computer codes were used for this purpose (Hökmark, 1991; Hökmark and Israelson, 1991). Thereby, theoretically, calculations of the effects of stress redistribution on the hydraulic characteristics of rock near the excavations become possible (Barton et al, 1992). The attempt to link changes in fracture aperture with changes in hydraulic conductivity was not completely accomplished within the project. However, the results of the calculations to quantify changes in fracture apertures were used, qualitatively, to interpret data derived from the *in situ* tests on the hydraulic properties of the stress disturbed zone.

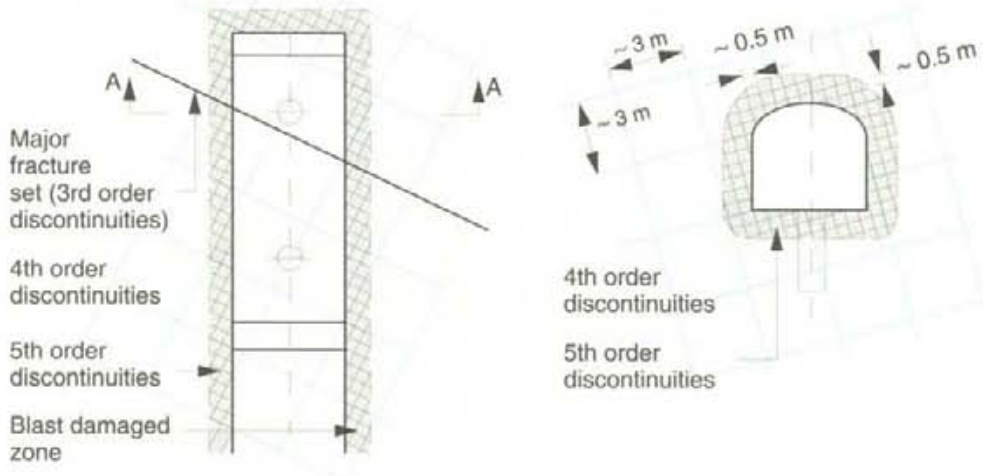

Figure 4-50 A simplified model of the possible fracture pattern in the rock around the experiment BMT room.

The deterministic methodology used to model the characteristics of EDZ adopted by the investigators responsible for the engineered barrier studies differed significantly from the stochastic processing applied by the natural barrier research group (Olsson, 1992). The use of different methodologies was necessary due to the different foci of the two groups and the significant differences between the geometric scales of the natural and engineered barriers studies. The natural barrier investigations were examining rock volumes of 10^6 m^3 or more. The engineered barriers studies focussed on rock volumes of about 3 500 m^3. A link between the two levels of modelling was not effected within the project and remains to be made.

Based on observations at Stripa and in other granitic formations in Sweden, Pusch et al (1991a) proposed that a characteristic series of discontinuities existed in the Stripa granite. Seven orders of discontinuities were identified. These ranged from 1st order discontinuities, which were regional fracture zones with a spacing of several kilometres, to seventh order discontinuities, which were local at the scale of millimetres. The J zone grouted in the fracture zone grouting experiment would fall in the third order in this classification system. Up to the fifth order, the fractures (discontinuities) were considered to conform and exist in orthogonal sets. This system was adopted for the numerical studies into the stress disturbed zone around the BMT.

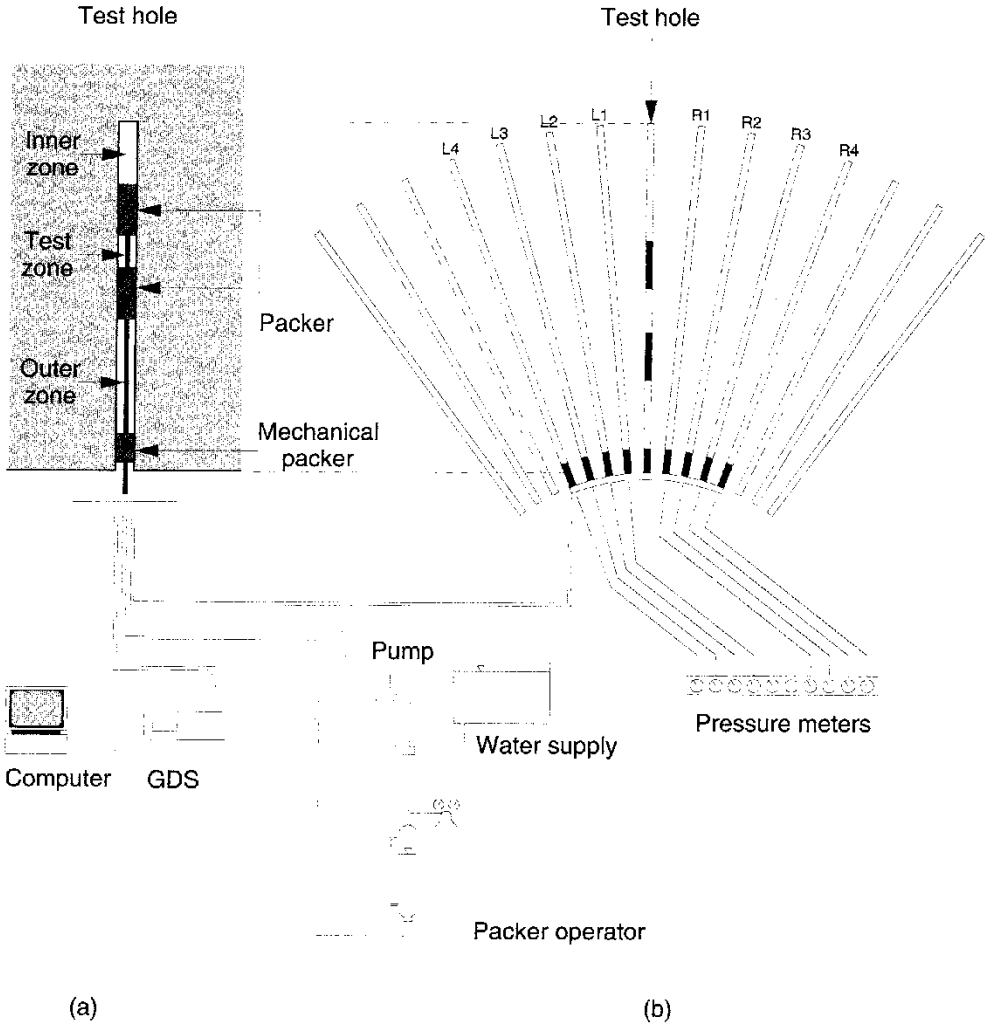

Figure 4-51 (a) the apparatus, and (b) the arrangement used to test the hydraulic properties of the rock around the borehole screens.

Examination of the surface of the room and data on the fracture characteristics obtained from core samples and borehole logging led to the model shown in Figure 4-50 for the fracture sets in the rock in which the BMT room had been excavated. Using the known information on the natural stress field in the rock and parameters for the constitutive behaviour of the rock mass and the discontinuities derived from the investigations into the natural barriers a numerical simulation of the processes of room excavation, backfilling and heating was made for the two dimensional case shown in cross section in Figure 4-50. The results indicated that fractures should have been opened to the east, above and to the east, and below the room (Hökmark, 1991). While the opening of the fractures could be reflected in higher hydraulic conductivities in the rock at the locations identified, the limitations of an analysis in two dimensions of the configuration shown in Figure 4-50 were recognized. The lack of confidence in the results of the calculations demonstrated an awareness of factors that limit available technologies for enumerating the effects of stress disturbance on hydraulic conditions in fractured rock bodies. The work clarified the relative importance of some of these factors.

Before grouting, the water bearing properties of the rock penetrated by the borehole curtains and the slots were measured using three separate methods. First, the rates at which water flowed into each of the curtain boreholes and slots were measured. Inflows were measured both before and after the application of the Procoat sealant to the surface of the tunnel. Second, with a packer set in the outer 0.5 m of each of the boreholes, water was injected into the rock. The water filled borehole was pressurized to 200 kPa above the natural groundwater pressure which had previously been measured. The rate at which water flowed out of the borehole was measured and the average hydraulic conductivity of the rock penetrated by the enclosed 6.5 m length of borehole was calculated. The two boreholes neighbouring the one in which the test was being carried out were sealed with a 6.5 m long packer. Tests were carried out only before the surface of the room was treated with Procoat. Third, to provide information on the variations in hydraulic conductivity along the length of selected boreholes, the system shown in Figure 4-51 was used to measure the hydraulic conductivity of the rock around 0.5 m lengths of the boreholes. Pressure decay and constant pressure flow tests were carried out. The third method was used in boreholes where simpler tests of the second type had indicated that the overall hydraulic conductivity of the rock was higher than 10^{-10} m/s. This latter value was the limit of resolution of the second testing method. The third test method was able to provide measurements of hydraulic conductivity down to 10^{-12} m/s.

The rates at which water flowed into each of the curtain boreholes and into the slots are shown in Figure 4-52. The flows into the boreholes in the floor at the outer screen are not shown. The application of the surface seal did not significantly influence the rates of flow. The results from the inner borehole curtain and slot show higher flows into the quadrants defined by the eastern wall and floor of the room and tend to agree with the predictions from the deformation model. However, the results from the outer screen are inverse. In both the inner and outer screens the flows into the basal quadrants were higher than those into any of the other three quadrants in the same screen.

The hydraulic conductivity measurements over the entire length of the boreholes using the second test method indicated that, in the main, the average hydraulic conductivity of the rock intersected by the boreholes was less than 10^{-10} m/s. Higher hydraulic conductivities were not measured in the segments and

quadrants in which the higher inflows shown in Figure 4-52 occurred. No clear trends in hydraulic conductivity with depth were obtained from the results of the detailed tests using the third test method. Measured values of hydraulic conductivity generally varied in the range 10^{-12} m/s < k < 10^{-10} m/s.

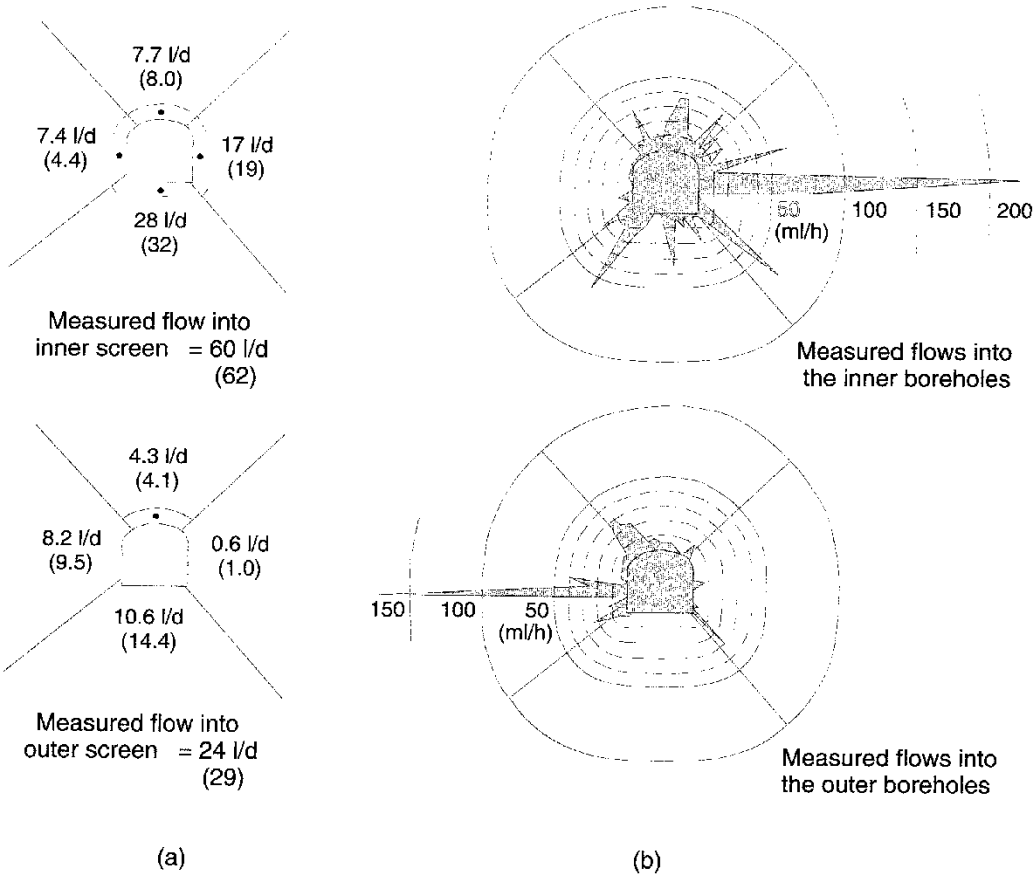

Figure 4-52 Natural rates of water flow into the screens showing (a) by quadrant, the total rates of water flow into the curtains (boreholes plus slots), and (b) the rates of flow into the boreholes. The numbers in brackets in (a) were recorded after the surface had been sealed with Procoat. All other values were measured before the seal was applied.

In brief, the results of the hydraulic measurements in the screens prior to the execution of the main axial flow tests neither substantiated nor obviated the hydraulic significance of either the BDZ or the stress disturbed zone. The results of the axial flow tests and associated analyses are discussed along with the grouting experiments in the following section.

4.5.3 Grouting, test results and analysis

In addition to measuring the hydraulic properties of the EDZ, the original intentions of the experiment included two separate phases in which the BDZ and the stress disturbed zones were to be grouted. The effects of grouting on the hydraulic properties of the zones were to be measured. The BDZ was to be grouted through a large number of short (1 to 1.2 m long) boreholes drilled from the surface of the room. The stress disturbed zone was to be grouted

through a curtain of deeper boreholes drilled in fan-like array inside the outer screen as shown in Figure 4-47. Due to delays in the programme arising from the difficulties encountered in sealing and pressurizing the room, the test of grouting the stress disturbed zone was not completed and the array of boreholes for grouting shown in Figure 4-47 was not drilled.

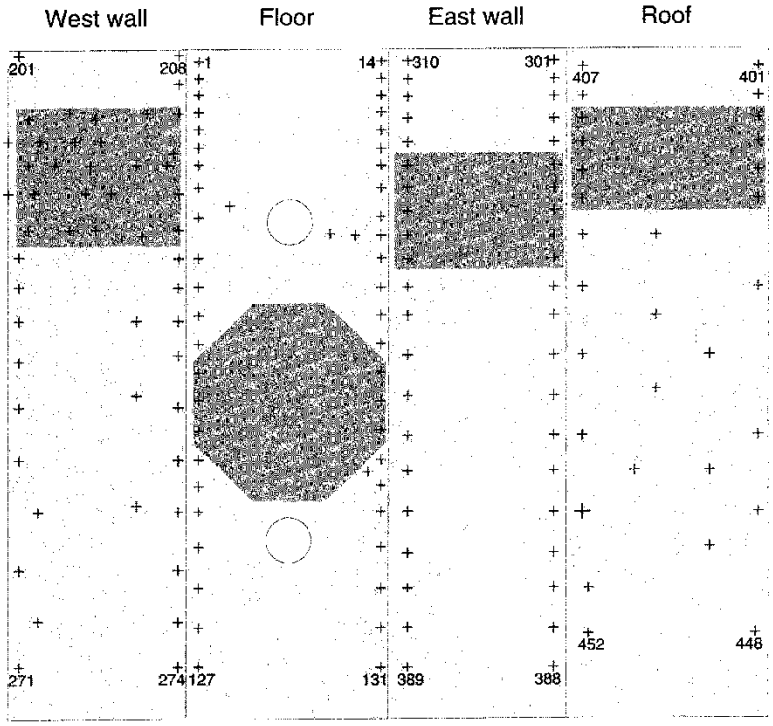

Figure 4-53 The pattern used for the grout holes and the areas in which detailed hydraulic conductivity measurements were made.

To grout the BDZ, a total of three hundred and forty nine holes (ϕ = 56 mm) were percussion drilled in the floor, walls and ceiling of the room in the arrays shown in Figure 4-53, in which the numbers used to code the holes are also identified. The holes were approximately equally spaced and were more concentrated at the end than in the body of the room, where, approximately, the holes were 0.5 to 1 m apart. Before grouting, a series of pressure-flow ("Lugeon" type) tests were carried out in the holes in the darker areas marked in Figure 4-53 to measure the hydraulic conductivity of the EDZ. The lugeon tests were carried out by packing off the outer 0.2 m and pressurizing the remainder of the hole within the inner end of the packer and the tip of the hole, which in the floor was 1.2 m from the surface and in the walls and ceiling was 1.0 m from the surface. The tests in the percussion drilled boreholes on the western wall were supplemented by tests in six supplementary holes which were diamond drilled close to the junction between the floor and the wall. The results from the tests are presented by Börgesson et al (1992a). The hydraulic conductivity of the BDZ was measured to vary significantly within metres and in the range $10^{-11} < k < 10^{-7}$m/s. The tested volume of rock in the western wall had the highest mean hydraulic conductivity, generally in the order of 10^{-8} m/s with specific values as high as $5 \cdot 10^{-5}$ m/s. The ceiling had the lowest mean hydraulic conductivity, which, generally, was in the order of 10^{-10} m/s. In the walls and the floor there was a general tendency for the hydraulic conductivity

to increase with distance from the junctions between the vertical and horizontal faces of the excavations. The results clearly showed that, in planes normal to the boreholes (i.e. with the main axis of the drift) the hydraulic conductivity of the BDZ is 2 to 4 orders of magnitude higher than that of the undisturbed rock mass and the stress disturbed zone.

Alofix-MC cement was used to grout the BDZ. The *W/CM* and the superplasticizer content were varied as shown in Table 4-7. Higher water contents were required when static pressure grouting was used to produce equiviscous behaviour during static and dynamic grouting. The rationale for changing the mix proportions during static pressure injection is not clear. The decision to use static injection techniques for the major part of the work was made after attempts to grout parts of the floor using the dynamic technique had been completed. Precise surveys of dowels cemented in the floor before and after grouting showed that the dynamic injection technique caused lateral and vertical (upward) displacements of the floor of the room. The possibility of such movements during the grouting of the walls and ceiling raised concerns for the safety of the operators.

Table 4-7 Materials and methods used to grout the BDZ.

Surface	Hole Nos.	*W/CM*	Superplasticizer content (%)	Injection method and pressure (kPa)*
Floor	34 to 39, 41 to 121, 123 to 131	0.45	1.4	Dynamic (800)
	1 to 33, 40 and 122,	0.6	1.5	Static (400)
Ceiling	401 to 452	0.6	1.5	Static (400)
Eastern wall	301 to 326 327 to 348, 356	0.60	1.5	
	360 to 362 365 to 389 349 to 355 357 to 359	0.50	3.0	Static (400)
	363 to 364	0.70	1.5	
Western wall	Percussion drilled holes			
	201 to 218, 224, 224, 233, 239, 242, 245, 249, 257,264, 271	0.60	1.5	Static (400)
	Rest	0.70	1.5	
	Diamond drilled holes			
	291 to 296	0.60	1.5	

* The pressure stated for the dynamic injection is the average value applied during injection.

The boreholes were flushed with water prior to grouting. For the walls and ceiling, the holes were flushed immediately after they had been drilled. The flushing water and inflows from the rock naturally drained out of the holes in the ceiling and the walls. The holes in the floor were flushed immediately prior to grouting after which they were emptied of water by blowing with compressed air. The outer 100 to 200 mm of the grout holes were sealed with packers which were designed to allow for the grout holes to be deaired. The packed-off grout holes were deaired and completely filled with grout prior to the application of pressure. Dynamic injection under a mean injection pressure of about 800 kPa was completed in each of the boreholes in approximately 30 s. The static injection took about 5 minutes. Generally, pressures were locked in the grout holes for a period of 24 h before the packers were removed.

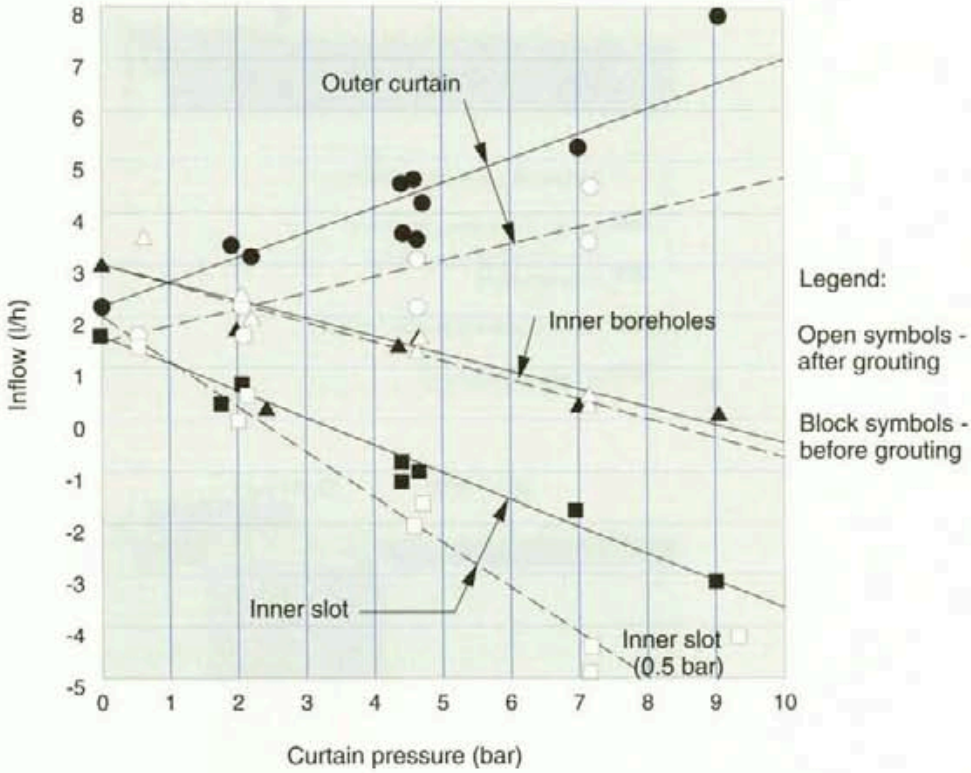

Figure 4-54 The effects of pressure in the inner curtain on the rates of water flow into and out of the inner and outer curtains before and after grouting. Solid symbols and lines are from results before grouting. Open symbols and dotted lines are from results after grouting.

Five of the holes (97, 226, 233, 236 and 421) were not used for grouting. A comparison between the hydraulic conductivity values derived from Lugeon type tests carried out in these holes pre- and post-grouting indicated that the grouting had not decreased the hydraulic conductivity of the BDZ. This result was supported by those of the large scale flow tests, which are shown in Figure 4-54. The figure presents data from tests in which, before and after grouting the BDZ, with the experiment room filled with clay slurry, the flows into and from the inner and outer screens were measured as the pressure in the inner screen was progressively raised to 10 bars (approximately 1 MPa). This pressure was significantly less than that of the groundwater, which decametres into the rock from the excavation was measured to be about 1.4 MPa.

Generally, the flow tests were effected with the slurry pressure of about 50 kPa higher than the water injection pressure. This ensured that none of the injected water flowed towards the slurry filled chamber. Comparisons of the absolute values presented in Figure 4-54 are not entirely satisfactory since leakage from the slurry in the test chamber during the second phase of the measurements, after the grouting had been done, was higher than that which occurred in the first phase. However, the slopes of the lines allowed for an examination of the gross effects of the grouting. The slopes of the lines were not significantly changed by the grouting. From these results and associated analyses it was concluded that the hydraulic conductivity of the BDZ had not been measurably affected by grouting (Börgesson et al, 1992a).

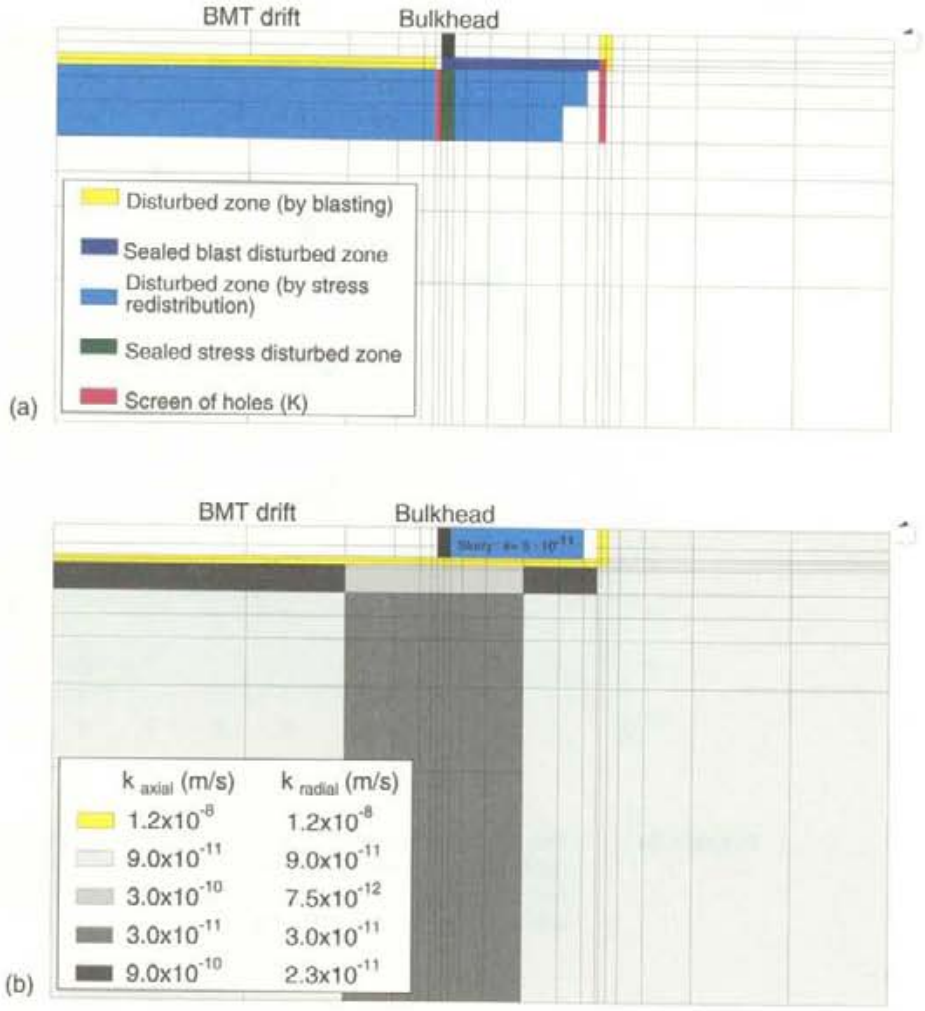

Figure 4-55 Two finite element, equivalent porous medium models (a) used to predict, and (b) derived from the test results.

Throughout the progress of the experiment porous media models were developed and used to attempt to predict and explain the water flows into the room and the pressure responses in the groundwater at different stages of the test. Figure 4-55(a) shows the finite element model that was initially used and developed using information that was available from the SAC macropermeability test, the BMT tests and the natural barrier studies at the start of Phase 3

of the project. Figure 4-55(b) shows a model that evolved from 4-55(a) and incorporated the results of the EDZ grouting experiment. Both models are simplified insofar as they are symmetrical about the longitudinal axis of the drift. The initial model distinguishes between a BDZ, a stress disturbed zone and the undisturbed host rock. The derived model adds complexity, allowing for different hydraulic conductivities in the host rock, spatial variations in the hydraulic conductivities of the stress disturbed zone and includes the clay slurry as a pressurized zone with an hydraulic conductivity of $5 \cdot 10^{-11}$ m/s. In both the original and the derived models the hydraulic conductivity of the stress disturbed zone was considered to be less than the axial value. Hydraulic pressures of 1400 kPa (the approximate measured value) were provided at the outer boundary. In all calculations, the open tunnel was ascribed a boundary pressure of 0 kPa. Unfortunately, this modelling activity was not subjected to the rigorous validation procedures used for the SCV exercise (see Volume II).

The rates at which water flowed into the excavations and the borehole curtains at different stages of the grouting experiment and during the SAC macropermeability experiment were calculated using the two models. The results of these calculations are compared with the measured values in Table 4-8. Both models fairly represent measured influx. The derived model is marginally more accurate. In this regard it is noted here that applying an hydraulic pressure of 1400 kPa to the outer boundary of a simple cylindrical porous medium model with an internal, open tunnel diameter of 4 m, an outside diameter of 25 m, and in which the hydraulic conductivity of a single medium is taken as $5 \cdot 10^{-11}$ m/s (the average of values taken for the host Stripa granite) yields an influx of approximately 3.0 l/h over a 50 m length of tunnel. This is remarkably similar to the quantity measured in the SAC macropermeability experiment. Thus, the total inflow into a tunnel may not be the appropriate measurement to evaluate the usefulness of these models. Under the boundary conditions used, total influx may only be sensitive to spatial variations in the properties of the undisturbed rock mass.

Table 4-8 Calculated and measured values of water flows at different stages of the hydraulic testing of the rock around the BMT drift.

Test	Sink or source	Predicted rate of flow of water into sink (original model) (l/h)	Predicted rate of flow of water into sink (derived model) (l/h)	Measured rate of flow of water into sink (l/h)
SAC Macro-permeability experiment	BMT room	2.25	2.59	3.00
Phase 3 - Grouting experiment				
Curtain inflow test	Inner curtain	3.33	3.52	3.25
	Outer curtain	6.29	1.26	1.25
Slurry leak test	Σ of inner and outer curtains		2.49	2.40
Macro-flow test*	Inner curtain	-9.07	-8.65	-8.50
	Outer curtain	6.61	4.73	4.75

* Inner curtain pressurized. Negative sign signifies flow of water out of the curtain.

Alternative tests for the models include an ability to describe the variations in groundwater pressure in the rock near the test tunnel at different stages of the experiment. At steady state, the simple cylindrical single porous medium model described above would predict a linear change in water pressure between the outer boundary and the tunnel surface. As shown in Figure 2-17 this was not the condition measured during the SAC macropermeability experiment. Mean water pressures calculated using the derived model (Figure 4-55(b)) are compared with the values measured during the macropermeability experiment in Figure 5-56. The calculated pressures conform with the measured pressures. The agreement can be taken to suggest that the assumed values for the hydraulic conductivities of the rock near the surfaces of the excavation are reasonable reflections of reality.

The suggestion that the derived model reasonably reflects reality is further supported by the data shown in Figure 4-57. Here, the results of numerical simulations made of the variations in the groundwater pressure near the test tunnel and parallel with the tunnel axis at distances of 0.5 m and 3 m into the rock during the flow tests are compared with measured values. The numerical simulations were made using the derived finite element model. Reasonable agreement existed between the measured and calculated values.

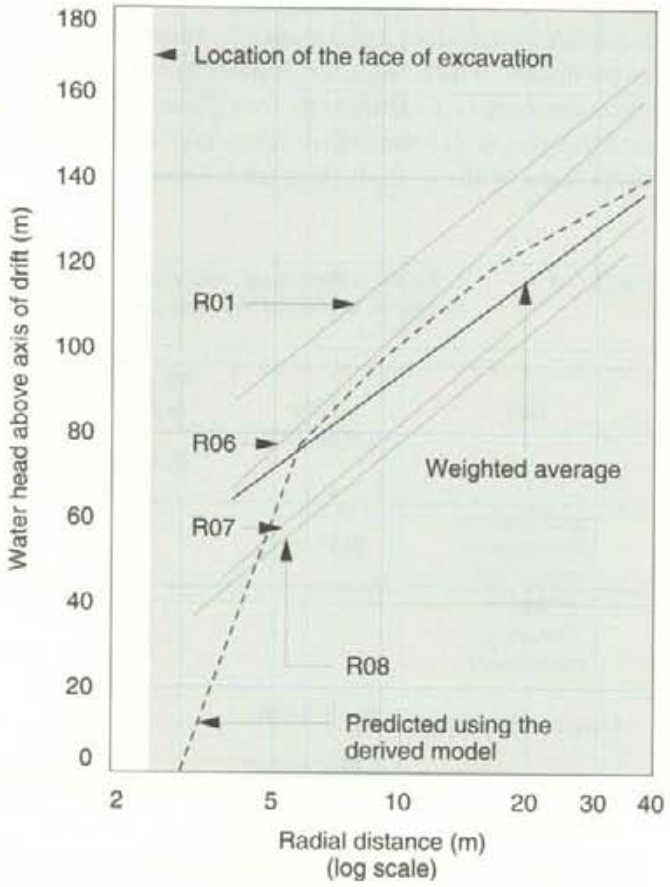

Figure 4-56 A comparison between the pressures measured in the groundwater around the BMT drift during the SAC macropermeability experiment and those predicted by the derived finite element equivalent porous media model.

The modelling activities and results sufficiently supported the data from the *in situ* experiments and measurements to indicate that to describe hydraulic phenomena around a tunnel in the Stripa granite it was appropriate to consider a blast damaged zone and a stress disturbed zone which had hydraulic conductivity properties that differed from each other and from those of undisturbed host media. The blast damaged zone could be generally ascribed an hydraulic conductivity of approximately 10^{-8} m/s but varied locally in the scale of metres within the range $10^{-11} < k < 10^{-6}$ m/s and may be anisotropic. The hydraulic conduction properties of the stress disturbed zone were generally anisotropic. For the purposes of the experiment the properties could be reasonably well described by axial (k_a) and radial (k_r) hydraulic conductivities of $5 \cdot 10^{-10}$ m/s and $5 \cdot 10^{-11}$ m/s, respectively. These hydraulic conductivities varied locally on the scale of tens of metres in the ranges $3 \cdot 10^{-10} < k_a < 9 \cdot 10^{-9}$ m/s and $2.3 \cdot 10^{-11} < k_r < 7.5 \cdot 10^{-12}$ m/s. The undisturbed rock could be considered as isotropic with hydraulic conductivities in the range $3 \cdot 10^{-11}$ to $9 \cdot 10^{-11}$ m/s and variable in this range on the scale of tens of metres. It is considered here that neither the modelling nor the measurements alone provided sufficient data for these final evaluations of the properties of the disturbed and undisturbed rock. The evaluations were made on the combined circumstantial evidence of the iterative modelling and repeated testing procedures.

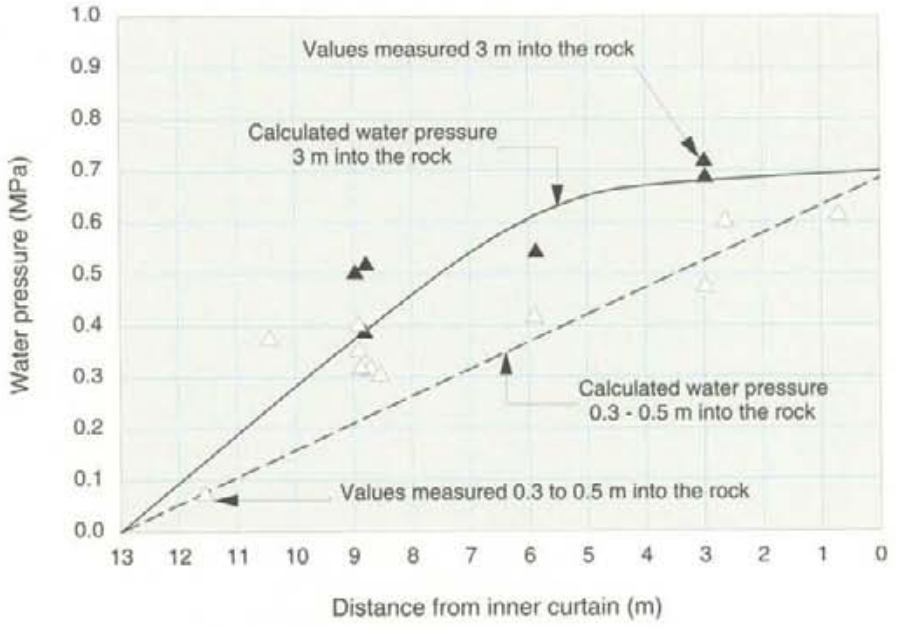

Figure 4-57 A comparison between the pressures measured in the rock parallel to the axis at 0.4 m and 3 m from the surface of the grouting test room with the pressures predicted using the derived finite element equivalent porous media model.

As described in sections 4.3 and 4.4, it was shown through the Stripa Project that grouts can be made to penetrate and reduce the permeability of granite with an average hydraulic conductivity of 10^{-8} m/s. The reasons explaining the inability to reduce the hydraulic conductivity of the BDZ surrounding the BMT room are not clear. Careful excavation of the grouted rock at the end of the experiment showed that the cement grout had penetrated fine fissures in the BDZ (Börgesson et al, 1992b). The spacing of the grout holes may not have been

sufficiently close to ensure continuous grout films in the hydraulic active fractures. It was shown in section 4.4 that a hole spacing of less than 0.5 m may be needed to decrease the hydraulic conductivity of fracture zones with mean hydraulic conductivities of 10^{-8} m/s or more. The procedures used for injecting the grout may need to be improved. The use of disposable packers which allow for the cement grout to set and harden under the injection pressure may be advisable. Thus, while, now, it may be concluded that the BDZ is a phenomenon with which repository design has to contend, it is possible that, if required, alternative methods and procedures for decreasing the hydraulic conductivity of these zones could be identified. These procedures could include the injection of grouts under high pressures around bulkheads placed strategically to divert water flow within a hydrogeological setting such as that shown in Figure 4-1. The second phase of the experiment to grout the disturbed zone was intended to test this aspect of repository engineering but, regrettably, was abandoned.

5 LONGEVITY OF SEALANTS

5.1 BACKGROUND AND SCOPE

Materials used and structures formed for any engineered system must possess longevity, i.e. they must be able throughout their design life to maintain performance under the range of physical and chemical conditions to which they will be subjected. The unique feature in the design of seals for an underground repository for heat-generating radioactive wastes is the design life, which, depending on the features of the waste form and the repository concept, can extend into periods of hundreds of thousands of years. Thus, ensuring the longevity of engineered barriers in a repository can require predictions of material behaviour and performance for periods longer than that during which humankind has been building towns, cities and all related infrastructure. From this viewpoint, longevity can be considered to be the least tractable factor in assessments of repository performance.

Table 5-1 Methods for the assessment of longevity

Method of assessment	Material types	Cautions
Examination of existing geological evidence	Naturally occurring	Provides no information on synthetic materials
Examination of archaeological evidence	Naturally occurring and man-made	Narrow observable range of materials and environments: time-scale less than 3000 years.
Laboratory experiments with accelerated reaction rates	All types	Can be misleading: reactions enter non-representative thermodynamic fields
Application of theoretical thermodynamics	All types	Problem can be indeterminate for complex repository situations

Four methods that can be applied in assessing the longevity of sealing materials and systems were identified by Mott et al(1985) and are shown in Table 5-1. The table also presents some limitations to the application of the methods which can be taken to indicate that, in isolation, none of the methods is entirely satisfactory.

The successful combined application of the four methods necessitates an understanding of the physical and chemical conditions and forces to which sealing materials will be subjected in a repository. These factors will be specific to the repository site, the design of the repository, the location and design of the sealing system within the repository and the required function of the seal. Reflecting these considerations, it was not possible within the Stripa Project to explore all the interests of all of the member countries. The studies were restricted to issues of general interest and those for which resolution was considered possible within the schedule and budget of the project.

Perforce, studies of the type indicated in Table 5-1 tend to be focussed on the very long term behaviour and performance of the materials. This can be considerably affected by the properties of the sealing material as placed, which can differ from those of laboratory prepared specimens. Moreover, the environmental forces that impinge on the materials from the instant that they are incorporated in the repository structure need to be considered.

Methods used to study the reactions between sealing materials, the rock and groundwater for a repository located under the water table in saturated granite, such as that represented by the Stripa site, for periods after a repository is closed (i.e. after waste has been deposited, the repository sealed and the water table restored) may need to differ from those used to study material performance factors while the repository is open. The significance of differences in hydraulic gradients, temperatures and other environmental factors acting during the two repository eras needs to be quantified. In this latter respect, it is evident from Chapters 2, 3 and 4 of this report that the physical conditions of the sealing materials depended on the method chosen for their use, the *in situ* rock conditions and the method and geometry of emplacement. For example, the properties of bentonite grouts, as placed, differed significantly from those of the HCB used in the Buffer Mass Test, which in turn were not the same as those of the less dense bentonites in the BMT backfills. Moreover, material properties changed with time under the varying temperatures, hydraulic pressures, temperature gradients and hydraulic gradients experienced in the *in situ* experiments at Stripa.

In light of the above, conditions in the Stripa mine during the conduct of the *in situ* investigations did not represent those in a closed repository and, in all likelihood, more closely resembled those that could exist during waste deposition in a repository in granite. In this context, and generally, it appears impractical to expect to be able to closely simulate *in situ* in underground laboratories the hydro-thermo-mechanical conditions that will act on engineered barrier materials in a closed repository setting. Thus, it does not appear to be possible to fully confirm, through *in situ* observations and monitoring, understanding of the long term performance of sealing systems. Alternative mechanisms to establish confidence in the predictions of system performance are required. The Stripa programme offered a case study of the application of longevity assessment methodologies outlined in Table 5-1 and assisted in defining some limitations to their application.

The four methods listed in Table 5-1 were used, to varying extent and as appropriate, to study the longevity of bentonite and cement based sealing materials. The work was principally carried out during Phase 3 of the project and focussed mainly on the longevity of grouts. However, the methodologies used and many of the results can be applied to other clay- and cement-based sealing materials, such as HCB and portland cement based concretes. The remainder of this chapter reviews, sequentially, the studies into clay- and cement-based materials. Attempts are made to identify, where clear, restrictions applying to the use of the longevity models generated through the Stripa investigations.

5.2 CLAY-BASED SEALING MATERIALS

Bentonite based materials were extensively studied during the Stripa Project. In Phases 1 and 2 of the project a specific bentonite product (MX-80) recompacted to very high densities was applied *in situ* to seal deposition holes, inves-

tigation boreholes, shafts and tunnels. Less dense mixtures of bentonite and sand were used to backfill and seal rooms. During Phase 3 of the project, alternative commercially available bentonites (principally Tixoton) were investigated for possible use in fracture grouting. In this latter application, it was necessary to use the materials at much lower densities than in the previous applications. Thus, studies were undertaken to investigate the longevity characteristics of bentonite products over a wide range of densities. These studies were focussed to evaluate possible mechanisms by which the sealing properties of the clays could be expected to change through time and to provide models by which the effects of any changes could be quantified. Reports by Pusch (1985) and Pusch et al (1991b) detail the work and form the basis of this section.

Changes in externally applied forces can mechanically disrupt materials. Alternatively, the internal structure of materials can alter such that they are no longer able to sustain the loads to which they are constantly subjected. In a repository, it is possible that the hydraulic conductivity, swelling properties, rheological characteristics and radionuclide sorption and transport properties of bentonite-based sealing materials and systems can be changed by either or both of the above mechanisms. Both of the processes of change were studied during the Stripa Project. Particular emphasis was placed on establishing an understanding of the processes of metamorphism in the clays with particular attention to the characteristics of the microstructure of the materials that control the rates of change in the clay. The effects of mechanical disruption were studied to a lesser extent. The work was carried out with the background of increasing levels of independent research and development into the properties of swelling clays relevant to the use of the materials in disposal schemes for heat-generating radioactive wastes (e.g. Engineering Geology Volume 28, 1990, and Canadian Geotechnical Journal, Dec.1992).

5.2.1 Microstructure, metamorphism and hydrothermal processes

Three internal processes were identified as possible mechanisms by which changes could be wrought in the sealing properties of bentonite clay. Namely, these processes were illitization, silicification and charge change. To more or less extent, the rates and consequences of these processes were studied in both HCB (Pusch, 1985) and the less dense bentonite grouts (Pusch et al, 1991b).

Illitization refers to the transformation of the smectite clay mineral montmorillonite to illite. Models for the crystal structure of montmorillonite are shown in Figure 2-5. A model for the crystal structure of the clay mineral illite is compared with the Endell/Hoffman/Wilm model for montmorillonite in Figure 5-1. Illitization involves the substitution of Al^{3+} for Si^{4+} within the montmorillonite layers, which causes an increase in the negative electrical charge on the crystal, and the fixation of K^+ between the highly charged layers. The illitization of Na-montmorillonite may proceed via the formation of beidelite in which Al^{3+} is substituted for Si^{4+} and the Na^+ on the exchange sites is replaced by divalent cations. This process can be termed beidelitization. Illite clay crystals are larger than those of montmorillonite. The clays are less active and, at the same clay density, illitic clays swell less than smectitic clays and have higher hydraulic conductivity.

Silicification is the deposition of silica within the structure of the clay. This causes changes in the swelling and rheological properties of the clay.

Beidelitization and illitization of the clays causes charge changes which influence both the swelling properties and the radionuclide retention and transport properties of the clay.

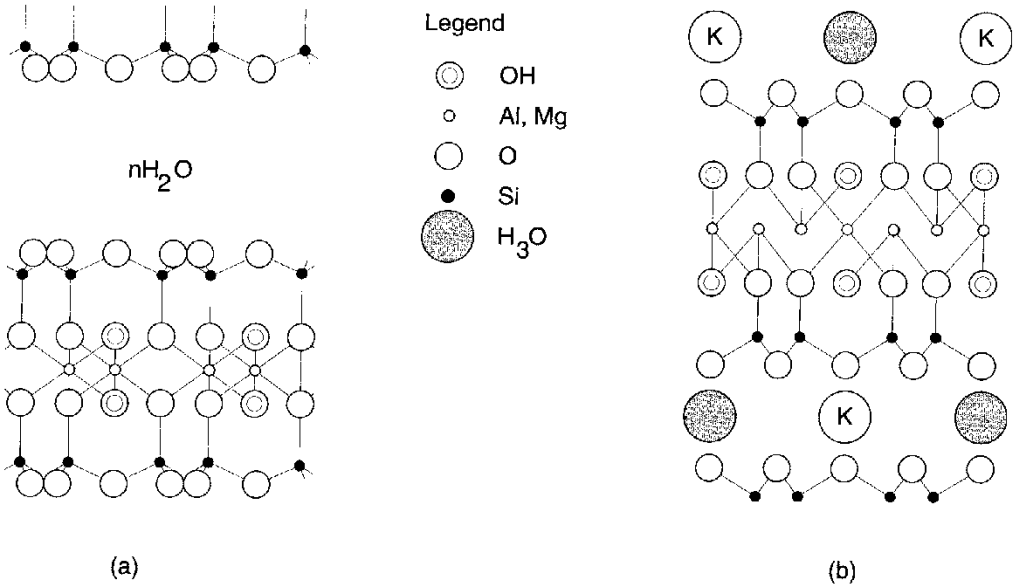

Figure 5-1 Crystal lattice models for (a) montmorillonite, and (b) illite.

Recourse to the literature (Pusch, 1985; Coons, 1987) revealed that there were many uncertainties involved in estimating the rates at which montmorillonite converts to illite. For the generalized reaction shown in Equation 5-1 (after Hower et al, 1976) studies had provided estimates of the activation energy from as low as about 3 kcal/mol (Howard and Roy, 1985) to as high as about 33 kcal/mol (Pytte, 1982).

$$\text{Smectite} + Al^{3+} + K^{+} \rightarrow \text{Illite} + Si^{4+} + H_2O \qquad (5\text{-}1)$$

The lower values were estimated from hydrothermal tests carried out in autoclaves in the laboratory. Higher values resulted from examination of the rates of transformation measured in natural bentonite formations. Using a value for the activation energy of 27 kcal/mol, derived from natural analogue studies, Pytte (1982) provided the estimates shown in Figure 5-2 for the time for conversion from smectite to illite at different temperatures. According to Equation 5-1, the presence of potassium and potassium bearing minerals is essential for the completion of these reactions. With this proviso, Figure 5-2 indicates that at 60°C negligible transformation would occur over a period of 100 000 years. At 130°C transformation could be significant after 50 years. Increasing the concentrations of alkali and alkaline earth cations, other than K^+, in the pore fluids appeared to decrease the transformation rate. However, the exact effects could not be quantified. Contrariwise, it was clear that hydrostatic and earth pressures did not significantly influence the reaction.

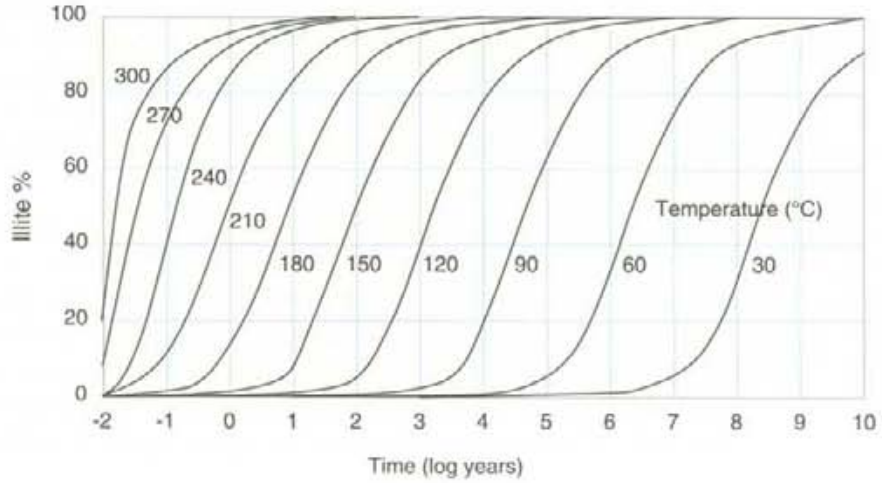

Figure 5-2 Calculated rate of transformation of smectite into illite (after Pytte, 1982). An activation energy for the reaction of 27 kcal/mol is assumed.

The silica released through the transformation described by Equation 5-1 could, by precipitation within the clay fabric, result in silicification of the bentonite and changes in properties. Evidence for this process was provided by Pusch (1983b), Pusch (1985) and Müller-Vonmoos et al (1990). Studies of the microstructure of a natural deposit of meta-bentonite of Ordovician age (~$4.5 \cdot 10^8$ years old) that had been subjected to temperatures of 110 to 150°C for several hundreds to, perhaps, 1000 years revealed nodules of siliceous, quartzitic material on the edges of the clay particles. These are seen in the photomicrograph presented in Figure 5-3.

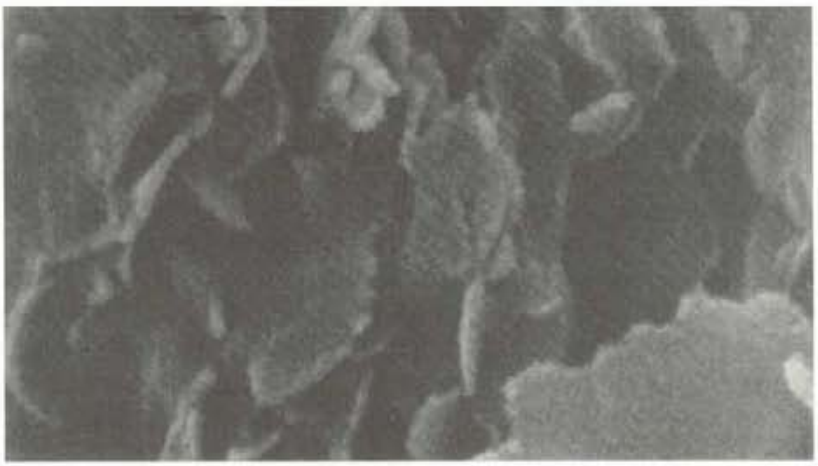

Figure 5-3 Scanning micrograph of Kinnekulle metabentonite (30 000 X). Siliceous nodules are identifiable at the edges of the clay particle (Pusch, 1985).

Samples of the HCB recovered from hole 1 of the BMT (see Chapter 2) were examined for evidence of illitization, beidelitization and silicification (Pusch, 1985). The clay had been heated for about 1 year to temperatures ranging from 72 to 125°C. The swelling properties and hydraulic conductivity of the materials were measured in concert with chemical analyses and examinations of the microstructure using scanning electron (SEM) and transmission electron (TEM) microscope techniques. X-ray diffraction (XRD) methods were used to evaluate possible mineralogical transformations. In view of the short time

scale and the high density of the clay it was generally shown and concluded that, as expected, the clay had not been significantly influenced by heating (Pusch, 1985). Swelling properties and hydraulic conductivity were not significantly altered. Only slight evidence existed for possible silicification and mineral transformation in samples recovered from next to the heaters, where temperatures were highest.

With the above background, for Phase 3 of the Stripa Project, series of autoclave and associated tests were carried out to further clarify the mechanisms of illitization and silicification. Moreover, samples from a number of natural deposits were collected. With an understanding of the geological situation from which samples were recovered and, through examination of the morphology and mineralogy of the samples, interpretations were made to identify the dominant and rate controlling processes of metamorphosis in the natural deposits.

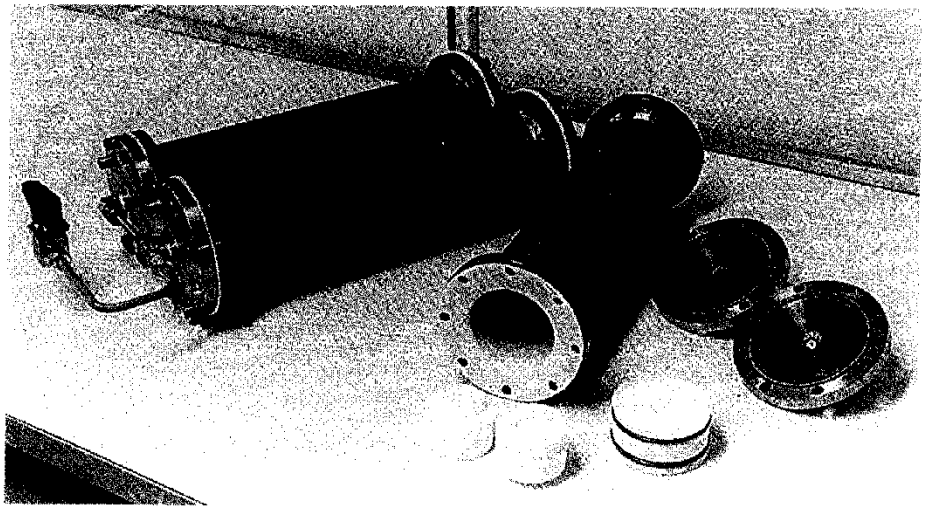

(a)

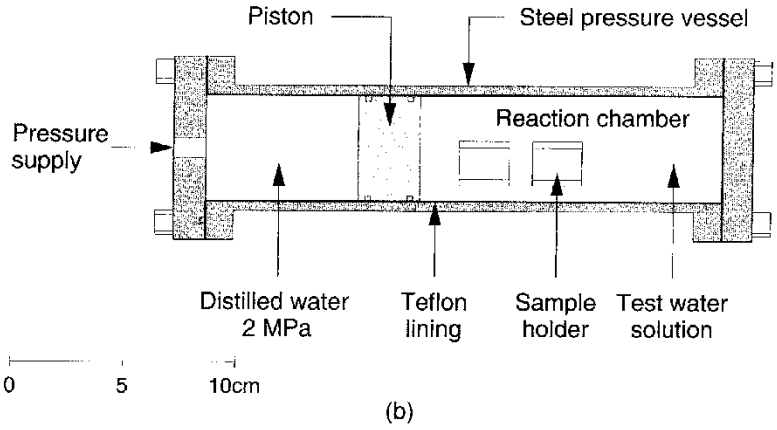

(b)

Figure 5-4 (a) A general view of the reaction vessels used to investigate clay-water interactions; and (b) the internal arrangement of the reaction vessels.

The autoclaves used to apply heat and water pressure to bentonite clay grout at $1.3w_L$ are shown in Figure 5-4. Na-bentonite, Ca-bentonite and bentonite-silica clays mixed with distilled deionized water were tested. Grout filled the 6 ml cylindrical sample holders which were immersed in one of three solutions: these were distilled deionized water, a Ca-rich solution and a Na-rich solution

and identical to the solutions described in section 4.2.2 in connection with the hydraulic conductivity tests on the grouts. The sealed chambers were maintained at constant temperatures of up to 200°C for periods of 10, 90 and 270 days. A pressure of 2 MPa was applied in all tests to prevent the water from boiling at the higher temperatures. After exposure, the hydraulic conductivities and undrained shear strengths of the specimens were measured. Undisturbed materials were examined for changes in microstructure and mineralogy. Changes in the pH of the solutions and concentrations in solution of selected cations were determined.

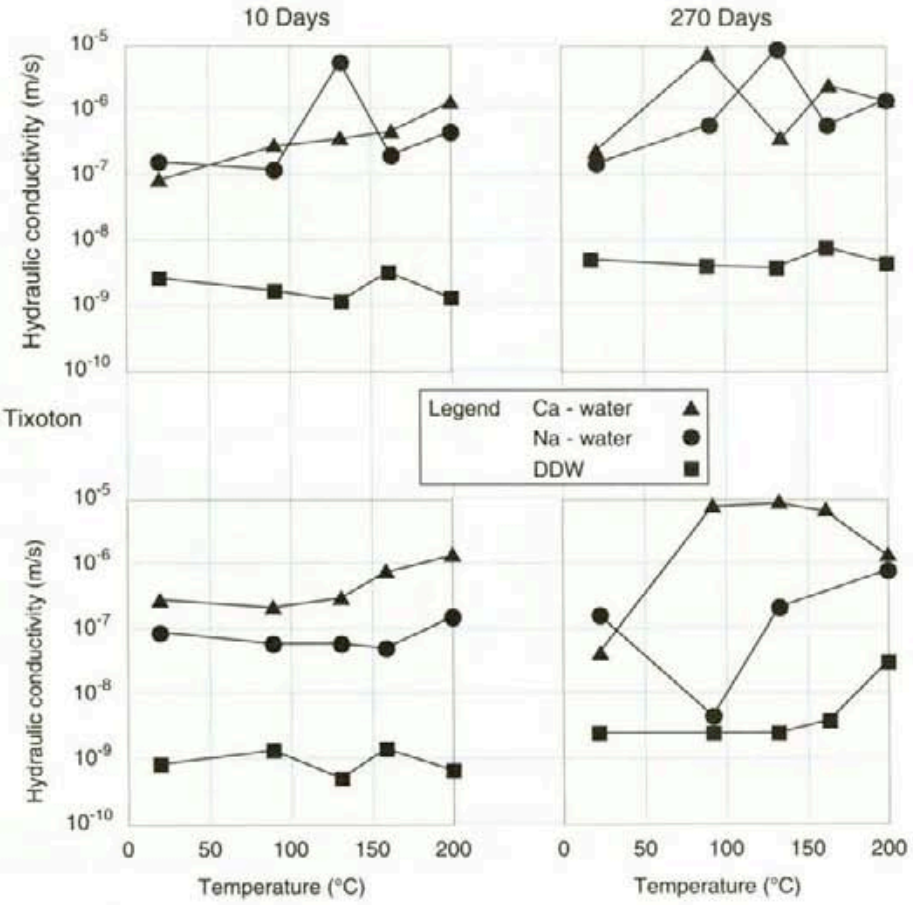

(a) 100% Tixoton

(b) 50% Tixoton / 50% silica

Figure 5-5 The influence of temperature, time, initial water composition and silica content on the hydraulic conductivities of Tixoton - water mixtures formed at 1.3 w_L.

Selected and representative data from the constant head (i = 33) hydraulic conductivity tests are presented in Figure 5-5. Distilled deionized water (DDW) was used as the permeant. The data are consistent with those from the hydraulic conductivity tests on freshly mixed grout presented in section 4.2.2. and show that for all mixtures hydraulic conductivity depended on the concentration and dominant ions of the solution. Hydraulic conductivity tended to increase in the order: DDW, Na-water, Ca-water. In accordance with conventional wisdom, exposure to the saltier water re-ordered (flocculated) the fabric of the clays within the first 10 days and increased the effective porosity of the grouts. Except for the specimen exposed for 270 days at 200°C, which

had an hydraulic conductivity of about $3 \cdot 10^{-8}$ m/s, the hydraulic conductivity of the grouts exposed to DDW did not vary significantly with either time or temperature and were between about 10^{-9} and 10^{-8} m/s. With more variabilty, and generally between about 10^{-7} and 10^{-5} m/s, the hydraulic conductivity of the grouts exposed to Na- and Ca-rich water tended to increase with temperature and become more variable with time and increasing silica content. The variability is attributed to leakage in the test cells between the specimen and the cell wall (Pusch et al, 1991b) and may be partly accounted for by difficulties in test interpretation due to changes in the hydraulic conductivity as the DDW permeated the clay and concomitantly changed its fabric.

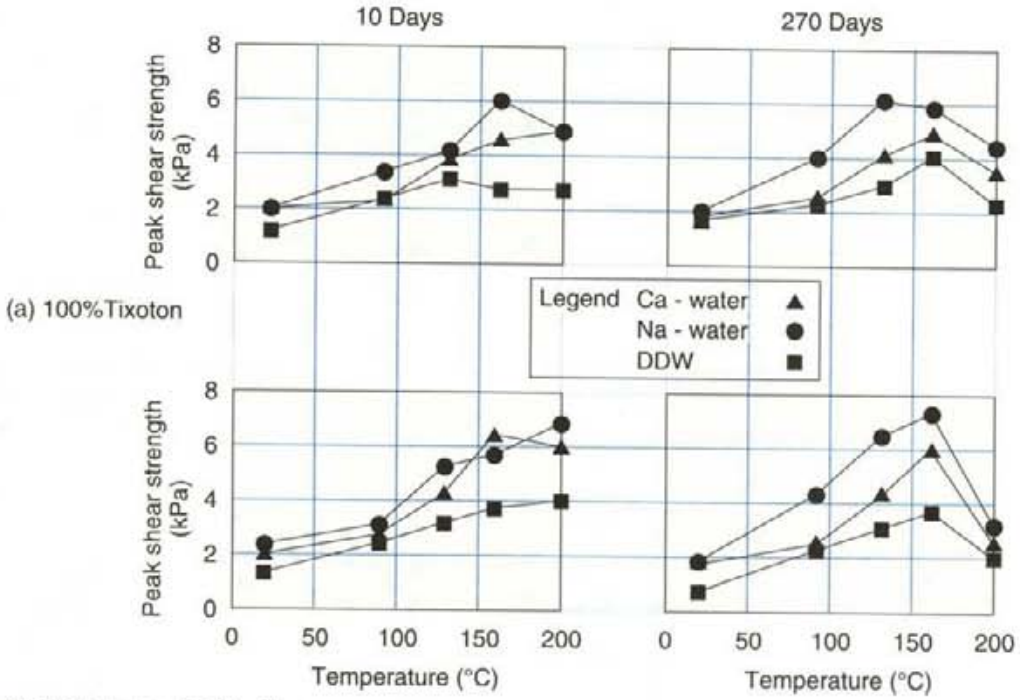

Figure 5-6 The influence of temperature, time and initial water composition on the ndrained shear strength of Tixoton - water mixtures formed at 1.3 w_L.

The vane test was used to measure the undrained shear strengths and strength behaviour of the hydrothermally treated clays. Stress-strain diagrams exhibited a maximum (peak) strength beyond which, with increasing strain, strength decreased. There was a tendency for the peak to become less pronounced with increasing temperature. The peak is typical of overconsolidated clays or thixotropic materials and is also seen in normally consolidated clays in which it is termed residual strength. The peak strengths recorded for bentonite and 50% bentonite - 50% silica mixtures after hydrothermal treatment for 10 and 270 days are shown in Figure 5-6.

The strengths of mixtures reacted with DDW tended to be less than those of equivalently treated grouts reacted with either the Ca- or Na-rich waters. Na-rich water tended to impart higher strengths to the mixtures than the Ca-rich waters. After 270 days of reaction, strengths increased with temperature to a maximum that occurred between about 130°C and 170°C. Increasing temperature above this value tended to decrease the shearing resistance of the clay. The

maximum was also indicated by the data obtained from specimens treated for 90 days. As shown in Figure 5-6, the maximum was less evident in materials that had only been reacted for 10 days. The increases in strength with temperatures up to 90°C were almost solely ascribed to temperature induced rearrangement of the clay particles (Pusch et al, 1991b). Strength increases at temperatures above about 120°C to 130°C were considered to be due to silicification. Decreases in strength at higher temperatures were associated with clay degradation (presumably illitization and beidelitization). These observations were made on the basis of analyses of the microstructural properties of the grouts and chemical analyses of the reacted solutions.

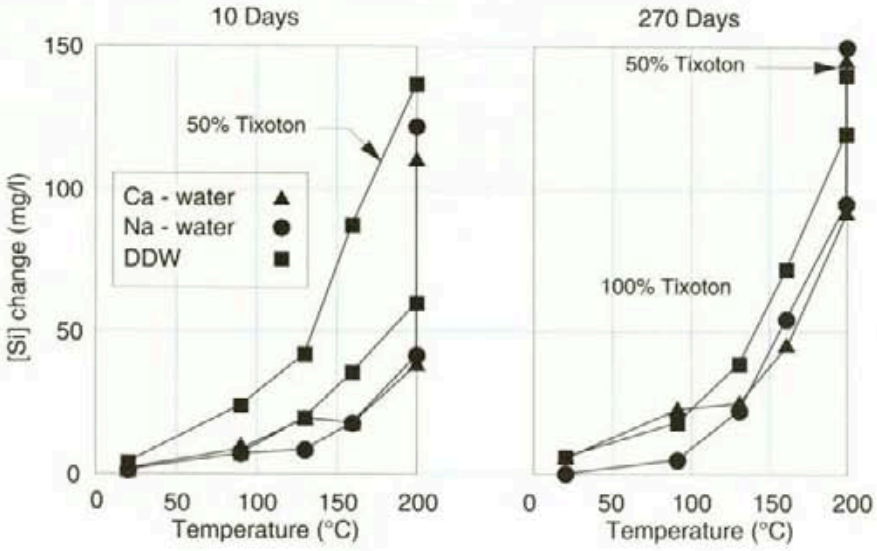

Figure 5-7 The influence of temperature, time, silica content and initial leachant composition on the quantities of silica released to the leachant from Tixoton-water mixtures at 1.3 w_L.

The quantities of silica released to the solutions from Tixoton and Tixoton-silica mixtures after 10 and 270 days are shown in Figure 5-7. The release increased with temperature and temperature effects became more pronounced at temperatures above 100°C. Due to solution saturation effects, little change in the quantities released occurred with time for the 50% clay - 50% silica mixtures. Above 100°C increasing time increased the quantities of silica released from the Tixoton until the solubility limits were approached. Depending on pH, the silica can be present in solution in the form of eiher H_4SiO_4 or $H_3SiO_4^-$. In general, more silica was released to DDW than to either of the salt solutions. Presumably, this reflects the negligible pH buffering capacity of DDW. The suppression of silica solubility was marginally more evident in the Ca-rich solutions than in the Na-rich solutions.

The changes in concentration in solution of silica provided a measure of the processes of silicification and beidelitization. Changes in the aluminium, magnesium and potassium concentrations provided information related to the processes involved in the neoformation of illitic minerals. The influences of temperature on the total quantities of all the four elements released from Tixoton to the three solutions over 270 days of reaction are shown in Figure 5-8. The data show that, congruent with silica release at temperatures above 120°C to 130°C, magnesium and potassium were taken up by the clay from the salt laden solutions with no significant release of these elements to the DDW. Moreover, ex-

cept for reactions with DDW at temperatures above about 150°C during which aluminium was released, the clay retained aluminium. These data were intepreted (Pusch, 1991b) to indicate that magnesium replaced aluminium which in turn replaced and allowed for release of the silica from the clay lamellæ. Despite the removal of potassium at high temperatures from the Ca-rich solution it was concluded (Pusch et al, 1991b) that K^+ had not been fixed by the clay and that the illitization reaction had not been completed. The release of silica from the clay was confirmed through chemical analyses of the solids remaining after reaction. The mean [Si]/[Al] ratio was observed to decrease from about 2.7 at 20°C to about 2.5 at 200°C. The value at 100°C was not significantly different from that at 20°C. Associated with the changes of concentrations of elements in solution, the pH of the solutions, cooled to ambient temperature, decreased with temperature at reaction temperatures above about 130°C (Pusch, 1991b). Below 130°C, pH of the cooled leachant was only marginally influenced by temperature changes. After 10 days, reaction time did not greatly influence pH. Pusch (1991b) reports that the pH of DDW reacted with clay at temperatures below about 130°C became alkaline and at 200°C became acidic. The significance of these pH results is uncertain.

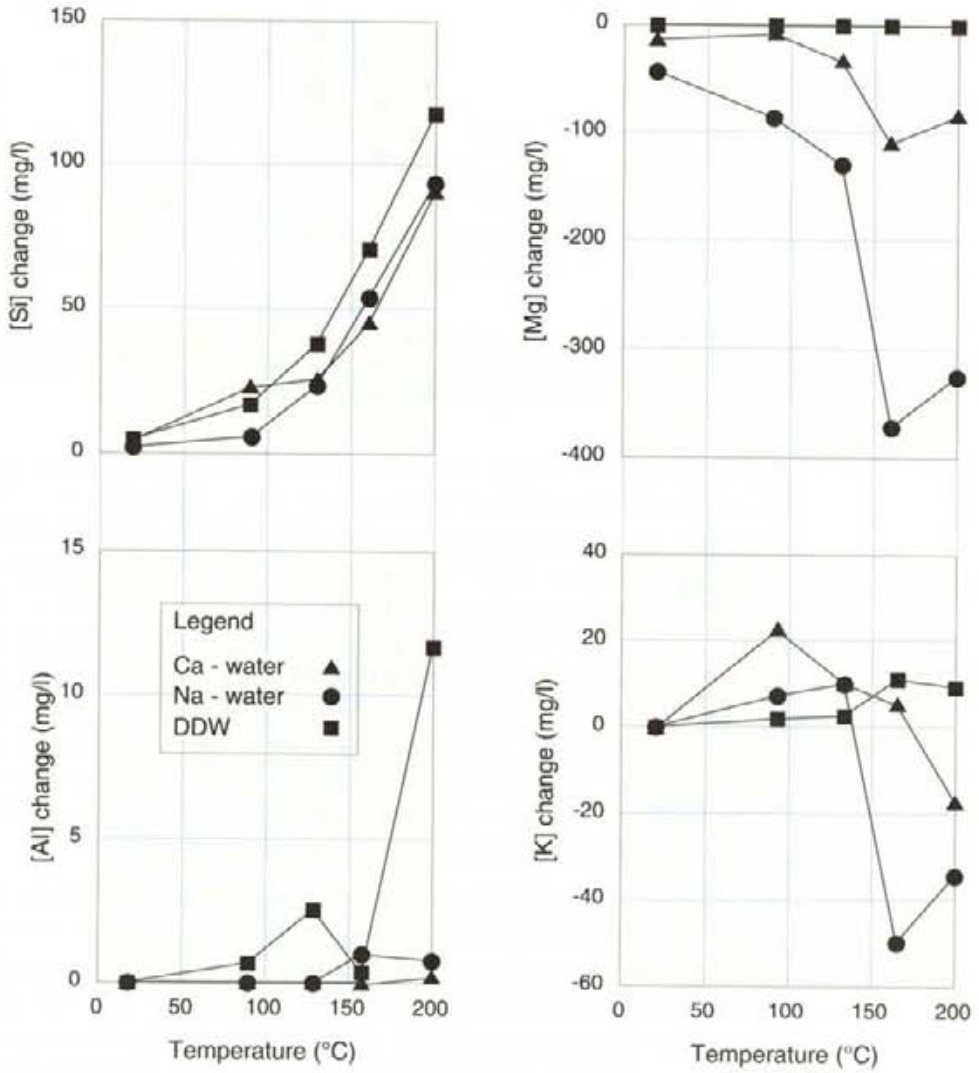

Figure 5-8 Changes in the concentrations of Si, Al, K and Mg in solution after 270 days of reaction over a range of temperatures with three waters of different initial chemical composition.

With the results from the first series of autoclave tests, the strong presence of potassium and magnesium in the solutions was seen as a determinant of the beidelitization and illitization reactions at temperatures at and above about 120°C. Thus, Na-Tixoton clay was reacted for one month with the following solutions: KCl (5 000 ppm), KCl and $MgCl_2$ (10 000 ppm), and KCl, $MgCl_2$ and NaCl (15 000 ppm). Analyses of the clays after reaction using X-ray diffraction (XRD) techniques showed small but clear signs of the formation of illitic (hydrous-mica) minerals. These were more pronounced in the clays reacted with the KCl solution than in those reacted with either of the other two solutions. It was suggested (Pusch et al, 1991b) that magnesium either hindered the transformation of montmorillonite through fixation on the surfaces of the clay particles in interlamellar positions or blocked the fixation of potassium by neo-formed beidellite. It was alternatively suggested that the high magnesium concentration may have favoured the formation of saponite over illite. In all respects evidence strongly supported the suggestion that, given access to K^+ at temperatures above about 120 to 130°C, hydrous-mica (illite) can be formed in the short time periods indicated by Howard and Roy (1985) and Pytte (1982) - see Figure 5-2. Using nuclear magnetic resonance (NMR) measurements of reacted and non-reacted bentonites, further investigations of the process of beidelitization and montmorillonite transformation added the condition that the completion of the metamorphic processes was conditional on the presence of a supply of magnesium, iron or aluminium to the clay. Examination of geological evidence generally confirmed these observations.

It was noted in Chapter 2 that the industrial grade bentonites used in the Stripa experiments are produced simply by drying, grinding and grading materials excavated from natural clay layers. Swelling bentonite clay layers are exploited throughout the world. During Phase 3 of the Stripa Project, the Task Force on Sealing Materials and Techniques witnessed such operations in Japan, Italy and the USA. Tests have been carried out to determine the properties of samples of a bentonite clay layer that is exploited in Canada (Oscarson et al, 1990). These show that the montmorillonite content is high (75 to 90 % of the clay fraction) and that the unprocessed material possesses the swelling, self sealing and low hydraulic conductivity properties deemed desirable in clay buffer and sealing materials. It is significant to note that these clay layers, like the deposits in Wyoming from which MX-80 is prepared, are found in sequences of the Upper Cretaceous epoch and are estimated to be older than 10^6 years. Details of the Canadian deposit are compared in Table 5-2 with those of natural clay deposits studied in Phase 3.

The table distinguishes between deposits that had and had not been subjected to temperatures above about 100°C. The North Sea sediments are from the same geological era as the Wyoming and Canadian bentonites and none of these materials had been subjected to high temperature excursions. Like the North American bentonite layers, the North Sea sediments contain high montmorillonite contents. In contrast, montmorillonite could not be identified in the clays from Kättelvik, Sweden (Silurian deposits with an age of about $4 \cdot 10^8$ years) which were known to originally contain significant quantities of smectitic minerals. The Kättelvik clay was found to be composed of hydrous mica, chlorite and quartz. Unlike the commercially exploited bentonite deposits, the Kättelvik clay had been exposed to the brackish waters of the Baltic sea which had an estimated K^+ content of 100 ppm when the clays were exposed. It was deduced that the Baltic waters had provided the K^+ needed for the conversion of smectites in the Kättelvik clay to hydrous mica.

Table 5-2 Properties and history of natural clay deposits.

Deposit, name and location	Geological era	Age (years)	Mean montomorillonite content (%)	Estimated thermal history
Avonlea*, Canada.	Upper Cretaceous	7 to $8 \cdot 10^7$	75 to 90	No significant elevation of T. Glaciation.
North Sea sediments	Upper Cretaceous	7 to $8 \cdot 10^7$	60 to 70	50 to 100°C
Burgsvik,Kättelvik, Sweden.	Silurian	$4 \cdot 10^8$	0	<100°C
Hamra, Gotland, Sweden.	Silurian	$4 \cdot 10^8$	~35	110 to 120°C for 10^7 a 20 to 110°C for rest
Busachi, Sardinia, Italy.	Tertiary	$3 \cdot 10^7$	80 to 90	>130°C for < 1 year
Kinnekulle, Sweden	Ordovician	$4.5 \cdot 10^8$	20 to 30	>130°C for 1000 years

• Data from Oscarson et al (1990). All other data from Pusch (1991b).

The Hamra clays are from the same geological sequence as the Kättelvik clays. With a residual montmorillonite content of about 35 %, 50 to 75 % of the original smectite in the Hamra clays was estimated to have been converted into hy-drous mica (Pusch et al, 1991b). In contrast with the Kättelvik clays, the Hamra clays had not been exposed to the Baltic sea waters and had been subjected to temperatures above about 120°C. The K^+ needed for the formation of hydrous micas in the Hamra clays was deduced to have been derived from the sedimentary limestones, mudstones and shales that confined the Hamra clays. With reasoned judgements relating to the concentrations of K^+ in the pore water in the confining layers and allowing for the complex geometry of the Hamra sediments, it was concluded that the conversions to hydrous-mica were consistent with diffusion of K^+ into clay beds with an effective diffusion coefficient (see Equation 2.1) for K^+ of between 10^{-11} to 10^{-10} m^2/s (Pusch et al, 1991b). This value is of the same order as that measured in the laboratory for dense smectitic clays. Applying this diffusion model to the North Sea sediments and to the Sardinian, Busachi, sediments resulted in estimates for the residual montmorillonite contents of the clays of 50 to 80 % and 70 to 90 %, respectively. These calculated values bounded those that were measured. Thus, it was concluded that the rate of conversion of montmorillonite to hydrous-mica in natural bentonite deposits is largely controlled by the supply of K^+ and the effective diffusion coefficient of K^+ in the clay. Logically, the commercially exploited bentonite beds had not been in contact with media that were rich in K^+.

The Sardinian bentonite and the clays from Kinnekulle in Sweden were of interest since both had been exposed to high temperatures. The Sardinian bentonite was overlain, in part, by rhyolite. The magma from which the rhyolite had formed had clearly heated the clay to high temperatures. The Kinnekulle bentonite was known to have been heated to temperatures in excess of 130°C for about 1000 years. Tests of the mechanical behaviour of the heat affected materials revealed that the clays had been embrittled by the temperature excursions (Pusch et al, 1988). Examination of the microstructure of the Kinnekulle clays provided evidence, such as that shown in Figure 5-3, for the occurrence of beidelitization and silicification of the clay. It is noteworthy that the application of the diffusion model to the Kinnekulle case using an effective diffusion

coefficient of $5 \cdot 10^{-11}$ m^2/s suggested that the residual montmorillonite content of the clay should be about 20 %. The measured values were between 20 and 30 %.

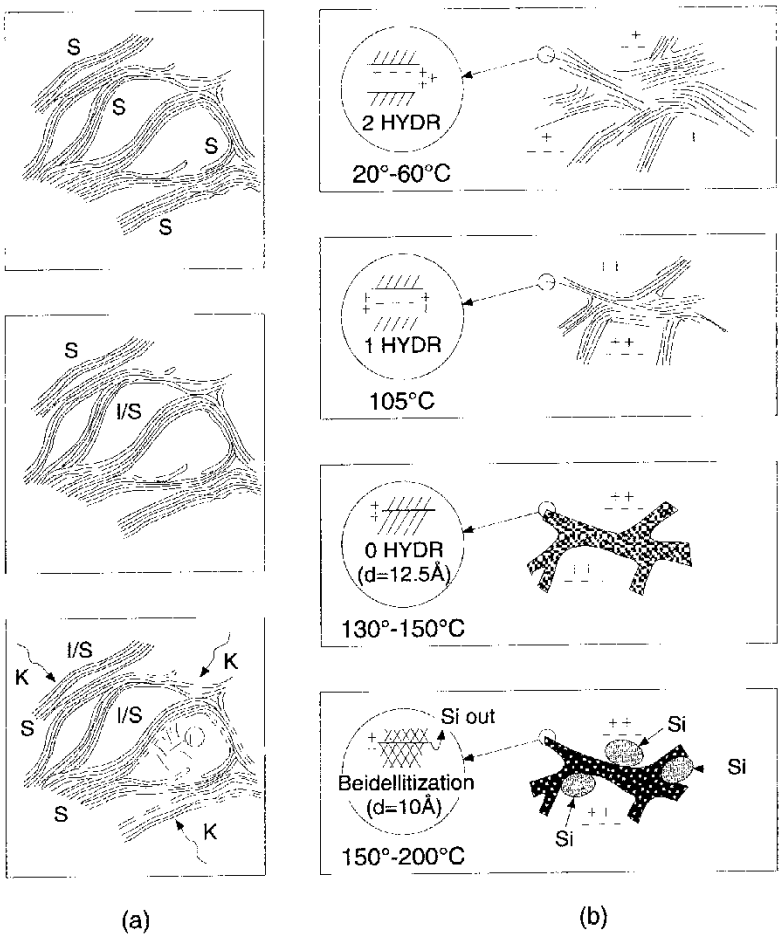

Figure 5-9 Major features of the smectite (S) to illite (I) alteration model. Column (a) shows congruent dissolution, the invasion of K^+, the transformation of the nerals and neoformation of hydrous mica. Column (b) shows heat induced contraction of smectite stacks, permanent collapse at a critical temperature and the precipitation of silica in closed conditions.

The results of the laboratory tests and the observations made from the natural deposits led to the model shown in Figure 5-9 of the chemical processes involved in the metamorphosis of natural bentonite clays and engineered bentonite clay barrier materials. Given the continuing presence of K^+, montmorillonite rich clays will convert to materials rich in hydrous-mica. The rate at which this change occurs and the mechanisms of metamorphosis vary with temperature.

It is suggested (Pusch et al, 1991b) that at temperatures below 100 to 130°C the smectitic clay dissolves congruently in the pore water and is converted to hydrous mica at a rate that depends on the supply of K^+. Increasing temperatures from about 60 to 100°C appears to cause some collapse of the hydrated smectite structure (i.e. the number of water layers bound between the clay crystals is decreased from 2 to 1). Presumably, the loss of the interlayer water causes changes in the pore size distribution in the materials and

associated changes in the hydraulic properties and mechanical condition of the clay. In this context it is noted that during extraction and production bentonite clay products are routinely kiln dried at temperatures about and above 100°C.

At temperatures of 130 to 200°C, in addition to the loss of the remaining inter-layer water and collapse of the hydrated clay crystal structure, given the presence of aluminium or magnesium, the beidelitization reaction proceeds in association with incongruent dissolution of silica from the clay and, in defined conditions, precipitation of silica in and consequent cementation of the clay. Thus, it is suggested that at the higher temperatures, given access to K^+, the smectitic clay transforms to hydrous mica either directly through the illitization reaction or via beidelitization and the associated formation of mixed-layer minerals. The physical properties of the clay will depend on the proportions of each of the possible reaction products present in the clay, the extent of silicification and the transformed microfrabric of the reaction products.

Over the full range of temperatures investigated it was concluded that the rate at which hydrous mica and mixed layer minerals are formed depends principally on the rate at which K^+ gains access to the reaction sites within the clay. For the purposes of estimating the performance of engineered bentonite barriers Fick's first law of diffusion was considered to provide a reasonable first estimate for the rate of this process (Pusch et al, 1991b). In this circumstance, the concentration and solubility of K^+ at the clay barrier boundaries, the dimensions of the clay barrier and the density, which bears on the porosity, pore size distribution, tortuosity and ion exclusion properties of the clay, will be determinants of the rates of metamorphosis and, hence, changes in the performance characteristics of the engineered clay barriers.

5.2.2 Expected performance

At the same clay dry density, clays with hydrous mica as the predominant clay mineral have higher hydraulic conductivity than otherwise equivalent clays with montmorillonite as the predominant clay mineral. Completely converted to hydrous mica, the hydraulic conductivity of the HCB tested in Phases 1 and 2 of the project will increase from about $5 \cdot 10^{-13}$ to about $5 \cdot 10^{-11}$ m/s. The hydraulic conductivity of the grouts examined in Phase 3 of the project will increase by about 5 orders of magnitude from about 10^{-10} to 10^{-5} m/s. These changes will be accompanied by decreases in the swelling ability of the clays, changes in the mechanical strength properties, decreases in the radionuclide sorption and retention properties, and increases in the effective diffusion coefficients for both K^+ and radionuclide transfer. The importance of these changes to the performance of a sealed repository depends on the degree of reliance placed on the clay barriers in the safety analysis of the repository design.

Using the K^+ diffusion model, estimates were made for the periods over which complete transformation of montmorillonite to hydrous mica will occur in clay grouts (Pusch et al, 1991b). The conditions used and results of these calculations are presented in Table 5-3. Conversion times of between less than 1 and as long as 500 years were predicted. It was considered that the lower values could be discarded. Shown by the autoclave tests, at times of 5 years or less the rate of dissolution of the clay is more likely to control the rate of conversion from montmorillonite to hydrous mica than the availability of K^+. Thus, based on an assessment of possible repository temperatures, groundwater conditions and seal geometries, it was concluded (Pusch, 1992) that bentonite

based grouts could persist without significant conversion from montmorillonite to hydrous mica for periods ranging from a few hundred years to hundreds of thousands of years.

Table 5-3 Time for conversion of montmorillonite to hydrous mica in bentonite grouts.

K^+ concentration in the groundwater (ppm)	D_e (m^2/s)	Conversion time* (years)
5	10^{-10}	500
5	10^{-8}	5
10	10^{-10}	25
10	10^{-8}	0.3

* Based on a maximum clay thickness of 10 mm. Clay at ρ_c = 0.16 Mg/m^3.

With $10^{-12} < D_e < 10^{-11}$ m^2/s and thicknesses of 250 mm or more the diffusion model predicts the time for conversion in HCB layers to be tens of thousands to millions of years. This is consistent with the observations made from the studies into the natural deposits which had clay dry densities of about 1.4 Mg/m^3 or more.

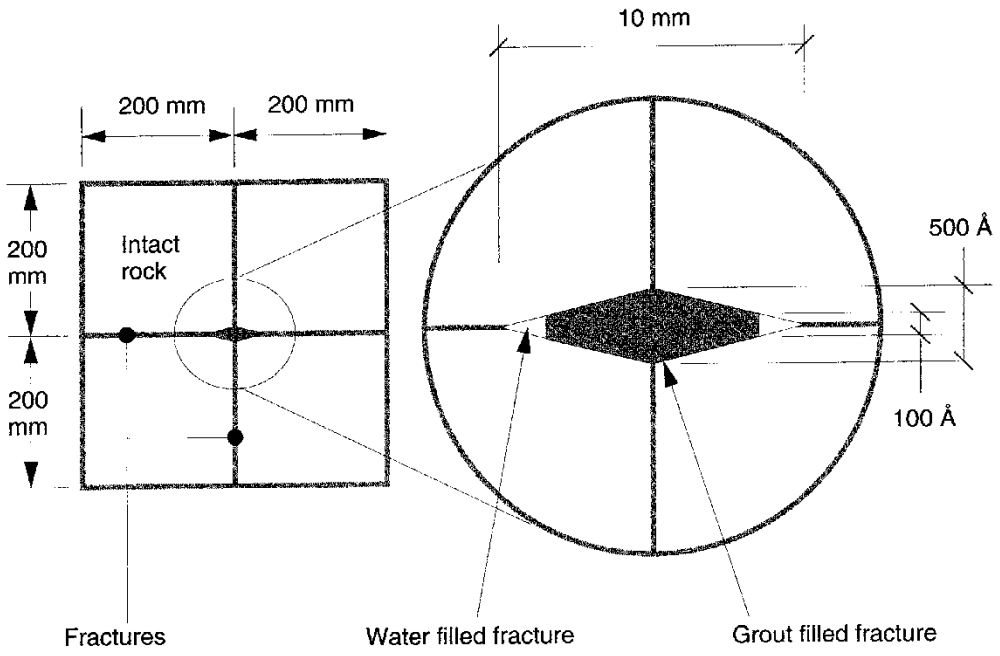

Figure 5-10 A unit of fractured rock with a channel of rhomboidal cross section that is partly filled with grout.

The effects of conversion on the sealing properties of the clay grout were estimated by reconsidering the results from the *in situ* and laboratory experiments. It was observed that clay grouts can penetrate and fill fractures as narrow as 10 μm. Based on the model for the fracture geometry in the Stripa granite established during the grouting experiments and described in Chapter 4 of this report, water flow was assumed to occur in a series of regular channels of rhomboidal cross section with the dimensions and spacing shown in Figure 5-10. Effects of filling these channels within practical limits with bentonite

grout and allowing for the complete conversion of the montmorillonite in the grout to hydrous mica were calculated (Pusch et al, 1991b). Results showed that with all apertures greater than 10 μm filled with bentonite grout the hydraulic conductivity of the grouted rock could be as low as about 10^{-11} m/s. With conversion to hydrous mica the hydraulic conductivity of the grouted rock increased to about 10^{-10} m/s. Using the same model, the hydraulic conductivity of the ungrouted rock was calculated to be about 10^{-8} m/s. Thus, after complete conversion of the montmorillonite to hydrous mica, the hydraulic conductivity of the grouted rock mass was calculated to remain about two orders of magnitude less than that of the ungrouted rock. It is important to recall that it has not yet been proven to be possible, either through the experiments in the Stripa mine (Pusch et al, 1991a; Börgesson et al, 1991; Börgesson et al, 1992b) or elsewhere (Gray and Keil, 1989), to reduce by grouting the hydraulic conductivity of fractured granite to values below about 10^{-10} m/s. Regardless of this fact, the calculations show that some benefits of grouting may be retained after conversion of the montmorillonite to hydrous mica.

It was noted in section 4.2.2 that it could not be concluded that admixing silica in the form of fine quartz powder improved the resistance of bentonite clay grout to piping. The strength and hydraulic conductivity tests on hydrothermally treated materials showed little benefit from adding the powder and there was some indication that at temperatures higher than about 130°C strength was decreased and the rate of silicification of the clay may have been enhanced. The apparent lack of benefit to the sealing properties of grouts and possible acceleration of the metamorphic processes at the higher temperatures led to the conclusion (Pusch et al, 1991b) that bentonite clay grouts should be as rich in clay minerals as possible and should not be diluted with quartzitic materials. Thus, the perceived advantages of higher swelling potential in the undiluted clay is not compromised. It is added here that where adding quartzitic materials offers engineering advantages, such as the incorporation of sand in the backfills examined in the BMT, and temperatures do not reach values above 120 to 130°C, there are no indications from the Stripa studies against the incorporation of these materials in bentonite-based repository seals.

5.3 CEMENT-BASED SEALING MATERIALS

Portland cements and cement-based concretes are used extensively in engineering practice. Accordingly, the open literature contains a wealth of information regarding the engineering properties of the materials, including durability. For the purposes of the Stripa studies, durability was distinguished from longevity and was defined as the resistance of a cement matrix to deleterious actions arising from internal, external, physical, chemical and physicochemical forces (Onofrei et al, 1991b). Unlike longevity, durability parameters can be measured and materials must possess properties that lie within specified measurable limits. Typically, the gross changes that occur in the strengths and volumes of materials as they are subjected to cycles of changing physical and chemical forces are measured. The durability properties and, by implication, the longevity of the materials depend explicitly

on their microstructure and physical properties. Generally, it has been concluded that increasing density and decreasing permeability decrease

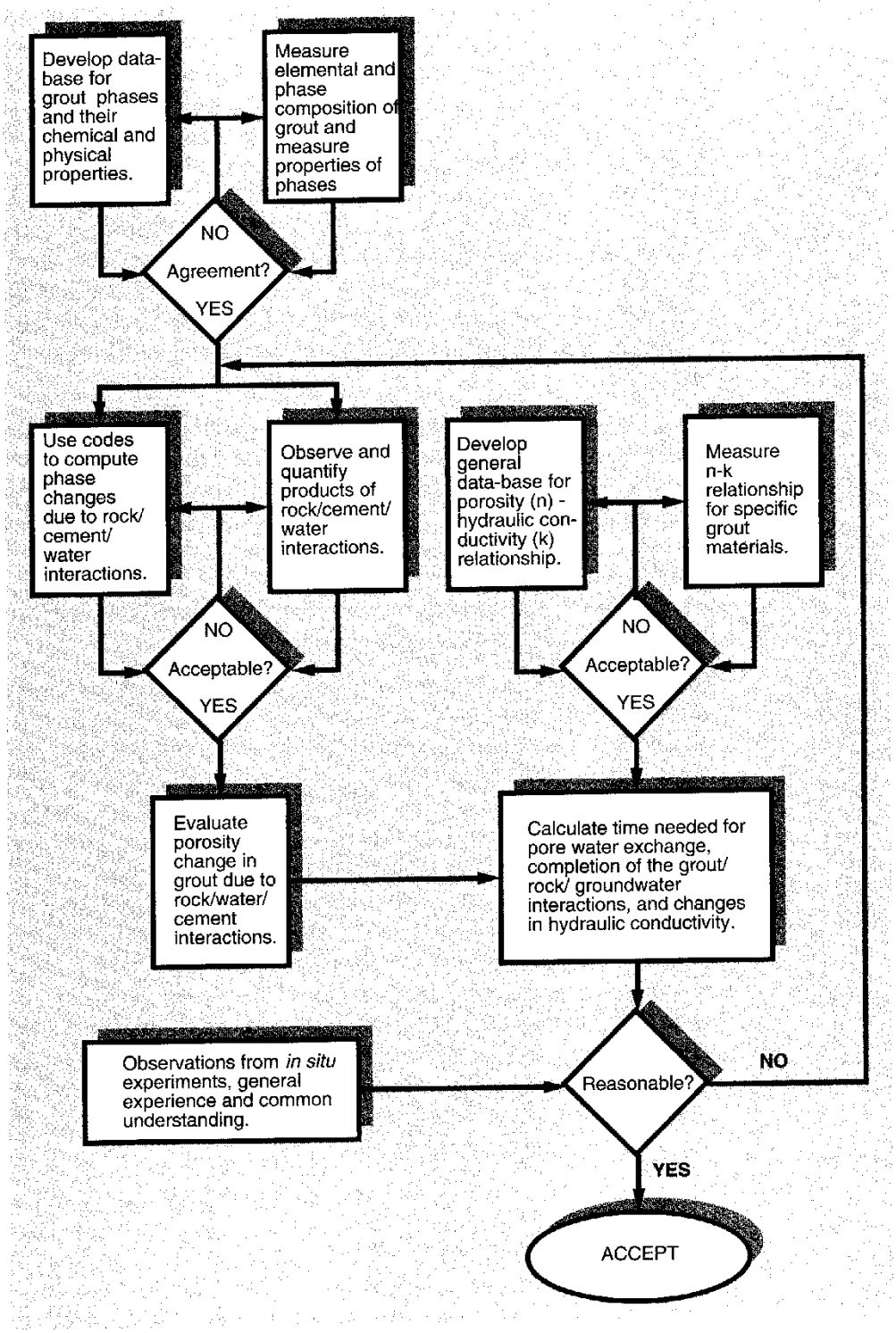

Figure 5-11 Flow diagram for the studies into the longevity of cement-based grouts.

the vulnerability of cement-based materials to environmental, particularly chemical, attack (Mehta, 1990). Understanding and craftsmanship in the application of the materials are seen to be as significant as constitution in

determining the microstructure and, hence, durability of cement-based materials (Neville, 1987). The high-performance cement-based grouts and advanced grouting technologies developed through the Stripa investigations have not been extensively used in engineering practice and it was not possible to evaluate the effects of craftsmanship. Thus, studies of longevity were limited to laboratory based investigations of material properties, behaviour and microstructure and appraisals of the effects of environmental factors and time on these properties. The latter was accomplished with the aid of specifically developed models of grout longevity that were founded on current understanding of the fundamental thermodynamic properties of the constituents of cement. The hydraulic conductivity was seen as the property of significance for grouts. Hence, the thermodynamic models were coupled with numerical models that replicated available information on the porosity (n)-hydraulic conductivity (k) relationships of hardened cements and concretes. The general, iterative scheme followed for the combined modelling and laboratory studies into cement grout longevity is shown in Figure 5-11.

To apply and develop thermodynamic models it was necessary to list the solid phases present in grouts and compile a data-base on the fundamental thermodynamic properties (Gibb's free energy of formation, solubility, etc.) of the phases. This was first accomplished through recourse to the literature on conventional cements and concretes. Continuing laboratory measurements made on high-performance grouts through the course of the investigations allowed for this data base to be adjusted and, consequently, led to refinements in understanding.

Preliminary calculations to explore possible chemical interactions between groundwater and grout were made using PHREEQE, which is a geochemical computer code developed by the United States Geological Survey (Alcorn et al , 1992; Parkhurst et al, 1980). Codes collectively known as EQ3NR/EQ6 (Alcorn et al, 1992; Wolery, T.J., 1983; and Wolery, 1984) were used later for broader ranging determinations of the paths that may be followed as grouts react with groundwater. Laboratory tests were also undertaken to provide direct observations on grout/groundwater/clay/rock reactions (Onofrei and Gray, 1988; Onofrei et al, 1990; Onofrei et al, 1991b; Onofrei et al, 1992; Pusch et al, 1988). These experiments provided supporting evidence for the veracity of the computer codes. Moreover, through the laboratory tests, reaction sites were identified, the influence of the reaction products on the reaction rates and physical properties of grout was measured and understanding of the influence of variables, such as clay type, temperature and the concentration of ions in the groundwater, on reaction processes was enhanced.

At the outset of the Phase 3 investigations, the almost impermeable character of hardened high-performance grouts shown in Chapter 4 of this report (from Onofrei et al,1992) was not known. National investigations (Atkinson and Hearne, 1984; Berner, 1987) were proceeding on the assumption that, in a repository setting, cements and concretes will degrade through dissolution of the cementitious solids in groundwater as it passed through the pores in the material. The dissolved solids were assumed to be removed from the sealant with the passage of slugs of groundwater. With some uncertainty, calculations based on these assumptions showed that grouts and concretes may be expected to persist for periods as short as a few hundred years (Atkinson and Hearne, 1984). The relationships between

porosity and hydraulic conductivity used to make these calculations were not agreed. Moreover, relationships established for conventionally used cements and concretes may not apply to high-performance grouts. Thus, through recourse to the literature, studies were undertaken to establish an understanding of porosity-hydraulic conductivity relationships in conventional cements and concretes. More directly, laboratory tests were undertaken to measure the hydraulic conductivity and associated porosity parameters of high-performance grout. Observations were also made on the effects of groundwater/grout interactions on the hydraulic conductivity-porosity relationships.

The results of the investigations into chemical interactions, which provided estimates of the changes with time in the volumes of pore space in grouts, were combined with the relationships between porosity and hydraulic conductivity. Thus, the changes in hydraulic conductivity with time were calculated. To effect this calculation reasonable assumptions on the evolution of the hydrogeological conditions that may be encountered in a repository in a rock mass such as that represented by the Stripa site were required and made. Moreover, assumptions on the initial porosity and condition of the grout were needed. To accommodate uncertainties in the assumptions, bounding deterministic calculations were effected.

The model developments proceeded in parallel with the laboratory investigations and *in situ* studies. Some important findings, such as the very low hydraulic conductivity of the high-performance grout, were not entirely evident until late in the investigations. Iterations in the longevity assessment process were required.

5.3.1 Grout composition

The major fraction of hydrated portland cement consists of an assemblage of hydrated ($H=H_2O$) phases formed from calcium ($C=CaO$), aluminium ($A=Al_2O_3$) and silicon ($S=SiO_2$) oxides. Hydrated phases containing ferric oxide ($F=Fe_2O_3$), magnesium oxide (MgO), sulphates (SO_3^-) and alkali metal oxides (K_2O, Na_2O) are also present in lesser proportions. In some circumstances, the minor constituents can be important to the character of the hydrated product. For example in conventional engineering practice, to limit the formation of the mineral ettringite ($Ca_6Al_{12}(SO_4)_3 \cdot 26H_2O$), the quantity of C_3A in the unhydrated cement is controlled to produce sulphate resisting portland cement (SRPC). During manufacture, the aluminate is incorportated with ferric oxide to form tetra-calcium alumino-ferrite (C_4AF).

The dominant phase in hydrated cements is CSH. This is a semi- or crypto-crystalline material that is sometimes referred to as tobermorite gel and is formed by the hydration of C_2S and C_3S compounds found in unhydrated cement products. The hydration reactions are exothermic and as a by-product yield CH, which in crystalline form is termed portlandite and is found in hydrated cements and concretes. Pozzolanas (see footnote 12) are often added to limit the quantities of portlandite, which is the most soluble product of the hydration reactions, and enhance the durability properties of grouts and concretes. Silica fume, which is a by-product of the ferro-silicon industry and consists of finely divided amorphous silica, was admixed as the pozzolana with SRPC to form the reference high-performance grout that was a focus for the Stripa investigations. In ideal circumstances the silica

fume would consume all CH present in the hydrated product to form more CSH. Moreover, the durability properties of the grout would be enhanced by the absence of formation of the swelling and physically disruptive ettringite.

The oxide compositions of the SRPC and the silica fume used in the Stripa studies are given in Table 5-4. Data for Alofix are included.

Table 5-4 Oxide compositions of the cements and pozzolanas studied at Stripa (after Onofrei et al, 1992).

Oxide	SRPC, % by mass	Alofix, % by mass	Silica fume, % by mass
SiO_2	21.6	30.0	94.0
Al_2O_3	3.1	12.2	0.8
TiO_2	0.2	0.6	N.D.
P_2O_5	0.1	0.2	N.D.
Fe_2O_3	4.0	1.3	0.3
CaO	61.4	47.2	0.3
SrO	0.0	0.1	N.D.
MgO	4.4	5.4	0.4
Na_2O	0.4	0.2	0.2
K_2O	0.5	0.4	0.8
SO_3	2.1	3.0	N.D.
Loss on ignition	1.3	0.5	2.8
Totals	100.7	99.9	100.0

Bogue (1955) provided relationships that allow for the computation of the complex oxide phases present in unhydrated portland cement. The chemical composition of the SRPC shown in Table 5-4 generally conforms to the international specifications for this material and can be ascribed the following Bogue oxide compositon by mass percentage: $40 \leq \%C_3S \leq 50$, $25 \leq \%C_2S \leq 35$, $0 \leq \%C_3A \leq 4$, and $10 \leq \%C_4AF \leq 20$. The Alofix , which is a blast furnace slag cement, differs from the SRPC by having higher silica and alumina contents: calcium and ferric oxide contents are lower. The MgO contents of both the SRPC and the Alofix exceed standard limits. The MgO is mostly derived from gypsum that is added mainly to control the setting time of the cement. The particle sizes of both the SRPC and the Alofix were finer than those found in conventional cements. Increased rates of reaction associated with the high specific surface areas of the cements were controlled by increasing the gypsum content of both cements above normally specified values.

Stoichiometrically, at $W/CM \geq \sim 0.3$, sufficient water exists in cement-water mixtures to satisfy the hydration reactions. The grouts used in the Stripa tests were mixed at *W/CM*'s of 0.4 or higher. Modern concretes and cements are placed at similar *W/CM*'s. The extra water was required to fluidify the grouts and is generally supposed to adversely affect durability by increasing porosity. Despite the presence of excess water, Onofrei et al (1992) note that examinations of the microstructures of both contemporary and historic cements and concretes typically reveal the presence of unhydrated materials. The fraction of unhydrated materials present is not clear but is considered to change with time. With the continuing deposition of new hydration prod-

ucts and changes in the morphology of the hydrated materials, the microstructure of cement pastes can be envisaged as dynamic and passing through a series of successive sets as the pastes age. In this context, conventional wisdom suggests that the tobermorite gel becomes increasingly crystalline with time. However, examination of the microstructures of the binding materials in ancient concretes and mortars has revealed amorphous and sub-crystalline silicate phases that appear to have changed little in periods as long as 3000 years (Roy and Langton, 1983; Steadman, 1989). The spacial arrangement of elements in the structure of tobermorite gel is not clearly defined. According to Onofrei et al (1992) alternative views include the Powers-Brunauer model, which considers that the CSH is ordered and layered with a specific surface area of about 180 m^2/g and a porosity of about 28%, and the Feldman-Sereda model, in which the CSH is visualized as being randomly arranged in layered particles with interlayer spaces of 5 to 25 Å.

The geochemical codes used to compute phase changes in cement require specific information on the thermodynamic properties of the phases being considered. It was not possible, either through recourse to the literature or by measurement during the course of the Stripa studies, to obtain the information for tobermorite gel. Similarly, data for other amorphous and cryptocrystalline phases present in cement paste were not nor are presently available. Thus, to apply the codes it was necessary to simplify the initial phase composition of grout to a series of reasonably well characterized crystalline phases for which the necessary thermodynamic data had been measured, could be inferred or attributed from expert judgement. The uncertainty caused by using the relatively simple thermodynamic data base for modelling is considered by Alcorn and Christian-Frear (1992) to introduce a maximum error in estimate of the performance life of grout of about +/- 5x. The effects of using the simplified composition of the grout cannot be quantified. Alcorn and Christian Frear (1992) note that the modelling results indicate that the service life of the multiphase grouts could be less than that of single phase tobermorite grout since the solubility of tobermorite is less than that those of the other phases in the multiphase grout. The modelled grouts were assumed to be composed of the hydrated phases shown in Table 5-5. The lack of unhydrated material was justified since, in the long term, it can be reasonably assumed that grouts will fully hydrate. The values of parameters determining the rate processes affecting the completion of the hydration reaction remain to be evaluated.

Table 5-5 Normative compositions of grouts that were modelled using the geochemical codes.

	Phase composition, mol %			
Grout phase	1 phase	3 phases	5 phases	6 phases
Tobermorite	100.0	91.7	77.7	71.6
Hydrogarnet	-	5.6	13.3	12.5
Ettringite	-	2.8	1.7	1.6
Fe-hydrogarnet	-	-	6.4	6.1
Fe-ettringite	-	-	0.9	0.9
Portlandite	-	-	-	7.3

Table 5-5 shows the four normative initial grout compositions that were modelled using the geochemical codes. To scope the exercise and test assumptions regarding the methodology being adopted to assess longevity a material comprised totally of crystalline tobermorite was reacted with groundwater using the PHREEQE code. Subsequently, reactions between groundwater, rock and grouts of increasingly complex phase composition were modelled using EQ3NR/EQ6. Increasing complexity in grout composition became possible as the data base on phases increased and as understanding of the complexities of the microstructure of high-performance grout was enhanced. The differences between the 5 and 6-phase-model grouts shown in Table 5-5 provide a notable example of the effects of laboratory measurements on the modelling process. The 6-phase-model includes portlandite (CH) which is absent from the 5-phase-grout. Initially, portlandite was omitted from the grout on the assumption that the silica fume in high-performance grout reacted with CH to produce CSH, which was reflected in increased fractions of tobermorite in the grout. However, examinations of the microstructure of the SRPC/10% silica fume mixtures revealed the presence of both unreacted silica fume and portlandite in the hardened pastes. The presence of excess silica in the grout was not sufficient to ensure consumption of all the CH evolved during cement hydration. Indirect evidence from leaching tests (Onofrei et al, 1991a) indicated that higher *W/CM* than the ones used in the high-performance grouts tested at Stripa may be needed to ensure completion of a number of reactions including that between CH and silica fume. Presumably increased porosity allows connections between the sites at which the reaction elements are located. This can be taken to confirm that microstructure and porosity influence grout/groundwater/rock interactions and may be as significant as phase composition to the durability characteristics of the grout.

5.3.2 Grout/groundwater/rock reactions

Details of the experiments carried out to measure reactions between grout, groundwater and rock are provided by Onofrei and Gray (1988), Onofrei et al (1991b), and Onofrei et al (1992). Briefly, specially prepared block specimens of grout that had been hardened for periods of up to 90 days prior to testing were reacted (leached) separately with known volumes of distilled deionized water (DDW) and two saline[18] waters. Coded WN-1 and SCSSS, the saline waters had TDS contents of 11 750 mg/l and 50 445 mg/l, respectively. The chloride content of SCSSS was about 5.5 time higher than that of WN-1. Calcium was the principal cation in SCSSS. Sodium and calcium were present in almost equal concentrations in WN-1. The cement, water and, in some cases, clay slurries were reacted at constant temperatures of 10, 25, 50, 85, 100 and 150°C for periods of up to 56 days. As many as six duplicate specimens were tested. Changes in the ionic concentrations in and the pH of the solutions were measured. Moreover, exposed and fractured surfaces of the reacted grout and the morphology of unreacted specimens were inspected using scanning electron microscopy (SEM) coupled with energy dispersive X-ray (EDAX) analyses and X-ray diffraction (XRD) techniques. Specimens that had been vacuum dried at 50°C were studied.

---

[18] The following classification based on total dissolved solids (TDS) is applied to waters: brines - TDS≥ 100 000 mg/l, saline - 10 000 mg/l ≤ TDS <100 000 mg/l, brackish - 1 000 mg/l≤ TDS < 10 000 mg/l, and fresh - TDS < 1 000 mg/l.

The pore size distributions in leached and unreacted specimens that had been vacuum dried were measured using mercury intrusion porosimetry (MIP).

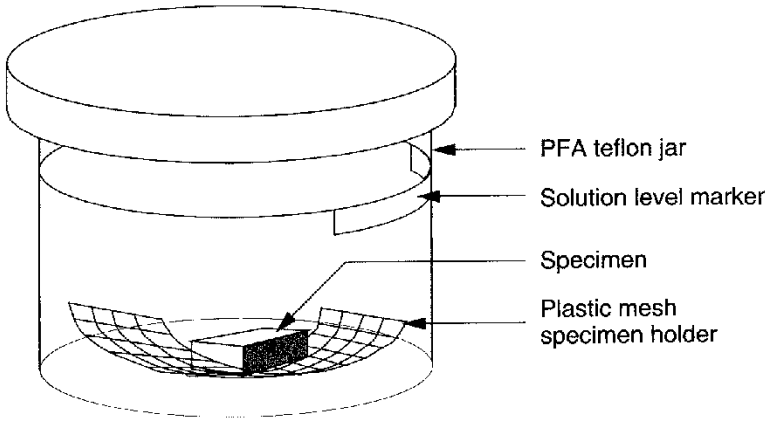

Figure 5-12 Arrangement of the static leaching test cells.

Cells configured as shown in Figure 5-12 were used to carry out static and pulsed leaching tests at temperatures up to 85°C. Static leaching tests were carried out by immersing the cell, assembled as illustrated, in a water bath maintained at the desired temperature and gently rocking the cell and its contents for the desired period. The contents of the cell were then analysed as previously described. The procedures used for the pulsed leach tests were the same as those for the static leach tests except that aliquots of the leachant were removed at specified times after the reaction was started. The volume of the fluid was maintained constant by replacing the removed volume of leachant with fresh solution or, in the cases when clays were present, with fresh slurry (the mass of clay in the slurry equalled the mass of the cement specimen). In both test types the ratio of the gross surface area of the specimen to the volume of leachant was kept constant at a value of 0.1 cm^{-1}.

Static and pulsed leach tests at temperatures of 100°C and above were carried out in titanium autoclaves equipped as shown in Figure 5-13. The external connections to the autoclaves permitted preconditioning of the temperature, pressure and chemical properties (gas content, Eh and pH) of the leachant. The system shown in Figure 5-13 was also used for dynamic leaching experiments in which DDW, WN-1 or SCSSS was passed through the cell and by cement specimens at controlled flow rates. Two test series were carried out with flow rates of 12 and 240 ml/d. At these flow rates the leachant volume in the cells would be exchanged in about 40 and 2 days, respectively.

Leach rates for Ca^{2+} and Si^{4+} in the static and dynamic leach tests were calculated using the expression given in Equation 5-2:

$$\text{Leach rate} = [X]\ (1/t)\ (V/SA) \qquad (5\text{-}2),$$

where [X] is the excess concentration of the element in solution at time t, V is the volume of the leachant and SA is the initial gross surface area of the specimen. In the dynamic leaching tests, V is the volume of leachant in the cell plus the product of flow rate and time. In contrast, cumulative release rates were calculated from the pulsed leach tests. The methodology is given by Onofrei et al (1991b). Cumulative release rates and leach rates cannot be

directly compared and discussion here is generally restricted to the results from the static and dynamic tests which formed the bulk of the work. Important findings of the pulsed flow tests are noted.

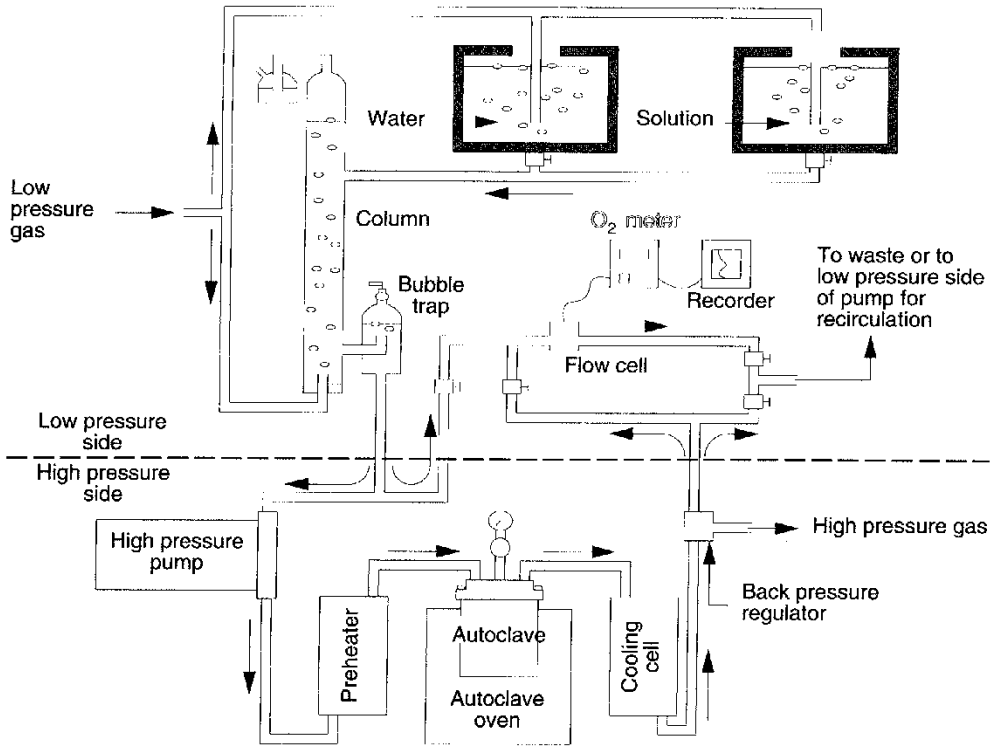

Figure 5-13 Arrangement of the dynamic leaching testing system.

The rates at which Ca^{2+} and Si^{4+} were leached by DDW in static tests on mixtures of 90% SRPC and 10% silica fume (the reference grout) at *W/CM* = 0.4 and 0.6 and from Alofix at *W/CM* = 0.7 are shown in Figure 5-14. The effects of temperature and time on the leach rates are shown. At both values of *W/CM*, Ca^{2+} was leached from the reference grout at rates that were between 30 to 80 times higher than those of Si^{4+} at the same temperature. After the same leaching time, the leach rates for Ca^{2+} steadily increased as temperature was increased from 10 to 150°C. In respect to the leach rates of Si^{4+} the effects of increasing temperature were much less consistent. Leach rates of Si^{4+} were less at 10°C and 150°C than at 50°C. Similar trends were exhibited by the leach rates from the Alofix cement. However, the Ca^{2+} and Si^{4+} leach rates from the Alofix were marginally lower and higher, respectively, than those from the reference grout. Increasing *W/CM* in the reference grout from 0.4 to 0.6 increased the leach rate of Ca^{2+}. However, the effects were slight and any other effects were not measurable.

In general the data in Figure 5-14 show virtually instantaneous release of both Ca^{2+} and Si^{4+}. Only at 10°C was the initial rate of release of Si^{4+} from all three of the grouts retarded. With slopes of between about -0.6 and -0.75, the virtually linear relationships in the log (leach rate)-log (time) coordinates used in figure 5-14 indicate continuing release of both Ca^{2+} and Si^{4+} with time from all the grouts studied. However, the rates are less than

those that would be predicted by a simple diffusion mechanism. This was attributed by Onofrei et al (1992) to an increase in the concentrations of elements in the leachants and, possibly and more importantly, to changes in the microstructure of the cement and the formation of surface layers that inhibited the release of elements to solution. Analyses of the surfaces of reacted cement specimens confirmed that a compound layer consisting of portlandite and calcite had formed. The observations indicated that the reaction layers tended to become increasingly dense with reaction time and that calcite tended to become more predominant at higher temperatures.

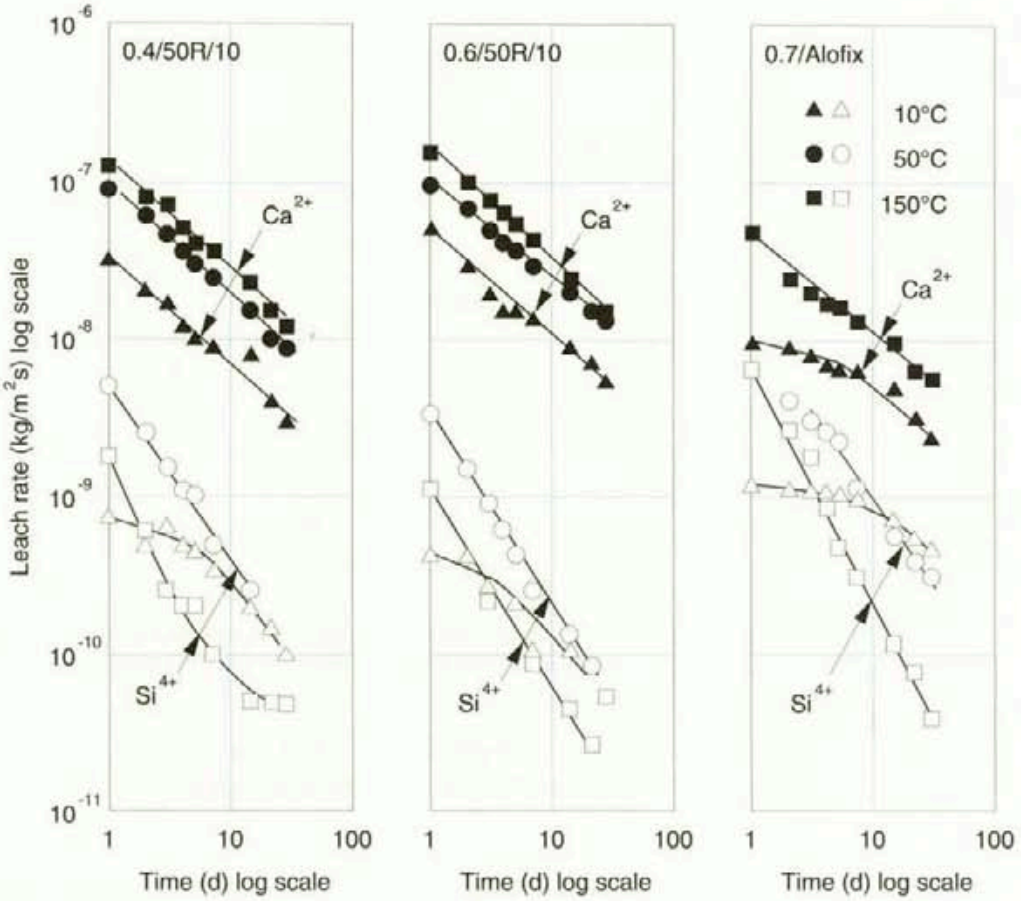

Figure 5-14 The effects of temperature and time on the rates at which calcium and silicon were leached in static tests on the reference grout at *W/CM*s of 0.4 and 0.6 and on Alofix at *W/CM* = 0.7 (after Onofrei et al, 1992).

The increase in the quantity of Ca^{2+} dissolved in the water with temperature is consistent with conventional wisdom. Moreover, the higher rates of release of Ca^{2+} than of Si^{4+} are consistent with the commonly observed incongruent[19] dissolution processes that occur during cement leaching. However, the concentrations of Ca^{2+} in solution were significantly less than the value of 0.02 mol/l observed by Atkinson and Hearne (1984) for water in equilibrium with CH and CSH. This is considered by Onofrei et al (1992) to provide further evidence of the limiting effects of the surface layers on the dissolution processes. The source of the Ca^{2+} that was incorpo-

19 During incongruent dissolution of a complex mixture of phases more than one phase is dissolving and the releases of elements to solution are not simply chemically equivalent to their concentratiorn in the solid phases.

rated in the surface reaction layers may have been the CH already present in the hydrated grout or the product of reaction between the leachant and any accessible unhydrated cement phases. In this latter respect the neoformation of CSH and CH in the grouts was identified by the SEM and associated studies of the leached specimens (Onofrei et al, 1992).

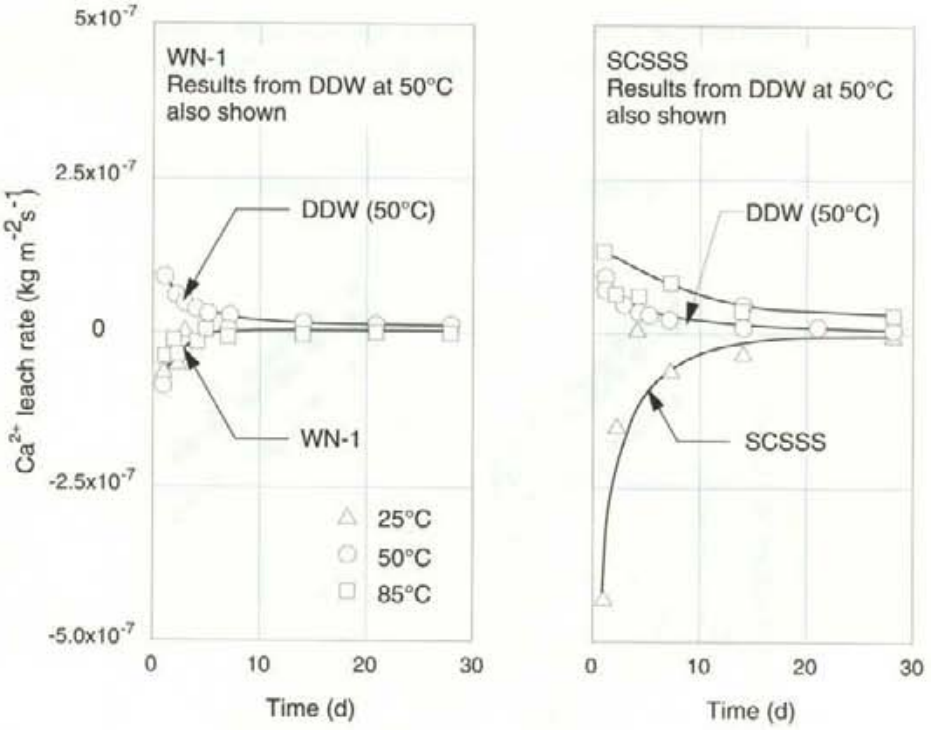

Figure 5-15 The effects of temperature, time and water composition on the rates at which calcium was leached from the reference grout at *W/CM* =0.4.

The effects of temperature, time and leachant composition on the leach rates for Ca^{2+} in static leach tests are shown in Figure 5-15. Where in some circumstances the leach rates were similar to those observed in DDW, in other circumstances negative leach rates were observed. Ca^{2+} was lost from solution. It is noteworthy that WN-1 and SCSSS are synthetic groundwaters that are considered to represent those encountered at repository depths in the Canadian Shield and other granite formations. Depending on conditions, the waters may be supersaturated with respect to the minerals calcite, portlandite, gypsum, brucite, sepiolite and hydrous mica (Goodwin and Munday, 1983). Examinations of the surfaces of the leached specimens and precipitates found in the reaction vessels showed that the temperature and pH changes had caused the depostion of brucite, portlandite and calcite. The brucite was found, mainly, on the surfaces of the specimens. The calcite and portlandite were found, mainly, as precipitates on the base of the vessel. In common with the calcite and portlandite layers found on the specimens leached in DDW, the density of the brucite layer was found to increase directly with leaching time. Accordingly, the tendency for the leach rate of Ca^{2+} to approach zero with time was linked to the presence of the reaction layer on the cement surfaces.

The crystalline morphology of the brucite formed on the surface of the reference grout at *W/CM* = 0.4 leached in WN-1 at 85°C is shown in the scanning electron micrograph presented in Figure 5-16. Perhaps of equal

significance, the micrograph, which is a representation of a cross-section through the surface layer down into the body of the grout, shows the extremely dense nature of the reference grout. The Alofix displayed similar morphology. Crystalline structures, if present, were not visible, even at the high magnifications used, in the unaltered body of the grouts. Moreover, larger pores were separated by the dense matrix.

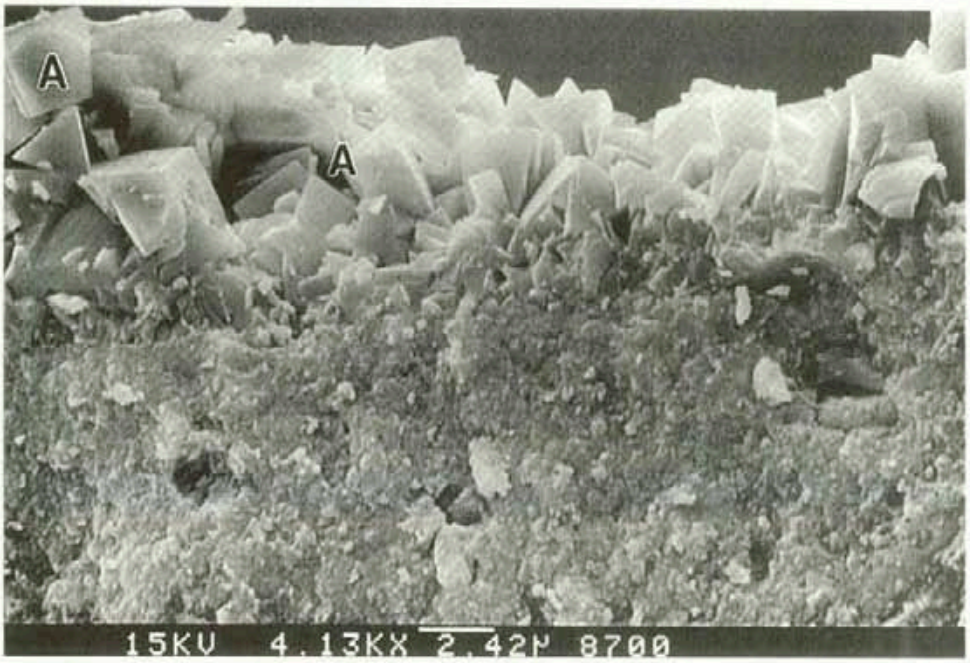

Figure 5-16 The structure of the reaction layers on the surfaces of the reference grout at *W/CM* = 0.4 leached in WN-1 at 85°C . A = brucite ($Mg(OH)_2$).

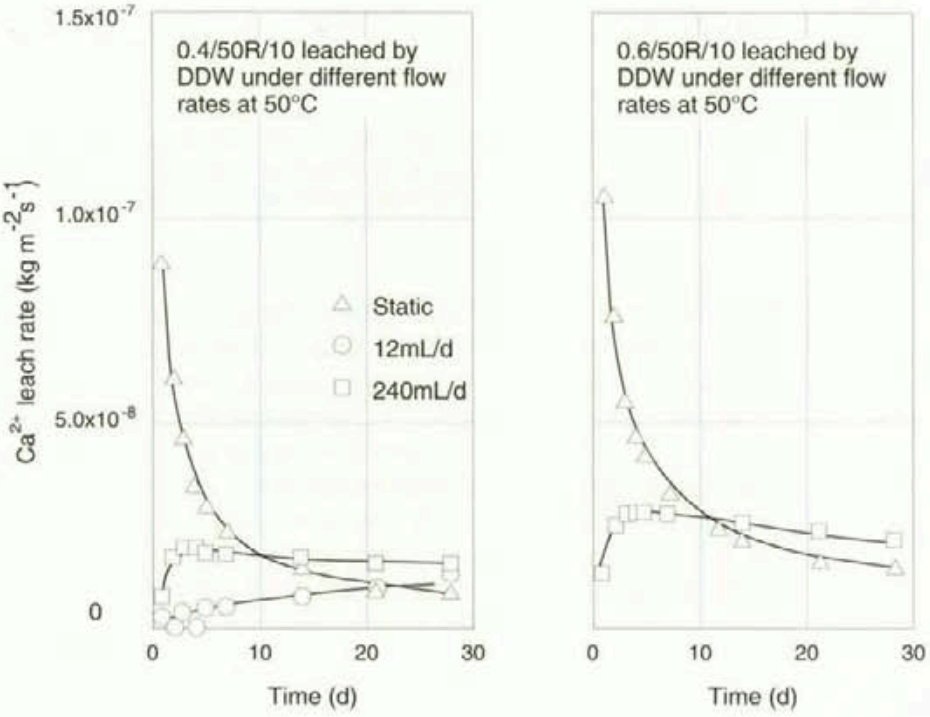

Figure 5-17 The effects of *W/CM* and flow conditions on the rates at which calcium was leached from the reference grout in tests at 50°C (after Onofrei et al, 1992)

In common with the results from the static leaching tests, after leaching, the surfaces of specimens examined in the dynamic leaching tests were coated with reaction layers. With DDW as the leachant at low temperatures, calcite was the main surface deposit. At higher temperatures and dynamically leached with saline groundwaters, the surface deposits varied with the cement type and *W/CM* . Brucite, ettringite and CSH phases with various Ca/Si ratios were observed both intermixed and as discrete layers. Independent of the character of the reaction layer, as shown in Figure 5-17, the leach rates for Ca^{2+} were almost independent of the leachant flow rate and were similar to those observed in the static leach tests.

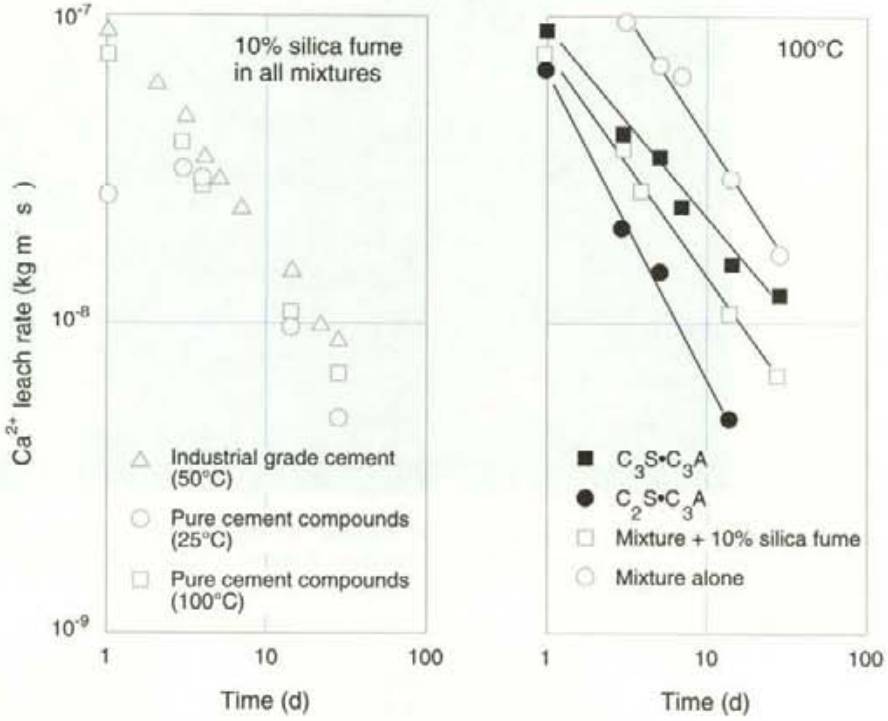

Figure 5-18 The rates at which calcium was leached into DDW during static tests on various hardened mixtures of primary cement compounds with and without silica fume. The leach rates from industrial grade materials are also shown (after Onofrei et al, 1992).

It was noted in Table 5-4 that industrial grade cements contain small quantities of impurities, which include alkali metal compounds, sulphates and phosphates. To determine the influence of these on the leaching properties of cements four of the main compounds in unhydrated portland cement (C_2S, C_3S, C_4AF and C_3A) were obtained in pure form from the American Concrete Institute. These compounds were mixed in various proportions and hydrated at *W/CM* = 0.35. In some cases, 10% silica fume was added. The hydrated products were subjected to static leaching tests similar to those conducted on the industrial grade products. The results of these studies are shown in Figure 5-18. The results from the tests carried out on the 90% SRPC, 10% silica fume mixture that was hydrated at *W/CM* = 0.4 are included for the purposes of comparison.

The results in Figure 5-18(a) show that the impurities did not significantly influence the leach rate of Ca^{2+}. The pure cement compounds were mixed in the mean proportions in which they are found in SRPC. The data shown

in Figure 4-18(b) show that admixing 10% silica fume decreased the Ca^{2+} leach rate by about one-half of an order of magnitude. Moreover, the C_3S•C_3A mixture released Ca^{2+} at faster rates than the equivalent C_2S•C_3A mixture. These data generally confirm the assumption that admixing silica fume should enhance the durability properties of cement based grouts. Moreover, it is commonly understood that C_3S hydrates more rapidly than C_2S (Neville, 1981). The higher release rates from the C_3S•C_3A than from the C_2S•C_3A mixture could reflect a higher degree of hydration and, hence, higher quantities of CH in the C_3S mixture. Alternatively, unhydrated C_3S would react more rapidly with the leachant than C_2S. The former explanation is considered here to be more likely and may indicate mechanisms through which the durability of cement-based grouts may be further enhanced.

Table 5-6 The solid reactants used and the predictions made by EQ6 of the solid products formed by reacting a total of 1000 ml of grout, granite and fracture minerals with 1000 ml of saline groundwater.

	Starting quantity in 1000 ml of solids Moles	Quantity of solids lost Moles	Volume of solids lost ml
Tobermorite	2.409	0.002	0.76
Hydrogarnet	0.421	0.176	26.45
Ettringite	0.052	0.052	37.08
Fe hydrogranet	0.204	0.176	27.50
Fe ettrignite	0.029	0.029	21.27
Portlandite	0.247	0.176	5.81
Quartz	20.100	0.000	0.00
Albite	7.390	0.176	17.60
Anorthite	2.450	0.176	17.70
Microcline	4.190	0.013	1.36
Calcite	1.350	0.000	0.00
Ca montmorillonite	0.140	0.176	30.62
Na montmorillonite	0.140	0.176	30.67
		Total	216.82
Products		**Quantity of solids gained Moles**	**Volume of solids gained ml**
Tobermorite	-	0.122	42.36
Calcite	-	0.062	2.28
Na nontronite	-	0.010	2.02
Quartz	-	1.131	25.67
Mesolite	-	0.314	162.68
Microcline	-	0.175	18.98
Strontianite	-	0.000	0.01
Ca saponite	-	0.002	0.30
Na saponite	-	0.001	0.20
		Total	254.50

The complex, heterogenous morphology and geometrical arrangement of the hydrated and unhydrated cement phases and the grout/groundwater reaction products revealed through the laboratory studies could not be numerically modelled. Moreover, because the laboratory and modelling studies proceeded in parallel, much of the information that became available on grout-groundwater-rock reactions through the laboratory studies was not available until late in the investigations. However, in terms of repository

design life the periods over which the laboratory experiments were carried out were very short and the modelling activities provide further insight into the anticipated longer term reactions and their consequences to repository seal performance.

The most complex system that was investigated using the computer codes EQ3NR/EQ6 was a mixture of the six phase grout, detailed in Table 5-5, with materials found in granite rock, including minerals present as infills on fracture surfaces, and, a saline groundwater. The solid phases had the initial molar composition shown in Table 5-6. The water had a TDS of 20 214 mg/l and, with a Ca^{2+} concentration of 4 540 mg/l, had a Ca^{2+}:Na^{+} ratio of 1.66.

The computer codes can be considered as reaction vessels in which the reactions were carried out by adding the solid constituents to the solution. Reflecting real systems, both the relative quantities and the order in which solid phases were added to the solution had consequences to the reaction products. Experience with the application of the codes and the consequences of sequencing was gained by the addition of equimolar proportions of the solid reactants in different order to 1000 ml of solution. The experience gained through this procedure was finally applied to reactions referred to as "relative rate basis titrations" by Alcorn et al (1992) through which the products of reaction detailed in Table 5-6 were identified. The reaction was considered to be completed when either all of the added solid phases were dissolved or equilibrium conditions in solution were attained. The details of the final calculations and the database used for their conduct are not reported and, if required, need to be obtained from the principal investigator. Hence, it is only possible to summarize the reported findings of the calculations and make appropriate inferences.

The most significant finding shown in Table 5-6 is that after reaction the volume of solids present in the system is predicted to exceed the initial volume. The original minerals (reactants) present decrease in volume by 216.82 ml and the reaction products occupy a volume of 254.50 ml. This is the smallest of the solid volume increases that were consistently shown by a series of different relative rate basis titrations. The principal reasons for the increase in volume are the formation of mesolite (zeolite), tobermorite, quartz and microcline. The quantities of the hydrogarnet and ettringite phases that were originally present in the grout were depleted along with all the smectite minerals present as fracture infill. In this latter respect, the results show that more smectite was lost than that which was originally present in the system. This reflects the imprecision of the code and the associated database. Moreover, when undertaking calculations as complex as those using the geochemical codes used for these studies, it is often necessary to make compromises that allow for the development of understanding. Based on the predicted increases in solid volumes it was concluded (Alcorn et al, 1992) that under low hydraulic gradients fractures filled with cement grout will progressively tighten due to reaction and alteration. It is specifically noted that the albite, anorthite and microcline components present in the granite also participated in the reaction. This was taken to suggest that the interface between the grout and the rock will interact chemically. These interactions may further enhance the sealing effects of the grout.

The calcite observed on the leached laboratory specimens was also found as a reaction product in the EQ3NR/EQ6 calculations. However, gypsum was not included as a reactant and the brucite observed in the leaching tests is not identified as a reaction product in Table 5-6. This may be a specific case in which apparently minor cement components have significant influence on the grout/groundwater/rock reactions. In this regard it is reported (Alcorn et al, 1992) that gypsum was revealed as a reaction product in the equimolar titrations.

5.3.3 Hydraulic conductivity/porosity relationships

With reasonably realistic assumptions for the hydraulic and temperature conditions that will exist in a repository, the modelling activities predicted that grout-groundwater interactions will result in decreases in grout porosity and concomitant decreases in hydraulic conductivity. This was verified in laboratory experiments. The following discussion focusses on the porosity and hydraulic conductivity of cement-based grouts and their relationship.

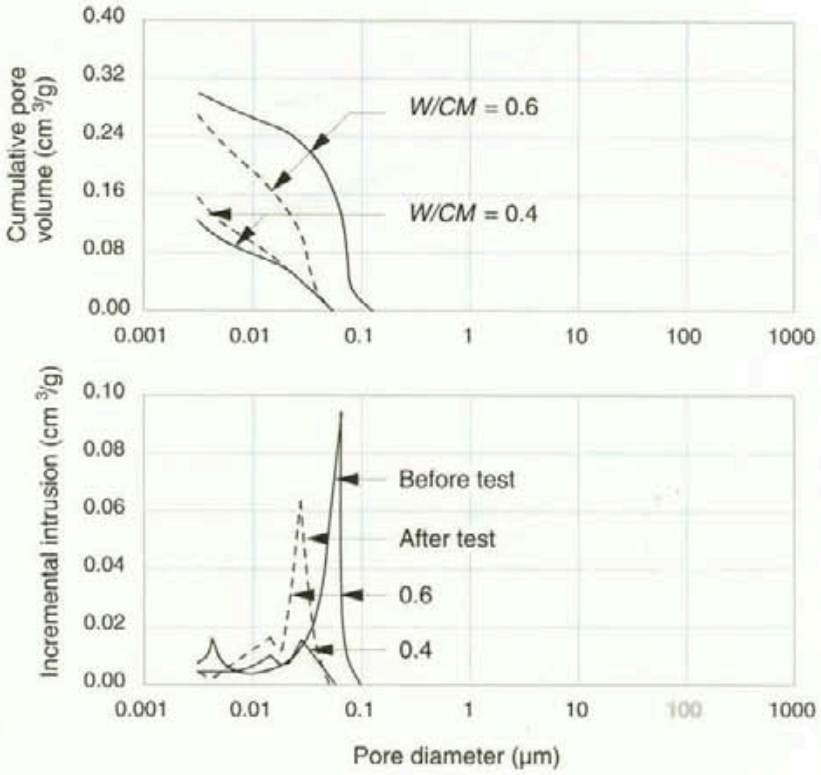

Figure 5-19 Pore size distributions in the reference grout at *W/CM* = 0.4 and 0.6 determined before and after the hydraulic conductivity tests.

A review of the literature on cements and concretes (Alcorn et al, 1992) led to the general relationship between hydraulic conductivity, k, and total porosity, n, given in Equation 5-3.

$$\Delta k = k_i \bullet 10^{7.39\Delta n} - k_i \qquad (5\text{-}3),$$

where k_i is the hydraulic conductivity of the grout at t = 0.

The value adopted for k_i was 10^{-12} m/s (Alcorn et al, 1992). It was shown in Chapter 4 (after Onofrei et al, 1992) that the hydraulic conductivities of bulk and thin film specimens of the reference cement-based grouts were less than 10^{-14} m/s. The higher assumed value was predicated on the assumption that $k \sim 10^{-12}$ m/s is a value that is commonly observed for concretes. Moreover, the higher value allows for uncertainties in the emplaced condition of the grout and is conservative insofar as calculations based on the higher value will give shorter times for longevity estimates.

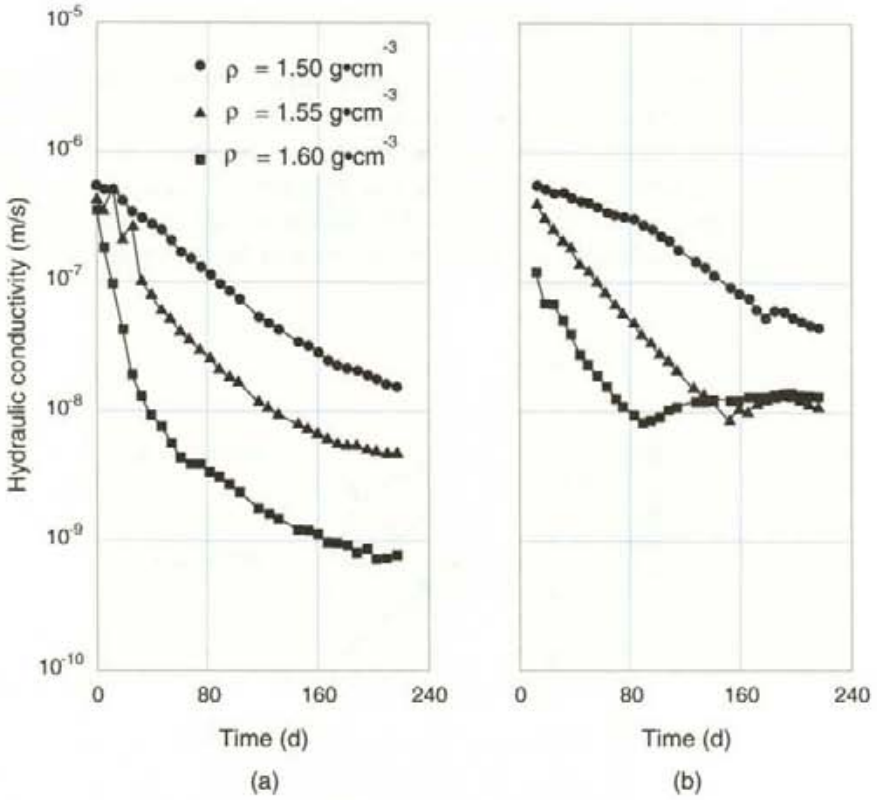

Figure 5-20 Changes in the hydraulic conductivity with time of recompacted granulated reference grouts made from (a) 50% 1.18 mm and 50% 0.3 mm fractions, and (b) 50% 2.36 and 50% 1.18 mm fractions.

The reasons for the very low hydraulic conductivities of the reference grouts were investigated through a series of laboratory tests and attempts were made to determine the k-n relationship for the reference grouts.

Figure 5-19 shows the results of MIP analyses on specimens of the bulk grout which had been tested in the radial flow hydraulic conductivity cells shown in Figure 4-14. The total intruded porosity and the pore size distributions measured in grouts with *W/CM* = 0.4 and 0.6 before and after the hydraulic conductivity tests are shown. The data show that increasing *W/CM* from 0.4 to 0.6 increased the intruded total porosity in the unpermeated grout from about 0.12 ml/g to about 0.3 ml/g. With time and increasing permeation of water through the specimens in the hydraulic conductivity tests, the total porosity and the pore size distributions were altered. Particularly, larger pores in the grout at *W/CM* = 0.6 were blocked. The data in Figure 5-19 show that the pores in the reference grout at *W/CM* of both 0.4 and 0.6 had diameters less than 0.1 mm. This tends to confirm

the observation by Mehta (1986) that pores with a diameter less than 0.1 mm do not contribute to the dynamic porosity of hardened cement pastes. Most of the flow through concrete takes place in pores larger than 0.1 µm. To explore the importance of larger sized pores to the hydraulic conductivity of grouts, two separate test series were carried out (Onofrei et al, 1992). In the first series, reference grouts at *W/CM* = 0.4 that had been hardened under water for 19 months were granulated. The granulated material was separated into size fractions which were recombined as required and compacted to known densities. The hydraulic conductivities of the compacted materials and the pore size distributions in the materials, before and after the hydraulic conductivity tests were carried out, were measured. In a second series of tests, the reference grout was prepared at high *W/CM* values of between 0.9 and 1.2. Special procedures were adopted to prevent settlement and bleeding of the high *W/CM* grouts during setting. The pore size distributions in the hardened high *W/CM* grouts were determined before and after hydraulic conductivities were measured.

The data from the hydraulic conductivity tests on the granulated grouts that are presented in Figure 5-20 show that at the start of the tests the materials had hydraulic conductivities between 10^{-7} and 10^{-6} m/s. Within this small range, hydraulic conductivity tended to decrease with increasing density. The results also show that hydraulic conductivity tended to decrease with increasing testing time. Hydraulic conductivity decreased by as much as two orders of magnitude after water had permeated the grout for 230 days. The decreases tended to be more pronounced in the denser systems. The hydraulic conductivities of the grouts made at high *W/CM* were about 4 orders of magnitude less than those of the granulated material and were in the range $2 \cdot 10^{-11} < k < 6 \cdot 10^{-11}$ m/s. In common with the results from the granulated grouts, k tended to decrease with increased density (decreased *W/CM*) and with increased testing time.

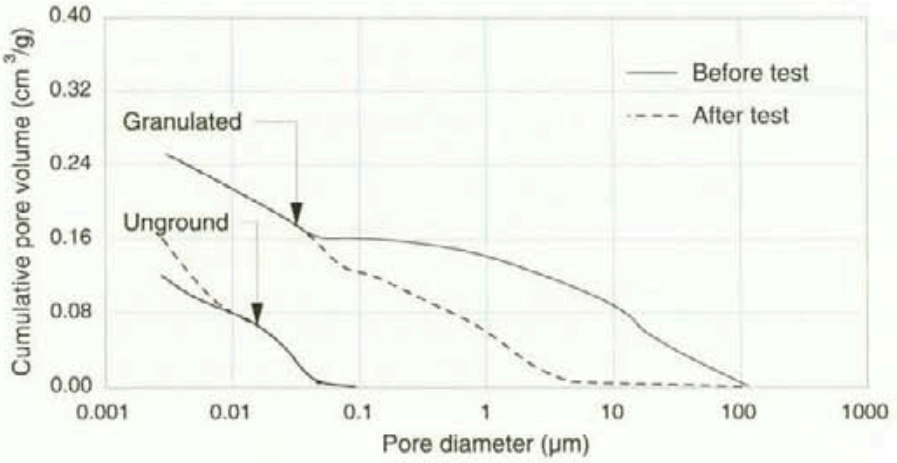

Figure 5-21 A comparison between the pore size distributions in the granulated grouts with those in the intact material at *W/CM* = 0.4 as determined before and after the hydraulic conductivity tests.

The total intruded porosity of the granulated grouts at a density of 1.6 Mg/m^3 was about 0.25 ml/g. Approximately 60 per cent of the porosity consisted of pores with diameters larger the 0.1 µm. Despite having lower

hydraulic conductivities than the granulated grouts, the total intruded porosity of the grouts mixed at high *W/CM* were higher. In the high *W/CM* mixtures, porosity values increased with *W/CM* from 0.59 ml/g at *W/CM* = 0.9 to 0.85 ml/g at *W/CM* = 1.2. The volumes of pores with diameters greater than 0.1 μm were similar to those in the granulated grout. Values ranged from about 0.1 ml/g to 0.24 ml/g. These data showed that there was no correlation between hydraulic conductivity and either the total porosity or the fraction of the volume with pore diameters greater than 0.1 μm. The fact that the grouts were not fully hydrated within the period of the tests may provide some explanation for the lack of correlation. However, the causes remains uncertain, and, with the available information, it can only be noted that neither the k-n relationship established for normal cements and concretes nor the significance of separating the pore volumes into fractions with diameters above and below 0.1 μm could be qualified for the reference grouts.

The decreases in hydraulic conductivity with time in the tests on both the granulated grouts and those with high *W/CM* were tentatively attributed to the deposition of reaction products in the pores. This was confirmed both by MIP test results and through examination of the microstructure of the permeated grouts. The results of MIP analyses on the granulated grout and the bulk grout before and after permeation are shown in Figure 5-21. The parallelism between the curves at pore sizes less than 0.1 mm indicates that the microstructure of the granules was virtually unchanged from that of the bulk material. The curves for the granulated grout show that during permeation the major quantities of the solid reaction products were deposited in the larger pores. These data, supported by the results from the cone-in-cone tests described in Chapter 4 and the results of the investigations into grout/rock groundwater reactions, confirm that if they are disrupted cementitious materials show a propensity to self-seal.

5.3.4 Expected performance

The laboratory tests showed that the hydraulic conductivities of high-performance cement grouts both in bulk and as thin films were significantly less than those of conventional hardened cement pastes, mortars and concretes. Laboratory and modelling studies of grout/groundwater/granite reactions showed that, in all likelihood, after reaction the volume of the solid phases present would exceed the solid volume present before the reaction and there would be a tendency for the hydraulic conductivity of the grouted system to decrease. Moreover, tests on both thin grout films and bulk mechanically disrupted grout specimens showed that the fractured materials have a propensity to self-seal. The leaching studies indicated that this ability arose from the formation of reaction products on the grout surfaces that were exposed to reaction with groundwater and that the reaction products may play a significant role in controlling the rates of the grout/groundwater reactions. All these data indicated that with good workmanship cement-based grouts and concretes may be expected to persist for long periods in repository settings such as that exemplified by the Stripa mine. The *in situ* tests coupled with the results of piping tests on unset grouts indicated that

during grouting operations care has to be taken to avoid exposing the fresh grout to excessively high hydraulic gradients.

To quantify the periods through which cement-based grouts may persist and function effectively in repository settings, coupled, iterative, deterministic calculations were made using EQ3NR/EQ6 and the k-n relationship given in Equation 5-3. In contrast with the evidence from the laboratory studies and from the thermodynamic modelling activities, for the purposes of the calculations, losses in solid mass were allowed and the resulting changes in hydraulic conductivity with time were calculated. Two major cases were studied. These were termed by Alcorn et al (1992) as the "open" and "equilibrium" systems. For the open system it was assumed that all the reaction products were swept away from the grout by flowing pore water. For the equilibrium system, 75% of the reaction products were assumed to precipitate in the pores of the grout. In common with the assumption that k_i for the grout is 10^{-12} m/s and the use of Equation 5-3, the assumption that reaction products are removed from the reaction sites is considered to add conservatisms to the estimates of durability. Significant increase in the hydraulic conductivity of the grout was taken as the durability criterion.

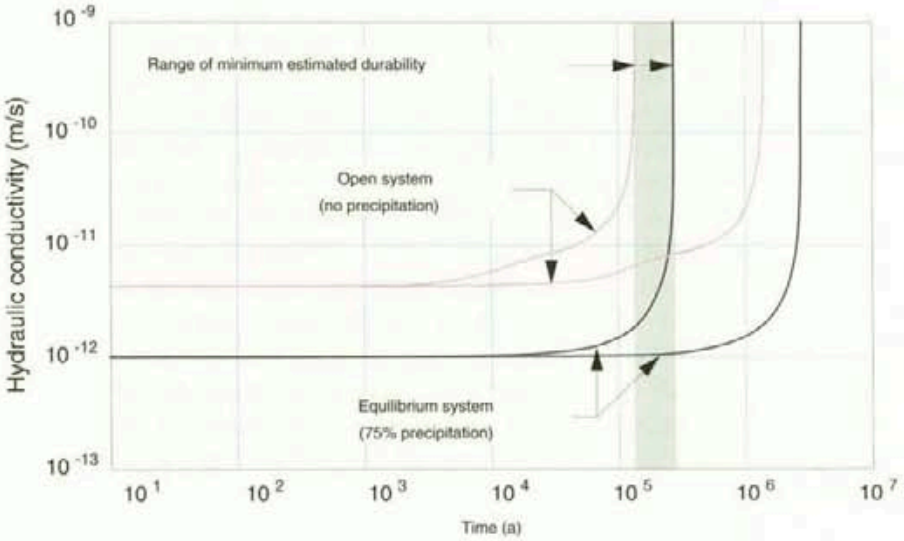

Figure 5-22 Calculated changes in hydraulic conductivity with time of the six-phase -grout in the presence of saline groundwater.

Both the hydraulic conductivities of porous media and the hydraulic gradients to which they are subjected affect the water flow velocity and thereby the rate at which pore water volumes are exchanged. After a repository in saturated granite is closed and sealed, some time will be required for the water table to become stable. During this period it is possible that seals will be subjected to higher hydraulic gradients than the low value of 0.01 suggested for the period after stability has been achieved (Chan, 1987). There are no verified estimates for the period during which the water table will rise and gradients at the repository depth will fall. For the purposes of the calculations it was assumed that the period would be about 100 years and that gradients of 1000 would act on the seals. Thereafter, it was assumed that the

gradients would adopt a value of 1. The high values assumed for the gradients were considered to result in an underestimate of the time needed for pore water exchange in the sealing materials and introduce conservatism to the predictions of performance life.

Series of calculations using the four different grout models listed in Table 5-5 were completed. Bounding calculations were made in an attempt to appraise the effects of the significant uncertainties that exist in the data base on the thermodynamic properties and a lack of crystallinity of the cement phases (Alcorn et al, 1992). The results shown in Figure 5-22 for both open and equilibrium system calculations in which the six-phase-grout was reacted with saline groundwater indicate that the grout may be able to resist significant changes in hydraulic conductivity for periods exceeding 100 000 years. The rapid increase in hydraulic conductivity at long times was caused by the loss of tobermorite from the grout. Discontinuities in the curves indicate loss of other grout phases. Use of the six-phase-model resulted in shorter periods of satisfactory performance than those predicted when the other models were used. This reflected the smaller fractions of tobermorite in the initial composition of the hydrated six-phase-grout model.

Examination of specimens of cement grout films recovered from the *in situ* experiments showed that Alofix grout in fractures with apertures wider than 30 to 50 μm was dense and homogeneous (Pusch, 1992). Narrower regions of the grouted fractures were filled down to 10 μm with more porous materials with heterogeneous microstructure. It was suggested that some of the materials filling the finer regions of fractures may have been precipitates resulting from grout/groundwater/rock reactions rather than injected grout materials. In both stagnant and flowing water, the islands of homogeneous material were projected to persist for the periods of hundreds of thousands of years predicted by the laboratory and modelling studies. It can be inferred that homogeneous mass concretes may be expected to possess similar longevity. In stagnant conditions, the more porous materials may also persist for very long periods. In flowing groundwater, the longevity of the more porous materials may be significantly decreased by erosional forces. Periods of a few hundred years were suggested (Pusch, 1992). Thus, it is concluded here that the results of the Stripa Project indicate that cement-based sealing materials can be used to seal a repository for heat-generating radioactive waste in granite. The available data indicate that with good workmanship and in zones of rock where groundwater flow is sluggish, cement-based seals with low hydraulic conductivity can be expected to persist for hundreds of thousands of years. To limit the bounds of speculation and, thereby, enhance confidence in the conclusion it would be necessary to further investigate the thermodynamic properties of phases present in cement, to measure the effects of elevated temperature on critical parameters such as hydraulic conductivity and porosity and to incorporate the complexities of progressively developing microstructure in the longevity models. Further *in situ* investigations may be necessary to confirm the suitability of the methodologies for grout injection developed for the Stripa Project in different geological circumstances and with different grouting patterns and procedures.

5.4 SUPERPLASTICIZERS

Superplasticizers are essential components of high-performance cement-based grouts and concretes. A number of different types of superplasticizer are commercially available. All types are synthetic organic molecules of large molecular weight which, when added to cement-water mixtures, tend to decrease the viscosity of the system. This renders the use of mixtures with low *W/CM* practical. Through modifications in the microstructure the benefits to the properties of the materials described in previous sections are accrued.

Concerns exist with the presence of organic materials in repositories for heat-generating radioactive waste. They provide sustenance for microorganisms and, either through kelation with specific radionuclides or through the formation of radionuclide-bearing colloids, may enhance the rates at which radionuclides migrate in groundwater. A review of literature and series of laboratory tests were undertaken to evaluate mechanisms by which the superplasticizer used in the Stripa studies may effect such changes in repository systems.

Two possible mechanisms by which the superplasticizer may enter the groundwater and be dispersed through a repository site were studied. First, bleed waters carrying the superplasticizer from the unset grouts may be injected into groundwater during grouting operations. Second, grout/groundwater reactions may result in dissolution of the superplasticizer from the hardened grout.

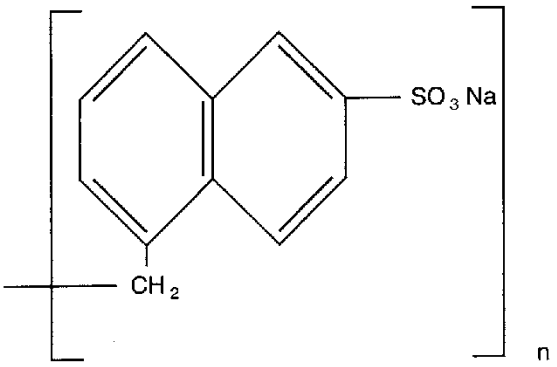

Figure 5-23 The unit cell of the sodium salt of sulphonated naphthalene formaldehyde which in condensed form (n~ 10) is the superplasticizer used in the Stripa studies.

The low value of *W/CM* and the lack of bleeding of the reference grout generally assures that the first mechanism of superplasticizer dispersal should be of little, if any, consequence. Moreover, studies of the mechanisms by which superplasticizers fluidify cement pastes suggested that the organic materials are sorbed on the surfaces of the hydrating solids (Aïtcin et al, 1989). Tests in which the superplasticizer contents in pore water that was extruded under very high pressures from reference grouts confirmed that 60 to 90 per cent of the superplasticizer added to the grout was fixed to the

solid shortly after the grouts were mixed (Onofrei et al, 1991a). Insofar as the proportions of superplasticizer sorbed tended to increase with *W/CM*, the grouts that were more likely to bleed had lesser possibility to release superplasticizer.

The microstructures generated in the period during which the grouts were fluid were studied using "humid cells" in the 3 MV electron microscope of the Laboratoire d'Optique Electronique du C.N.R.S., France. In addition to clarifying the processes by which superplasticizer delays setting in the reference grout, these studies indicated that any superplasticizer that was not sorbed on the solid surfaces was incorporated in the fluids held in the finer pores of the cement pastes (Pusch and Fredrikson, 1990). Further evidence supporting this suggestion was sought. Moreover, the solid phases where superplasticizer was sorbed were identified through a series of tests using superplasticizer that had been tagged with radioactive sulphur.

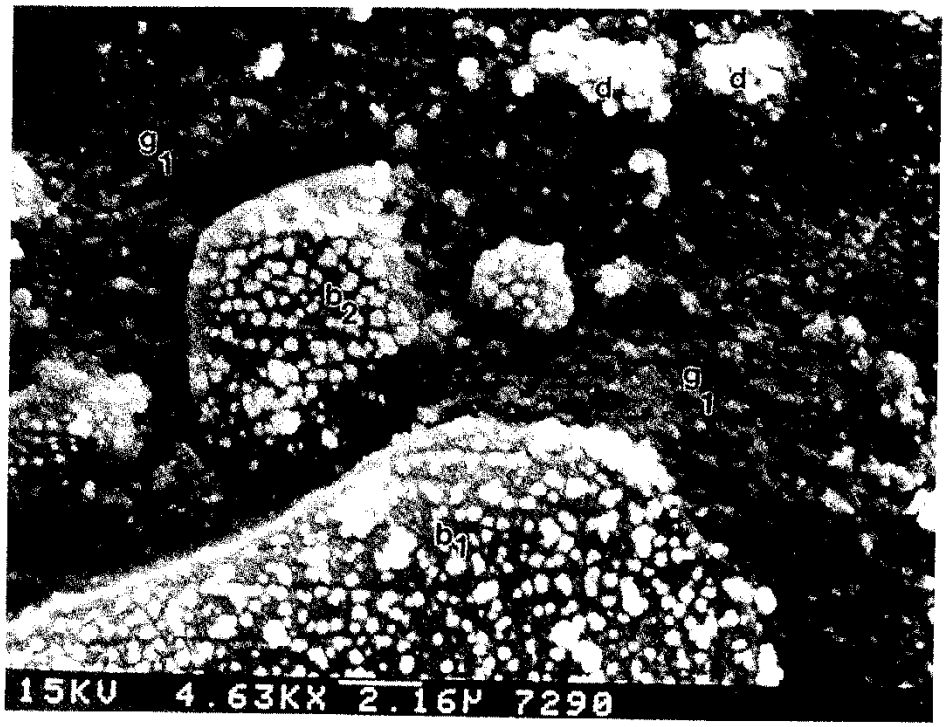

Figure 5-24 Electron micrograph of polished surfaces of reference grout at *W/CM* = 0.2 with 10% silica fume and incorporating 3% of ^{35}S-labelled superplasticizer. The bright spots indicate the locations of ^{35}S.

The superplasticizer studied in the Stripa Project was a condensed sodium salt of sulphonated naphthalene formaldehyde. The molecular arrangement of the unit cell that when polymerized (n ~ 10) forms the superplasticizer is shown in Figure 5-23. Sulphuric acid containing ^{35}S, a beta ray emitter, was used in the manufacture of a special batch of superplasticizer (Onofrei et al, 1991a). As much as 3% of the labelled superplasticizer was incorporated in reference grout mixtures with and without silica fume and at *W/CM* = 0.2 and 0.4. After hardening and curing, specimens of the grout were subjected to pulsed leaching tests as described in section 5.3.2 and the leached

concentrations of ^{35}S in the waters were determined by calibrated liquid scintillation counting. Three waters, DDW, WN-1 and SCSSS, were used to leach the grouts. Moreover, fractured surfaces of the grouts containing the labelled superplasticizer were examined for the presence of ^{35}S. This was achieved by coating the fractured surfaces with high resolution silver emulsions, exposing the emulsions to the emissions from ^{35}S and developing the film *in situ*. The developed surfaces were examined by SEM. Coupling the SEM observations with EDAX analyses led to identification of the cement phases in which ^{35}S resided.

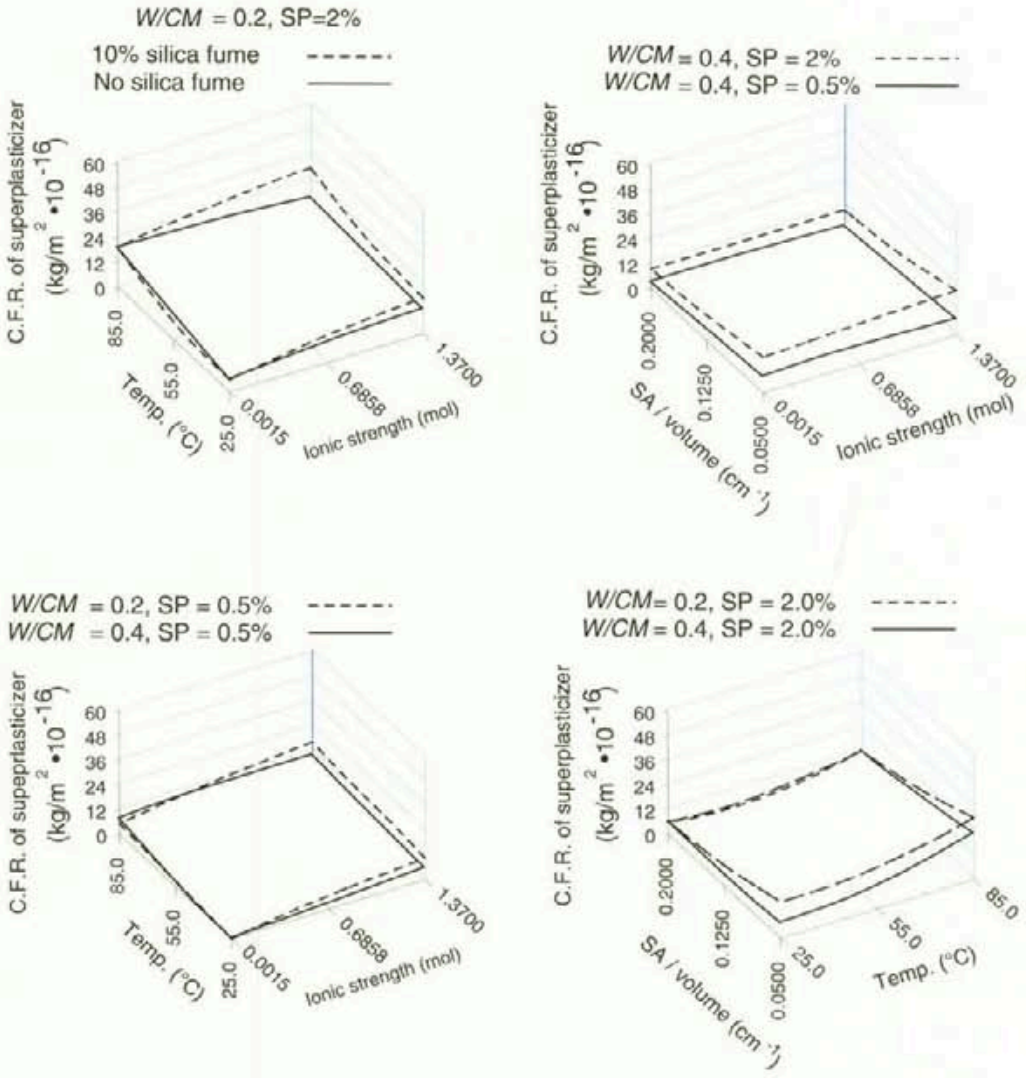

Figure 5-25 Results from the pulsed leaching tests showing the release of superplasticizer (SP) from SRPC cement-based grout under different environmental conditions. Except where indicated all mixtures contained 10% silica fume.

A typical result from the SEM studies is shown in Figure 5-24. The ^{35}S was not evenly distributed through the grout. EDAX analyses showed that the ^{35}S was located primarily in CSH and CAH phases. More specifically, the CSH phases were recognized as being rich in calcium and were considered to be the products of hydration of the C_3S phase in the unhydrated cement.

The ^{35}S was not found in silicon rich areas which were considered to be unreacted or partly reacted silica fume. The C_3S and C_3A phases in unhydrated cement are known to hydrate more rapidly than others present and the data supported suggestions, arising from the observed delays in setting time caused by adding superplasticizers to cement pastes, that superplasticizers fluidify fresh grouts by initially interfering with the hydration reactions. The principal mechanism by which the superplasticizers are incorporated with the CSH and CAH phases was suggested to be by association with the hydrating water molecules (Onofrei et al, 1991a).

The effects of grout composition, temperature, groundwater composition and grout surface area to leachant volume on the release of superplasticizer to solution are shown in Figure 5-25. The releases are expressed as cumulative fraction release (CFR). The CFR's for the superplasticizer are in the order of 10^{-16} to 10^{-15} kg/m^2. For the purposes of comparison, the CFR's of Ca^{2+} observed in pulsed leach tests were in the order of 10^{-7} kg/m^2. The small releases of superplasticizer tended to increase with increasing silica fume content, increasing temperature, increasing solid surface area to leachant volume ratio and increasing ionic strength of the leachant. The effects of changing *W/CM* varied with the test conditions. In some circumstances increasing *W/CM* decreased the quantity of superplasticizer released to solution. The reverse was also observed. Over the ranges tested, which were chosen to encompass expected repository conditions, the compound effects of all the variables was to change the small release rates by less than one to two orders of magnitude and the release patterns of the superplasticizer did not follow those of either Ca^{2+} or Si^{4+}. Thus it was generally concluded that the releases were mostly derived from the smaller pores that contained unreacted superplasticizer and were exposed to the leachant. Successive exposure of these pores to the groundwaters and dissolution of the CSH and CAH phases in which superplasticizers was incorporated may increase the releases to solution. The possibility that the products of reaction between grout/groundwater and rock identified through the Stripa studies may incorporate or otherwise limit the quantities of superplasticizer released to the groundwater was not explored.

The results show that the use of superplasticizers will increase the total organic load in groundwaters that pass through a repository for heat-generating radioactive waste. The total increases are likely to be significantly less than the quantities of superplasticizers used in the construction of seals. It is not possible to determine the significance of the effects of the increased organic load. These can only be estimated when realistic assessments of the quantities of naturally occurring organic matter and that introduced during repository construction and development are available. In view of the leaching data, the understanding developed of the microstructure and the virtually impermeable character of high-performance cements and concretes, it is concluded here that it appears possible and likely that the benefits in material properties and performance gained through the use of superplasticizers would outweigh any adverse effects of increased organic load.

6 COMMENTARY & CONCLUSIONS

The engineered barriers studies of the International Stripa Project have examined and resolved a range of scientific and technical issues related to the geological disposal of heat-generating radioactive wastes. Details can be found in the technical reports by the principal investigators. Findings that bear directly on repository system design and performance assessment are re-stated here with some discussion. General conclusions are drawn. Where appropriate, the conclusions accommodate the findings of the studies of the natural barriers as well as those of the engineered barriers and in some cases are also based on experiences gained in other underground laboratories and in national programmes.

Practical aspects of the in-floor borehole emplacement methodology were demonstrated, selected materials and methods for plugging investigation boreholes, tunnels and shafts were tested, and, grouting technologies for sealing the fractured rock that is accessible from repository excavations, including the excavation disturbed zone, were advanced and applied.

The properties of highly compacted bentonite (HCB) and the interactions between this material and granitic rock under a range of thermal and moisture regimes and in a number of geometrical arrangements were studied *in situ* and at scales approaching those that will be encountered in a repository for heat-generating radioactive waste. Although previously used in geotechnical applications, in view of the highly compacted form, the situations and the large scales in which bentonite was investigated, the Stripa investigations have introduced a novel material and technology for application in repository sealing. The technology has been sufficiently advanced to permit application in engineering projects. The properties of HCB have been measured and understanding of aspects of *in situ* performance has been increased.

The *in situ* tests at the Stripa mine showed that the hydraulic conductivity of drillholes and excavated openings could be returned to values similar to those of intact granite by the judicious use of HCB.

Models are now available to predict the response of HCB to changes in stress, thermal and hydraulic gradients. The models are not rigorously precise. Particularly, related to a lack of clear understanding of the constitutive stress-strain-time behaviour, difficulties remain in the analyses and predictions of the mechanical response of unsaturated highly compacted bentonite to water uptake and changing thermal and hydraulic boundary conditions. In contrast, thermal properties are reasonably well understood and heat fluxes through the material can be described.

The properties of advanced, high-performance bentonite- and cement-based materials pertinent to their successful injection as grouts in fractured rock have been well defined. Equipment and procedures for injection of the grouts have been developed and are available to the member countries for use in repository design and construction. The limits of the application of the selected materials and methodologies were defined for the Stripa granite. In the rock volume that is accessible from the excavations it appears to be possible to cut-off and divert water flows in naturally present fracture zones and moderately fractured rock with hydraulic conductivities as low as 10^{-9} to 10^{-8} m/s. The ability to effect the diversions can be assessed by measuring the hydraulic conductivity of the

rock using water injection procedures similar, but not limited, to those used in the "lugeon" test employed in conventional civil engineering practice.

It appears to be possible to numerically describe the effects of grouting on water flows and groundwater pressures using equivalent porous media models provided that sufficient information on the groundwater flow paths is available at the scale of interest. Data at the level of detail derived for the application and qualification of general groundwater flow models such as those examined in the natural barrier studies of the Stripa project are unlikely to provide sufficient information for grouting activities intended for repository sealing. A large number of boreholes with lengths of tens of metres emanating from the surfaces of excavations will be needed both to investigate the rock to be grouted and to effect the grouting. As at Stripa, the information gained from the grouting activities at repository sites will likely lead to revisions in understanding of the rock mass. This revised understanding can be used in the refinement of hydrogeological models, the detailed design of repositories and the assessment of their performance. Thereby, it is likely that repository safety will be enhanced along with confidence in the applicability of performance assessment calculations. These benefits can be achieved if the observational method and the consequent iterative approach to the design of geotechnical works associated with a repository is accepted by both designers and approving authorities. Management should be clear in its requirement for and intent to integrate the findings of site investigation activities with those of observations made during repository construction.

An excavation disturbed zone (EDZ) consisting of a blast disturbed zone enveloped by a stress disturbed zone was identified in the rock surrounding tunnels in the Stripa granite. In the absence of alternative, preferably repository site specific information, the EDZ of the blast disturbed zone in granitic rocks similar to those at Stripa can be taken to have an hydraulic conductivity of about 10^{-9} to 10^{-8} m/s. At the locations in the Stripa mine studied by the engineered barriers research group, the stress disturbed zone appeared to be more conductive parallel to the axis of the excavations ($3 \cdot 10^{-10} \leq k \leq 9 \cdot 10^{-10}$ m/s) than normal to it ($7.5 \cdot 10^{-12} \leq k \leq 2.3 \cdot 10^{-11}$ m/s). The hydraulic properties of both the stress and blast disturbed zones were variable at the scale of metres and could not be significantly modified by the application of the grouting technologies developed and applied through the project. In the event that excavation disturbed zones prove to be major determinants of the performance of repositories, materials or methodologies other than those examined through the Stripa Project will have to be developed.

Archaeological and geological analogues examined gave no indication that, if used appropriately, the clay- and cement-based sealants would not persist in repository settings. The results of laboratory tests and geochemical modelling coupled with examination of samples of sealing materials recovered from the *in situ* experiments were consistent with this finding. The processing involved with the production of bentonites and cements renders the materials inherently thermodynamically unstable . However, under the low hydraulic gradients expected in the groundwater in a sealed repository site, chemical transformation of the minerals in the sealants can be predicted, reasonably, to extend over tens of thousands to millions of years. The predicted period depends on the porosity of the as-placed materials and the ionic concentrations in the groundwater. Understanding of the materials and models for effecting the longevity calculations have been developed. For bentonite, longevity is primary controlled by the diffusion of K^+ in the clay. The extremely low hydraulic conductivity of

high-performance cement-based materials ($k < 10^{-14}$ m/s) controls their longevity.

The sealing properties of both clay- and cement-based sealants are most susceptible to change under high hydraulic gradients. Thus, both materials will be most vulnerable to adverse change during seal construction and the period over which the repository is open for the deposition of waste. Understanding of the conditions under which the sealants are placed, which can only be developed during repository construction, and careful control of the methodologies used for seal construction or grouting, are needed to ensure adequate seal performance. Consequent to the self sealing abilities of both clay and cement-based materials, mechanical disruption of the sealants after closing the repository can be concluded to be likely to be less than significant to the hydraulic conductivity and persistence of appropriately chosen and placed materials.

A review of the designs being proposed for repositories in granite by countries that were members of the Stripa Project shows that all include the possibility of using bentonite-based clay buffer materials. This may be taken, in part, to reflect the confidence built in the ability to engineer the materials and the common understanding of the performance characteristics of the clays developed through the Stripa project and associated studies.

No tests were undertaken in the Stripa mine to measure the rates at which radionuclides migrate through clay or cement-based sealants. The studies focussed on the ability of the materials to limit water flow rates. Translated to analyses of total system performance the results from the Stripa Project increased confidence that HCB can be used to decrease water flow rates near containers such that radionuclide movement in water staurated clay-barrier materials can be reasonably assumed to be controlled, principally, by fickian diffusion and associated processes. Similarly, the Stripa studies showed that where boreholes and large excavations penetrate the rock, the hydraulic conductivity of the openings can be returned to values equal to or less than those of the rock. Thus, once qualified, the models that describe radionuclide movement through the rock may be assumed to provide a conservative measure of the rate of radionuclide movement through sealed openings. In this regard it is pertinent to note that the natural barrier studies undertaken for the Stripa Project focussed on the development of groundwater flow models and validation processes. In common with the engineered barrier investigations, radionuclide movement in groundwaters under very low hydraulic gradients, and to which radionuclides may be released in a sealed repository in granite, was not measured. Due to the perturbations caused by the presence of excavations it may never be possible to physically examine in underground laboratories, or from excavations at repository sites, the conditions under which radionuclides will migrate within either the engineered barriers or the host rocks that form the waste isolation system.

For the models being used to assess the performance of repository systems *in toto*, it is reasonably assumed that radionuclides can only be released from breached containers after both the engineered and natural barriers become virtually saturated with water. The mechanisms that control the rates at which containers deteriorate and breach depend on the degree of saturation of the materials in which they are embedded. The period through which the changes in the groundwater flow paths and conditions caused by repository excavations condition the repository system remain uncertain. In this respect it was sug-

gested through the natural barrier investigations that some of the properties of the excavation disturbed zone may be explained through processes associated with desaturation. Moreover, it was shown that, in some conditions, heat fluxes in bentonite buffers will cause water to flow away from the container. By delaying the access of water to the waste, the time of onset of radionuclide release may be extended. Increased understanding of these resaturation periods and associated processes would provide for more realistic models for assessing the performance of repositories which include the use of natural and engineered clay-based barrier materials.

The engineered barriers studies of the Stripa Project arrived at different descriptions of the excavation disturbed zone than those concluded from the investigations into natural barriers. This may be related to the different locations and geological conditions at which the zones were studied within the Stripa mine. From this it may be concluded that the EDZ can be expected to be variable between sites and, perhaps more importantly, within a repository. In addition to geological factors, the excavation methods used and time are likely to influence the properties of the EDZ. In light of the demonstrated inability to effectively grout the EDZ at Stripa and in the absence of alternative information, it remains necessary to consider the implications on repository performance of a zone of rock around excavations with higher permeability than the host rock. In common with considerations of the performance of the engineered and natural barriers, the assessments are required to focus on radionuclide movement in the disturbed zone under low hydraulic gradients. The results of such assessments may differ significantly from those of physical and numerical appraisals of water movement under high hydraulic gradients.

The International Stripa Project was undertaken as a combined research programme by organisations intent on the resolution of technical issues connected with the geological disposal of heat-generating radioactive wastes. The scope of work was constrained to common concerns. Moreover, for each of the phases of the project specific objectives were identified. This restricted the periods over which issues could be addressed. During Phase 1 of the project, the behaviour of clay buffers and backfills were examined; during Phase 2, clay seals for boreholes, tunnels and shafts were studied; in Phase 3, grouts were investigated. With these constraints it was not always possible to resolve issues that arose from the studies and were of possible concern to repository performance. Such issues include the following:

- the examination of alternative technologies for the application of sand-bentonite backfills at higher densities than those attained in the BMT;
- the development of more appropriate instrumentation for monitoring the *in situ* performance of bentonite-based backfill and buffer materials;
- the installation of instrumentation to more precisely define groundwater conditions in grouting experiments;
- the investigation of the effects of temperature on the hydraulic conduction properties of cement-based materials;
- the development of an agreed data base on the thermodynamic properties of the phases present in high-performance cementitious materials;
- determination of the rates at which groundwater conditions return to relatively stable conditions after a repository is closed;

- evaluation of the importance of the excavation disturbed zones to repository performance and, if necessary, measurement of the radionuclide transmission properties of these zones under conditions other than those studied at Stripa;
- evaluation of the periods over which sealing materials such as HCB become fully saturated with water; and, more generally,
- a more comprehensive investigation of alternative materials and methods for sealing repositories.

These and other, associated and unresolved issues that have been raised in the body of this text could be considered for resolution in future collaborative studies or national programmes.

REFERENCES

Abelin, H. and Birgersson, L. (1987). 3-D migration experiment - Report 1 - Site preparation and documentation. Stripa Project TR 87-19. SKB, Stockholm, Sweden.

Abelin, H. and Gidlund, J. (1985). Migration in a single fracture - Instrumentation and site description. Stripa Project IR 85-02, SKB, Stockholm, Sweden.

Abelin, H., Neretniks, I., Tunbrant, S. and Moreno, L. (1985). Final report of the migration in a single fracture - Experimental results and evaluation. Stripa Project TR 85-03, SKB, Stockholm, Sweden.

Abelin, H. and Birgersson, L. and Gidlund, J. (1987a). 3-D migration experiment - Report 2 - Instrumentation and tracers. Stripa Project TR 87-20. SKB, Stockholm, Sweden.

Abelin, H. and Birgersson, L., Gidlund, J., Moreno, L., Neretniks, I., Widén, H. and Ågren, T. (1987b). 3-D migration experiment - Report 3 - Performed experiments results and evaluation. Stripa Project TR 87-21, SKB, Stockholm, Sweden.

Abelin, H., Birgesson, L. and Ågren, T. (1990a). The channeling experiment - Instrumentaiton and site preparation. Stripa Project TR 90-12, SKB, Stockholm, Sweden.

Abelin, H., Birgesson, L., Widén, H., Ågren, T., Moreno, L. and Neretniks, I. (1990b). Channeling experiment. Stripa Project TR 90-13, SKB, Stockholm, Sweden.

Aïtcin, P-C., Onofrei, M. and Gray, M.N. (1989). Superplasticizers. AECL Research Technical Record, TR-447, Whiteshell Laboratories, Pinawa, MB, Canada.

Alcorn S.R. and Christian-Frear, T.L. (1992). Geochemical modelling of grout-groundwater-rock interactions at the seal-rock interface. Stripa Project TR 92-17, SKB, Stockholm, Sweden.

Alcorn, S.R., Coons, W.E., Christian-Frear, T.L. and Wallace, M.G. (1991). Theoretical investigations of grout seal longevity. Stripa Project TR 91-24. SKB, Stockholm, Sweden.

Alcorn, S.R., Coons, W.E., Christian-Frear, T.L and Wallace, M.G. (1992). Theoretical investigations of grout seal logevity - final report. Stripa Project TR 92-23, SKB, Stockholm, Sweden.

Al-Manaseer, A.A. and Keil, L.D. (1990). Physical properties of cement-based grout containing silica fume and superplasticizer. Proc. CSCE Annual Conference, Hamilton, Ontario.

Andersson, J. and Dverstorp, B. (1987). 3-D migration experiment - Report 4 - Fracture network modelling of the Stripa 3-D site. Stripa Project TR 87-22. SKB, Stockholm, Sweden.

Andersson, B. and Halén, P.-A. (1978). Mining methods used in the underground tunnels and test rooms at Stripa. Swedish-American cooperative program on radioactive waste storage in mined caverns in crystalline rock. SAC Report 08. SKB, Stockholm, Sweden.

Atkinson, J.H. and Bransby, P.L. (1978). The mechanics of soils: An introduction to critical state soil mechanics. McGraw-Hill, London, UK.

Atkinson, A. and Hearne, J.A. (1984). An assessment of the long-term durability of concrete in radioactive repositories. UK Atomic ENergy Authority Report, AERE-R-11465.

Barton, N ., Makurat, A., Monsen , K., Vik, G. and Tunbridge, L. (1992). Rock mechanics characterization of the distrubed zone phenomena at Stripa. Stripa Project TR 91-12. SKB , Stockholm, Sweden.

Berner, U. (1987). Modelling the incongruent dissolution of hydrated cement minerals. Radiochemica Acta, Proc. Int. Conf. "Migration 87".

Bogue, R.H. (1955). The chemistry of portland cement. Reinhold Publishing Corporation, New York.

Börgesson, L. (1982). Buffer Mass Test - Predictions of the behaviour of the bentonite-based buffer materials. Stripa Project TR 82-08, SKBF/KBS, Stockholm, Sweden.

Börgesson, L. (1985). Water flow and swelling pressure in non-saturated bentonite-based clay barriers. Engineering Geology, 21: 229-237.

Börgesson, L., Pusch, R., Fredrikson, A., Hökmark, H., Karnland, O. and Sandén, T. (1991). Final report of the rock sealing project - Sealing of the near field rock around deposition holes by use of bentonite grouts. Stripa Project TR 91-34. SKB, Stockholm, Sweden.

Börgesson, L., Pusch, R., Fredrikson, A., Hökmark, H., Karnland, O. and Sandén, T. (1992a). Final report of the rock sealing project -Identification of zones disturbed by blasting and stress release. Stripa Project TR 92-08. SKB, Stockholm, Sweden.

Börgesson, L., Pusch, R., Fredrikson, A., Hökmark, H., Karnland, O. and Sandén, T. (1992b). Final report of the rock sealing project - Sealing of zones disturbed by blasting and stress release. Stripa Project TR 92-21. SKB, Stockholm, Sweden.

Brandberg, F. and Skagius, K. (1991). Porosity, sorption and diffusivity data compiled for the SKB 91 study. SKB Technical Report 91-48. SKB, Stockholm, Sweden.

Bresler, E. (1973). Anion exclusion and coupling effects in non steady state transport through unsaturated soils: I Theory. Soil Sci. Soc. America Proc. 37.

British Standards Institute (1975). Methods of testing soils for civil engineering purposes. BS 1377.

Chan, T.C. (1987). An overview of groundwater flow and radionuclide transport modelling in the Canadian Nuclear Fuel Waste Management Program. Proc. of US/DOE Conf. Geostatistical, Sensitivity, and Uncertainty methods for groundwater flow and radionuclide transport modelling. San Francisco.

Chan, T.C. and Stanchell, F. (1990). A numerical study of some effects of nuclear fuel waste vault construction, closure and evolution on convective transport in the geosphere. Proc. of the 1st annual meeting international high-level waste radioactive waste management. American Nuclear Society, Las Vegas, Apr 8-12.

Cheung, S.C.H., Gray, M.N. and Dixon, D.A. (1987). Hydraulic and ionic diffusion properties of bentonite-sand buffer materials. Coupled processes in nuclear waste repositories. Academic Press Inc. Vol 30.

Coons, W.E. (Ed.) (1987). State-of-the-art report on potentially useful materials for sealing nuclear waste repositories. Stripa Project TR 87-12, SKB, Stockholm, Sweden.

Dixon, D.A., Gray, M.N. and Thomas, A.W. (1985). Studies of compaction properties of potential clay-sand buffer mixtures for use in nuclear waste disposal. Engineering Geology 21, 247-255.

Dixon, D.A., Gray, M.N. and Hnatiw, D. (1992a). Critical gradients and pressures in dense swelling clays. Canadian Geotechnical Journal, (in press).

Dixon, D.A., Hnatiw, D.S.J. and Walker, B.T. (1992b). The bentonite industry in North America: suppliers, reserves, processing capacity and products. AECL Report 10587.

Dunnicliff, J. (1988). Geotechnical instrumentation for monitoring field performance. John Wiley and Sons, New York.

Gale, J.E., Witherspoon, P.A., Wilson, C.R. and Rouleau, A. (1983). Hydrogeological characterization of the Stripa site. Proceedings of a workshop on geological disposal of radioactive waste - In situ experiments in granite. Stockholm, Sweden 25-27 October 1992. OECD/NEA. Paris.

Gens, A. and Alonso, E.E. (1992). A framework for the behaviour of unsaturated expansive clays. Canadian Geotechnical Journal 29:6.

Goodwin, B.W. and Munday, M. (1983). A reference guide to SOLMQ - an interactive solution-mineral equilibrium program. AEL-report, AECL-7800, AECL-Research, Whiteshell Laboratories, Pinawa, Canada.

Government of Hong Kong (1979). Geotechnical manual for slopes. Geotechnical Control Office, Public Works Department, Government of Hong Kong.

Graham, J., Saadat, F., Gray, M.N., Dixon, D.A. and Zhang, Q-Y. (1989). Strength and volume change characteristics of sand-bentonite mixtures. Canadian Geotechnical Journal 26. pp. 292-305.

Gray, D.H. (1969). Coupled flow phenomena in clay-water systems. Ph.D dissertation, University of California, Berkeley.

Gray, M.N. and Keil, L.D. (1989). Field trials of superplasticized grout at AECL's underground research laboratory. Third Int. Conf. on super-plasticizers and other additives in concrete. Ottawa, Ontario, Canada.

Gray, M.N., Cheung, S.C.H. and Dixon, D.A. (1985). Swelling pressures of compacted bentonite-sand mixtures. MRS, Scientific Basis for Nuclear Waste Management. Vol. 44. pp. 523-530.

Hodgkinson, D. and Cooper, N. (1992). A comparison of measurements and calculations for the Stripa validation drift inflow experiment. Stripa Project TR 92-07. SKB, Stockholm, Sweden.

Hökmark, H. (1991). Distinct element method modelling of fracture behaviour in near field rock. Stripa Project TR 91-01. SKB, Stockholm, Sweden.

Hökmark, H. and Israelson, J. (1991). Distinct element modelling of joint behaviour in nearfield rock. Stripa Project TR 91-22. SKB, Stockholm, Sweden.

Hood, M., Carlsson, H. and Nelson, P.H. (1979). Some results of a field investigation of thermo-meachnical loading of a rock mass when heaters are emplaced in the rock. Swedish-American cooperative program on radioactive waste storage in mined caverns in crystalline rock. SAC Report 26. SKB, Stockholm, Sweden.

Howard, J.J. and Roy, D.M. (1985). Develoment of layer charge and kinetics of experimental smectite alteration. Clays and Clay Minerals, Vol 29, 136 -147.

Hower, J., Eslinger, W.V., Hower, M.E. and Perry, E.A. (1976). Mechanisms of burial metamorphism of argillaceous sediment: 1. Mineralogical and chemical evidence. Geological Society of America Bulletin, Vol 87, 725-737.

IAEA (1985). Deep underground disposal of radioactive wastes: near field effects. Technical Report No. 251, International Atomic Energy Agency, Vienna.

IAEA (1989). Guidance for regulation of underground repositories for disposal of radioactive wastes. Safety Series No 96, International Atomic Energy Agency, Vienna.

IAEA (1990). Sealing of underground repositories for radioactive wastes. Technical Series No. 319, International Atomic Energy Agency, Vienna.

ICRP (1977). Recommendations of the international commission on radiological protection. ICRP publication 26, Annals of the ICRP, 1:3. Pergamon Press, Oxford, U.K.

ICRP (1985). Radiation protection principles for the disposal of solid radioactive waste. ICRP publication 46, Annals of the ICRP, 15:4. Pergamon Press, Oxford, U.K.

ICRP (1991a). 1990 recommendations 0f the international commission on radiological protection. ICRP publication 60, Annals of the ICRP, 31: (1-3).

ICRP (1991b). Annual ICRP limits on intake of radionuclides by workers based on the 1990 recommendations. ICRP publication 61, Annals of the ICRP 21:4.

Kelsall, P.C. and Shukla, D.K. (1980). Shaft and tunnel sealing considerations. Proc. OECD/USDOE Workshop on Borehole and Shaft Plugging. Columbus, Ohio, USA. ISBN 92-64-02114-0. pp 99 - 114.

Knutsson, S. (1983). Buffer Mass Test - Thermal calculations for the high temperature test. Stripa Project TR 83-03. SKBF/KBS, Stockholm, Sweden.

Lambe, T.W. and Whitman, R.V. (1969). Soil mechanics. Wiley and Sons, New York.

Mehta, P.K. (1986). In Concrete structure, properties and materials (Ed. W.J. Hall). Prentice-Hall International Series in Civil Engineering and Engineering Mechanics. Prentice-Hall Inc., Englewood Cliffs, New Jersey 07632.

Mehta, P.K. (1990). Durability of concrete - Fifty years of progress? American Concrete Institute, SP 126-1, 1-31.

Mitchell, J.K. (1976). Fundamentals of soil behaviour. Wiley and Sons, New York.

Mitchell, J.K. (1991). Conduction phenomena: from theory to geotechnical practice. Géotechnique 41(3), 299-340.

Mott, Hay and Anderson. (1985). The backfilling and sealing of radioactive waste repositories. EUR 9115 (2 vols), Commission of European Communities, Luxembourg.

Müller-Vonmoos, M., Kahn, G., Bucher, F. and Madsen, F.T. (1990). Investigation of metabentonites aimed at assessing the long-term stability of bentonites under repository conditions. Engng. Geology Vol. 28.

NAGRA (1985). Project Gewähr 1985 - Nuclear waste management in Switzerland: Feasibility studies and safety analyses. NAGRA, Baden, Switzerland.

Neville, A. (1981). Properties of concrete. John Wiley and sons, London, UK.

Neville, A. (1987). Why we have concrete durability problems. American Concrete Institute, SP 100, 21-30 (Ed. J.M. Scanlan)

Nilsson, J., Ramqvist, G. and Pusch, R. (1984). Buffer Mass Test - Heater design and operation. Stripa Project TR 84-02. SKBF/KBS, Stockholm, Sweden.

OECD/NEA (1980). Borehole and shaft plugging. Proceedings of a workshop. Columbus, Ohio, USA.

OECD/NEA (1988). Geological disposal of radioactive waste - *In situ* research and investigations in OECD countries. OECD/NEA, Paris.

Ohnishi, Y. (1988). FE coupled process analysis of buffer mass test in Stripa Project. 2nd International Symposium of Field Measurements in Geomechanics, Sakurai (Ed.) Balkema, Rotterdam. pp. 1019-1026.

Olsson, O. (Ed.) (1992). Site characterization and validation - Final report. Stripa Project TR 92-22. SKB, Stockholm, Sweden.

Onofrei, M. and Gray, M.N. (1988). The effect of W/C ratio and cement type on the longevity of grouts for use in a nuclear fuel waste disposal vault. Proc. MRS Fall Meeting, Boston, Mass.

Onofrei, M. and Gray, M.N. (1989). Adsorption studies of ^{35}S labelled superplasticizer in cement-based grouts. Proc. 3rd Int. Conf on superplasticizers and other additives in concrete. Ottawa, Ontario, Canada.

Onofrei, M., Gray, M.N. Keil, L.D. and Pusch, R. (1988). Studies of cement grouts and grouting techniques for sealing a nuclear fuel waste repository. Proc. MRS Annual Meeting, Symposium N, Boston.

Onofrei, M., Gray, M.N., Breton, D. and Ballivy, G. (1990). The effect of leaching on the pore structure of cement-based grouts for use in nuclear fuel waste disposal. Proc. MRS Fall Meeting, Boston, Mass.

Onofrei, M., Gray, M.N. and Roe, L. (1991a). Superplasticizer function and sorption in high-performance cement based grouts. Stripa Project TR 91-21. SKB, Stockholm, Sweden.

Onofrei, M., Gray, M.N. and Roe, L. (1991b). Cement based grouts - Longevity: laboratory studies of leaching behaviour. Stripa Project TR 91-33. SKB, Stockholm, Sweden.

Onofrei, M., Pusch, R., Gray, M.N., Börgesson, L., Karnland, O., Shenton, B. and Walker, B. (1992). Final report of the rock sealing project - Sealing properties of cement based grout materials. Stripa Project TR 92-28, SKB, Stockholm, Sweden.

Oscarson, D., Dixon, D.A. and Gray, M.N. (1990). Swelling capacity and permeability of an unprocessed and processed bentonitic clay. Engineering Geology 28. pp 281-289. Elsevier Scientific Publishing Company.

Oscarson, D.W., Sawatsky, N.G., Hume, H.B. and Cheung, S-C. H. (1991). Diffusion of iodide in compacted bentonite. Journal of the American Society of Soil Science.

Parkhurst, D.L., Thorstenson, D.C. and Plummer, L.N. (1980). PHREEQE - A computer program for geochemical calculations. U.S. Geological Survey, Water Resources Investigations.

Peck, R.B. (1969). Advantages and limitations of the observational method in applied soil mechanics. Ninth Rankine Lecture. Géotechnique 19:171-187.

Philip, J.R. and DeVries, D.A. (1957). Moisture movement in porous materials under temperature gradients. Trans. Am. Geophys. Union 38, 222-237.

Pusch, R. (1980a). Swelling pressures of highly compacted bentonite. SKBF/KBS Technical Report 80-13. SKBF/KBS, Stockholm, Sweden.

Pusch, R. (1980b). Permeability of highly compacted bentonite. SKBF/KBS Technical Report 80-16, SKBF/KBS, Stockholm, Sweden.

Pusch, R. (1983a). Stability of bentonite gels in crystalline rock - Physical aspects. SKBF/KBS 83-04, SKBF/KBS, Stockholm, Sweden.

Pusch, R. (1983b). Stability of bentonite gels in crystalline rock - Chemical aspects. SKBF/KBS 83-04, SKBF/KBS, Stockholm, Sweden.

Pusch, R. (1985). Final report on the Buffer Mass Test - Volume III: Chemical and physical properties of the buffer materials. Stripa Project TR 85-14, SKB, Stockholm, Sweden.

Pusch, R. (1992). Executive summary and general conclusions of the rock sealing project. Stripa Project TR 92-27. SKB, Stockholm, Sweden.

Pusch, R. and Börgesson, L. (1983). Buffer Mass Test-Improved models for water uptake and redistribution in the heater holes and tunnel backfill. Stripa Project TR 83-16, SKBF/KBS, Stockholm, Sweden.

Pusch, R. and Fredrikson, A. (1990). High voltage microscopy of the hydration of cement with special respect to the influence of superplasticizers. Stripa Project TR 90-03. SKB, Stockholm, Sweden.

Pusch, R. and Gray, M.N. (1989). Sealing of radioactive waste repositories in crystalline rock. Proceedings of an NEA/CEC Workshop held in Braunshweig, Germany. OECD/NEA, Paris. pp. 214-228.

Pusch, R. and Nilsson, J. (1983). Buffer Mass Test - site documentation. Stripa Project IR 83-04, SKBF/KBS, Stockholm, Sweden.

Pusch, R., Börgesson, L. and Nilsson, J. (1982). Buffer Mass Test - Buffer materials. Stripa Project TR 82-06, SKBF/KBS, Stockholm, Sweden.

Pusch, R., Forsberg, T., Nilsson, J., Ramqvist, G. and Tegelmark, S-E. (1984). Buffer Mass Test - Instrumentation. Stripa Project TR 84-06, SKBF/KBS, Stockholm, Sweden.

Pusch, R., Börgesson, L. and Ramqvist, G. (1985a). Final report on the Buffer Mass Test - Volume II: test results. Stripa Project TR 85-12, SKB, Stockholm, Sweden.

Pusch, R., Nillson, J. and Ramqvist, G. (1985b). Final report on the Buffer Mass Test - Volume I: scope, preparative field work and test arrangement. Stripa Project TR 85-11, SKB, Stockholm, Sweden.

Pusch, R., Erlström, M. and Börgesson, L. (1985c). Sealing of rock fractures. A survey of potentially useful methods and substances. SKB Technical Report 85-17. SKB, Stockholm, Sweden.

Pusch, R., Börgesson, L. and Ramqvist, G. (1987a). Final report of the borehole, shaft and tunnel sealing test - Volume I: borehole plugging. Stripa Project TR 87-01. SKB, Stockholm, Sweden.

Pusch, R., Börgesson, L. and Ramqvist, G. (1987b). Final report of the borehole, shaft and tunnel sealing test - Volume II: shaft plugging. Stripa Project TR 87-02. SKB, Stockholm, Sweden.

Pusch, R., Börgesson, L. and Ramqvist, G. (1987c). Final report of the borehole, shaft and tunnel sealing test - Volume III: tunnel plugging. Stripa Project TR 87-03. SKB, Stockholm, Sweden.

Pusch, R., Börgesson, L., Fredrikson, A., Markström, L., Erlström, M., Ramqvist, G., Onofrei, M. and Coons, W.E. (1988). Rock Sealing - Interim report on the rock sealing project (Stage 1). Stripa Project TR 88-11. SKB, Stockhlm, Sweden.

Pusch, R., Börgesson, L., Karnland, O. and Hökmark, H. (1991a). Final report on test 4 - Sealing of natural fine-fracture zone. Stripa Project TR 91-26. SKB, Stockholm, Sweden.

Pusch, R., Karnland, O., Hökmark, H., Sandén, T. and Börgesson, L. (1991b). Final report of the rock sealing project - sealing properties and longevity

of smectitic clay grouts. Stripa Project TR 91-30. SKB, Stockholm, Sweden.

Pytte, A.M. (1982). The kinetics of the smetite to illite reaction in contact metamorphic shales. Thesis M.A., Dartmouth College, N.H., USA.

Radhakrishna, H.S. (1984). Thermal properties of clay-based buffer materials for a nuclear fuel-waste disposal vault. Atomic Energy of Canada Limited Report, AECL-7805, AECL-Research, Pinawa, Manitoba, Canada.

Radhakrishna, H.S., Chan, H.T., Crawford, A.M. and Lau, K.C. (1989). Thermal and physical properties of candidate buffer-backfill materials for a nuclear fuel-waste disposal vault. Canadian Geotechnical Journal: 26(4), 629-639.

Riekkola, R. (1989). Personal communication to the Stripa Task Force on Sealing Materials and Techniques. In minutes of meeting held in Zurich, Switzerland.

Roy, D.M. and Langton, C.A. (1983). Charactertization of cement-based ancient building materials in support of repository seal materials studies. BMI/ONWI-523.

Selig, E.T. (1964). A review of stress and strain measurement in soil. Proc. Symp. on soil-structure interaction. University of Arizona, Tucson, AZ. 172-186.

Shackelford, C.D. (1988). Diffusion as a transport process in fine-grained barrier materials. Geotechnical News 6(2), 24-27.

Sposito, G. (1984). The surface chemistry of soils. Oxford University Press N.Y/ Clarendon Press, Oxford.

Steadman, J. (1989). Studies of the properties of cements used in Hadrian's Wall. Personal communication. Minutes of the task force on sealing materials and techniques. OECD/NEA Stripa Project.

Taguchi, G. (1978). Off-line and on-line quality control system. International Conference on Quality Control, Tokyo, Japan.

Thorpe, R. (1979). Characterization of the discontinuities in the Stripa granite time-scale heater experiment. Swedish American Cooperative Program SAC-Report 20. Lawrence Berkeley Laboratory, Earth Sciences Division, Report LBL-7083.

Thomas, H.R. (1992). On the development of a model of coupled heat and moisture transfer in unsaturated soil. Canadian Geotechnical Journal 29(6).

Van Olphen, H. (1963). An introduction to clay colloid chemistry. J. Wiley and Sons, New York.

Watanabe, K. (1991). Evaporation measurement in the Validation Drift. Stripa Project TR 91-06. SKB, Stockholm, Sweden.

Watanabe, K., Yanagisawa, K., Pusch, R., Sakuma, H., Aizawa, T., Yamamoto, H. and Kanda, N. (1989). Evaporation measurement to map the groundwater discharge on a tunnel wall of low permeable rock mass. J. Japan Soc. Engineering Geology: 31.

Wilson, C.R., Long, J.C.S., Galbraith, R.M., Karasaki, K., Endo, H.K., DuBois, A.O,. McPherson, M.J. and Ramqvist, G. (1981). Geohydrological data from the macropermeability experiment at Stripa, Sweden. Swedish-American co-operative program on radioactive waste storage in mined caverns in crystalline rock. SAC-Report 37, SKB, Sweden.

Wolery, T.J. (1983). EQ3NR, a computer program for speciation-solubility calcultaions: user's guide and documentation. Lawrence Livermore National Laboratory, UCRL-53414.

Wolery, T.J. (1984). EQ6, a computer program for reaction path modeling of aqueous geochemical systems: user's guide and documentation. Lawrence Livermore National Laboratory, UCRL-51 (Draft).

Yong, R.N. and Warkentin, B.P. (1975). Soil properties and behaviour. Elsevier, Amsterdam.

BIOGRAPHY-Dr. Malcolm N. Gray, P.Eng.

Malcolm Gray was born in Birkenhead, England in 1945. In 1967 he graduated with a B.Sc. in Civil Engineering from the University of Leeds, England and, in 1972, the same university awarded him a Ph.D. degree for research into soil stabilization. Dr. Gray has been engaged since in civil engineering practice, teaching and research. Between 1972 and 1980, he was employed by the Governments of Kenya and Hong Kong and also worked as a consulting engineer. From 1980 to 1983 he taught at the Department of Civil and Structural Engineering at University College, Cardiff, Wales. In 1983 he joined AECL Research, Canada, where he is currently head of research into repository sealing. Dr. Gray represented AECL Research on the TSG-2 of Phases 1 and 2 of the Stripa Project and, during Phase 3 of the project, was a member and *ad hoc* chairman of the Task Force on Sealing Materials and Techniques. In addition, he was one of the two Canadian representatives on the TSG. Dr. Gray is a registered professional engineer in the Province of Manitoba, Canada, and an Adjunct Professor in the Department of Civil Engineering at the University of Manitoba.